A comparison of HIV-1 and HIV-2 *gag* gene expression

Gemma L. Watkins

A thesis submitted for the degree of Doctor of Philosophy

University of Warwick, School of Life Sciences

September 2011

Contents

Acknowledgements

There are numerous people who deserve thanks for assisting with the work in this thesis. Though I only acknowledge a few of them here, I am also grateful to the many others who provided help along the way.

Firstly, I would like to thank my supervisor Dr Emma Anderson for the considerable advice, guidance and enthusiasm throughout my PhD and for the consistent support, help and encouragement given whilst writing my thesis; none of this work would have been possible without you.

I am also most grateful to members of the Anderson lab, especially Cyril Barbezange and Michela Marongiu, for their abundant supply of patience, motivation and technical advice. Additionally, I thank members of the Evans lab, in particular Kym Lowry, Andy Tuplin, Crystal Hornsey, Chris Bull and Estelle Dumas, for allowing me to gatecrash so frequently, for significant advice on protocols, lending of equipment, reagents, and the provision of much humour.

I would also like to thank Professor David Evans and Dr Keith Leppard for their interesting conversations and technical knowhow, Sue Morris, Phil Gould and Bo Meng for additional assistance, and Cathy Parry and Gill Scott for being truly superb technicians.

I wish to thank all my friends at the University of Warwick for making my time there so enjoyable, my family; Ma, Pa, Kate, Ben and Joe for their endless love and support, and Joshua for his computing genius and for making me smile when times were tough.

Finally, I acknowledge generous financial contributions from both the Medical Research Council and the University of Warwick.

Declaration

This work was completed at the University of Warwick between October 2008 and September 2011 and has not been submitted for another degree. The work is original and, unless otherwise stated in the text, has been completed by the author.

Gemma L. Watkins September 2011

Summary

Despite being closely related viruses with similar replication cycles, HIV-2 replicates more slowly than HIV-1 and produces fewer particles, resulting in a lower plasma viral load. Expression of the major structural gene, *gag*, from HIV-1 and HIV-2 proviruses was compared to investigate whether this could play a role in the difference in particle production observed between HIV-1 and HIV-2 infection.

Using quantitative RT-PCR, significantly less full-length HIV-2 gag mRNA was found to be transcribed from its provirus than for HIV-1. Sub-cellular fractionation allowed us to determine HIV-1/2 gag mRNA levels in the nucleus and cytoplasm throughout a time course. RNA export of HIV-2 gag mRNA was shown to be slower than for HIV-1 gag mRNA.

HIV-2 full-length gag RNA was shown to be translated much less efficiently than HIV-1 in a range of cell lines. Both HIV-1 and HIV-2 Gag have been proposed to be translated by internal ribosome entry. Shutting down cap-dependent translation (by poliovirus-mediated eIF4G cleavage) significantly reduced translation from both HIV-1/2 gag RNAs, with no evidence of compensatory IRES activity. This suggests that cap-dependent translation is the predominant mechanism for translation of both HIV-1 and HIV-2 RNA.

Additional work explored HIV RNA-protein interactions by UV cross-linking experiments using cellular proteins. Several proteins differentially binding to HIV-1/2 5' UTR RNAs were identified and, in particular, a 45 kDa protein binding only to the HIV-1 5' UTR. Attempts were made to characterise the proteins binding with different affinities to HIV-1 and HIV-2 RNAs.

Confocal microscopy was used to visualise HIV-1/2 Gag expression within the cell. Both HIV-1 and HIV-2 Gag expression was shown to be reduced when siRNA was used to inhibit the cellular clathrin adaptor protein AP-1.

In conclusion, HIV-2 Gag gene expression was found to be less efficient than HIV-1 at the level of transcription, RNA export and translation. Future work will continue to investigate the mechanisms behind these differences.

Abbreviations

Ab	antibody
ActD	actinomycin D
Ag	antigen
AIDS	acquired immune deficiency syndrome
AP	adaptor protein
ARD	arginine rich domain
ARV	AIDS-associated retrovirus
AZT	3-azido-2-3-dideoxythymidine
BIV	bovine immunodeficiency virus
bp	base pairs
BSA	bovine serum albumin
CA	Capsid
$CaCl_2$	calcium chloride
CAEV	caprine arthritis-encephalitis virus
CDC	Centers for Disease Control and Prevention
cDNA	complementary DNA
CIAP	calf intestinal alkaline phosphatase
CMV	cytomegalovirus
CpG	cytosine-phosphate-guanine
CRFs	circulating recombinant forms
Ct	cycle number
CTD	C-terminal domain
CTS	central DNA synthesis termination site
DAPI	4',6-diamidino-2-phenylindole dihydrochloride
DEPC	diethyl pyrocarbonate
DIS	dimer initiation site
DMEM	Dulbecco's modified Eagle's medium
DTT	dithiothreitol
E.coli	*Escherichia coli*
EDTA	ethylenediaminetetraacetic acid
eEF	eukaryotic elongation factor
EGTA	ethylene glycol tetraacetic acid
EIAV	equine infectious anemia virus
eIF	eukaryotic initiation factor
Env	Envelope glycoprotein
eRF	eukaryotic release factor
ESCRT	endosomal sorting complexes required for transport
FCS	foetal calf serum
FIV	feline immunodeficiency virus
Gag	Group-specific antigen
GAPDH	glyceraldehyde-3-phosphate dehydrogenase
GFP	green fluorescent protein
GMEM	Glasgow minimum essential medium
GRID	gay-related immune deficiency
HAART	highly active antiretroviral therapy
HIV	human immunodeficiency virus
HK	housekeeping
hnRNP	heterogeneous nuclear ribonucleoprotein
HRP	horse radish peroxidase
HRV-2	human rhinovirus 2
HTLV	human T-lymphotrophic viruses
IDAV	immunodeficiency-associated virus
IFN	interferon
IN	Integrase
IP	immunoprecipitation
IRES	internal ribosome entry site
ITAF	IRES *trans*-acting factor
KCl	potassium chloride
kDa	kilodaltons
La	lupus autoantigen
LAV	lymphadenopathy-associated virus
LB	lysogeny broth medium
LepB	leptomycin B
LPS	lipopolysaccharide
LTNP	long-term non-progressors
LTR	long terminal repeats
MA	Matrix
MAb	monoclonal antibody
MALT	mucosal-associated lymphoid tissue
µCi	microcurie
$MgCl_2$	magnesium chloride
$Mg(OAc)_2$	magnesium acetate solution

MHC I/II	major histocompatibility complex class I/II
m.o.i.	multiplicity of infection
MOPS	3-(N-morpholino) propanesulfonic acid
MP	Maxiprep
MS	mass spectrometry
MTC	mother-to-child
MVB	multivesicular body
MW	molecular weight
myDC	myeloid dendritic cell
NaOAc	sodium acetate
NaOH	sodium hydroxide
NC	Nucleocapsid
NEB	New England Biolabs
NES	nuclear export signal
NFκB	nuclear factor kappa B
NIBSC	National Institute for Biological Standards and Control
NLS	nuclear localisation signal
NMD	nonsense mediated decay
NNRTI	non-nucleoside reverse transcriptase inhibitor
NRTI	nucleoside/nucleotide reverse transcriptase inhibitors
NSI	non-syncytia inducing
nt	nucleotides
NTD	N-terminal domain
ORF	open reading frame
PABP	poly(A) binding protein
PBS	phosphate buffered saline
PBS	primer binding site
pcDC	plasmacytoid dendritic cell
PCR	polymerase chain reaction
PEG	polyethylene glycol
pfu	plaque-forming units
PI	protease inhibitor
PIC	pre-integration complex
PKR	protein kinase R
PLB	passive lysis buffer
PLV	puma lentivirus
PPT	polypurine tract
PR	Protease
PRF	programmed ribosomal frameshifting
PV	poliovirus
RAC	RNA affinity chromatography
RBD	RNA-binding domain
RER	rough endoplasmic reticulum
RNP	ribonucleoprotein
RPC	ribosome peptidyl centre
RPM	revolutions per minute
RPMI	Roswell Park Memorial Institute medium
RRE	Rev responsive element
RRL	rabbit reticulocyte lysate
rt	room temperature
RT	Reverse transcriptase
RTC	reverse transcription complex
qPCR	quantitative real- time PCR
S100	supernatant from centrifugation at 100,000g
SA	splice acceptor
SD	splice donor
SDS-PAGE	sodium dodecyl sulphate polyacrylamide gel electrophoresis
SI	syncytia inducing
SIV	simian immunodeficiency virus
SOC	super optimal broth with catabolite repression
Sp1/Sp2	spacer peptide 1/2
SQ	saquinavir
SRP	signal recognition particle
SU	surface subunit
TAK	Tat-associated kinase
TAR	*trans*-activation response element
TBE	Tris/borate/EDTA
TBS-T	Tris-buffered saline tween20
TCA	trichloroacetic acid
TM	transmembrane subunit
TRBP	TAR RNA-binding protein
Tris	Tris (hydroxymethyl) aminoethane
U	units
uORF	upstream open reading frame
UTR	untranslated region
UV	ultraviolet
VLP	virus-like particle
VMV	visna-maedi virus
Vol.	volume

CHAPTER 1: INTRODUCTION

1.1 The origin of HIV

Human immunodeficiency virus (HIV) is a lentivirus of the family *Retroviridae* and subfamily *Orthoretrovirinae*. HIV is the causative agent of acquired immune deficiency syndrome (AIDS). Lentiviruses are characteristically responsible for long-term illnesses: commencing with subclinical infection and a prolonged incubation period, and progressing insidiously to degenerative disease syndromes (Narayan and Clements, 1989). Other lentiviruses include bovine (BIV), feline (FIV), and simian (SIV) immunodeficiency viruses, caprine arthritis encephalitis virus (CAEV), equine infectious anemia virus (EIAV), puma lentivirus (PLV) and visna-maedi virus (VMV) [figure 1]. Lentiviruses are distinguished from other retroviruses by their morphologically distinct, cone-shaped nucleoid in mature virus particles and the presence of regulatory elements *rev* and *tat*. Infection with lentiviruses is also species-specific (Coffin, J.M. *et al.*, 1997).

There are two types of HIV: HIV-1 and HIV-2. HIV-1 is the predominant subtype and is found globally, whereas HIV-2 is largely confined to West African countries such as Senegal and Ivory Coast (Coffin, J.M. *et al.*, 1997). Until recently, three major groups of HIV-1 had been identified; group M (Main) which is responsible for the majority of global infections, group O (Outlier group) mainly responsible for infections in Cameroon, France and Gabon and the rarer group N (non M or O) discovered in Cameroon (Levy, J., 2007; Sleasman and Goodenow, 2003). Additionally, group M has 9 distinct subtypes known as ‘clades’: A, B, C, D, F, G, H, J and K [figure 2]. Genetic recombination between different HIV-1 subtypes has also resulted in many HIV-1 variants known as circulating recombinant forms (CRFs) (Coffin, J.M. *et al.*, 1997; Sharp *et al.*, 2001). Recently, transmission of a gorilla retrovirus (SIV_{gor}) into humans has been reported and will potentially form a new, fourth HIV-1 group classified as Group P (Broder, 2010). The HIV-2 virus is divided into 8 groups: A-H, of which groups A and B are the most prevalent whereas groups C-H have only been isolated from one person (Santiago *et al.*, 2005).

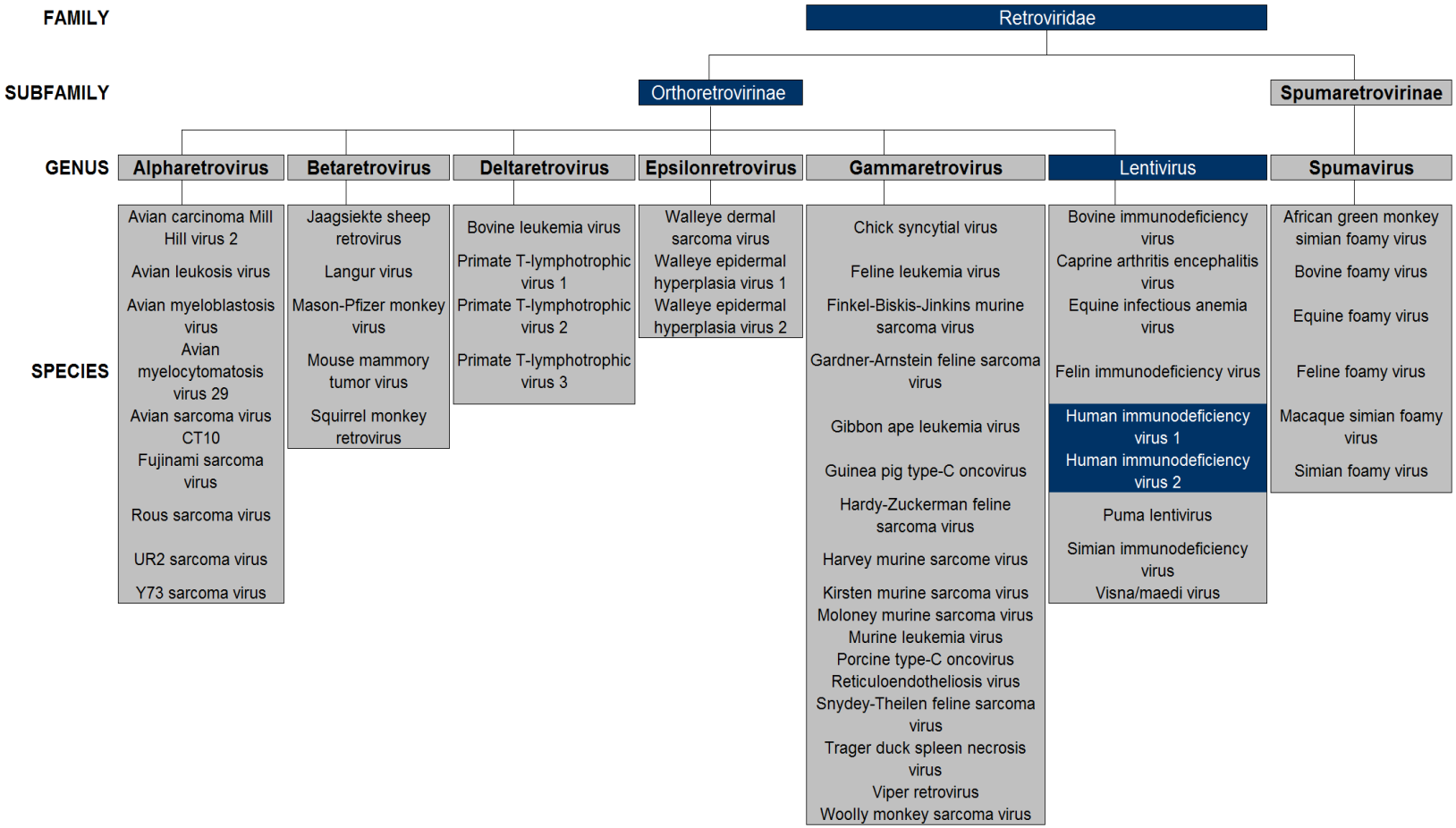

Figure 1: Taxonomy of HIV highlighted in blue: the HIV species is classified as part of the *Retroviridae* family, *Orthoretrovirinae* subfamily, and *lentivirus* genus [International Committee on the Taxonomy of Viruses (ICTV): http://www.ictvonline.org/virusTaxonomy.asp?version=2009].

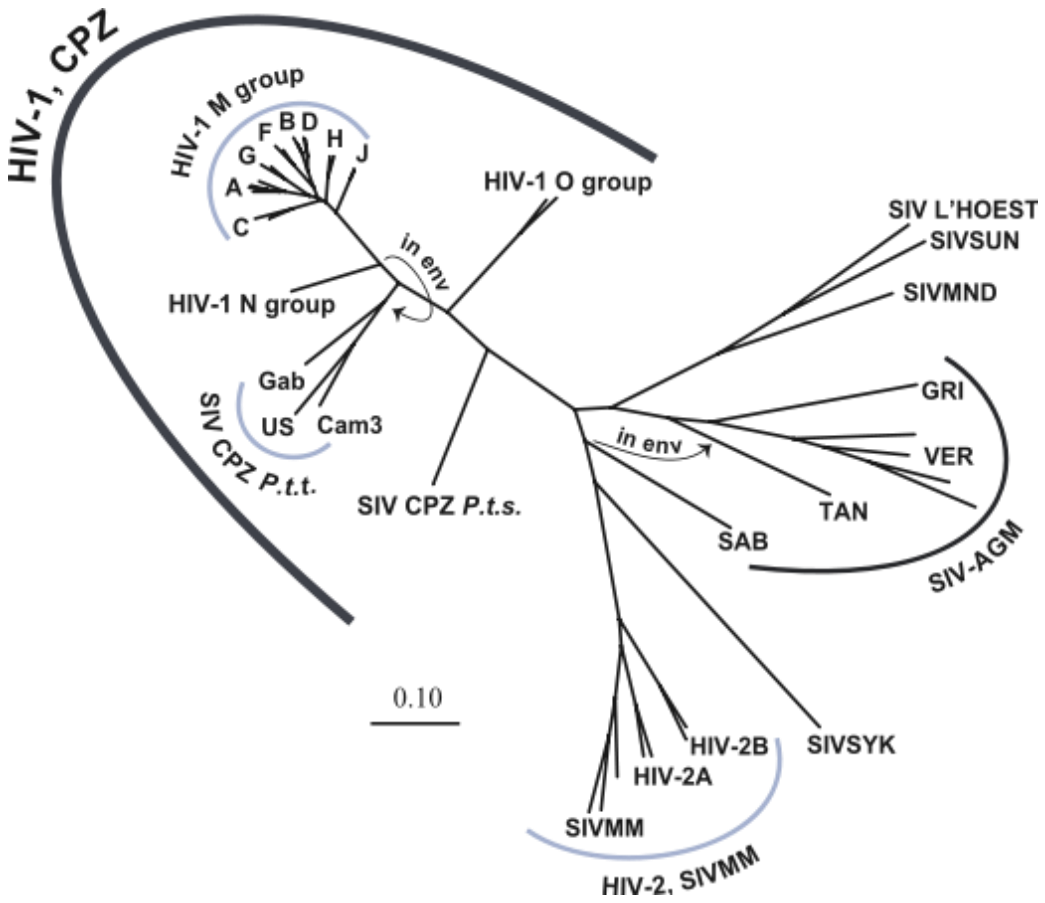

Figure 2: Phylogenetic tree of primate lentiviruses based on the similarities within the HIV *pol* gene region. The relationship of HIV-1 (groups M, N and O) to SIV_{cpz} and HIV-2 to SIV_{smm} are shown [Image: http://svr225.stepx.com:3388/hiv and description from (Reeves and Doms, 2002)].

It is thought that cross-species transmission events are responsible for the presence of HIV in humans. Viruses related to HIV-1 have been identified in chimpanzees (*Pan troglodytes*) (Sharp *et al.*, 2001). In particular, phylogenetic analysis has shown that another lentivirus - chimpanzee simian immunodeficiency virus (SIV_{cpz}) - is closely related to, and therefore believed to be the origin of, HIV-1 groups M, N and O (Chen, Z. *et al.*, 1997). SIV_{cpz} infection is non-pathogenic in chimpanzees and is not accompanied by the vast destruction of immune tissue seen in HIV-1 infection of humans (Forsman and Weiss, 2008). Sooty mangabey simian immunodeficiency virus (SIV_{smm}) which infects sooty mangabeys (*Cercocebus atys*) closely resembles HIV-2 and sooty mangabeys are native to western Africa; coincident with endemic HIV-2 (de Silva *et al.*, 2008). It is believed that

SIV_{smm} crossover into the human population may have occurred on at least 8 occasions resulting in the HIV-2 subgroups A-H (Broder, 2010; de Silva *et al.*, 2008). Independent transmission events from primates infected with genetically distant lentiviruses are therefore thought to account for the emergence of both HIV-1 and HIV-2.

In terms of timing, HIV-1 M group isolates have been detected in samples from as far back as 1931, yet the HIV virus was not detected until considerably later during the 20^{th} century (Chen, Z. *et al.*, 1997). However, symptoms of HIV infection are diverse, not easily recognisable and manifest in a way that makes HIV infection difficult to distinguish from other autoimmune diseases. Coupled with a latency period of around ten years between HIV infection and AIDS, HIV may thus have gone undetected (Chevret *et al.*, 1992). This may account for the extended period between the first, dormant cases of HIV within the human population and its actual detection and recognition as part of the AIDS epidemic in the 1980s (Yusim *et al.*, 2001).

Although unreported incidents of the disease may have existed earlier, the first identified cases of AIDS occurred in June 1981. Immune deficiency was identified following an unusually high incidence of rare, opportunistic infections: *Pneumocystis carinii* pneumonia and Kaposi's sarcoma, amongst previously healthy, homosexual men living in Los Angeles (Gottlieb *et al.*, 1981). The disease was therefore, initially, termed gay-related immune deficiency syndrome (GRID). However, after subsequent detection of disease in patients outside of the gay community, the disease was given the name AIDS (acquired immunodeficiency syndrome) by the Center for Disease Control and Prevention (CDC).

In 1983 Luc Montagnier isolated a new virus from the swollen lymph nodes of AIDS patients, which resembled another retrovirus: equine infectious anemia virus (EIAV). Initially called lymphadenopathy-associated virus (LAV), Montagnier subsequently relabelled the virus immune-deficiency-associated virus (IDAV) due to its isolation from AIDS patients, and confirmed an association with AIDS pathogenesis (Barre-Sinoussi *et al.*, 1983; Montagnier

et al., 1984). Around a similar time, in 1984, Robert Gallo identified a new retrovirus which was isolated from AIDS patients and shared several features of previously identified human T-lymphotrophic viruses (HTLV). Named HTLV-III, this new retrovirus was distinguishable from HTLV-I/II due to its morphological, biological and antigenic differences. Gallo suggested that HTLV-III was the causative agent of AIDS (Gallo *et al.*, 1984). In 1985 Jay Levy isolated AIDS-associated retrovirus (ARV) from homosexual men and showed this to be the cause of neurological syndromes presented in AIDS patients (Levy, J.A. *et al.*, 1985). In the same year, HTLV-III, LAV and ARV were shown to be genetic variants of the same virus (Ratner *et al.*, 1985). Consequently, these viruses were grouped and collectively coined HIV in 1986 (Coffin, J. *et al.*, 1986).

In 1985, a new retrovirus was isolated from AIDS patients in West Africa (Clavel *et al.*, 1986). Although related to HIV, this new virus was distinct and its envelope glycoproteins more closely resembled those of simian retroviruses. However, in 1987 it was shown that this new retrovirus also caused AIDS. The virus was, therefore, named HIV-2 and its predecessor became known as HIV-1 (Le Guenno *et al.*, 1987).

1.2 HIV pathology

1.2.1 The global disease burden of HIV

Currently, 33.3 million people are infected with HIV, with 2.6 million new infections, and 1.8 million deaths from AIDS occurring during 2009 [figure 3]. The highest prevalence of HIV is in Sub-Saharan Africa with 22.4 million people living with HIV (UNAIDS, 2010).

Subtypes A, B and C (group M) are the most prevalent amongst HIV-1 patients with subtype C responsible for nearly 50% of infections. Geographically, subtype A is found in Central/East Africa and East Europe, subtype B is primarily located in Central/West Europe, Australia, the Americas, North Africa, Southeast Asia and the Middle East, whilst subtype C is predominant in Africa and India. The burden of infection is not evenly

distributed as around 80% of all global infections are found in Africa and India, coincident with the dominance of subtype C (Buonaguro *et al.*, 2007).

Total: 33.3 million (31.4 million - 35.3 million)

Area	Estimated adult and child deaths due to AIDS
Sub-Saharan Africa	1300000
South & South-East Asia	260000
Eastern Europe & Central Asia	76000
Central & South America	58000
East Asia	36000
North America	26000
Middle East & North Africa	24000
Caribbean	12000
Western & Central Europe	8500
Oceania	1400
TOTAL	**1801900**

Figure 3: The number of adults and children living with HIV and the distribution of adult and child deaths due to AIDS in 2009 (UNAIDS, 2010).

The range of HIV-2 infection is more limited, occurring principally in West Africa and Europe. The majority of HIV-2 infections in Guinea-Bissau and Europe, are due to subtype A, whereas HIV-2 subtype B infections are found more commonly in Ghana and the Ivory Coast. The highest diversity of HIV-2 is found in Sierra Leone, with identifed subtypes A, B, E and F causing infection (Reeves and Doms, 2002). Dual infection (with HIV-1 and HIV-2) has also been identified in areas with increasing HIV-1 prevalence and endemic HIV-2 (Reeves and Doms, 2002). This introduces the possibility of recombination between the two types of HIV, although this has not yet been detected. Interestingly, whilst the prevalence of HIV-1 continues to increase, the prevalence of HIV-2 is declining. A simple explanation is the low viral load, and thus inefficient transmission efficiency, of the HIV-2 virus (de Silva *et al.*, 2008).

1.2.2 HIV transmission

Transmission of HIV occurs via direct sexual contact, through blood, by perinatal transmission from mother to child (MTC) or through breast milk (Coffin, J.M. *et al.*, 1997). 85% of HIV-1 infections are transmitted heterosexually (Forsman and Weiss, 2008). Although MTC transmission of HIV can occur, due to the limited lifespan of infants born with HIV, the virus is

rarely transmitted further (Forsman and Weiss, 2008). The rate of MTC transmission varies according to different regions. In Europe, HIV-1 MTC transmission occurs for 15-20% of AIDS patients, whereas the rate is much higher in Africa at 25-35%. Breast feeding contributes to MTC transmission statistics. Notably, HIV-2 MTC transmission rates, at 0-1.2%, are much lower than for HIV-1 (O'Donovan *et al.*, 2000). Risk factors for MTC transmission include obstetric issues, nutritional deficiency, advanced disease status and a low CD4 cell count (O'Donovan *et al.*, 2000). HIV transmission is also 26-fold more likely during stages of primary infection than during stages of asymptomatic, chronic infection. It has thus been estimated that 23% of transmission events occur whilst HIV positive individuals are experiencing primary infection (Forsman and Weiss, 2008).

Genetic factors can also influence HIV transmission: some individuals show a genetic predisposition to be more resistant to HIV infection. For example, a homozygous CCR5Δ32 deletion prevents HIV infection via the chemokine receptor CCR5, resulting in resistance to strains dependent on this co-receptor. Additionally, variations in host restriction factors, such as APOBEC3G and Trim5α, have also been shown to confer resistance to HIV infection (Forsman and Weiss, 2008).

Although equivalent routes of transmission are used by HIV-1 and HIV-2, transmission of HIV-2 is much less efficient (Reeves and Doms, 2002). Overall, it has been estimated that HIV-1 has a transmission rate of 24.4% compared to only 4.0% for HIV-2 (O'Donovan *et al.*, 2000).

1.2.3 HIV target cells

Several tissues host HIV replication including the spleen, lymph nodes, lymph cells and macrophages (Wei *et al.*, 1995). Initial infection may target mononuclear phagocytes which provide a means for early dissemination of the virus and are, therefore, important in establishing early infection and subsequent pathogenesis (Gartner *et al.*, 1986). HIV is able to proliferate in $CD4^+$ T-lymphocytes (T-cells), macrophages and both plasmacytoid (pcDC) and myeloid (myDC) dendritic cells (Forsman and Weiss, 2008; Patterson *et al.*, 2001). HIV tropism is governed by the presence of suitable cell surface

receptors which are required for virus attachment and entry (Forsman and Weiss, 2008). CD4 is the primary HIV receptor whilst accessory chemokine receptors CCR5 and CXCR4 are co-receptors (Patterson *et al.*, 2001). CCR5 is the receptor most commonly used by HIV variants, although during later stages of infection variants which use the CXCR4 receptor tend to emerge (Forsman and Weiss, 2008).

Co-receptor usage largely determines virus tropism, although additional host factors can also affect virus dissemination. Cell tropism also varies between different HIV isolates. $CD4^+$ T-cells remain the prominent target of all HIV viruses, although other cells provide targets for HIV infection based on receptor compatibility with the infecting strain (Reeves and Doms, 2002). HIV isolates have, thus, been divided into groups based on their cellular tropism. X4 tropic viruses use the CXCR4 co-receptor and have a characteristically rapid replication rate leading to high virus titres in $CD4^+$ T-cells. Additionally, X4 tropics induce the formation of giant, multi-nucleated cells, or syncytia, *in vitro* and are therefore sometimes referred to as SI (syncytia-inducing) isolates (Reeves and Doms, 2002). Non-syncytia inducing (NSI) strains preferentially infect macrophages using the CCR5 co-receptor. These isolates are sometimes called R5 tropic strains and typically replicate more slowly and to a lower titre than X4 tropic strains (Reeves and Doms, 2002). An additional group of HIV variants has been identified with an ability to infect both $CD4^+$ T-cells and macrophages. These strains use both the CXCR4 and CCR5 co-receptors and are therefore referred to as R5/X4 tropic strains. Individuals lacking the CCR5 co-receptor have proven more resistant to HIV infection (Reeves and Doms, 2002).

1.2.4 HIV disease progression

There are essentially four phases of HIV disease progression; primary infection, clinical latency, symptomatic disease and progression to AIDS.

1.2.4.1 Primary infection

Following exposure and infection with HIV, there is a period of incubation lasting between 2-6 weeks. This is followed by primary infection which is

marked by a 4-8 week period of acute disease (Forsman and Weiss, 2008) [figure 4].

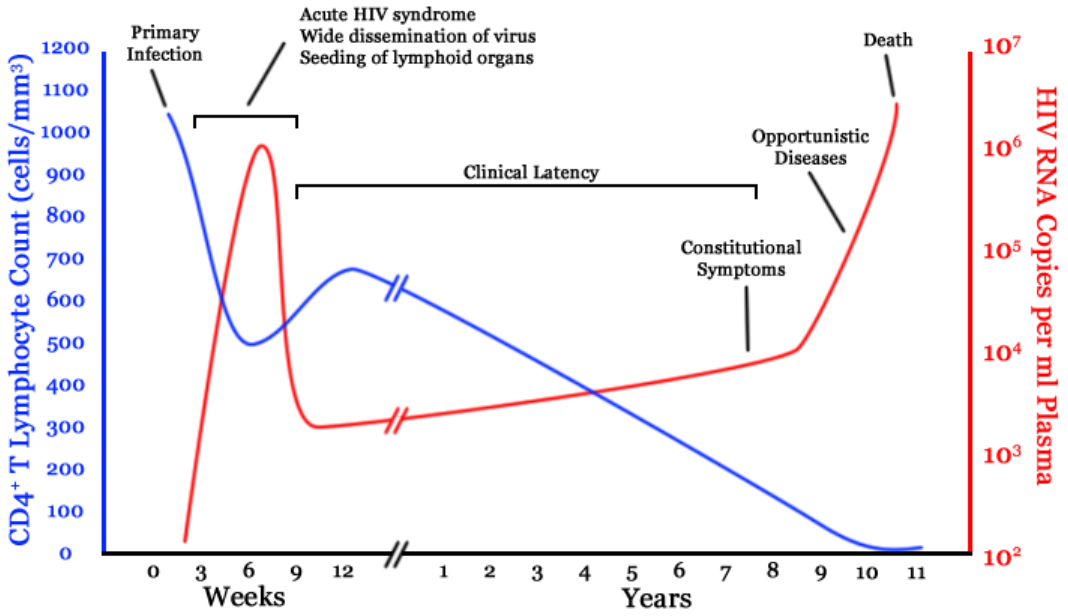

Figure 4: A time course of HIV infection showing primary infection, clinical latency, symptomatic disease and progression to AIDS resulting in death. The relationship between viral load (the number of copies of HIV RNA per ml of plasma) and the level of $CD4^+$ T-lymphocytes (CD4 count in cells per µl) during an untreated HIV infection are indicated. Following primary infection, wide dissemination of the virus results in $CD4^+$ T-cell destruction (blue). Virus load (red) peaks during primary infection and, after a period of clinical latency, increases with the onset of AIDS [http://svr225.stepx.com:3388/hiv].

Swollen lymph nodes (lymphadenopathy), fever, muscle pain (myalgia), nausea, fatigue and a sore throat (pharyngitis) are common symptoms of acute infection (Rogowska-Szadkowska and Chlabicz, 2008). During primary infection, HIV-1 replicates rapidly within $CD4^+$ T-cells in mucosal-associated lymphoid tissue (MALT). Mass destruction of $CD4^+$ T-cells is associated with damage to the mucosal epithelium. Subsequently, commensal organisms gain entry to the MALT where the presence of bacterial lipopolysaccharides (LPS) triggers an inflammatory immune response (Forsman and Weiss, 2008). In response to this, the peripheral viral load begins to increase.

HIV infection causes $CD4^+$ T-cell destruction both directly, from cellular virus infection, and via the adaptive immune response. Immune activation is also

elevated by bystander effects including activation and apoptosis of neighbouring, uninfected $CD4^+$ T-cells, and translocation of microbial LPS across damaged mucosa. Consequently, dissemination of virus particles into the blood results in extensive, systemic viremia. The humoral immune response is activated in response to the copious number of infected $CD4^+$ T-cells circulating in the blood (Coffin, J.M., 1995). The immune system begins to clear the infection by producing HIV-specific, $CD8^+$ cytotoxic T-cells which kill virus-infected cells via antibody cytotoxicity (Forsman and Weiss, 2008). Innate immunity also has a role in clearing viral infection through the complement system, which causes opsonisation and destruction of viral particles. Viral destruction of target cells may result in insufficient $CD4^+$ T-cell levels for continued viral replication. Additionally, impairment of thymic function prevents T-cells from regenerating, preventing sustainance of T-cell reservoirs and replacement of destroyed $CD4^+$ T-cells (Forsman and Weiss, 2008). Thus, at this stage, further viral replication is hindered and viral load begins to decrease.

1.2.4.2 Latency and asymptomatic infection

The subsequent decline in the level of circulating virus marks the onset of asymptomatic infection, during which few or no apparent symptoms are observed, before the final stage of HIV infection emerges in the form of AIDS. During asymptomatic infection, although cellular and integrated proviral levels are similar for both HIV-1 and HIV-2, HIV-1 viral mRNA levels are higher and the HIV-1 plasma viral load is up to 30 times greater than HIV-2 (de Silva *et al.*, 2008). Despite the lack of outward symptoms, the period of clinical latency conceals a dynamic phase of virus replication. The average lifespan of a HIV infected cell is 2.2 days and plasma virions have a lifespan of 0.3 days. *In vivo*, the minimum HIV-1 life cycle lasts an average of 2.2 days with a generation time (from the release of virus particles, subsequent infection of a new host cell and the release of further viral progeny from that cell) of 2.6 days. During a productive infection, individuals produce daily an average of 10.3×10^9 virions via continuing replication in $CD4^+$ T-cells. (Perelson *et al.*, 1996). Consequently, there is a high level of infected $CD4^+$ T-cell turnover; low levels of virus are constantly produced by replication and

removed by the host immune response (Coffin, J.M., 1995). However, initially, the immune system is able to regenerate at a sufficient rate to maintain the level of $CD4^+$ T-cells.

It may take up to 10 years for progression to AIDS. Individuals failing to progress to AIDS within 15 years are called long term non-progressors (LTNPs) (Forsman and Weiss, 2008). With an incubation period spanning months or years, the mechanisms of HIV infection are therefore the antithesis of those used by viruses causing acute disease (Narayan and Clements, 1989). This is reflected by recovery failure in HIV infected individuals. Individuals infected with HIV-2 often undergo a longer period of clinical latency and progress more slowly to AIDS. This is represented by a reduced viral load during asymptomatic stages of infection (Chen, Z. *et al.*, 1997). Consequently, the rate of mortality for HIV-2 infected patients is only 1/3 of the rate for HIV-1 (Reeves and Doms, 2002). Additionally, not all HIV-2 infections progress to AIDS (Poulsen *et al.*, 1997). However, once the onset of AIDS occurs, viral load, disease progression and the outcome of HIV-1/2 infection are comparable (Reeves and Doms, 2002).

During a HIV infection around 10^9 $CD4^+$ T-cells are destroyed and replenished daily. This puts a substantial strain on the host immune system to compensate for the huge $CD4^+$ T-cell turnover. Following such a long period of intense cell turnover and replacement, the body's ability to mount an immune response is strained and slowly eroded (Coffin, J.M., 1995). Eventually, persistent T-cell activation depletes the reserves of naïve and memory $CD4^+$ T-cell pools such that the the number of $CD4^+$ T-cells in the host steadily decline [blue line, figure 4] (Brenchley *et al.*, 2006). The regenerative capacity of the host immune response cannot continue indefinitely and immune reserves can no longer compensate for the mass destruction of $CD4^+$ T-cells (Ho *et al.*, 1995). It is this slow, continual erosion, rather than a pinnacle event, which results in the inevitable collapse of the immune system. Failure to mount an appropriate immune response coincides with a peak in viremia [red line, figure 4]; opportunistic infections persist and an accumulation of infections and disease syndromes indicative of

immunodeficiency are recognisable. Thus the clinical features of AIDS commence.

1.2.4.3 Symptomatic infection and AIDS

Human immunodeficiency virus causes a chronic and progressive disease culminating in the onset of clinical AIDS, cachexia (wasting) and, ultimately, death (Narayan and Clements, 1989). The progression of an HIV infection is measured by monitoring both the patient's viral load and $CD4^+$ T-cell count. AIDS is defined as a $CD4^+$ T-cell count of less than 200 cells/µl (Forsman and Weiss, 2008).

Clinical features such as weight loss are the most overt sign of HIV infection. HIV infection of cells in the central nervous system may result in dementia, seen in some AIDS patients. HIV can infect microglial cells and infiltration of the brain can occur via infected macrophages (Forsman and Weiss, 2008). AIDS deaths usually result from opportunistic infection due to a compromised immune system. Both virus infection and treatment, particularly with immunosuppressive anti-viral drugs for transplant patients, weaken host immunity such that candida, CMV (cytomegalovirus), pneumocystis, and tuberculosis infection are common amongst AIDS sufferers (Forsman and Weiss, 2008). Abnormal cellular proliferation is often seen in AIDS patients and oncogenic diseases such as cervical carcinoma, Kaposi's sarcoma and non-Hodgkin's lymphoma can result from re-emerging infection caused by resident viruses which are no longer under the control of the host immune system (Forsman and Weiss, 2008).

1.2.5 AIDS Therapy

Resolving the HIV epidemic is hindered by the lack of an adequate vaccine or effective therapeutic interventions. However, reducing the risk of transmission can be achieved through measures such as screening blood donors, practising safe sex and testing for HIV. Infectious particles can be inactivated by detergents which disrupt the viral lipid envelope, preventing fusion with host cells (WHO, 2009). Therefore, simple precautions and education on transmission prevention may extend a long way towards reducing the global impact of HIV.

The use of highly active antiretroviral therapy (HAART) is effective at prolonging the longevity of HIV infected individuals although the effectiveness of this treatment is challenged by the development of resistance to antiviral drugs (Bousquet *et al.*, 2008; Venkat *et al.*, 2008). The best prospect for combating HIV, therefore, lies in research and education. Further understanding of the way in which HIV replicates will provide better information about how this virus functions, thus enhancing the prospect of producing a therapeutic remedy or vaccine to combat HIV.

1.2.5.1 AIDS therapy: vaccination

At present, there is no vaccine offering total protection against HIV infection. Likewise, knowledge of both host and viral factors conferring protection against HIV infection and disease is currently lacking. Infection with HIV-2 does not confer protection from infection with HIV-1 (de Silva *et al.*, 2008). HIV-2 infection cannot thus be viewed as a mechanism of protecting against infection with the more rapidly progressing HIV-1 virus. However, vaccines designed against the HIV-2 virus may provide a proof of concept for HIV-1 vaccine development (de Silva *et al.*, 2008). The provision of considerable resources and funding to develop either prophylactic or therapeutic vaccines demonstrates the magnitude of the global HIV burden and the importance of therapeutic developments to ease this burden.

Primary strategies for combating the virus focus on preventing viral-mediated destruction of immune cells, rather than enhancing lymphocyte regeneration. However, visna-maedi, like HIV, is a lentivirus which causes chronic pulmonary disease (maedi) and brain disease (visna) in sheep. Infection progression with visna-maedi virus is similar to that observed during AIDS; most notably disease of the central nervous system and wasting syndromes. However, the visna-maedi virus only infects dendritic cells and macrophages. It is likely that $CD4^+$ T-lymphocyte infection by HIV is an additional emergence through adaption to CD4 receptor usage. Therefore, it is unknown whether combating immunodeficiency caused by $CD4^+$ T-cell depletion will prove sufficient to halt the progression of HIV infection to AIDS (Forsman and Weiss, 2008).

Irrespective of the prospects of curing AIDS, current progress in slowing the process which links HIV infection to AIDS has provided significant benefit to patients (Ho *et al.*, 1995). Likewise, the related social and economic benefits of a prolonged life for HIV sufferers in countries where HIV is endemic are irrefutable.

There are several routes for potential vaccine therapy. In an ideal situation, a HIV vaccine would induce sterilizing immunity, conferring complete protection against HIV infection and thus halting transmission. As an alternative, HIV vaccination could promote transient infection, whereby infection occurs but the host immune system, as a result of vaccination, is equipped to deal with the infection and remove it. Vaccination could, alternatively, permit control of long-term infection resulting in undetectable HIV levels, no harmful decline of $CD4^+$ T-cells and a reduced transmission rate. Despite some failures, several vaccine candidates look promising. The GeoVax HIV-1 vaccine (http://www.geovax.com) targeting HIV-1 subtypes A, B and C (group M) has been shown to induce a strong cellular and humoral immune response in primates and is, therefore, currently undergoing stage II clinical trials to assess its suitability for use as a human vaccine. Additionally, the RV 144 vaccine, developed by Sanofi Pasteur (http://www.sanofipasteur.com), has shown promising results in phase III clinical trials in Thailand, lowering the rate of HIV infection by 31.2% compared to a placebo control (Rerks-Ngarm *et al.*, 2009). This priming ALVAC® HIV and boosting AIDSVAX® B/E combination vaccine provides the first evidence that a HIV vaccine is feasible. Further developmental work is ongoing before this product will be suitable for licensing and global use (Ledford, 2008).

1.2.5.2 AIDS therapy: drug development

Despite vaccine difficulties, the last 25 years have seen enormous progress in the treatment of HIV. Whereas HIV was once thought to be an essentially untreatable retroviral disease, it is now recognised that HIV is susceptible to several antiviral agents. HIV patients have witnessed a reduction in the death rate associated with infection and, additionally, both an enhanced quality and

length of life attributed to long-term management of the virus via antiretroviral therapy (Broder, 2010).

25 therapeutic agents are now available for the treatment of HIV (de Béthune, 2010) [table 1]. These are predominantly orally administered. Currently, antiretroviral drugs mainly target enzymatic products of the HIV *pol* gene: RT (Reverse transcriptase), IN (Integrase) and PR (Protease) (Broder, 2010).

Drug class	#
Protease inhibitor [PI]	10
Nucleoside (nucleotide) RT inhibitor [N(t)RTI]	8
Non-nucleoside RT inhibitor [NNRTI]	4
Integrase inhibitor	1
Fusion inhibitor	1
CCR5 inhibitor	1

Table 1: The number of HIV drugs in each class approved for use by HIV patients. HAART therapy recommends combining several classes of drugs from the 25 therapeutic agents currently available (de Béthune, 2010).

Two main classes of HIV drug target the viral RT; nucleoside/nucleotide reverse transcriptase inhibitors (NRTIs/N(t)RTIs) and non-nucleoside reverse transcriptase inhibitors (NNRTIs) (Haubrich *et al.*, 2008). The first HIV antiretroviral agent, Zidovudine (3-azido-2-3-dideoxythymidine, AZT), was a nucleoside reverse transcriptase inhibitor (NRTI) approved for use in 1987 (de Béthune, 2010). NRTIs inhibit the reverse transcription step of HIV replication: copying viral single-stranded RNA (ssRNA) into double-stranded DNA (dsDNA) prior to integration. NRTIs are functional analogues of deoxynucleotides lacking a 3' OH group. They competitively inhibit DNA synthesis by incorporating into the nascent DNA and, instead of extending the DNA chain by formation of a phosphodiester bond, inducing chain termination. Combination therapy still uses AZT and other NRTIs such as didanosine (Broder, 2010). Alternatively, NNRTIs directly block virally encoded RT by binding to an allosteric site on RT and disrupting catalytic activity (Haubrich *et al.*, 2008).

It is recommended that HIV is treated with a combination of three antiretroviral drugs. This is called highly active antiretroviral therapy (HAART) (Daugas *et al.*, 2005). Drug treatment regimes typically include treatment with two NRTIs and either a PI (Protease inhibitor) or an NNRTI [table 2] (Haubrich *et al.*, 2008).

Drug Target	Brand	Generic Names	Manufacturer	Date
Nucleoside Reverse Transcriptase Inhibitors (NRTIs)	Retrovir	Zidovudine, azidothymidine, AZT, ZDV	GSK	1987
	Epivir	Lamivudine, 3TC	GSK	1995
	Epzicom	Abacavir, lamivudine	GSK	2004
Non-Nucleoside Reverse Transcriptase Inhibitors (NNRTIs)	Viramune	Nevirapine, NVP	Boehringer Ingelheim	1996
	Intelence	Etravirine	Tibotec Therapeutics	2008
Protease Inhibitors (PIs)	Invirase	Saquinavir mesylate, SQV	Hoffman-La Roche	1995
	Crixivan	Indinavir, IDV	Merck	1996
	Prezista	Darunavir	Tibotec, Inc.	2006
Fusion Inhibitors	Fuzeon	Enfuvirtide, T-20	Hoffman-La Roche & Trimeris	2003
Entry Inhibitors (CCR5 antagonists)	Selzentry	Maraviroc	Pfizer	2007
HIV Integrase Strand Transfer Inhibitors	Isentress	Raltegravir	Merck & Co.	2007
Multi-class Combination Products	Atripla	Efavirenz, emtricitabine, tenofovir disoproxil fumarate	Bristol-Myers Squibb & Gilead Sciences	2006

Table 2: Some of the HIV-1 antiretroviral products used in single or combination therapy (Broder, 2010).

HAART results in a reduction in viral load. Secondary benefits of HAART include a reduction in HIV transmission associated with a lower viral load (Montaner *et al.*, 2010). Therapy has been shown to have an astonishing effect on patients such as reversing neurological symptoms and brain abnormalities. Drastic improvements in patient focus, memory and coordination have also been observed (Broder, 2010). It is now projected that, with appropriate therapy, a person infected with HIV at the age of 20

may live to 60 years or more, unless they develop resistance to multiple drugs (The Antiretroviral Therapy Cohort Collaboration, 2008).

1.2.5.3 AIDS therapy: drug resistance

HIV demonstrates a spectacular capacity to adapt to antiretroviral therapy; wild-type HIV strains are rapidly replaced by drug-resistant strains within 14-28 days (Wei *et al.*, 1995). Treatment with antiretroviral drugs results in an increase in circulating CD4+ T-cells. However, a rising level of mutant genomes and a decline in drug susceptibility coincide with a decrease in CD4+ T-cells back to pre-therapy levels (Coffin, J.M., 1995). The number of replicative cycles occuring within an HIV infected individual is extraordinarily high and presents a unique feature of HIV infection (Coffin, J.M., 1995). Furthermore, the virus exhibits an unusually high rate of mutation. Each HIV nucleotide exhibits a mutation rate of between 10^{-4}-10^{-5} per replication cycle. Subsequently, during infection, a single position within the HIV genome is subject to 10^{4}-10^{5} point mutations per day (Coffin, J.M., 1995; Perelson *et al.*, 1996). Consequently, both of these features give rise to a large amount of genetic variation. Whilst most mutations may prove deleterious to the virus, or have little effect on inducing protection to antiviral therapy, only one escape mutant is necessary to promote resistant viral replication and thereby confer drug resistance (Coffin, J.M., 1995). HIV mutants existing in numerous combinations present a pre-existing barrier to antiviral therapy and it is likely that the presence of mutants in an HIV infected individual predate the introduction of antiretroviral drugs and emerge once treatment is initiated (Coffin, J.M., 1995).

Early treatment to block viral replication is therefore important in order to avoid the establishment of a reservoir of HIV mutants with the capacity for drug resistance (Coffin, J.M., 1995). However, it is often difficult to intervene immediately after exposure to HIV as the generic nature or lack of early stage symptoms often prevents easy recognition of the virus. However, hope remains as HIV mutants, albeit resistant to therapeutic interventions, are likely to be more defective at replicating than wild type virus. Therefore any mutations upheld within the emerging virus population are likely to be

detrimental to its infective capacity. Subsequently, it may be that the most effective compounds to treat HIV are not those which directly target the wild type virus, but instead, those therapies which cause the only escape mutants emerging to be severely crippled in function (Coffin, J.M., 1995). In the case of the HIV virus, effective treatment cannot result from antiviral agents which are overcome by resistance resulting from a single point mutation. Rather, effective therapy must elude viral resistance by necessitating multiple, simultaneous viral mutations (Perelson *et al.*, 1996). The concurrent use of numerous antiviral agents against multiple HIV targets thus presents the contemporary approach to regulating HIV infection.

Currently, mutants showing resistance to all therapeutic compounds have been identified and are thus now deemed to be an inevitable artefact of antiretroviral therapy (Coffin, J.M., 1995). The wild type HIV-2 virus has demonstrated resistance to Selzentry: currently the only entry inhibitor available. However, HIV-2 still shows susceptibility to newly developed Integrase inhibitors (de Silva *et al.*, 2008). Likewise, Etravirine (an NNRTI) is a promising drug candidate to control HIV infection as it presents a difficult genetic challenge for the development of virus resistance [figure 5] (Broder, 2010). Trials are also currently underway to investigate whether drugs can be administered as a pre-exposure prophylaxis (PrEP) (Broder, 2010).

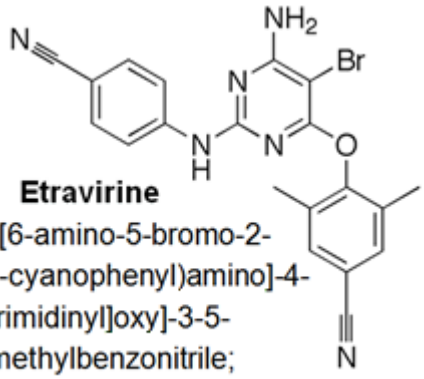

Figure 5: Etravirine: presenting a high genetic barrier for the emergence of resistant HIV strains [http://www.ask.com/wiki/Etravirine].

The challenges remaining in combating HIV are numerous and varied. In the long term, eradicating HIV may prove difficult due to the presence of HIV reservoirs. These include; latently infected memory T-cells, where the virus remains inactive and non-productive; chronically producing cells, which have

an extended life-span and therefore release virus for long periods of time; and cells infected with defective provirus, which are not recognised by the immune system as they do not produce either active virus or viral components eliciting an immune response. HIV reservoirs not only facilitate evasion of the immune response, they also provide a source of former viral genotypes allowing infection to persevere in spite of antiviral interventions (Coffin, J.M., 1995). Integrated provirus may remain latent and re-emerge to cause infection when treatment is interrupted or discontinued. A better understanding of viral latency and the mechanisms by which it is established and maintained will be required before the lifelong treatment of HIV patients is no longer a necessity (Marcello, 2006).

Administering effective therapy is also hindered in developing countries by obstacles such as high prevalence, lack of access to drugs, cost, sustainability and poor infrastructure (Broder, 2010). The need for life-long therapy, drug associated toxicity and the inadvertent side-effects of treatment also generate a complex situation for HIV sufferers. Additionally, factors such as; high viral genetic variation, the emergence of drug resistance and the potential for new cross-species events to facilitate the transmission of viruses from previously unrecognised retroviral reservoirs into humans, all pose a threat to the future control and containment of HIV. These challenges will all have to be addressed before the control and potential eradication of HIV are a possibility.

1.3 The HIV life cycle

1.3.1 The viral particle

HIV particles are predominantly spherical in shape, with a distinctive cone-shaped core [figure 6b]. Although the diameter of each virus particle can vary from 106-183 nm, the overall structures are analogous (Briggs *et al.*, 2006). The particle core is comprised of 1000-1500 Capsid proteins assembled into a hexameric lattice (Chen, J. *et al.*, 2008). It encloses two copies of the RNA viral genome bound to Nucleocapsid proteins in a ribonucleoprotein complex, and viral enzymes Reverse transcriptase and Integrase [figure 6a] (Lever, 2005). Numerous cellular proteins such as APOBEC3G and Cyclophilin A are

also found within the viral core (Arhel, 2010). A lipid bilayer, underlined by a shell of Matrix proteins, surrounds the core and the viral Protease enzymes (Cannon *et al.*, 1997). The lipid bilayer encompasses transmembrane envelope proteins which anchor the exterior surface envelope proteins (Kwong *et al.*, 1998; Sleasman and Goodenow, 2003). The complete viral particle comprises 35% lipid, 65% protein and 1-2% RNA (Coffin, J.M. *et al.*, 1997).

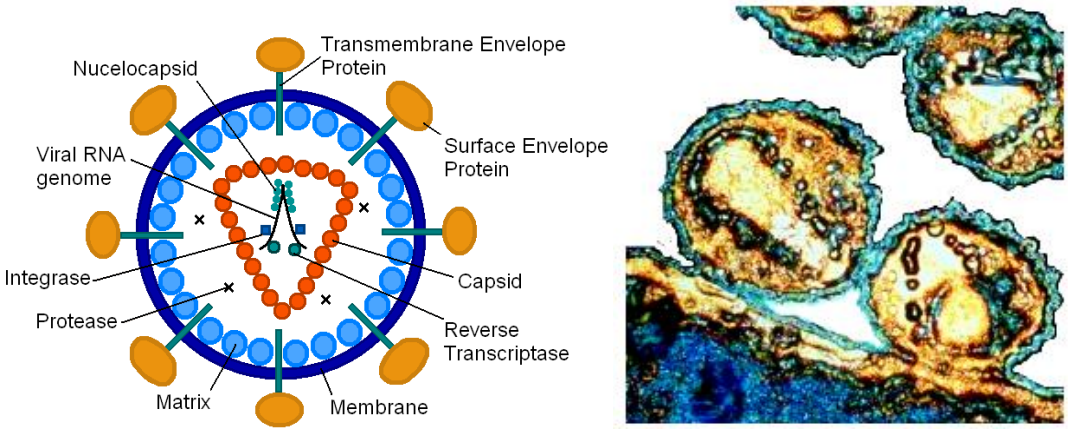

(A) **(B)**

Figure 6: Retrovirus particle showing assembled Gag proteins (Matrix, Capsid and Nucleocapsid), Pol enzymes (Reverse transcriptase, Integrase and Protease) and Env proteins (transmembrane and surface Envelope) (A) [adapted from (Freed, 2001)]. A transmission electron micrograph of HIV (B) [http://www.profimedia.si/picture/aids-virus-tem/0041375286/].

1.3.2 The HIV genome and viral proteins

The HIV positive-sense, ssRNA genome is roughly 9.3kb in length, has a 5' cap and 3' polyadenylation, and exists as a non-covalent dimer (Jacob and DeStefano, 2008). A total of 15 viral proteins are encoded by nine open reading frames within the virus genome (Briggs *et al.*, 2006). There are three principal open reading frames; '*gag'* encoding structural proteins Matrix (MA), Capsid (CA) and Nucleocapsid (NC) and smaller peptides: Sp1, Sp2, p6; '*env'* encoding Envelope proteins (TM and SU); and '*pol'* encoding viral enzymes: Protease (PR), Integrase (IN) and Reverse transcriptase (RT) (Sleasman and Goodenow, 2003). Six smaller accessory genes; *nef, vpu, vpr, vif, tat* and *rev* (Lever, 2005) are also encoded by the HIV genome, which is flanked by long terminal repeats (LTRs) (Marcello *et al.*, 2004). The

viral 5' LTR contains an RNA packaging signal (ψ) and a *trans*-activation response (TAR) element (Lawrence *et al.*, 2003; Ricci *et al.*, 2008) [figure 7].

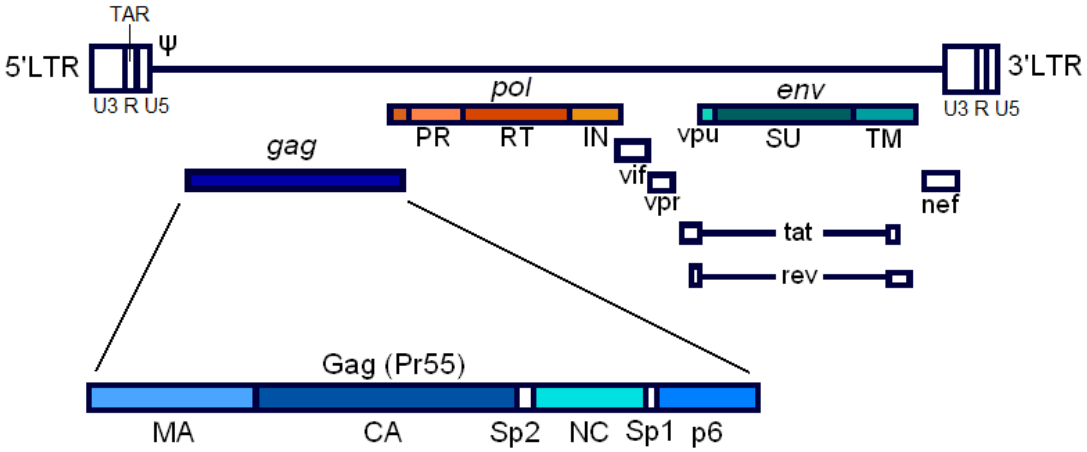

Figure 7: The HIV genome showing *gag*, *pol* and *env* open reading frames and smaller accessory genes; *vif, vpr, vpu, tat, rev* and *nef*. The structural proteins MA, CA and NC in addition to smaller peptides Sp1, Sp2 and p6 encoded by *gag* are also shown [adapted from (Freed, 2001)].

The HIV genome exhibits a high level of RNA structure (discussed further in Chapter 4) which plays a role in several stages of the virus life cycle such as initiating reverse transcription, altering reading frame usage, modulating RNA export from the nucleus, dimerization of the genome and viral packaging. Protein activity is also modulated by the structure of HIV RNA. Protein junctions are encoded by regions of highly-structured RNA which cause the ribosome to slow or pause during elongation. This provides time for the nascent protein to fold as it is translated; thus the RNA structure also provides a means of managing protein expression. Additionally, there are a large number of interactions between the HIV genome and both host and viral proteins (discussed further in Chapter 5) which serve to regulate viral gene expression (Watts *et al.*, 2009).

1.3.3 Binding/entry

The start of the HIV life cycle is marked by binding of virus particles to target cells [figure 8].

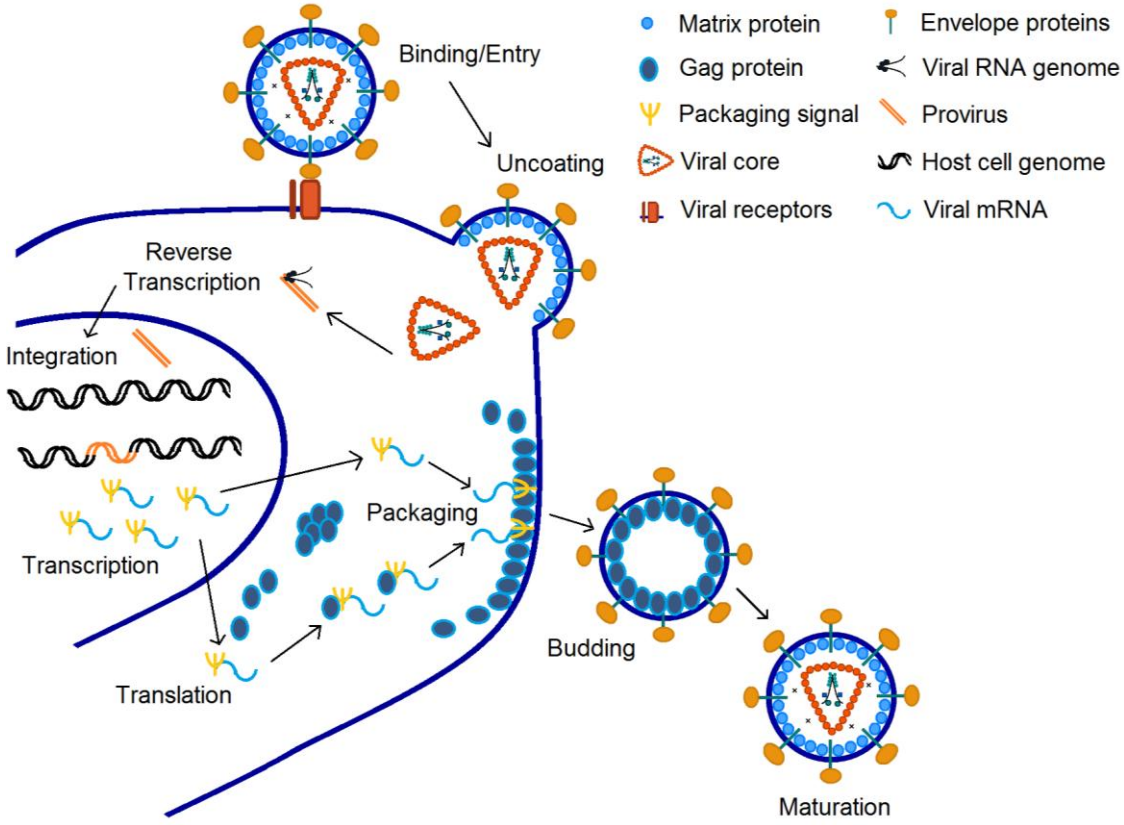

Figure 8: The HIV replication cycle showing stages of the viral life cycle from binding, fusion, proviral integration, transcription, translation, assembly and budding through to maturation.

Multiple viral and cellular protein interactions occur during the stages of binding and entry. Binding is initiated by the two Env glycoproteins: gp120 (surface subunit, SU) and gp41 (transmembrane subunit, TM) which bind to each other non-covalently, and form a trimeric spike structure on the surface of virions (Chan and Kim, 1998). Gp120 binds to the primary HIV receptor CD4 (a co-receptor of MHC II) present on the surface of target cells such as T-cells or macrophages (Chan and Kim, 1998). The CD4 receptor consists of four immunoglobulin-like domains; HIV gp120 binds to the amino-terminal domain (Kwong *et al.*, 1998). Enhanced binding is provided by viral co-receptors: the chemokine receptors CXCR4 and CCR5 [figure 9] (Sleasman and Goodenow, 2003).

Binding of the Env surface subunit induces a conformational change in the shape of gp120/gp41 revealing a highly conserved fusion peptide at the N-terminus ectodomain of gp41. The fusion peptide adopts an extended

conformation and elicits fusion by inserting into the host cell lipid bilayer (Chan and Kim, 1998). Folding of the N-terminus ectodomain into a bundle of six helices brings the virus and host membranes into alignment (Freed, 2001). Subsequent fusion occurs with the viral membrane merging with the target cell membrane. The contents of the viral particle are consequently exposed, resulting in the release of the viral core into the cell cytoplasm.

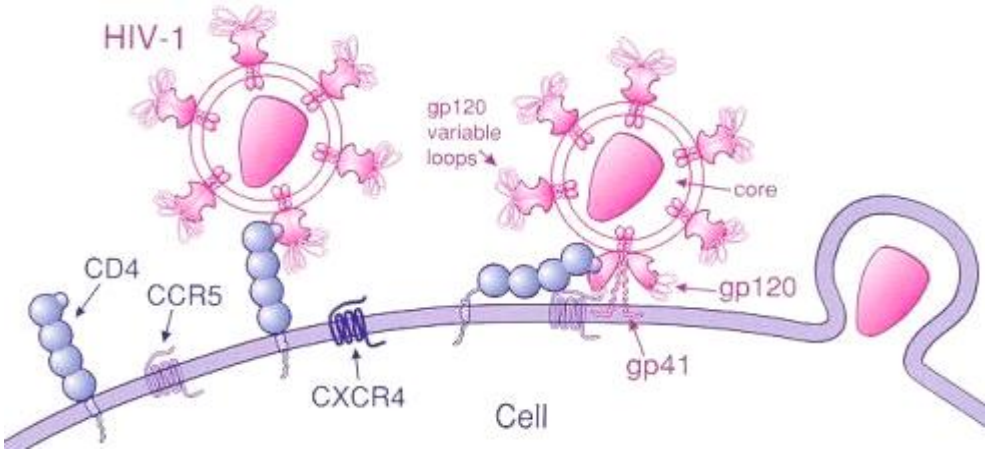

Figure 9: Binding of HIV to host cells is mediated by the viral gp120 receptor interacting with CD4 on the surface of target cells. Viral co-receptors CCR5 and CXCR4 enhance virus binding. Fusion with the host cell is promoted by an extended conformation of the fusion peptide within the viral envelope. Following fusion, the viral core is released into the host cell cytoplasm [Image: https://dokuwiki.noctrl.edu/doku.php?id=bio:440:hiv_-_group_1#retrovirus_replication].

1.3.4 Uncoating

Following entry, the viral core is uncoated by disassembly of Capsid proteins. Little is known about the mechanism of uncoating, although there is evidence to suggest that this stage is cell-cycle dependent. In particular, cellular factors activated during the G_0-G_1 transition of the cell cycle have been shown to be specifically required for uncoating (Auewarakul *et al.*, 2005). Likewise, the exact cellular location of uncoating remains contentious; it is believed that this event occurs post-entry to the cytoplasm but pre-nuclear import. Viral uncoating may be promoted by the change in environment experienced by viral cores released into the cell cytoplasm. Alternatively, the loss of high concentrations of loose Capsid proteins, which are present in the viral particle and contribute to core stability, may trigger uncoating. Timing is

an essential feature of viral uncoating; HIV particles which undergo premature core disassembly cannot undertake reverse transcription. Likewise virus particles containing Capsid mutants with enhanced or diminished stability show compromised infectivity. This indicates that both the stability of the HIV core and the timing of uncoating are important during the early stages of infection (Arhel, 2010). Uncoating of the viral core releases a reverse transcription complex (RTC) consisting of Nucleocapsid proteins, Integrase and Reverse transcriptase enzymes, and the accessory protein Vpr (Arhel, 2010; Freed, 2001).The nucleoprotein RTC promotes reverse transcription of the viral positive-sense ssRNA genome into dsDNA.

1.3.5 Reverse transcription

HIV genomic RNA is reverse transcribed into dsDNA; a defining characteristic of retroviral infection (Lever, 2005). Viral Reverse transcriptase is an RNA- and DNA-dependent polymerase which catalyses this process (Isel *et al.*, 2010). HIV RT is a heterodimer composed of two similar subunits; p51 (51 kDa) and p66 (66 kDa). HIV Protease removes a 15 kDa (RNaseH) domain from p66 to produce p51 [figure 10]. Although the two RT subunits are similar in terms of protein content, the conformations they assume are very different (Freed, 2001).

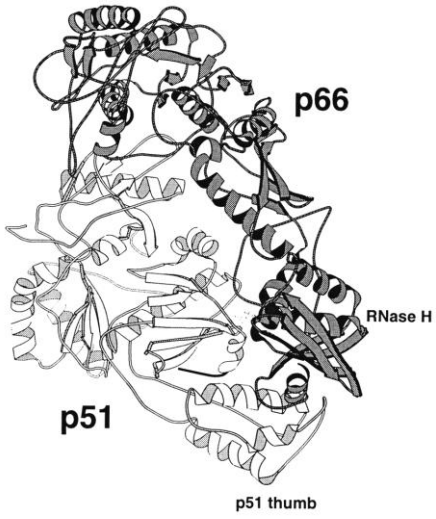

Figure 10: Structure of the HIV Reverse transcriptase heterodimer showing subunits p51 and p66 (including RNaseH) (Cameron *et al.*, 1997).

Retroviruses are unique in that the virus particles contain diploid genomes. This allows recombination events to feature as part of viral replication. During a process termed copy choice, the RT enzyme is able to switch between the

two HIV genomic RNA templates. Genetic recombination may thus result if the two genomic sequences are divergent (Ramirez *et al.*, 2008). Moreover, the high error rate of HIV RT contributes to mutations which enhance the genetic variability of HIV virions (Mansky and Temin, 1995).

The process of reverse transcription is a multi-step process including two strand transfer events and several stages of RNaseH digestion [figure 11].

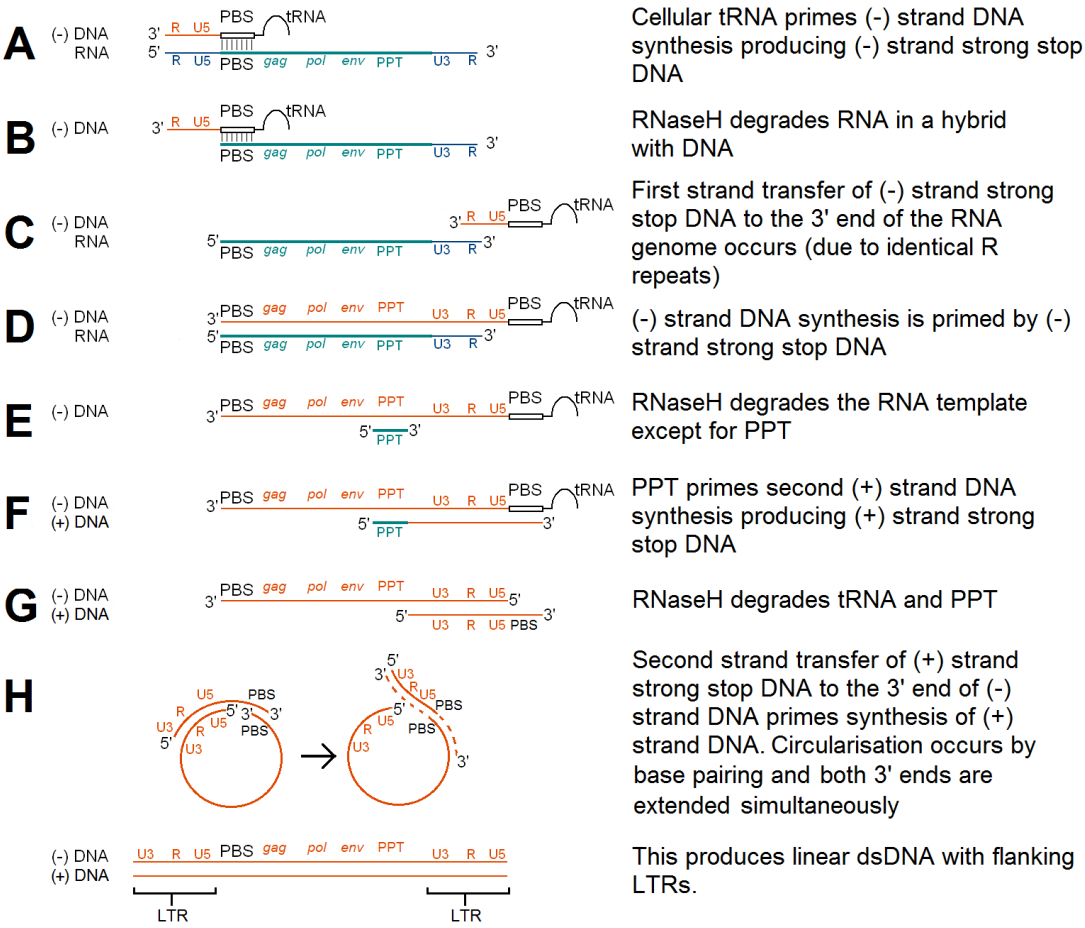

Figure 11: Reverse transcription of HIV genomic ssRNA to produce dsDNA [Adapted from (Sarafianos *et al.*, 2001)].

Reverse transcription is initiated by priming of the 5' end of the HIV RNA with cellular $tRNA_{Lys}$, which is packaged into virions [figure 11A] (Isel *et al.*, 2010). Initiation takes place at a location within the HIV 5' UTR called the primer binding site (PBS). 5' to 3' DNA synthesis produces a hybrid of viral RNA and newly synthesised DNA. RNaseH digests most of the RNA component of the RNA-DNA hybrid [figure 11B]. A section of DNA, complementary to the viral genome, remains and is referred to as minus (-) strand strong stop DNA

(Freed, 2001). First strand transfer of (-) strand strong stop DNA from the 5' R region to the 3' R region of genomic RNA occurs [figure 11C]. This is permitted by template homology (Basu *et al.*, 2008). Subsequent (-) strand DNA synthesis, primed by (-) strand strong stop DNA, occurs in a 3'-5' direction along the RNA template [figure 11D]. Following (-) strand synthesis, RNaseH degrades the RNA template. A small section of 3' RNA within the polypurine tract (PPT) is resistant to RNaseH digestion [figure 11E]. This 3' PPT RNA segment is able to prime synthesis of a plus (+) DNA strand using the (-) DNA strand as a template (Ramirez *et al.*, 2008; Suzuki and Craigie, 2007). HIV-1 has another, centrally located PPT (cPPT) region which acts as an additional primer of (+) strand DNA (Basu *et al.*, 2008). (+) strand synthesis from the 3' PPT to the 5' end of (-) strand DNA produces (+) strand strong stop DNA [figure 11F], which undergoes second strand transfer to the 3' end of (-) strand DNA using homologous PBS regions. During this process, further degradation by RNaseH removes $tRNA_{Lys}$ and PPT [figure 11G]. Second strand transfer of (+) strand strong stop DNA to the 3' end of (-) strand DNA primes second strand synthesis of (+) strand DNA [figure 11H]. Due to the complementarity of the DNA ends, circularisation occurs and DNA synthesis extends the 3' ends to produce dsDNA flanked by long terminal repeats (LTRs) (Basu *et al.*, 2008). As the central DNA synthesis termination site (CTS) is positioned 100 nucleotides 3' of the cPPT, an excess of (+) strand DNA is produced. This central section of DNA is important for transport of dsDNA to the nucleus (Freed, 2001). The reverse transcription of genomic ssRNA, and subsequent integration of viral dsDNA into the host cell chromosome, is a defining feature of retroviral replication.

1.3.6 Nuclear targeting/integration

Following synthesis of full-length dsDNA (now termed proviral DNA) a pre-integration complex (PIC) is formed (Arhel, 2010). The PIC functions to target proviral DNA to the nucleus and facilitate its integration into the host cell genome. Both cellular and viral factors contribute to PIC formation (Miller *et al.*, 1997; Popov *et al.*, 1998). Specific sequences within the cPPT region of viral DNA are involved in nuclear import through binding to Integrase proteins within the PIC (Schröder *et al.*, 2002). Viral proteins Vpr and MA contribute to

PIC formation whilst RT has also been shown to co-localize to the PIC [figure 12] (Miller *et al.*, 1997). The mechanism by which the PIC migrates to the nucleus remains unclear, although it has been shown that the Vpr protein contains a nuclear localisation signal (NLS) which may aid this transport (Fouchier *et al.*, 1998).

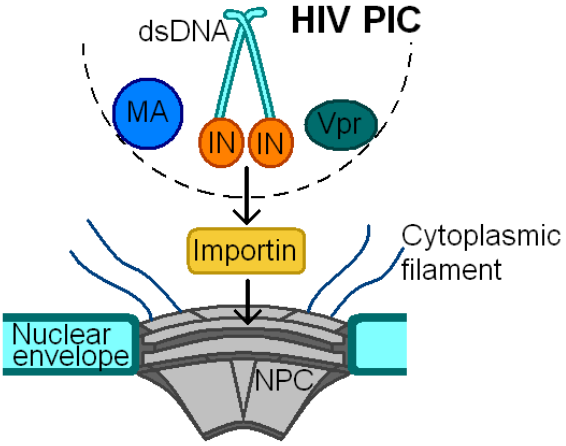

Figure 12: The HIV pre-integration complex (PIC), composed of Matrix (MA), Vpr, Integrase (IN) and the central polypurine tract (cPPT) region of viral DNA, assists transport of dsDNA through the nuclear pore complex (NPC). The importin pathway is implicated in transport of the PIC from the cytoplasm to the nucleus [Adapted from (Suzuki and Craigie, 2007)].

Once in the nucleus, proviral dsDNA is integrated into host DNA; viral Integrase plays a key role in this process. Two activities are catalysed by Integrase; the 3' processing of viral DNA and DNA strand transfer (integration) (Savarino, 2007). During the first stage of integration, Integrase catalyses the removal of two nucleotides from the 3' end of each provirus DNA strand (Craigie, 2001; Shun *et al.*, 2007). Terminal nucleotide cleavage exposes 3' hydroxyl groups at each end of the viral DNA (Miller *et al.*, 1997). 3' processing of viral DNA can take place soon after reverse transcription and before nuclear entry, when Integrase binds to both ends of newly transcribed DNA as part of the PIC (Savarino, 2007; Shun *et al.*, 2007).

After nuclear entry, the second stage of integration, termed DNA strand transfer, involves insertion of the viral DNA strand into host DNA [figure 13] (Craigie, 2001). Integrase cuts the host cell genome producing staggered ends 5 base pairs apart on the target DNA (Craigie, 2001; Shun *et al.*, 2007).

The 3’ OH provirus ends form phosphodiester bonds with the exposed 5’ phosphates of the cut host DNA (Shun *et al.*, 2007). During a repair process, likely undertaken by cellular repair enzymes, the two unpaired nucleotides at each end of the proviral DNA are removed, the five nucleotide gap adjoining each proviral DNA/host DNA junction is filled and ligation of the provirus into the target DNA is achieved (Savarino, 2007). The nuclear protein LEDGF/p75 regulates the activity of viral Integrase by tethering it to chromatin and preventing its degradation. Reducing the Integrase binding capacity of LEDGF/p75 inhibits viral replication (Poeschla, 2008).

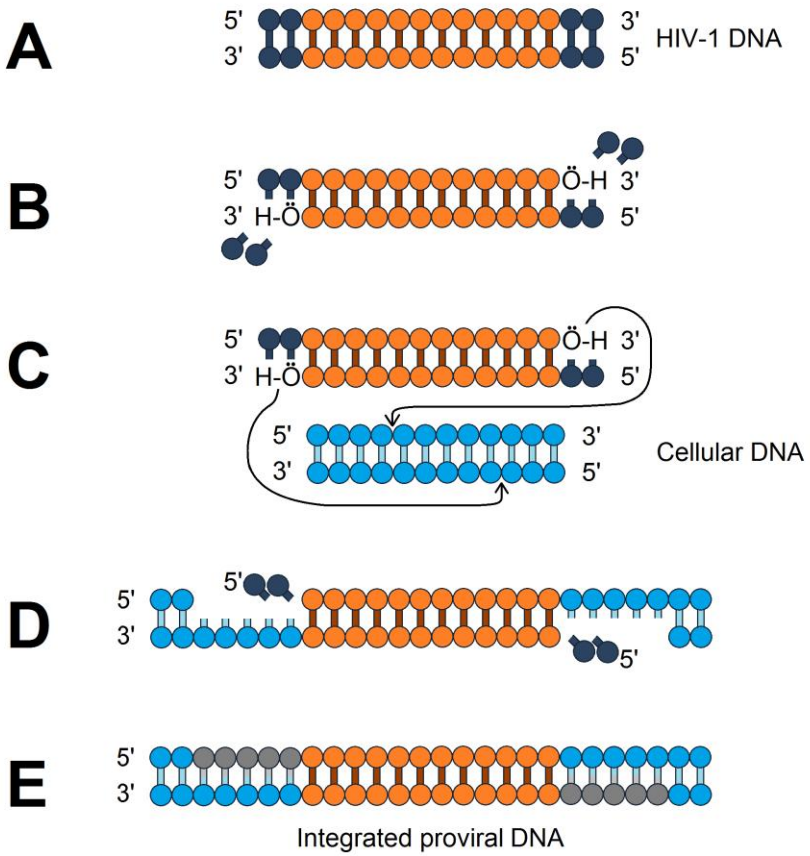

Figure 13: HIV integration of dsDNA provirus (A). During the first stage of integration, 3’ processing of viral DNA occurs via viral integrase (B). Strand transfer is catalysed by viral Integrase to integrate proviral DNA into the host chromosome (C). DNA repair is undertaken by cellular enzymes to remove unpaired nucleotides (D), fill in nucleotide gaps and complete ligation of provirus into the host genome (E). [Adapted from (Savarino, 2007)].

There is little specificity as to the site of provirus integration which can, essentially, occur at any location within the host chromosome. However,

evidence suggests that integration may be favoured at gene-rich areas within target DNA and, in particular, at the site of actively transcribing genes (Lever, 2005; Mitchell *et al.*, 2004; Schröder *et al.*, 2002). Retroviral vectors capable of inserting genes directly into the host genome of target cells are potentially a powerful tool for therapeutic intervention. However, retroviral integrations near transcriptional start sites can disrupt or enhance the normal levels of cellular transcription. This may lead to oncogenesis and thus poses a barrier to the success of retroviral gene therapy (Ambrosi *et al.*, 2008).

1.3.7 Dormancy and reactivation

The human genome contains evidence of ancient integration events and a substantial proportion of the human genome consists of endogenous retroviruses or retroviral elements. This characteristic of retroviruses contributes to the dormancy evidenced in HIV infected patients. Following integration of the HIV provirus, the virus may remain dormant within the cell until an activation event occurs.

Latency can result from integration into quiescent or non-dividing cells where transcription factors, needed to promote viral transcription, are at a low level (Mok and Lever, 2007). Dormant HIV provirus provides a viral reservoir, protected from clearance by the host immune response and immune to the effects of antiretroviral therapy. Thus latency presents a significant obstacle in curing HIV patients as seemingly virus-free individuals may relapse years later when undetected, latent virus is reactivated. The mechanism of HIV dormancy remains unclear, although the local environment and the site of provirus integration may be contributing factors (Mok and Lever, 2007). Recruitment of cellular proteins HDAC-1 (histone deacetylase type 1), HP1 (heterochromatin protein 1) and Suv39H1 (histone methyltransferase) to chromatin surrounding the HIV LTR can also promote latency (Blazkova *et al.*, 2009). Alternatively, methylation of DNA at cytosine-phosphate-guanine (CpG) sites within the HIV LTR has been shown to suppress HIV transcription and regulate reactivation (Blazkova *et al.*, 2009).

Reactivation of integrated viral genes can occur spontaneously, or activation may be triggered by chemical or physical stimuli (Leib-Mösch *et al.*, 1990).

Likewise, T-cell activation signals, cellular NFκB, proinflammatory cytokines and viral Tat can promote reactivation. The HIV-1 promoter within the LTR contains numerous binding sites for transcription factors such as NFκB. Thus a complex and diverse regulatory network may be involved in the activation of provirus transcription (Yang *et al.*, 2009). Blocking NFκB induction can prevent reactivation and, furthermore, silence LTR-driven transcription of HIV provirus (Blazkova *et al.*, 2009).

During activation, Tat also functions in a positive feedback loop [figure 14] to drive provirus transcription and establish stable transcription of viral genes. Tat may therefore be an evolutionary development designed to enhance the virus' ability to counteract gene silencing. Consequently, the timely alignment of several factors either promotes entry of the virus into latency or, alternatively, permits reactivation (Mok and Lever, 2007).

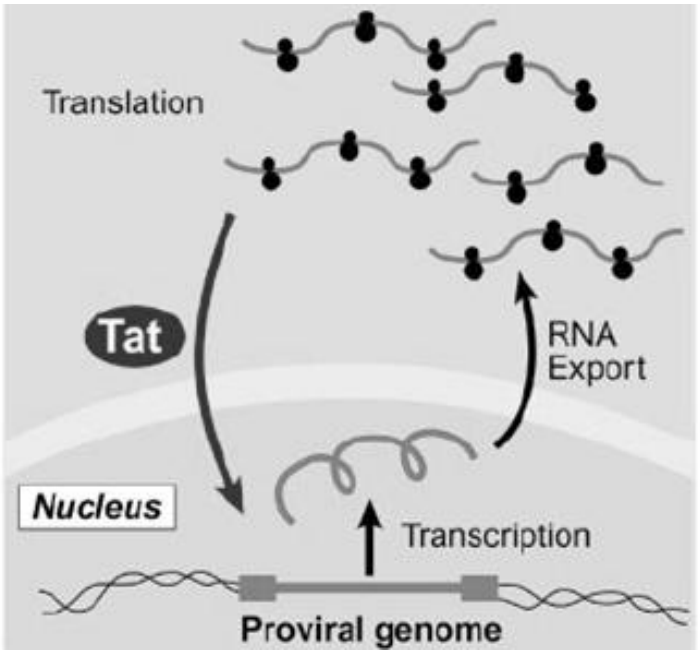

Figure 14: The Tat feedback loop: transcribed mRNA encoding Tat is exported to the cytoplasm; translated Tat shuttles back to the nucleus where it enhances viral transcription (Karn, 1999).

Irrespective of how latency is achieved and established, once integrated into the host genome the provirus is an established artefact of the host cell. In this

way, HIV hijacks the host cell and proviral genes utilise the same cellular transcription machinery as normal, cellular genes to produce viral mRNAs.

1.3.8 HIV Gene expression

1.3.8.1 HIV transcription

Transcription of proviral DNA occurs alongside cellular genes and therefore RNA polymerase II and the same host transcriptional machinery are required (Sleasman and Goodenow, 2003). The HIV LTR directs the production of viral mRNA by enhancing and promoting transcription (Mok and Lever, 2007). Alike to cellular mRNA, viral RNA is capped and polyadenylated (Watts *et al.*, 2009). The metabolic environment within the cell is influential to the rate of transcription as this process is reliant on cellular transcription factors; NFκB, NFAT, Sp1 and AP-1, which bind to the HIV LTR and regulate the activity of the HIV promoter (Wu, Y. and Marsh, 2003). T-cell activity is also promoted by these factors therefore activation of infected T-cells corresponds with the promotion of HIV transcription. HIV is unusual in that transcription may occur from both integrated and non-integrated DNA (Wu, Y. and Marsh, 2003).

Transcription of HIV RNA is inefficient in the absence of Tat. Tat is one of the earliest viral proteins to be expressed (see below) and localises to the nucleus to *trans*-activate viral transcription.

Spliced HIV-1 *env* mRNA is translated to produce Tat (*trans*-activator of transcription): a small 86-102 AA RNA-binding protein (Ponti *et al.*, 2008). Tat binds to the t*rans*-activation response (TAR) element at the 5' end of the viral RNA, and enhances the level of transcription and gene expression. Cells over-expressing TAR RNA are more resistant to HIV-1 replication through sequestering viral Tat (Svitkin, Y.V *et al.*, 1994).

Tat binds specifically to the U-rich bulge within TAR; mutations in this region abolish Tat-activated transcription (Braddock *et al.*, 1993). Cellular proteins, such as Tat-associated kinase (TAK) also bind to the TAR stem-loop (Coffin, J.M. *et al.*, 1997). TAK is composed of a kinase component called CDK9 and a cyclin component: CyclinT_1 [figure 15]. Conformational changes within Tat,

induced by CyclinT$_1$, stabilise and enhance Tat interactions with TAR. Mutations in the TAR apical loop inhibit Tat activity, even though this region is not involved in Tat binding. This suggests that binding of cellular co-factors, such as TAK, is essential for Tat activity (Braddock *et al.*, 1993).

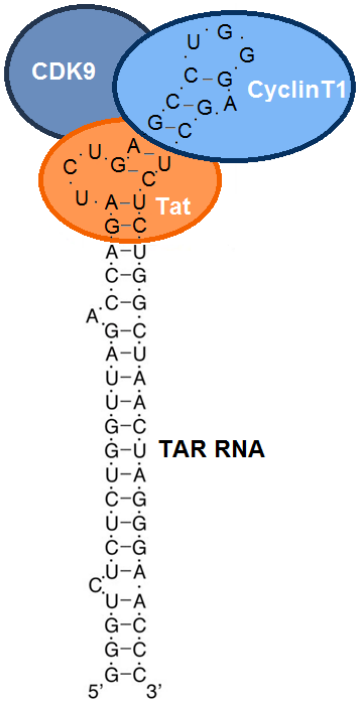

Figure 15: Recognition of HIV TAR RNA by viral Tat and TAK (CyclinT$_1$ and CDK9) [adapted from (Karn, 1999)].

During transcription initiation, the CDK7 kinase of initiation factor TFIIH activates RNA polymerase II by phosphorylating its carboxyl terminus domain (CTD). Tat stimulates additional phosphorylation via TAK; the protein kinase (CDK9) component of TAK hyper-phosphorylates the RNA polymerase II CTD [figure 16]. This enhances the activity of RNA polymerase II and allows efficient read through of RNA structure. Consequently, the presence of Tat effects more frequent RNA polymerase II binding to the HIV promoter and increased processivity. This results in an increased rate of transcription initiation and more efficient elongation. Furthermore, in the presence of Tat, a greater proportion of initiation events result in the production of full-length RNA. If Tat is absent, RNA polymerase frequently dissociates from template RNA resulting in truncated transcripts. Thus Tat imparts a significant contribution to HIV transcription (Karn, 1999).

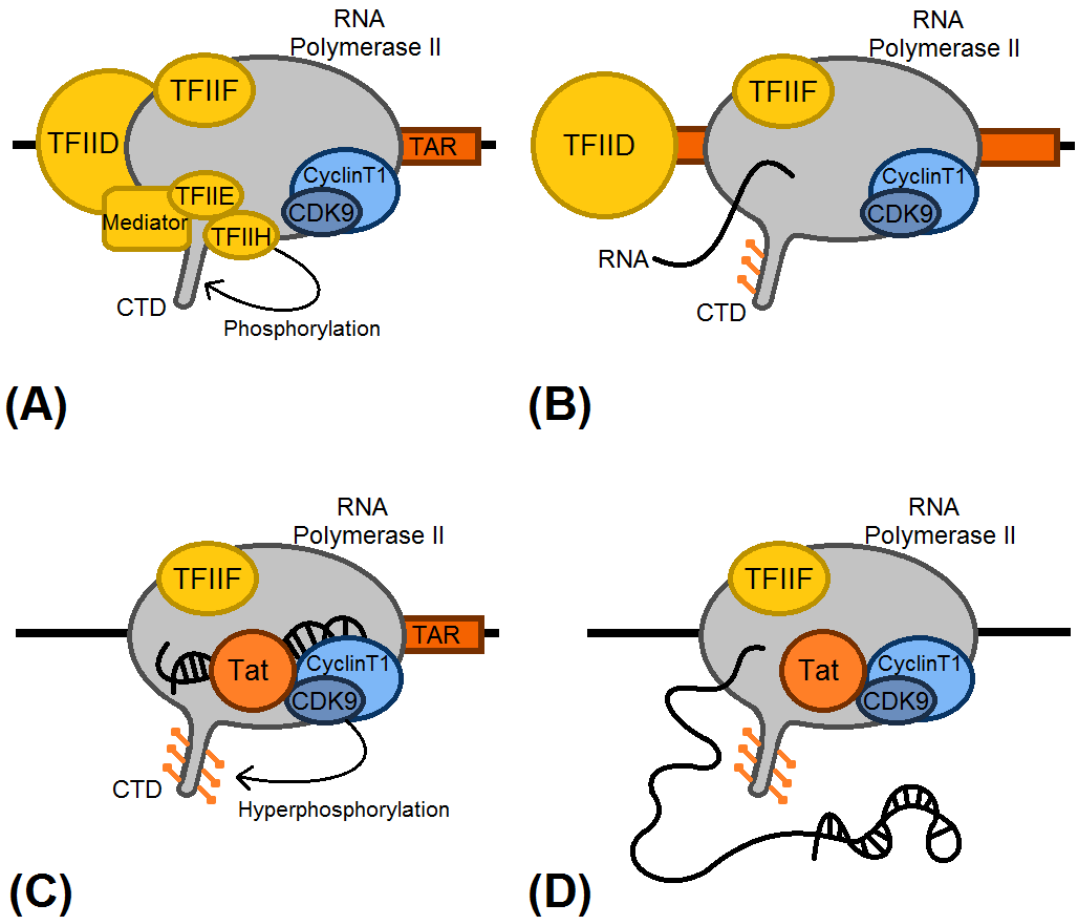

Figure 16: Activation of RNA polymerase II by cellular co-factors and viral Tat. RNA polymerase II is recruited to the HIV LTR for transcription initiation (A). The TFIIH CDK7 kinase phosphorylates the CTD of RNA polymerase II, which clears the promoter region and commences transcription of TAR (B). Nascent RNA, corresponding to TAR, folds and binds to RNA polymerase II. Tat binds to TAR RNA and forms a complex with TAK (C). Activated TAK kinase hyperphosphorylates the RNA polymerase II CTD; TAR is displaced from RNA polymerase II and transcription continues (D) [adapted from (Karn, 1999)].

1.3.8.2 Splicing

Both nascent transcribed host and viral mRNA associate with numerous proteins that carry out processes such as capping, polyadenylation, the removal of introns by splicing and transport of mature transcripts to the cytosol. Transcription and splicing occur simultaneously therefore the removal of introns also progresses in a 5'-3' direction (Bohne *et al.*, 2005). Although transcription of provirus DNA generates a single RNA, more than 40 HIV transcripts can be produced through alternative splicing (Madsen and Stoltzfus, 2006; Watts *et al.*, 2009).

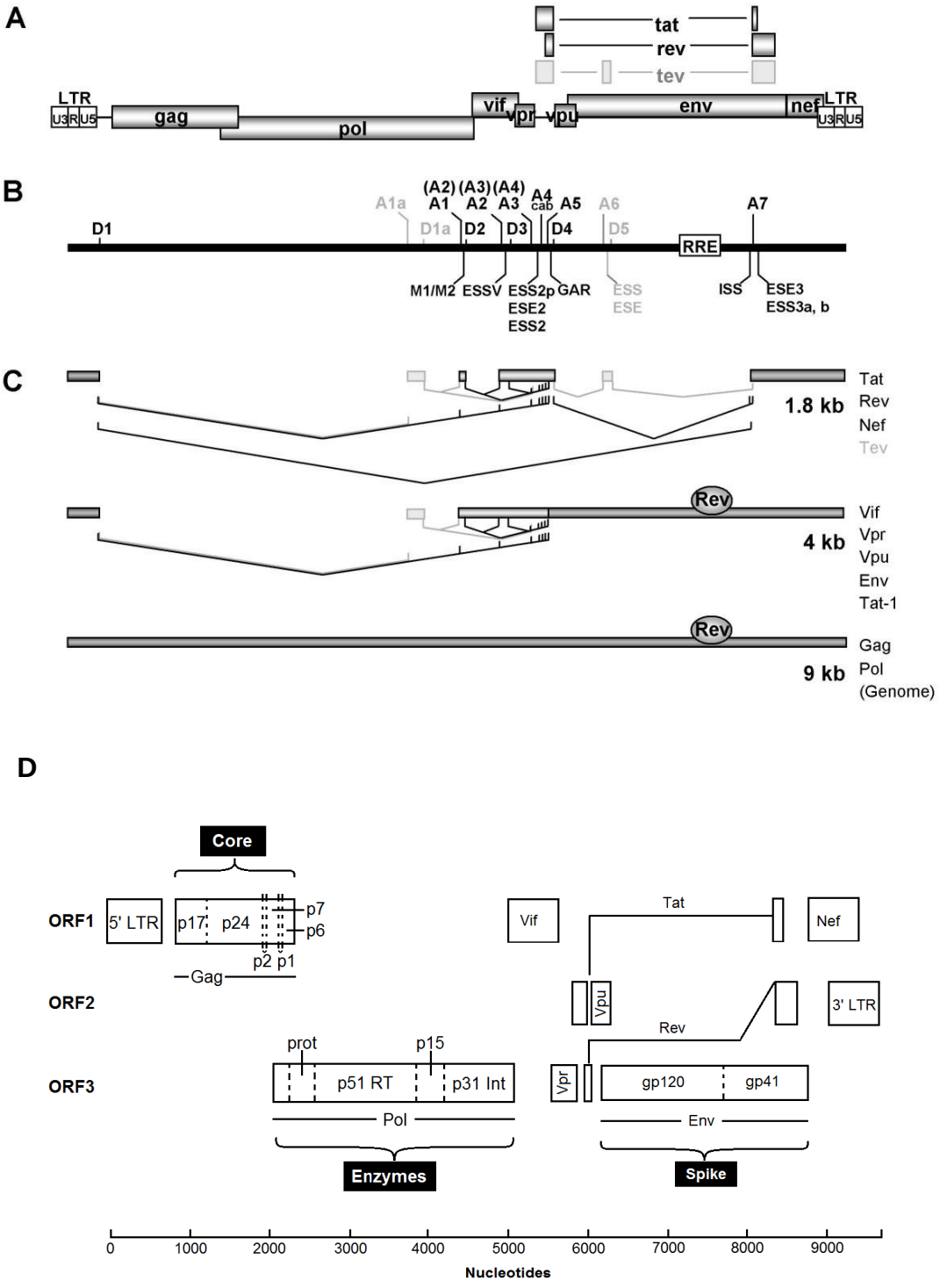

Figure 17: The HIV genome (A) and alignment of mRNAs to show the locations of known splice sites (B). Proteins produced from different splicing patterns are grouped by mRNA class with obligatory sequences represented by dark boxes and sequences produced by alternative splice sites usage shown by light boxes (C). Export of 4 kb and 9 kb mRNAs requires the viral Rev protein. The reading frame usage to produce differing mRNAs is also indicated (D) (Dimmock *et al.*, 2001; Kammler *et al.*, 2006).

HIV RNA undergoes a complex pattern of splicing to produce both Env RNA, with removed Gag and Pol coding regions, as well as several smaller proteins important in coordinating viral replication. Full-length HIV RNA contains 4 5' splice donors (SD) and 8 3' splice acceptors (SA) which contribute to the intricate splicing of HIV transcripts (Kammler *et al.*, 2006; Purcell and Martin, 1993). Additionally, HIV transcripts contain several features which alter splicing efficacy. Suboptimal splice sites, not easily recognised by cellular splicing machinery, result in inefficient splicing. Likewise exonic splicing enhancers and both exonic and intronic splicing silencers interact with cellular proteins to induce or inhibit splicing of adjacent splice sites. Inefficient splicing increases the number of HIV transcripts available for translation by differential processing of nascent mRNA (Madsen and Stoltzfus, 2006). HIV RNAs can be singly-spliced (producing mRNAs that encode Env, Vif, Vpr, and Vpu), multiply-spliced (encoding Tat, Rev, and Nef) or unspliced (encoding Gag and Gag-Pol) (Asai *et al.*, 2003).

1.3.8.3 Nuclear export

During replication, the expression of early genes and late genes requires temporal regulation to ensure that the correct levels of each viral protein are expressed at the required time. The export of viral mRNAs from the nucleus governs their temporal expression. Completely spliced RNAs are exported using the cellular mRNA export pathway. However, singly-spliced and unspliced RNA are retained in the nucleus due to the presence of introns which restrict their export (Li *et al.*, 2006). Splicing of pre-mRNA and nuclear export are coupled events; recruitment of nuclear export factors such as Aly to the mRNA-protein splicing complex targets spliced transcripts for export (Luo *et al.*, 2001). Therefore, in the absence of extenuating factors, intron-containing mRNA cannot exit the nucleus and therefore splicing is a pre-requisite for nascent mRNA export.

Three early, regulatory proteins; Nef, Rev and Tat, are encoded by fully-spliced HIV transcripts. Tat functions as a *trans*-activator of transcription through interactions with the TAR region of the HIV 5' UTR (see above). Nef (negative regulatory factor) indirectly enhances transcription by promoting

transcription factors such as NFκB, NFAT and AP-1 (Wu, Y. and Marsh, 2003). The transition from expression of early genes to late genes is controlled by an 18 kDa viral protein Rev (regulator of expression of viral proteins) (Pollard and Malim, 1998). Rev significantly contributes to the success of the viral life cycle through its role in regulating the transport of unspliced and singly spliced mRNA from the nucleus to the cytoplasm (Peterlin and Trono, 2003).

The levels of Rev determine which transcripts are expressed, and the Rev-RRE interaction (see below) alleviates the necessity for multiple pools of RNA by allowing temporal regulation of splicing (Purcell and Martin, 1993). In the absence of nuclear Rev, fully-spliced mRNA is able to undergo export directly. This favours expression of early, multiply-spliced gene products which encode regulatory proteins. However, in the presence of Rev, the rate of RNA export of singly-spliced and unspliced mRNAs is accelerated such that there is a limited time for splicing. Consequently, singly-spliced or unspliced transcripts encoding structural proteins are exported (Wu, Y. and Marsh, 2003). The export of unspliced transcripts requires the Rev/RRE pathway. Rev binds to the Rev responsive element (RRE) which is a large RNA structure within the *env* coding region of incompletely spliced, intron-containing mRNA (Dayton, 2004; Pollard and Malim, 1998). The Rev protein is composed of two domains; an amino-terminus arginine rich domain (ARD) and a carboxyl terminus leucine-rich region containing a nuclear export signal (NES). The Rev ARD functions as both a nuclear localization signal (NLS) and an RNA-binding domain (RBD). Both of the Rev domains are involved in Rev-mediated export of viral mRNA [figure 18] (Pollard and Malim, 1998).

A nuclear protein, Ran, regulates transport between the nucleus and cytoplasm (Seewald *et al.*, 2002). In the nucleus, Ran-GDP is converted to Ran-GTP by Ran-guanine exchange factor (Ran-GEF). CRM-1 (sometime called exportin 1 or XPO1) binds to both Ran-GTP and to Rev via its NES. This enables RRE-containing viral mRNA to be exported from the nucleus by the CRM-1 complex. The DDX3 helicase binds to CRM-1 and helps to mediate mRNA export by unwinding RNA secondary structure, making it easier for mRNA cargo to pass through nuclear pores. Once exported to the

cytoplasm, Ran-GTP is converted to Ran-GDP by Ran-GTPase-activating protein (Ran-GAP) causing the release of CRM-1, Rev and the mRNA cargo (Dayton, 2004). Following the successful export of viral mRNA, Rev is recycled back to the nucleus; the ARD of Rev binds to importin-β and both are translocated into the nucleus (Wu, Y. and Marsh, 2003).

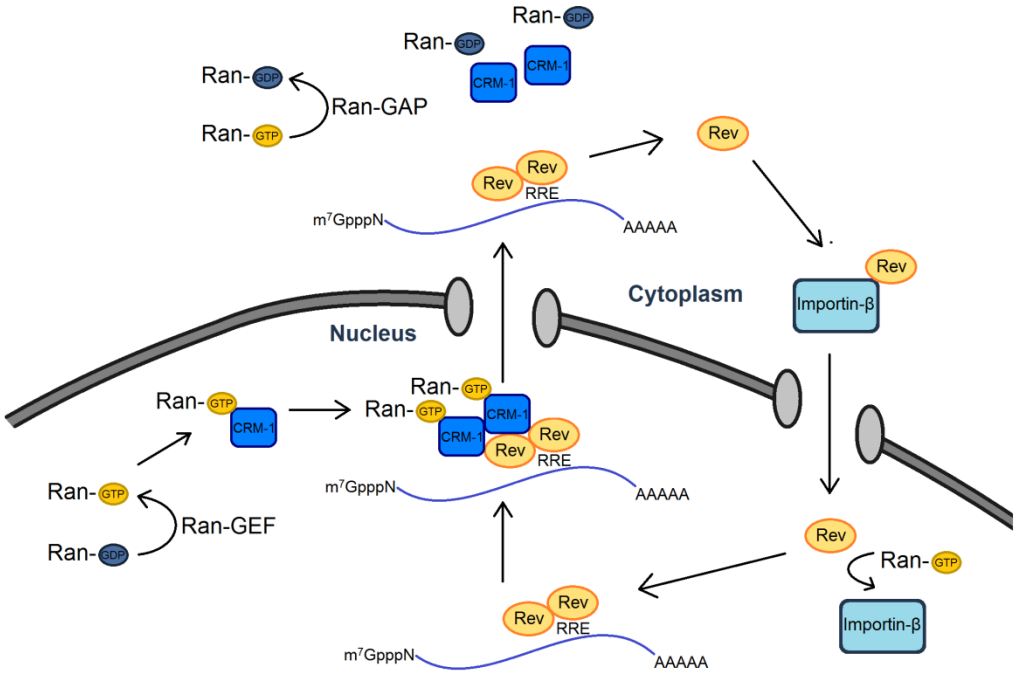

Figure 18: Rev/RRE mediated CRM-1 dependent transport of viral mRNA from the nucleus to the cytoplasm. Rev forms a complex with Ran-GTP-bound CRM-1 and viral mRNA through binding to the RRE. Following nuclear export of the CRM-1 complex, conversion of Ran-GTP to Ran-GDP in the cytoplasm causes the release of Rev and its viral mRNA cargo. Rev is recycled back to the nucleus through interactions with importin-β.

In the nucleus, Ran-GTP interacts with importin-β resulting in the release of Rev which is then available to continue shuttling more viral mRNA to the cytoplasm (Pollard and Malim, 1998). Ran-GAP and Ran-GEF are asymmetrically distributed between the cytoplasm and nucleus therefore producing a constant Ran-GDP/Ran-GTP gradient. This permits ongoing CRM-1 recycling and Rev/RRE export to occur (Dayton, 2004).

1.3.8.4 HIV translation: viral proteins

Following export to the cytoplasm, viral mRNAs are translated by host cell ribosomes and associated translation factors to produce viral proteins. The

mechanism and regulation of HIV translation will be considered in greater detail in Chapter 4. Translation of viral mRNA produces all of the proteins necessary to produce new viral particles.

HIV proteins: Gag and Gag-Pol

Unspliced genomic RNA contains the *gag* open reading frame (ORF) [figure 7] which is translated into a Gag precursor polyprotein ($Pr55^{Gag}$ for HIV-1 and $Pr57^{Gag}$ for HIV-2) [figure 19].

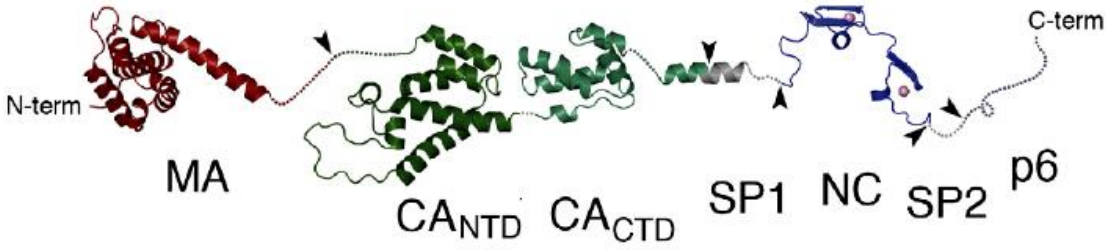

Figure 19: Model of the HIV-1 Gag polyprotein showing the N-terminus Matrix (MA), Capsid (CA) N-terminal and C-terminal domains (NTD/CTD) and C-terminus Nucleocapsid (NC) domain (Ganser-Pornillos *et al.*, 2008).

HIV-1 Gag is cleaved into mature, structural proteins by viral Protease during maturation. This produces several smaller proteins; p17 (Matrix, MA), p24 (Capsid, CA), p7 (Nucleocapsid, NC), p6 and two spacer peptides (Sp1 and Sp2) (Ganser-Pornillos *et al.*, 2008).

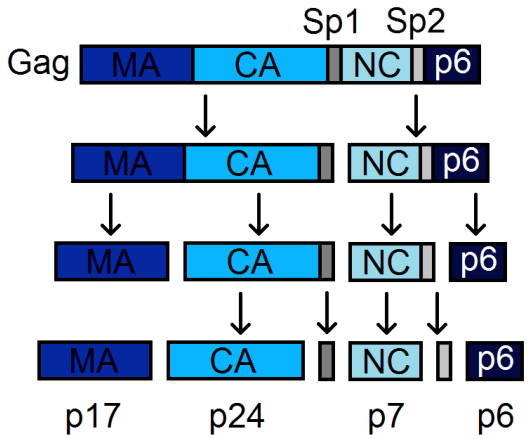

Figure 20: Processing intermediates and structural proteins produced from cleavage of the HIV-1 Gag precursor (p55) [adapted from (Clavel and Mammano, 2010)].

Within viral particles undergoing maturation, the first cleavage event separates NC from CA downstream of a 14 amino acid peptide, Sp1. Next, CA is cleaved from MA at around the same time as p6 is cleaved from NC

downstream of a second linker peptide, Sp2. Finally both linker peptides are cleaved; Sp1 from CA and Sp2 from NC [figure 20] (Clavel and Mammano, 2010).

Alternatively, during translation a (-1) frameshift event can occur at the frameshifting signal within the *gag* ORF (Ganser-Pornillos *et al.*, 2008). The frameshifting signal is a downstream, structural RNA element near the 3' end of the Gag coding region [figure 21] (Dulude *et al.*, 2008). Ribosome stalling is induced by the hairpin structure which presents a barrier to translational machinery. Pausing of the ribosome at a heptameric slippery sequence (UUUUUUA) subsequently promotes mRNA realignment such that the ribosome slips a nucleotide backwards towards the 5' end of the mRNA and translation continues in a -1 frame (Dulude *et al.*, 2008; Mazauric *et al.*, 2009). This results in the extension of the *gag* ORF by continued translation into the *pol* ORF generating a Gag-Pol fusion protein, Pr160 (Buck *et al.*, 2001).

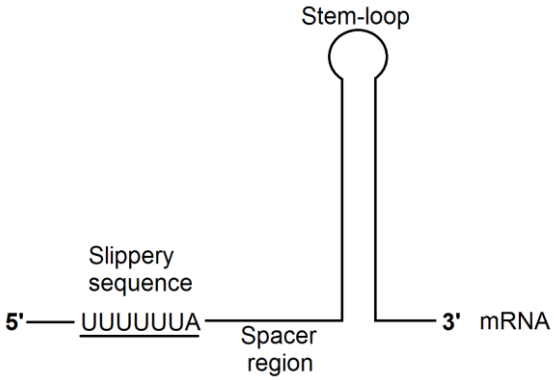

Figure 21: The HIV frameshifting signal consisting of a slippery sequence and stem-loop structure separated by a spacer region (Gaudin *et al.*, 2005; Watts *et al.*, 2009).

Programmed ribosomal frameshifting (PRF) occurs for around 5-10% of ribosomes and provides a method of controlling both the rate of translation and the ratio of viral proteins produced (Clavel and Mammano, 2010; Ganser-Pornillos *et al.*, 2008). The level of programmed ribosomal frameshifting is considerably higher than the amount of frameshifting caused by ribosomal error due to the combined effect of the slippery sequence and RNA structural element (Gaudin *et al.*, 2005). The Gag-Pol frameshift protein is cleaved to produce viral enzymes; PR, IN, and RT, in addition to Gag cleavage products (Lever, 2005).

HIV proteins: Env

The HIV *env* gene is expressed from genomic RNA which has undergone splicing to remove *gag* and *pol* coding regions (see figure 17) (Lever, 2005). Leaky scanning of ribosomes past the *rev* and *vpu* start codons is responsible for production of Env and Nef proteins (Buck *et al.*, 2001). Translation of *env* to produce envelope proteins takes place on endoplasmic reticulum-bound ribosomes. The amino terminus of the translating polyprotein contains a hydrophobic signal peptide. Recognition by signal recognition particle (SRP) results in transport to the rough endoplasmic reticulum (RER) where the envelope protein is co-translationally translocated into the RER [figure 22].

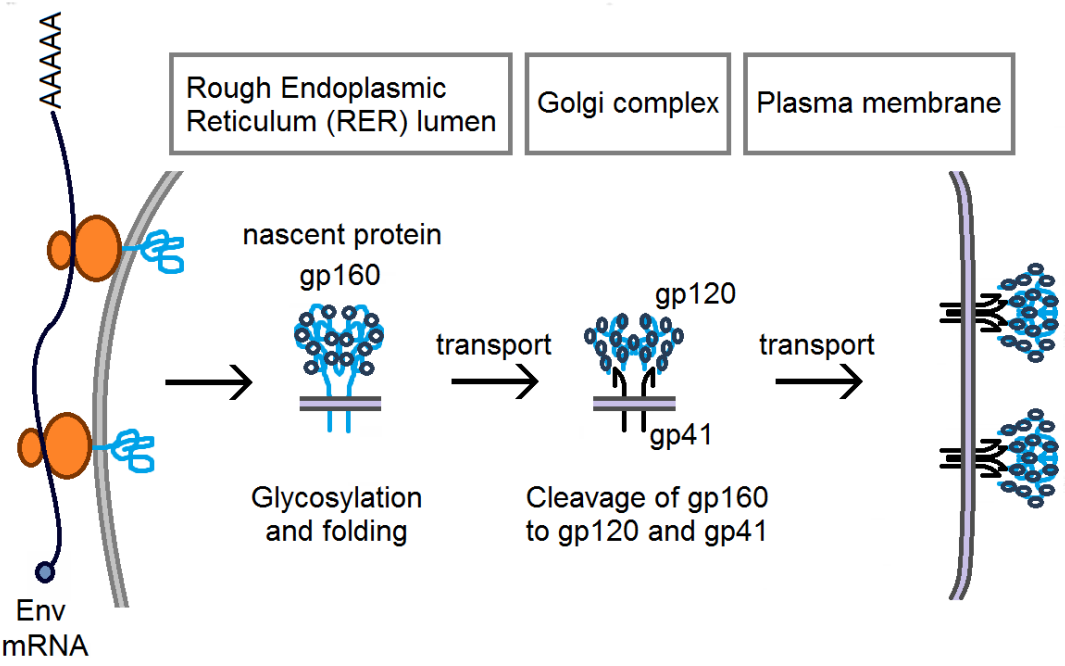

Figure 22: 160 kDa HIV Env proteins (gp160) are co-translationally transported to the rough endoplasmic reticulum (RER) where they undergo glycosylation and folding. Following transport to the Golgi, cleavage of gp160 by cellular proteases produces surface gp120 proteins which are non-covalently bound to transmembrane gp41 proteins. Env proteins are subsequently transported to the plasma membrane and incorporated into new virus particles [Image adapted from http://legacy.lclark.edu/~Ebkbaxter/200lecture/lecture_images/4_16_env_maturation.jpg].

HIV-1 *env* encodes gp160; a 160 kDa precursor protein (140 kDa for HIV-2) which undergoes cleavage by cellular proteases to make surface (SU) gp120

and transmembrane (TM) gp41 glycoproteins (gp125 and gp36 for HIV-2) (Reeves and Doms, 2002). Cleavage and further processing in the Golgi precedes protein transportation, via cellular mechanisms, to the cell surface where proteins are assembled into new particles (Lever, 2005).

The HIV gp120 SU protein contains conserved disulphide bonds, multiple glycosylation sites, and 5 conserved (C1-5) and variable (V1-5) domains (Reeves and Doms, 2002). Variable domains within HIV gp120 are responsible for much of the virus' genetic diversity and are therefore an indispensible part of viral strategy to evade the host immune response (Watts *et al.*, 2009). Non-covalent bonding associates the Envelope SU protein with the TM protein. The N-terminus of the HIV TM protein contains a fusion peptide important in entry to host cells, the central region consists of a membrane-spanning domain and the C-terminus contains an amphipathic intracellular domain (Reeves and Doms, 2002).

The HIV genome also encodes six smaller proteins; Tat, Rev, Nef, Vif, Vpr and Vpu. Whilst the regulatory proteins Tat and Rev are essential for virus replication (see above), Nef, Vif, Vpr and Vpu are accessory proteins which, although not crucial *in vitro*, serve to enhance HIV replication (Le Rouzic and Benichou, 2005).

HIV accessory proteins: Nef

One of the first viral proteins expressed is the 27 kDa Nef (negative factor) protein which plays an important role in enhancing HIV pathogenicity. Nef binds to cellular membranes through myristylation of its N-terminus, and regulates the intracellular trafficking of cell surface CD4, promoting its endocytosis through interactions with the CD4 cytoplasmic tail (Waheed and Freed, 2009). Recruitment of AP-2, involved in the formation of clathrin coated vesicles, is also enhanced by Nef. These two activities serve to encourage the intracellular transport of CD4 to endosomes and finally lysosomes where it is degraded (Malim and Emerman, 2008). Additionally, Nef engineers suppression of the major histocompatibility complexes (MHCI and MHCII) which are important in antigen presentation on T-cells; this prevents T-cell activation (Waheed and Freed, 2009). Thus Nef down-

regulates the expression of cell surface molecules important in provoking an immune response and thereby promotes viral survival (Malim and Emerman, 2008). Although it remains unclear whether Nef fundamentally enhances HIV replication, or whether Nef itself is a pathogenic agent, deletions in Nef severely attenuate the pathogenicity of HIV indicating the importance of this factor for viral infectivity (Foster and Garcia, 2008).

HIV accessory proteins Vpr (and Vpx)

Viral protein R (Vpr) is a multifunctional, 14 kDa accessory protein encoded by HIV-1 and HIV-2. Vpr has been implicated in numerous processes within the virus life cycle including accurate reverse-transcription, the regulation of cell cycle progression, apoptosis, and permissible macrophage infection (Fouchier *et al.*, 1998). Additionally, Vpr contains a nuclear localisation signal which permits targeting of the pre-integration complex to the nucleus. Although expressed during the late stages of the virus life cycle, Vpr is found both in virus particles and within the host cell and is therefore present for early stages of replication as it is released from infectious particles post-entry. Vpr has also been isolated from the sera of AIDS patients and therefore may operate via a diverse range of methods (Le Rouzic and Benichou, 2005). Cell death results from Vpr expression, although it is unknown whether this is attributed to induced apoptosis, or the Vpr-mediated arrest of cells at the G2 stage of the cell cycle (Malim and Emerman, 2008).

HIV-2 and SIV_{SMM} encode both Vpr and a Vpx gene whereas HIV-1 and other SIVs express only Vpr (Le Rouzic and Benichou, 2005). Consequently, for HIV-2, the functions of Vpr in HIV-1 are shared; Vpx permits macrophage infection and Vpr is responsible for cell cycle arrest. It has also been suggested that Vpx may counteract the host defence protein TRIM5α and target it for destruction. Consequently, the presence of Vpx in viral cores means that it may be directly introduced into target cells to overcome host restriction factors during the early stages of infection (Malim and Emerman, 2008).

HIV accessory proteins: VIF

Vif (viral infectivity factor) is a 23 kDa protein which counteracts the antiviral function of the host protein APOBEC3G: a DNA-editing enzyme which can enter HIV virions (Harris and Liddament, 2004; Madani and Kabat, 1998). If incorporated into virus particles, APOBEC3G renders them non-infectious as it induces mutations into reverse transcribed viral DNA in subsequent cells. Vif suppresses APOBEC3G via two mechanisms: inhibiting translation of APOBEC3G mRNA and inducing proteasomal degradation of cellular APOBEC3G proteins [figure 23] (Stopak *et al.*, 2003).

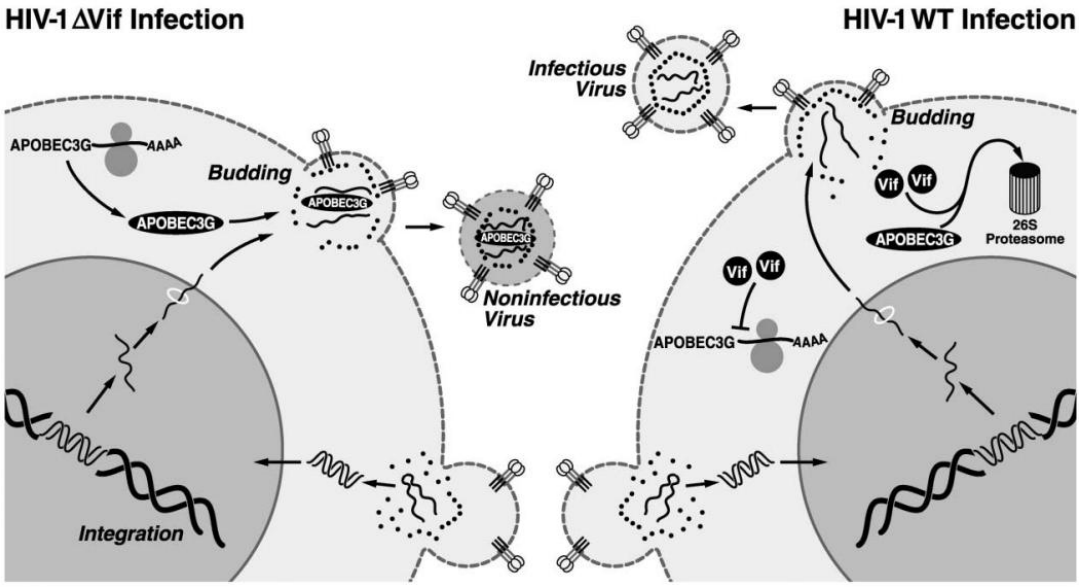

Figure 23: Vif counteracts the antiviral activity of cellular APOBEC3G by impairing APOBEC3G mRNA translation and targeting APOBEC3G proteins for degradation via the proteasome. These mechanisms prevent APOBEC3G from becoming incorporated into budding virions. In the absence of Vif, APOBEC3G is incorporated into virions where it induces damaging mutations into the reverse transcribed viral DNA within subsequently infected cells. This renders APOBEC3G containing virions non-infectious (Stopak *et al.*, 2003).

HIV accessory proteins: Vpu

Vpu (Viral protein U) is an 81 AA, type 1 membrane protein produced from the same mRNA as the Envelope glycoproteins. Vpu is unique to HIV-1 and has two main roles during infectivity; facilitating the release of viral particles from the cell surface by sequestering tetherin and, like Nef, inducing CD4 degradation through interactions with the CD4 cytoplasmic tail (Levesque *et al.*, 2003). In this way, Vpu monitors the expression of cell surface immune

markers and therefore regulates viral replication and persistence. Activation of antiviral agents can impair HIV replication. Type 1 interferon (in particular IFNα) induces the restriction factor tetherin which impairs release of viral particles. Vpu overcomes this resistance both by suppressing immune activation via cell surface markers, and sequestering tetherin molecules from the cell surface (Malim and Emerman, 2008). As HIV-2 does not encode Vpu, an alternative counteractive strategy involving HIV-2 Env is employed to overcome host restriction by tetherin. Both HIV-1 Vpu and HIV-2 Env can promote removal of tetherin from the cell surface. However, HIV-1 can additionally mediate a reduction in the total level of tetherin within the cell; a factor not attributed to HIV-2 Env (Hauser *et al.*, 2010).

1.3.9 Retrovirus assembly, budding and maturation

1.3.9.1 Assembly

Retrovirus assembly results in the construction of virus particles composed of viral proteins and containing genomic viral mRNA. Within T-cells, viral RNA, Gag and Env proteins are transported on endosomes to the plasma membrane to form immature virions. However, in primary human macrophages translated Gag proteins target to intracellular multivesicular bodies (MVB) and are likely released via exosomal pathways. Despite targetting of Gag to MVB, virions are still released with high efficiency from macrophages (Ono and Freed, 2004). Two groups of proteins associate with Gag during cell trafficking; MVB and clathrin adaptor (AP) proteins. ESCRT (endosomal sorting complexes required for transport) recognise and sort ubiquitinated cargo proteins into the intralumenal vesicles of MVBs. AP proteins sort target proteins into clathrin coated transport vesicles (Camus *et al.*, 2007).

The major structural determinant of virion construction is the Gag polyprotein. In fact, if only Gag proteins are expressed they produce extracellular, virus-like particles (VLP) which are indistinct from immature virions (Bieniasz, 2009). Gag translation occurs on free ribosomes within the cell cytoplasm. Resulting Gag proteins are involved in directing budding, regulating virion size and packaging other virion components. The mechanism by which Gag

proteins travel to the cell surface is unknown. However, host proteins, such as Arf and the GGA proteins, have been shown to play a role in the intracellular transport of Gag (Joshi *et al.*, 2008). The Gag matrix domain, which has an N-terminal myristate group and α-helical stalk, also facilitates targeting of Gag to the cellular membrane (Bieniasz, 2009). HIV-1 Gag proteins cannot travel to the cell surface by attachment to Golgi apparatus as Brefeldin A, a drug which disrupts this secretory pathway, does not disrupt the efficiency of Gag budding (Pal *et al.*, 1991). It is therefore thought that Gag trafficking to the plasma membrane may follow the pathways used by cellular proteins, travelling to the plasma membrane following synthesis on free, cytosolic ribosomes (Coffin, J.M. *et al.*, 1997). Additionally, it is unclear whether Gag monomers are singly transported or whether they co-localise to form multimeric proteins in the cytoplasm before encountering the plasma membrane at assembly sites (Bieniasz, 2009).

HIV Gag targets the more ordered lipid raft regions of the plasma membrane which are abundant in cholesterol and sphingolipids. Tetherin, which restricts HIV particle release, is a raft-associated protein. Likewise, the raft marker GM1 has been shown to co-localise with HIV Gag (Waheed and Freed, 2009). A phosphoinositide, PI(4,5)P_2, resides in the plasma membrane of host cells. Recognition of PI(4,5)P_2 by the matrix domain of Gag aids targeting of Gag to the plasma membrane and moreover stabilizes this association during assembly of virions. A bipartite motif within the matrix domain contains a covalently bound myristic acid and several positively charged amino acids. This positively charged surface is suitably placed to interact with the negatively charged interior of the plasma membrane. Thus the matrix domain helps Gag molecules to engage with the plasma membrane (Waheed and Freed, 2009).

Once at the plasma membrane, Gag molecules initiate or contribute to already forming Gag protein shells (Bieniasz, 2009). The N-terminal matrix domain of Gag associates with the host cell membrane which later forms the membrane of the viral envelope. As the particle assembles, Gag proteins are radially aligned with the N-terminals at the viral membrane and the C-

terminals pointing towards the centre of the forming virus particle [figure 24] (Briggs *et al.*, 2006).

Forming HIV virions contain two copies of positive-sense full-length genomic RNA (Berkhout *et al.*, 2011). The dimerization of two viral RNA strands results in packaging signals positioned in close proximity. Disruption of RNA dimers can impair the efficiency of viral encapsidation (Kaye and Lever, 1999). The mRNA produced during a HIV-1 infection consists of a single pool which is used interchangeably as both mRNA for translation and genomic RNA for packaging. Conversely, HIV-2 RNA is packaged primarily in *cis*, with nascent Gag proteins packaging the message from which they were synthesised (Paillart *et al.*, 2002).

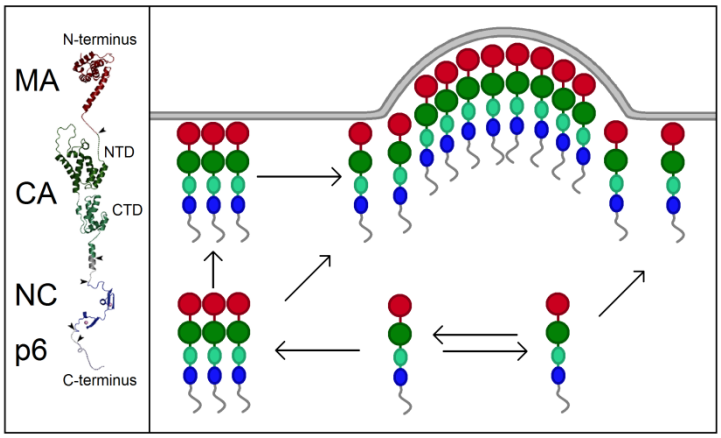

Figure 24: A structural model of HIV Gag showing Matrix (MA), Capsid (CA), Nucleocapsid (NC) and p6 domains. Several possible methods of Gag monomer assembly contribute to the Gag shell forming at the plasma membrane [adapted from (Bieniasz, 2009)].

It is thought that the matrix domain of Gag is responsible for stimulating translation at low Gag concentrations. At high Gag concentrations, binding of Gag to the packaging signal occurs through the Gag nucleocapsid domain, and directs encapsidation of the genome into new virus particles. Since HIV mRNA serves as both a translational template and genomic RNA for packaging, there is competition between these processes. Consequently, before packaging can proceed, there must be sufficient Gag molecules already synthesised to produce viral particles. Additionally, this suggests that

the Gag protein is responsible for controlling the switch between translation and packaging (Anderson and Lever, 2006).

HIV RNA contains a multipartite packaging signal; the primary packaging signal (Psi, Ψ) is located within the 5' UTR of mRNA although additional 5' UTR structures: DIS, poly(A), TAR and the Gag coding region have also been shown to contribute to optimal packaging (Paillart *et al.*, 2002). Gag molecules interact with the packaging signal within the 5' UTR of transcribed viral mRNA and this drives the multimerization of Gag (Bieniasz, 2009). During assembly, homologous regions of Gag monomers bind, causing alignment and non-specific binding of their NC domain along the viral RNA in an RNA/NC complex. It is thought that the Gag interaction with RNA provides a nucleation site, allowing more Gag proteins to assemble until an immature viral particle is formed. Pol proteins are linked to Gag before maturation and therefore also become incorporated into new virions (Kaye and Lever, 1999).

Like Gag, Env protein is targeted to lipid raft regions of the cell membrane via myristoylation and palmitoylation signals. Whereas Gag binds to the inner leaflet of the plasma membrane, Env is independently transported to the outer leaflet where it is acquired by budding virus particles (Jolly and Sattentau, 2007). It has been proposed that Env is incorporated into forming virus particles via the cytoplasmic tail of gp41 which interacts with the Gag matrix domain (Waheed and Freed, 2009).

Generation of virus particles commences with the formation of a protein sphere composed of Gag molecules. This occurs on the cytoplasmic face of the host cell lipid bilayer meaning that particle assembly and envelopment occur simultaneously [figure 25] (Bieniasz, 2009).

The C-terminal domain of Gag, p6, contains a docking site for proteins associated with the ESCRT. Separation of the virion envelope from the host cellular membrane relies on ESCRT-associated proteins (Bieniasz, 2009). HIV particles budding from the membrane of host cells are immature and non-infectious (Briggs *et al.*, 2006).

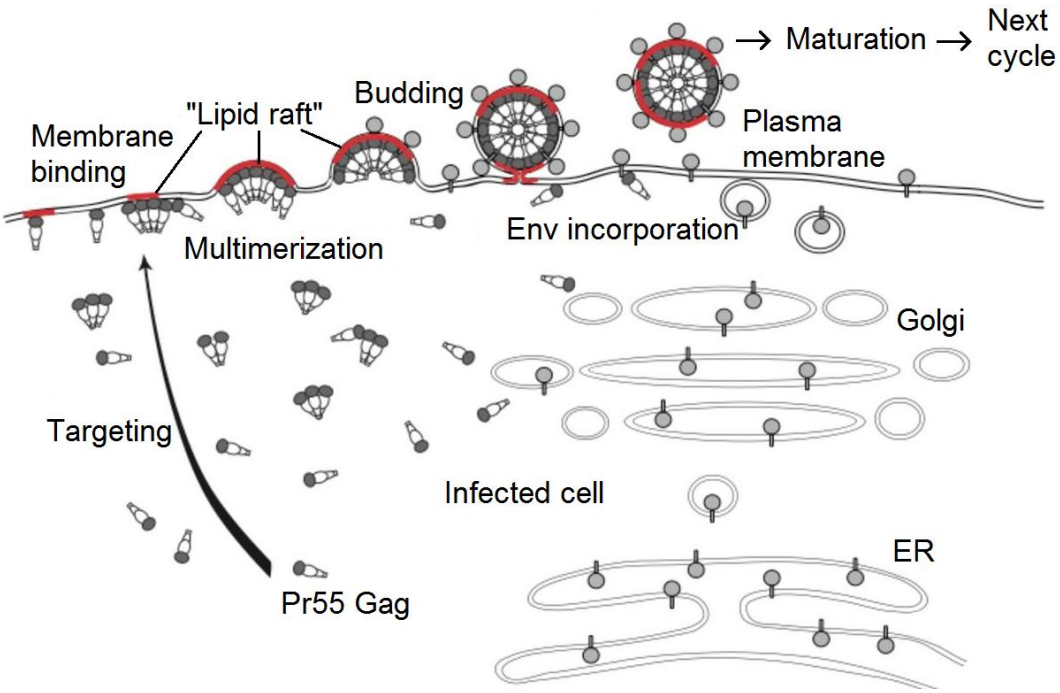

Figure 25: Assembly of HIV virions at lipid raft (red) regions of the plasma membrane (Waheed and Freed, 2009).

1.3.9.2 Budding

Following detachment of the formed virion from the host cell surface, it would seem that the virus particles should be free move away from the cell. However, a retention mechanism involving a host inhibitor, tetherin, can block viral release [figure 26].

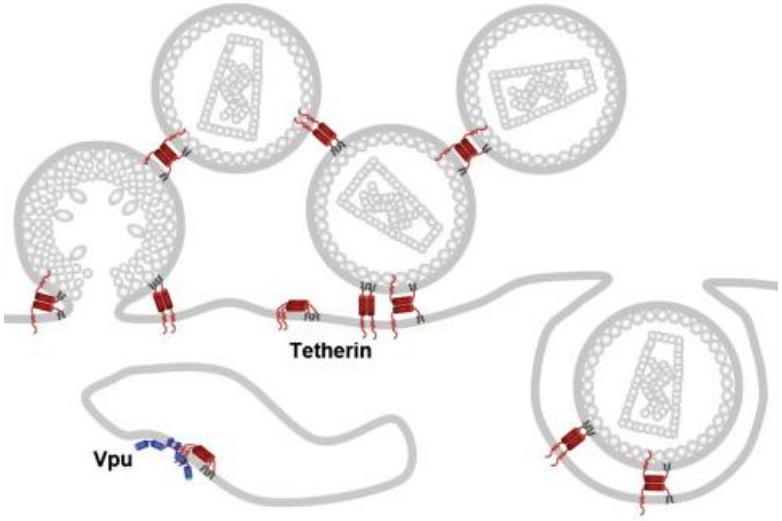

Figure 26: A model for tetherin retention of budding virus particles. Tetherin is an integral membrane protein which prevents particle release by causing virions to become tethered to each other and the cell membrane. Sequestering of tetherin

through the viral protein Vpu leads to its removal from assembly sites thereby allowing release of budding viral particles (Bieniasz, 2009).

Tetherin is an integral membrane protein induced by interferon (IFN). The protein is composed of an N-terminal cytoplasmic tail and an extracellular coiled-coil held in place by a central, transmembrane anchor. The C-terminal also forms a glycophosphatidylinositol lipid anchor. Thus tetherin is unusual in that it contains two membrane anchors (Bieniasz, 2009). Consequently, non-permissive cells expressing tetherin can restrict the ability of HIV to release viral particles. However, HIV has overcome this form of resistance via the viral protein Vpu. The N-terminal domain of Vpu forms a transmembrane anchor whilst the cytoplasmic C-terminal domain contains two helices and a phosphorylation site. Vpu is able to sequester tetherin and subsequently enhance viral release by removing tetherin from viral assembly sites (Bieniasz, 2009).

1.3.9.3 Maturation

Cleavage of nascent HIV polyproteins is required for viral maturation. The HIV-1 dimeric aspartic Protease (PR) catalyses polyprotein processing (Adachi *et al.*, 2009). However, the HIV genome only encodes one subunit of the HIV PR which is translated as part of the Gag-Pol polyprotein. Therefore dimerization of Gag-Pol (encoding PR) is first required to allow configuration of the PR active site and thus form an active Protease (Wan *et al.*, 1996).

During budding, or shortly afterwards, viral Protease cleaves Gag and Gag-Pol polyproteins to release several viral proteins (MA, CA, NC and PR, IN, RT). Considerable morphological change and restructuring of the immature viral particle follows polyprotein cleavage resulting in capsid formation and maturation of the virus into an infectious particle (Briggs *et al.*, 2006; Lever, 2005). Within the mature virus particle, Matrix proteins remain bound to the membrane. The core condenses into a ribonucleoprotein (RNP) complex of genomic RNA bound to Nucleocapsid proteins surrounded by a shell of Capsid proteins (Briggs *et al.*, 2006). The characteristic cone shape of the core results from the way the Capsid proteins elongate [figure 27].

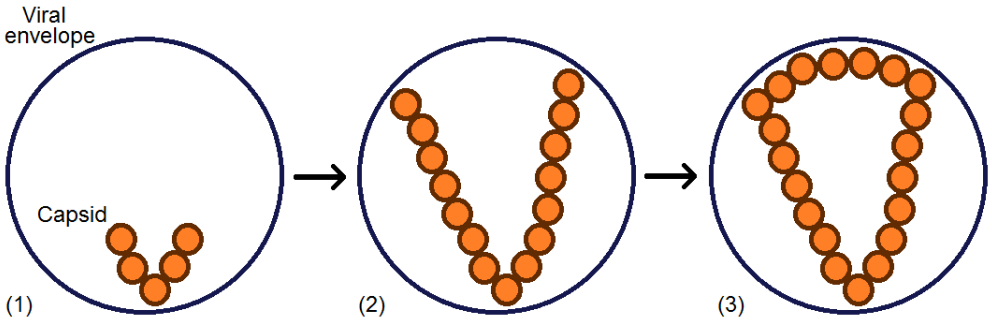

Figure 27: Assembly of the HIV mature core is coordinated to ensure cores of a homogeneous shape and size are formed. Assembly of the core initiates from a narrow point (1). Elongation is limited by the virion diameter (2) before growth along the inside of the viral envelope closes the cone (3) (Briggs *et al.*, 2006).

Maturation of immature virus particles by Protease cleavage and restructuring produces fully infectious virions which are subsequently poised to go on and infect naïve cells which they encounter. Viruses are obligate intracellular pathogens which subvert cellular replicative machinery to produce new progeny. Consequently, virus particles require access to cellular receptors on targets cells in order to bind and initiate infection. Classical models of virus infection focus on cell-free virus particles attaching to receptive target cells. However, an additional model has been proposed whereby some viruses, including HIV, may transition directly from host cells to target cells via cellular synapses. This could provide an important means of transmission for cells residing in close proximity to infectious cells; in particular, between cells of epithelial surfaces and lymphoid tissue. Likewise, the formation of a synapse between antigen presenting cells and T-cells is well characterised. Target cells may thus assist their own infection by forming synapses with HIV-infected cells and, moreover, provide a means for viruses to rapidly and covertly undergo cell-cell dissemination. This method would avoid complications posed by obstacles such as receptor binding, and, furthermore, would permit viral evasion of the antibody or complement aspects of the host humoral immune response (Jolly and Sattentau, 2004).

1.4 A comparison of HIV-1 and HIV-2

HIV-1 and HIV-2 are closely related lentiviruses which both cause AIDS. However, HIV-1 evolved from chimpanzee simian immunodeficiency virus

(SIV_{cpz}) and was identified in 1983, whereas HIV-2 evolved independently from sooty mangabey SIV (SIV_{smm}) and was first recognised in 1985. HIV-1 is found globally whereas HIV-2 infection is confined to West Africa (Sleasman and Goodenow, 2003).

HIV-1 is much more prevalent than HIV-2 and is the primary source of global AIDS cases. A causal factor is that HIV-2 is less pathogenic than HIV-1 and has a longer incubation stage. Both types of HIV show tropism for $CD4^+$ T-cells and mononuclear phagocytes (Lever, 2005). However, *in vivo*, lower viral RNA levels are seen in HIV-2 infection than HIV-1, despite similar proviral DNA levels, resulting in a significantly lower viral plasma load (MacNeil *et al.*, 2007).

Unlike HIV-1, HIV-2 is not transmitted vertically and, furthermore, perinatal transmission is less efficient (Coffin, J.M. *et al.*, 1997). HIV-2 is also associated with a higher proportion of long-term non-progressors than HIV-1, and the average disease progression in untreated infections is a few years longer with HIV-2 than HIV-1, despite the establishment of a stable and integrated proviral infection. Infection with HIV-2 is less virulent than HIV-1 infection and results in fewer individuals who progress to AIDS (Forsman and Weiss). However, once AIDS has developed the infection outcome is the same. Evidence suggests that a better immune response during HIV-2 infection may control replication of the HIV-2 virus, although HIV-2 infected individuals who do progress to AIDS show a similar level of immune response activation to HIV-1 infected individuals (Forsman and Weiss; Leligdowicz *et al.*, 2007). In contrast to HIV-1 infection, HIV-2 infected individuals can produce normal levels of $CD4^+$ T-cells which are able to specifically recognise HIV, replicate, and produce IFN-γ and IL-2 (Duvall *et al.*, 2006). Moreover, when $CD4^+$ T-cell levels are equivalent, the proportion of $CD4^+$ T-cells able to produce IL-2 during a HIV-2 infection is greater than for HIV-1 infection (Reeves and Doms, 2002). During a HIV-2 infection, a greater number of $CD8^+$ T-cells are also able to maintain production of IFN-γ and IL-2 than during a HIV-1 infection. Consequently, this suggests a different immune response to HIV-1 infection than infection with HIV-2, which may account for the lower replication rate witnessed during HIV-2 infection.

However, in tissue culture, where differences in the immune system are irrelevant, HIV-2 also has a lower replication rate than HIV-1 suggesting that additional factors influence the lower replication rate of HIV-2 (Blaak *et al.*, 2006).

Several distinguishing differences between infection with HIV-1 and HIV-2 viruses are discussed below and listed in table 3.

	HIV-1	HIV-2
Clinical illness	Majority develop AIDS	20-25% develop AIDS, the remainder are LTNPs
Plasma viral load	High in acute phase and during disease (10^5-10^7 RNA copies/ml), may be undetectable in asymptomatic phase	High in progressors (10^5-10^7 RNA copies/ml), undetectable in LTNPs
$CD4^+$ count	Decreases during acute infection, returns to normal and then declines over time	Normal in LTNPs, reduced count in progressors
$CD4^+$ depletion in gut associated lymphoid tissue	Massive depletion	Unknown
Vertical transmission	Up to 40%	<4%
Immune activation	Elevated even when viral load is undetectable	Not elevated in LTNPs, increased in progressors and predicts disease progression
T-cell proliferation	Increased $CD4^+$ and $CD8^+$ T cell turnover	Unknown
Thymopoiesis	Reduced	Enhanced (maintains $CD4^+$ T-cells)
T-cell apoptosis	Increased	Lower than HIV-1
Virus-specific $CD8^+$ T-cell response	Vigorous. Gag-specific response correlates with reduced virus load	Vigorous. Magnitude and Gag peptide specificity inversely correlate to virus load
Selection of cytotoxic T-cell escape variants	Frequently occurs. Associated with clinical decline	Unknown
Virus-specific $CD4^+$ T-cell response	IFNγ response present throughout infection. IL-2 secretion and proliferation correlate with LTNP status	IFNγ response present in most patients, IL-2 secretion and proliferation correlate with LTNP status

Table 3: A comparison of infection with HIV-1 and HIV-2 [modified from (de Silva *et al.*, 2008)].

HIV-1 and -2 have different long terminal repeats which could result in dissimilar expression of mRNA (de Silva *et al.*, 2008). Alternatively, the

difference in production of viral mRNA suggests that HIV-2 transcription may be more tightly controlled than for HIV-1 (de Silva *et al.*, 2008). The level of proviral DNA is comparable during a HIV-1/2 infection. Thus differences in viral gene expression may account for the reduced viral load associated with infection by HIV-2 (Reeves and Doms, 2002). *In vitro*, HIV-2 replicates more slowly and to lower titres than HIV-1. However, it is currently unknown why fewer viral particles are produced during a HIV-2 infection.

Work published during the completion of this thesis has suggested that HIV-1 and HIV-2 may have different translation strategies. *In vitro*, the addition of cap analogue inhibits translation of HIV-1 Gag but has less of an effect on Gag production in HIV-2. This suggests that translation of HIV-1 Gag may be more cap-dependent than HIV-2 (Ricci *et al.*, 2008). HIV-2 RNA also has a longer 5' UTR than HIV-1, with complex secondary structure which may hinder translation. Some regions of the HIV-1 and -2 genomes show considerable homology, whereas other regions are less homologous (Lever, 2005). For example, the HIV-1/2 Gag-Pol coding region shows 60% homology whereas the Env coding region only has 30-40% homology (de Silva *et al.*, 2008). The two strains also respond to differing cellular stimuli, indicating differences in the mechanism of gene expression (MacNeil *et al.*, 2007).

It has been shown that HIV-2 is unable to bud out of yeast spheroplasts whilst HIV-1 can. Defective HIV-2 Gag assembly in *S.cerevisiae* resulted in the accumulation of Gag proteins at the plasma membrane but a lack of budding (Morikawa *et al.*, 2007). This suggests that particle formation and budding could also differ between HIV-1 and -2. Additionally, HIV-2 MA does not bind as strongly to the plasma membrane as HIV-1 MA, which may contribute to a lower rate of particle production (Lever, 2005).

Since HIV-1 infection is responsible for the globally devastating AIDS pandemic, whereas HIV-2 has restricted endemicity, HIV research has principally focused on understanding how HIV-1 functions. Currently, a definitive study of the differences between the HIV-1 and HIV-2 viruses has not been carried out. Although differences in disease pathology, structural

variations and varying cellular interactions have been highlighted between these two viruses, it remains unclear as to the cause of the diminished replication levels seen during a HIV-2 infection. Identifying the underlying mechanisms for the failure of HIV-2 to present itself as such a severe pathogen, in contrast to the global dominance of the HIV-1 virus, may highlight a means to restrict the impact of HIV-1 through therapeutic intervention. Likewise, it remains to be seen whether the less effectual impact of the HIV-2 virus is attributable to one particular stage of the virus life cycle or whether it is the due to accumulative inefficiencies at various replicative stages.

1.5 Project aims

A greater understanding of the relationship between viral strategies and pathogenesis may provide an outlet for future therapeutic interventions, thus reducing the global impact of HIV. Consequently, the focus of my project lies in identifying and characterising the differences between HIV-1 and HIV-2 replication at the level of gene expression, with a particular focus on the potential differences between translation of HIV-1 and HIV-2 RNAs. A greater understanding of the relationship between viral strategies, and the implications for pathogenesis, is an important consideration when designing therapeutic measures or vaccines, and may go a long way to reducing the global disease burden of HIV.

CHAPTER 2: MATERIALS AND METHODS

2.1 Materials

2.1.1 Antibodies

Antibody	Dilution	1°/ 2°	Target	Supplier
Rabbit MAb anti-p24	1:2000	Primary	HIV-1 p24	NIBSC Centre for AIDS Reagents
Sheep MAb anti-p27	1:2000	Primary	HIV-2 p27	NIBSC Centre for AIDS Reagents
Rabbit polyclonal to eIF4G1	1:1000	Primary	eIF4G1 (220 kDa)	Abcam
Purified Mouse MAb Anti-adaptin γ	1:5000	Primary	AP1α (104 kDa)	BD Transduction Laboratories™
Mouse monoclonal anti-La/SSB (22A):sc-80655	1:500	Primary	Human cellular La protein (48 kDa)	Santa Cruz Biotechnology, Inc.
Mouse anti-luciferase	1:2000	Primary	Luciferase (61 kDa)	Sigma
Rabbit anti-GAPDH	1:1000	Primary	GAPDH	Abcam
Goat anti-rabbit IgG HRP	1:5000	Secondary	HIV-1 p24/GAPDH secondary	Santa Cruz Biotechnology, Inc.
Rabbit-anti-sheep IgG HRP	1:5000	Secondary	HIV-2 p27 secondary	Santa Cruz Biotechnology, Inc.
Goat-anti mouse IgG HRP	1:5000	Secondary	AP1 secondary	Sigma
Alexa Fluor 488-tagged goat anti-mouse IgG	1:500	Secondary	AP1 secondary	Invitrogen
Alexa Fluor 594-tagged goat anti-rabbit IgG	1:500	Secondary	HIV-1 p24 secondary	Invitrogen
Alexa Fluor 594-tagged donkey anti-sheep IgG	1:500	Secondary	HIV-2 p27 secondary	Invitrogen

Table 4: The antibodies used for experiments. The protein target, dilution and supplier are indicated.

2.1.2 Plasmids

Plasmid	Description	Digested with	Source
PJLuc	Plasmid containing a T7 promoter and gene encoding firefly luciferase	Sal1	Emma Anderson
HIV-1 MP	HIV-1 UTR-Gag-Luc reporter plasmid (PJLuc)	Nhe1	Made
HIV-1 MA2 MP	HIV-1 MA2 UTR-Gag-Luc reporter plasmid (PJLuc)	Nhe1	Made
HIV-2 MP	HIV-2 UTR-Gag-Luc reporter plasmid (PJLuc)	Nhe1	Made
SVC21ΔBgl	HIV-1 Env-deleted provirus (HXB2 strain)	Sal1	Prof. Andrew Lever
SVC21ΔBgl MA2	HIV-1 Env-deleted provirus (HXB2 strain) with the matrix region of HIV-2 (MA2)	Sal1	Emma Anderson
SVRΔNB	HIV-2 Env-deleted provirus (ROD strain)	Sal1	Prof. Andrew Lever
PRHCVF	Bicistronic plasmid with cap-dependent *Renilla* and Hepatitis C (HCV) IRES-driven firefly luciferase. Linearised to make bicistronic RHCVF RNA. Linearised to make cap-dependent *Renilla* luciferase RNA.	BamH1 Xba1	Prof. Anne Willis
PRHRVF	Bicistronic plasmid with cap-dependent *Renilla* and human rhinovirus (HRV) IRES-driven firefly luciferase. Linearised to make cap-dependent *Renilla* luciferase RNA.	BamH1	Prof. Anne Willis
pcDNA GFP	Plasmid encoding green fluorescent protein (GFP). Used as a non-specific translation control.		Emma Anderson
pcDNA GAG	HIV Gag coding plasmid. Used as a specific translation control.		Emma Anderson
PV1 Q746	Poliovirus 1 (PV1) IRES under the control of a T7 promoter.	BamH1	Prof. Richard Jackson
HVPΔEC puroΔB14	HIV provirus with a large deletion in Gag-Pol and puromycin replacing Nef.		Emma Anderson
pT7HRV2	Used to make HRV-2 RNA.	Acc65I	Prof. Tim Skern

pcDNA3-2A	HRV-2 2A protease (cap-dependent) in a pcDNA3 plasmid.	HindIII	Made
pcDNA3-2A-IRES	pcDNA3 plasmid containing HRV-2 2A under the control of an EMCV IRES.		Made
pT7Ev7ΔP1	Full-length echovirus-7 with capsid genes removed. Encodes 2A protease to make 2A RNA.	Xho1	Kym Lowry & Prof. David Evans
pJHRV GCC	Mutant HRV-2 IRES under the control of a T7 promoter.		Emma Anderson
PJHRV 10-605	HRV-2 IRES under the control of a T7 promoter.	BamH1	Prof. Richard Jackson
HIV-1ΔTAR	HIV-1 MP with TAR deletion in the 5'UTR.	Nhe1	Made
HIV-1 MA2 ΔTAR	HIV-1 MA2 MP with TAR deletion in the 5'UTR.	Nhe1	Made
HIV-2 ΔTAR	HIV-2 MP with TAR deletion in the 5'UTR.	Nhe1	Made
PGEM-T easy	Plasmid containing SP6 and T7 promoters flanking a multiple cloning site (MCS) within the coding region of the β-galactosidase enzyme. Insertional inactivation of the α-peptide permits recombinant clones to be identified on indicator plates by colour screening.		Kym Lowry & Prof. David Evans
pTK Renilla	*Renilla* luciferase under the control of a HSV thymidine kinase promoter.		Sue Morris & Dr Keith Leppard.

Table 5: The plasmids used for experiments. The plasmid name, content and restriction enzyme used for digestions are indicated alongside the plasmid source.

2.1.3 Plasmids produced

2.1.3.1 HIV Gag-Luc reporter plasmids

The 5' UTR and *gag* coding region from HIV-1 (SVC21ΔBgl) (primers #1, 2) and HIV-2 (SVRΔNB) (primers #3, 4) DNA plasmid templates were amplified by PCR. Sal1 restriction sites were included on forward and reverse primers, with the inclusion of an additional 15 nucleotide Gly(4)Ser linker on reverse primers. PCR products and a pJLuc plasmid encoding firefly luciferase were digested with Sal1 [NEB]. The pJLuc plasmid was dephosphorylated with

CIAP [Fermentas]. PCR products were ligated into pJLuc using T4 DNA ligase [NEB] and transformed into TG1 *E.coli*. Screening for the correct plasmid insert size and orientation was carried out by Sal1 and Sfo1 digests respectively of extracted bacterial DNA. Plasmids with the correctly orientated inserts were amplified by Maxiprep [Qiagen]. See appendix 1 for plasmid maps.

2.1.3.2 HIV ΔTAR Gag-Luc reporter plasmids

Forward primers were designed to bind after the TAR structure at the 5' end of the HIV-1/2 5' UTRs. Subsequently, the HIV-1 (primers #2, 16,) and HIV-2 (primers #4, 17) 5' UTR (ΔTAR) and *gag* coding region were amplified by PCR from HIV-1 (SVC21ΔBgl) and HIV-2 (SVRΔNB) DNA plasmid templates. Sal1 restriction sites were included on forward and reverse primers and an additional 15 nucleotide Gly(4)Ser linker included on the reverse primers. HIV-1 and HIV-2 ΔTAR PCR products were purified by gel extraction and, alongside pJLuc, digested using Sal1 [NEB]. The pJLuc plasmid was dephosphorylated using CIAP [Fermentas]. Following DNA extraction of digests, HIV-1/2 (ΔTAR) UTR-gag DNA was ligated into pJLuc using T4 DNA ligase [Fermentas] and ligated plasmids transformed into TG1 *E.coli*. Resultant colonies were cultured by Miniprep and bacterial DNA isolated. Sequencing was carried out on the resulting plasmids to check the 5' UTR-Gag coding region was correctly inserted and affirm the deletion of HIV-1/2 TAR sequences. See appendix 2 for plasmid maps.

2.1.3.3 pcDNA3-2A

The HRV-2 2A protease was amplified by PCR (using primers #5, 6) from pT7HRV-2 (encoding human rhinovirus 2). The forward primer contained a HindIII restriction site and the reverse primer contained an XbaI restriction site. The PCR product and a pcDNA3 plasmid (under T7 promotion) [Invitrogen] were digested with HindIII and XbaI [NEB] and the plasmid dephosphorylated with CIAP [Fermentas]. The digested HRV-2 2A PCR product was ligated into pcDNA3 using T4 DNA ligase [NEB] and used to transform TG1 *E.coli*. Sequencing of DNA extracted from bacterial colonies

was carried out to ensure the presence of the correct insert. The resulting plasmid was named pcDNA3-2A. See appendix 3 for plasmid map.

2.1.3.4 pcDNA3-2A-IRES

Cloning was carried out to express HRV-2 2A under the promotion of an EMCV IRES. The encephalomyocarditis virus (EMCV) IRES (nucleotides 1230-1840) was amplified by PCR (primers #7, 8) from a prB322 plasmid containing the EMCV IRES replicon [a gift from Kym Lowry and Professor David Evans]. The EMCV IRES PCR product was Klenow treated [Fermentas] according to the manufacturer's instructions to produce blunt ends. Previously made pcDNA3-2A was digested with HindIII, Klenow treated to produce blunt ends and dephosphorylated with CIAP [Fermentas]. A blunt end ligation using T4 DNA ligase [NEB] was carried out to insert the EMCV IRES into pcDNA3-2A; the resulting plasmid was called pcDNA3-2A-IRES. See appendix 4 for plasmid map.

2.1.4 Primers

NB: Primers were used at 20 µM diluted from 100 µM stock.

#	Primer	Sequence	Source
1	Sal1 HIV-1 (26)	TAGCTAGTCGACGGTCTCTCTGGTT	Sigma
2	Sal1 Linker Gag1 (131)	TAGCTAGTCGACAGAGCCTCCGCCTC CTTGTGACGAGGGGTCG	Invitrogen
3	Sal1 HIV-2 (133)	TAGCTAGTCGACGGTCGCTCTGCGG	Invitrogen
4	Sal1 linker Gag2 (132)	TAGCTAGTCGACAGAGCCTCCGCCTC CCTGGTCTTTTCCAAAGAG	Invitrogen
5	2A protease FWD	CTAGCAAGCTTATGGGCCCCAGTGACA TG	Invitrogen
6	2A protease REV	CCTAGTCTAGACTATTGTTCTTCAGCA C	Invitrogen
7	EMCV IRES FWD	GACCACAACGGTTTCCCT	Invitrogen
8	EMCV IRES REV	TATTATCGTGTTTTTCAAAGG	Invitrogen
9	HIV-1 Gag (Pfo1)	TCAGAAGCAGGAGCCGATAG	Invitrogen
10	HIV-2 Gag (Pfo1)	CTTGCTGCACCTCAATTCTC	Invitrogen
11	HIV-1 T7ΔTAR UTR FWD	TAGCTAATACGACTCACTATAGGGACT GCTTAAGCCTCAATAAAGC	Invitrogen
12	HIV-2 T7ΔTAR UTR FWD	TAGCTAATACGACTCACTATAGGGCCA CGCTTGCTTGCTTAAAAACC	Invitrogen

13	HIV-1 T7 UTR FWD	TAGCTAATACGACTCACTATAGGGTCT CTCTGGTTAGACCAGATC	Invitrogen
14	HIV-2 T7 UTR FWD	TAGCTAATACGACTCACTATAGGGTCG CTCTGCGGAGAGGCTGGC	Invitrogen
15	Nhe1-Luc REV	CGATGACCCTGCTGATTGGTTCGCTGA	Invitrogen
16	Sal1 HIV-1ΔTAR	TAGCTAGTCGACACTGCTTAAGCCTCA ATAAAGC	Invitrogen
17	Sal1 HIV-2ΔTAR	TAGCTAGTCGACCCACGCTTGCTTGCT TAAAAACC	Invitrogen
18	GAPDHf	TCTCCTCTGACTTCAACAGCGAC	Invitrogen
19	GAPDHr	CCCTGTTGCTGTAGCCAAATTC	Invitrogen
20	Pre-GAPDHf	CCACCAACTGCTTAGCACC	Invitrogen
21	Pre-GAPDHr	CTCCCCACCTTGAAAGGAAAT	Invitrogen
22	Gag1_1412f	GGCAAGAGTTTTGGCTGAAG	Invitrogen
23	Gag1_1584r	CACATTTCCAACAGCCCTTTT	Invitrogen
24	Gag2_1457f	AAGCTTGAGGGCAGAACAAA	Invitrogen
25	Gag2_1651r	AGGGCCTCTGCCATTAATCT	Invitrogen
26	H2 spliced FWD	ACTAGCAGTCGCCGC	Invitrogen
27	H2 spliced REV	TGCCACTAGATGTCTCCGCAC	Invitrogen
28	H2 unspliced FWD	CCTCTTAATAAAGCTGCCAGTTAG	Invitrogen
29	H2 unspliced REV	ACTCAGCGGTATATGGGTGTAG	Invitrogen
30	Renilla FWD	ATGATAACTGGTCCGCAGTG	Invitrogen
31	Renilla REV	GCGCTACTGGCTCAATATGT	Invitrogen
32	T7 Sequencing primer	TAATACGACTCACTATAGGG	Bo Meng & Prof. Andrew Easton

Table 6: Primer names and primer sequences used for experiments. The primer number and source are shown.

2.2 Methods

2.2.1 Tissue culture

HeLa and COS-1 cells were cultured in Dulbecco's modified Eagle's medium (DMEM) supplemented with 10% FCS at 37ºC/5% CO_2. When confluent, HeLa were split 1/10 and COS-1 split 1/5 twice weekly. Jurkat cells were grown in suspension at 37ºC/5% CO_2 in Roswell Park Memorial Institute medium (RPMI) supplemented with 10% FCS and split 1/10 twice weekly. BSRT7 cells were grown alternatively in Glasgow minimum essential medium (GMEM) and GMEM-G418 (supplemented with Geneticin, G418) at 37ºC/5% CO_2. In both cases media was supplemented with FCS (5%), glutamine (0.25%), Penstrep (0.25%), and cells were split 1/6 when confluent.

2.2.2 Plating out cells (for transfection)

Confluent BSRT7, COS-1 or HeLa cells were washed in PBS and extracted from flasks by incubation with 3 ml trypsin-EDTA at 37ºC/5% CO_2 for 5 min. Trypsin reactions were quenched with 7 ml media. Cell suspensions were diluted 1/8 (HeLa), 1/4 (COS-1) in DMEM and seeded into 6-well (2 ml per well) or 12-well (1 ml per well) plates and incubated overnight at 37ºC/5% CO_2.

Jurkat cells grown in suspension were centrifuged at 1,500 rpm for 5 min. The supernatant was discarded and the remaining cell pellet resuspended in 10 ml RPMI. 10 µl cells were stained with 10 µl Trypan blue [Sigma] and the cell concentration determined by counting using a haemocytometer. Cells were plated at a concentration of 0.8-1.6 x 10^6 cells/ml diluted in RPMI and grown overnight at 37ºC/5% CO_2.

2.2.3 Transfection of cells

Cells at 70% confluency were transfected with DNA or RNA via a lipid transfection system. Lipofectamine^{TM}2000 [Invitrogen] was diluted 1/50 (BSRT7, COS-1, HeLa) or 1/25 (Jurkat cells) in OPTIMEM and incubated for 20 min with nucleic acid also diluted in OPTIMEM. Cell media was replaced before the nucleic acid/Lipofectamine/OPTIMEM suspension was added to cells. Transfected cells were incubated at 37ºC/5% CO_2. Conventionally, DNA transfections were harvested after 24 h and RNA transfections after 6 h and RNA or protein extracted for downstream expression analysis.

Actinomycin D treatment: Cellular transcription was shut down by substituting cell media for media containing 5 µg/ml actinomycin D [Sigma] at 24 h post-transfection.

Leptomycin B treatment: To shut down CRM-1-dependent nuclear export, cell media was supplemented with 15 nM leptomycin B [Sigma-Aldrich] at 24 h post-transfection.

Poliovirus infections: For shutdown of cap-dependent translation, HeLa cells were infected with poliovirus diluted to a concentration of 3.8 x 10^6 pfu/well in DMEM (with 10% FCS) for 1 h prior to transfections (at an m.o.i of 10). Media

containing poliovirus was removed and cells were washed twice with 1 ml PBS before new media was replaced onto cells and transfection carried out.

Saquinavir treatment: For some transfections, HIV Protease cleavage of Gag was inhibited by supplementing the media of treated cells with 1 µM saquinavir.

siRNA treatment: Where stated, cells were treated with either 50 nM AP-1 siRNA or 50 nM negative control siRNA [Ambion] by transfection with Lipofectamine^{TM}2000 [Invitrogen].

2.2.4 Protein extraction from transfected cells

Following incubation at 37ºC, media was removed from transfected BSRT7, COS-1 or HeLa. Cells were washed with PBS before adding 200 µl 1x PLB [Promega] and lysing cells on a Luckham R100 Orbital Shaker for 20 min. Lysed cells were centrifuged for 2 min at 13,000 rpm. The supernatant, containing total cellular protein, was removed to a fresh Eppendorf and stored at -20ºC. Jurkat cells grown in suspension were first centrifuged at 2,000 rpm for 1 min to pellet cells. Cell pellets were washed with 200 µl PBS and centrifuged again at 2,000 rpm for 1 min, before discarding the supernatant and lysing cells by adding 50 µl 1x PLB.

2.2.5 Sub-cellular fractionation of cells for qPCR

At stated time points, the media was removed from cells and the monolayer washed in PBS. 200 µl Trypsin-EDTA was added for 5 min at 37°C. Cells were dislodged, transferred to an Eppendorf and rinsed in 1 ml DMEM (10% FCS). After centrifugation at 4000 rpm for 5 min, the supernatant was discarded and cell pellet washed in 1 ml PBS. Following further centrifugation for 3 min at 4,000 rpm, the cell pellet was either resuspended in 200 µl ice-cold PBS for total RNA extraction, or further processed for nucleus/cytoplasm separation.

Cell pellets for nucleus/cytoplasm separation were resuspended in 1 ml RSB (10 mM Tris pH 7.5, 10 mM NaCl, 10 mM $MgCl_2$) and incubated on ice for 3 min. After centrifugation at 4,000 rpm for 3 min, the cell pellet was resuspended in 200 µl RSBG40 (10 mM Tris pH 7.4, 10 mM NaCl, 3 mM

$MgCl_2$, 10% glycerol, 0.5% NP40, 0.5 mM DTT, 4000U RNase inhibitor) and centrifuged at 7,000 rpm for 3 min. 200 µl of the supernatant was removed to a new Eppendorf for cytoplasmic RNA extraction. Excess supernatant was discarded and the pellet vortexed slowly in 100 µl RSBG40 with 1/10 detergent mix (3.3% wt/wt sodium deoxycholate, 6.6% Tween40). After incubation on ice for 5 min, the pellet was centrifuged at 7,000 rpm for 3 min and the supernatant discarded before resuspension in 100 µl RSBG40. After centrifuging at 10,000 rpm for 5 min, the pellet was resuspended in 200 µl for nuclear RNA extraction. RNA was extracted from total, nuclear and cytoplasmic samples using Trizol.

2.2.6 RNA isolation from cells: Trizol extraction

After vortexing in 1 ml Tri Reagent® [Sigma-Aldrich], samples were incubated for 5 min at rt. 200 µl chloroform was added and samples were shaken by hand for 15 sec before leaving for 2 min (rt). After centrifuging at 12,000 g (10 min), the aqueous phase containing RNA was removed into 0.5 ml isopropanol, mixed by inverting, and placed at -20ºC overnight to precipitate RNA. Following centrifugation at 12,000 g (10 min), the supernatant was discarded and the pellet washed with 1 ml 75% ethanol. After vortexing and re-pelleting the sample at 12,000 g (5 min), the Eppendorf lid was left open to air dry the pellet for 10 min. Pelleted RNA was re-suspended in 30 µl DEPC-treated H_2O.

2.2.7 RNA isolation: phenol extraction

Nuclease-free water was added to nucleic acid samples to produce a total volume of 150 µl or 200 µl. An equal volume of phenol/chloroform/isoamyl alcohol (25:24:1) [Fisher BioReagents] was added to each sample. Following vortexing and centrifugation for 2 min (13,000 rpm), the aqueous phase containing nucleic acid was removed to a fresh Eppendorf. An equal volume of isopropanol was added before overnight precipitation at -20ºC. Following overnight precipitation, the sample was centrifuged for 8 min at 13,000 rpm and the pellet resuspended in 20 µl nuclease-free H_2O.

Alternatively, RNA was extracted using an RNeasy Mini Kit [Qiagen] as per the manufacturer's instructions.

2.2.8 DNase treatment

RNA samples were treated with 2 µl DNaseI (2 U/µl) in 50 µl 1x DNase1 Buffer [Ambion] to remove template DNA. Reactions were incubated at 37°C for 30 min, before phenol extraction of DNA.

2.2.9 DNA isolation: phenol extraction

DNA products were purified by phenol/chloroform extraction and ethanol precipitation. Reaction volumes were adjusted to 200 µl with nuclease-free H_2O and an equal volume of phenol/chloroform/isoamyl alcohol (25:24:1) mix [Fisher BioReagents] was added to each sample prior to vortexing and centrifugation at 13,000 g for 2 min. The upper aqueous phase was removed to a fresh Eppendorf and DNA precipitated overnight at -20°C in 1/10 3 M NaOAc and 2.5 vol. 100% ethanol. The next day, samples were centrifuged at 13,000 rpm for 8 min and the supernatant discarded. The remaining DNA pellet was resuspended in 20 µl nuclease-free H_2O.

Alternatively, DNA reactions were cleaned up using the MinElute Reaction Cleanup Kit [Qiagen] according to the manufacturer's instructions.

2.2.10 Determining the concentration of nucleic acids

A Nanodrop 1000 Spectrophotometer [Thermo Scientific] was used to determine the concentration of DNA or RNA preparations.

2.2.11 *In vitro* DNA transcription (mMESSAGE mMACHINE® T7 kit)

1 µg linearised DNA was transcribed into capped RNA using a mMESSAGE mMACHINE® T7 kit [Ambion] for 2 h at 37°C. Capped RNA was polyadenylated using a Poly(A) Tailing kit [Ambion] and template DNA was degraded by incubation with TURBO DNase [Ambion mMESSAGE mMACHINE® T7 Kit] at 37°C for 30 min before extraction of capped and polyadenylated RNA by phenol extraction. Reactions were carried out according to the manufacturer's instructions.

To produce uncapped RNA, the cap-NTP mix contained in the mMESSAGE kit was exchanged for 7.5 mM NTPs, preventing the addition of a cap-structure to the mRNA.

2.2.12 *In vitro* DNA transcription (MAXIscript® kit)

The Ambion MAXIscript® kit was used to make radiolabelled RNA from 1 µg linearised DNA plasmids. Reactions were incubated with 1x Transcription Buffer, 0.5 mM ATP, 0.5 mM CTP, 0.5 mM GTP, 0.05 mM UTP, 20 µCi α-^{32}P UTP (10 µCi/µl) [Perkin Elmer] and enzyme mix as per the manufacturer's instructions at 37°C for 1 h. Subsequent TURBO DNase [Ambion mMESSAGE mMACHINE® T7 Kit] treatment removed template DNA. Radioactive RNA was isolated using the RNeasy Mini Kit [Qiagen].

2.2.13 *In vitro* DNA transcription (biotinylated RNA)

Biotinylated RNA was produced for RNA affinity chromatography. 1 µg of linearised DNA was used in a reaction with 2 µl of Biotin RNA Labelling mix [Roche Applied Science], 1x Transcription Buffer and 2 µl RNA T7 polymerase [Ambion]. Samples were incubated at 37°C for 2 h before DNase treatment at 37°C for 15 min. Biotinylated RNA was extracted using phenol/chloroform. To make radioactively labelled biotin RNA, 2 µl α-^{32}P UTP (10 µCi/µl) [Perkin Elmer] was added to transcription reactions.

2.2.14 *In vitro* DNA transcription/translation (TnT)

100 ng of DNA plasmid was used in an *in vitro* TnT Quick Coupled Transcription/Translation system [Promega] with ^{35}S-methionine (0.01 µCi). Reactions were carried out at 30°C for 1.5 h according to manufacturer's instructions. Proteins produced were used for luciferase assays or in a SDS-PAGE; gels were vacuum dried and exposed to KODAK™ Biomax® MR 1 Film [Perkin Elmer].

2.2.15 *In vitro* RNA translation (rabbit reticulocyte lysate)

800 ng RNA was translated in a Flexi® Rabbit Reticulocyte Lysate System [Promega] supplemented with amino acid (minus methionine) [Promega], 60 mM or 100 mM KCl, 1/10 HeLa S100 extract and ^{35}S-methionine (0.01 µCi). Reactions were incubated for 1.5 h at 30°C before 10 µl RNase STOP solution (50 µg/ml RNase A, 10 mM EDTA pH 7.5) was added and the reactions incubated at 37°C for a further 15 min before heating to 85°C for 10 min. 2.5 µl radioactively labelled proteins were used in a luciferase assay or

added to 2x SDS sample buffer and used in a SDS-PAGE; gels were vacuum dried and exposed to KODAK™ Biomax® MR 1 Film [Perkin Elmer].

2.2.16 Luciferase assays

The amount of firefly and *Renilla* luciferase in 5 µl of extracted protein sample, or 2.5 µl TnT reaction, was quantified using a Dual-Luciferase® Reporter (DLR™) Assay System [Promega]. 25 µl of luciferase assay reagent II (LARII) was added to each sample in a 96-well, flat-bottomed, white plate [Greiner Bio-One] and the luminescent signal read on a Luminoskan Ascent luminometer [Thermo Labsystems]. After firefly luciferase quantification, the reaction signal was quenched, and the *Renilla* luciferase simultaneously activated, by adding 25 µl Stop & Glo® Reagent [Promega] to each sample. *Renilla* luciferase luminescence was quantified by once more reading the plate on the luminometer.

2.2.17 SDS-PAGE and western blotting

Protein samples were diluted in 2x SDS sample buffer (100 mM Tris Cl pH 6.8, 4% SDS, 20% glycerol, 0.2% bromophenol blue, 5% β-mercaptoethanol) and heated at 100ºC for 5 min before loading onto a 10% SDS-PAGE gel (composed of a 5% stacking layer and 10% resolving layer). 10 µl of a PageRuler™ Plus Prestained Protein Ladder [Fermentas] was run alongside samples for sizing. Samples were separated at 30 mA in 1x protein gel running buffer (0.1% SDS, 0.03% Tris, 1.44% Glycine) for 2 h. A nitrocellulose filter was used for western blotting of resolved protein gels, sandwiched between layers of 3 mm Whatman® Chromatography Paper, at 400 mA for 2 h. Western blotting was carried out in 1x transfer buffer (0.3% Tris, 2.88% glycine, 20% methanol) at 4ºC.

2.2.18 Immunoprobing

After western blotting, nitrocellulose filters were blocked overnight in 5% dried milk Marvel TBS-T (0.1% Tween). The filter was probed with primary antibody diluted in 5% Marvel TBS-T for 1 h and secondary antibody diluted in 5% Marvel TBS-T for 1 h. After each incubation, 3x 10 min washes were

carried out using TBS-Tween. The filter was developed using an ECL™ Advance Kit [Amersham] according to the manufacturer's instructions.

2.2.19 Gel staining and vacuum drying

Gels were stained by immersion in Coomassie Brilliant Blue for 2 min followed by destain (10% acetic acid, 10% methanol, H_2O). Gels for mass spectrometry were stained with Instant Blue™ [Expedeon] according to the manufacturer's instructions. The Silver Stain Plus kit [Biorad] was used to stain RNA affinity chromatography SDS-PAGE gels. Staining was carried out according to the manufacturer's instructions. After staining, the gels were placed onto two layers of 3 mm Whatman® Chromatography Paper and covered with cling film before vacuum drying at 80°C for 1 h on a Slab Gel Dryer Sr. SE1160 [Hoefer Scientific Instruments]. Dried gels were exposed to photographic Fuji Medical X-Ray Film [Fujifilm] or KODAK™ Biomax® MR 1 Film [Perkin Elmer] for the stated exposure time before developing films using a Curix60 Developer [AGFA].

2.2.20 Mass spectrometry

Instant Blue stained gel pieces were excised, cut into smaller segments using a scalpel and placed into 200 µl H_2O. Mass spectrometry was carried out by the Warwick/Waters Centre for Biomedical Mass Spectrometry and Proteomics facility within the School of Life Sciences, University of Warwick. The gel sample was processed and digested by trypsin according to the MassPrep robotic protein handling system manufacturer's instructions. Peptides extracted from each sample were analysed by nanoLC-ESI-MS/MS using the NanoAcquity/Synapt HDMS instrumentation and a 45 minute LC gradient. Data was corrected for mass drift using reference data from the Human [Glu^1]-Fibrinopeptide B [Sigma] sampled for each minute of data collection. Resulting data was used to interrogate the UniProt databases (http://www.ebi.ac.uk/integr8) using ProteinLynx Global Server v2.4. Proteins identified from the database search were presented in an Excel document.

2.2.21 Confocal microscopy

Prior to transfection, HeLa cells were seeded into 12-well plates containing 16 mm glass cover-slips. Following transfection, cell media was removed and cells were fixed for 10 min with 10% (v/v) liquid formalin diluted in PBS and permeabilised with 0.5% (v/v) NP40 in PBS for 10 min. Non-specific binding was blocked by treating cells with 10 mg/ml BSA in PBS for 1 h. Cells were washed in PBS before incubation with primary antibody for 1 h diluted 1:500 in 1% BSA PBS. Following washes in PBS, cells were incubated for 1 h with a secondary Alexa Fluor® antibody [Invitrogen] diluted 1:500 in PBS with 1% BSA. Incubation steps were repeated with subsequent primary and secondary antibodies to target additional proteins. DAPI nuclear stain [Sigma] at 1 µg/ml in PBS was applied for 5 min. Slides were mounted using Vectashield® Mounting Medium [Vector Laboratories] and sealed using clear nail varnish before viewing on a SP2 confocal microscope [Leica Microsystems].

2.2.22 Reverse transcription: making cDNA

For qPCR experiments, between 2-4 µg of Trizol extracted RNA was DNase treated to remove template DNA. cDNA was produced from 500 ng RNA using the High Capacity RNA-to-cDNA kit [Applied Biosystems] according to the manufacturer's recommendations. Reactions were carried out in a TC-3000 Personal 25-well Thermal Cycler [Techne] with the following conditions: 60 min at 37°C, 5 min at 95°C, reactions held at 4°C.

2.2.23 PCR

For PCR, 50 ng plasmid template DNA or 1 µl of cDNA were amplified by 30 cycles of PCR using 20 µM forward and reverse primers and 2x Biomix [Bioline]. Reactions were carried out in a TC-3000 Personal 25-well Thermal Cycler [Techne] with the following conditions: denaturation for 2 min at 96°C, 30 cycles of: 1 min at 96°C, 1 min at 55°, 2 min at 72°C and a final extension at 72°C for 10 min.

2.2.24 Quantitative real-time PCR (qPCR)

qPCR master mixes were prepared in a MicroAmp® Optical 96-well Reaction Plate [Applied Biosystems] with 2x Fast SYBR® Green Master Mix [Applied Biosystems] according to the manufacturer's recommendations. Plates were sealed with an Optical Adhesive Cover [Applied Biosystems]. Master mixes contained 20 µM forward and reverse primers and 2 µl reverse transcribed cDNA template in a total reaction volume of 20 µl. Amplification of cDNA was carried out by real-time quantitative PCR and detected using an ABI 7000 Sequence Detection System [Applied Biosystems]. Gene expression was normalised to housekeeping genes and samples were run alongside RT negative cDNA (produced without reverse transcriptase) and H_2O controls. Data was evaluated using 7500 Fast System SDS Sequence Detection Software (version 1.4) [Applied Biosystems] with a threshold bar setting of 1.00; results were exported into an Excel document for further analysis.

2.2.25 Denaturing RNA gel electrophoresis

Denaturing gels were prepared using 1% nuclease-free Agarose-LE [Ambion], 6% formaldehyde and 10x MOPS gel running buffer [Ambion] diluted to a total volume of 20 ml in DEPC-treated water. Samples were added to 3x loading dye [Ambion] (with 10% β-mercaptoethanol) and heated to 65°C for 15 min before loading onto the gel. A 5x ssRNA Millenium marker [Ambion] was loaded alongside samples for sizing. Electrophoresis was carried out at 30 mA in 1x MOPS running buffer [Ambion].

2.2.26 DNA agarose gel electrophoresis

Unless otherwise stated, agarose gels were prepared using 0.75% agarose [Gibco-BRL] in 1x TBE buffer with 0.02% ethidium bromide [Sigma]. Samples to be separated by gel electrophoresis were mixed with 6x DNA loading dye (0.625% SDS, 62.5% glycerol, 0.125% bromophenol blue) and loaded onto the gel. Electrophoresis was carried out at 30 mA in 1x TBE buffer and gels were visualised using UV illumination. A 1 kb DNA ladder [Invitrogen] was used to size fragments.

2.2.27 Gel extraction of DNA and purification of restriction digests

The correct fragment on a 0.75% agarose gel was viewed on a Transilluminator 4000 UV light box [Stratagene], excised with a scalpel and purified using a QIAquick Gel Extraction Kit [Qiagen] according to the recommended procedure.

2.2.28 Restriction enzyme digests

PCR DNA digestion: 25 µl of PCR product was digested with a restriction enzyme for 2 h according to the manufacturer's instructions. DNA was isolated by phenol extraction.

Plasmid digestion and dephosphorylation: 5 µg of plasmid was typically digested with 2 µl restriction enzyme for 2 h according to the manufacturer's instructions. After 2 h, an additional 2 µl of enzyme was added and the reaction incubated for a further 2 h. Plasmids digested for use as vectors in ligation reactions were dephosphorylated to prevent self-ligation by treatment of the entire restriction digest volume with 1 µl calf intestinal alkaline phosphatase (CIAP) in 10x NEBuffer 3 [NEB] at 37°C for 15 min, according to the manufacturer's instructions. DNA was isolated by phenol extraction.

2.2.29 Ligation

Restriction digested inserts and plasmids were ligated at a molar ratio of 3:1 insert: vector with T4 DNA ligase [NEB] at 16°C overnight in accordance with the manufacturer's instructions.

2.2.30 Transformation of *E.Coli* and purification of bacterial DNA

50 µl of *E.coli* TG1 competent bacteria were transformed with 5 µl ligation reaction or 1 µl plasmid DNA. Reactions were incubated on ice for 20 min before heat-shock at 42°C for 45 sec followed by placement on ice for 1 min. 200 µl SOC was added to each sample and the bacteria incubated for 1 h at 37ºC. 200 µl bacteria were plated onto selective LB plates containing ampicillin at 100 µg/ml and incubated at 37ºC overnight.

Provirus DNA was transformed into TOP10F cells according to the manufacturer's recommendations [Invitrogen] and plates incubated at 30ºC for 24 h.

2.2.31 Sequencing

250 ng DNA samples were sequenced in a 10 µl reaction volume with 5.5 pmol T7 primer. Sequencing was carried out in house on a PRISM 3130XL Genetic Analyser [Applied Biosystems].

2.2.32 DNA Miniprep

Resulting colonies from transformations were grown up in 2 ml LB-medium supplemented with 100 µg/ml ampicillin. After growth overnight at 37°C in an Orbital Incubator [Gallenkamp], each culture was decanted into a 1.5 ml Eppendorf and centrifuged for 2 min at 13,000 rpm. The supernatant was discarded and bacterial DNA extracted using reagents from the Plasmid Maxi Kit [Qiagen]: the pellet was resuspended in 100 µl P1, 100 µl P2 and 100 µl P3 sequentially, inverting the Eppendorf after each addition. DNA was extracted using phenol/chloroform.

2.2.33 DNA Maxiprep

For large scale plasmid preparation, transformed bacterial colonies were isolated and initially incubated for 5 h in 2 ml LB-medium supplemented with 100 µg/ml ampicillin before transferring 50 µl of the resulting culture into a 1 litre conical flask, containing 250 ml LB-medium with 100 µg/ml ampicillin, and incubating overnight. Incubations were carried out at 37°C in an Orbital Incubator [Gallenkamp] or 30°C for amplification of provirus DNA in TOP10F cells. Cultures were centrifuged for 10 min at 5,000 rpm in a JA10 Rotor [Beckman] to pellet bacterial cells and bacterial DNA was purified using the Plasmid Maxi Kit [Qiagen] according to the manufacturer's instructions. Centrifugation steps were carried out with a JA20 Rotor [Beckman] and DNA was eluted in 400 µl H_2O and stored at -20ºC.

2.2.34 Making HeLa cell extract

HeLa S10 extract [a gift from Professor Richard Jackson] was adjusted to 0.5 M KCl by dropwise addition. Following 30 min incubation on ice, the extract was layered onto a 5 ml glycerol cushion (25% glycerol, 0.5 M KCl, 20 mM MOPS pH 7.2, 6 mM $Mg(OAc)_2$, 2 mM EGTA, 2 mM DTT). After centrifugation for 3.5 h at 28,000 rpm, 4°C, in a Beckman XL-70 Ultracentrifuge with a SW40Ti rotor [Beckman], extract was dialyzed in 3 ml (10K) Slide-A-Lyzer G2 Dialysis Cassettes [Thermo Scientific] against H100 buffer (20 mM HEPES pH 7.5, 100 mM KCl, 2 mM DTT) overnight at 4°C. The resulting HeLa S100 extract was stored at -80°C.

2.2.35 UV cross-linking

The MW of HIV RNA binding proteins were determined by UV cross-linking. Each 10 µl reaction was incubated for 15 min at 30ºC in a 96-well, U-Bottom, Flexible Plate [BD Falcon™] with 2 µl HeLa S100 extract, 1 mg/ml tRNA, 0.1 M KCl and 2 µl α-^{32}P UTP labelled RNA in binding buffer (at a final concentration of 10 mM HEPES pH 7.5, 3 mM $MgCl_2$, 5% glycerol, 1 mM DTT). Non-specific, specific or unlabelled RNA competitors were added at specified molar excess ratios. Samples were kept on ice and cross-linked by exposure to UV light at 3x 0.800 J/cm^2 using a UV cross-linker CL-E508 [Uvitec]. Unbound RNA was degraded with 4 µl of RNase mix: 10 mg/ml RNaseA and Cobra venom RNase V_1 [Ambion] diluted 1/30 in buffer (at a final concentration of 10 mM Tris/HCl pH 7.8, 1 mM $MgCl_2$, 100 mM KCl) for 15 min at 37°C. 15 µl 2x SDS sample buffer was added and samples boiled at 100°C for 5 min. Protein-RNA complexes were separated by 10% SDS-PAGE alongside 10 µl of PageRuler Plus™ Prestained Protein Ladder [Fermentas]. The resolved gel was Coomassie stained and destained before vacuum drying at 80°C for 1 h. Protein-RNA complexes were identified by autoradiography and sized by comparison to the protein marker.

2.2.36 UV cross-linking and La immunoprecipitation (Protein G agarose)

UV cross linking was carried out using HeLa S100 extract, followed by La immunoprecipitation. 400 µl NET Buffer (50 mM Tris pH 7.6, 150 mM NaCl,

0.01% NP40) and 1 µl La antibody [Santa Cruz Biotechnology, Inc.] were added to each UV cross-linking reaction and incubated for 1 h at 4°C. Precipitated proteins were pelleted by centrifugation at 8,000 rpm for 2 min. A 50% slurry of hydrated Protein G agarose beads [Sigma] washed in 1 ml NET buffer (150 mM NaCl, 1 mM EDTA, 50 mM Tris pH 8) was added to each sample and incubated on a Spiramix 5 tube rotator [Denley] for 20 min at 4°C. Beads were centrifuged at 13,000 rpm for 1 min; the supernatant was discarded and the pellet was washed 3 times with RIPA buffer (1% NP40, 0.5% sodium deoxycholate, 0.1% SDS, 150 mM NaCl, 50 mM Tris pH 7.8). The pellet was resuspended in 25 µl 2x SDS sample buffer before heating at 100°C for 5 min. Precipitated proteins were separated by SDS-PAGE; the gel was subsequently Coomassie stained, destained, vacuum dried at 80°C for 1 h and exposed to Fuji Medical X-Ray Film [Fujifilm].

2.2.37 La immunoprecipitation (Dynabeads)

La immunoprecipitation was carried out using recombinant La [Prospec-Tany Technogene Ltd] and HeLa cell extract. 1.5 mg of magnetic Dynabeads® Protein G [Invitrogen] were removed from solution by placing on a MagnaRack™ [Invitrogen] and used in a binding assay with 2 µg mouse anti-La antibody [Santa Cruz Biotechnology, Inc.] at rt, for 10 min with rotation on a Spiramix 5 tube rotator [Denley]. Beads were placed on the magnet and the supernatant discarded. The remaining bead-antibody complex was washed by gentle pipetting in 200 µl PBS with (0.02%) Tween (PBS-T) followed by 2 washes in 200 µl conjugation buffer (20 mM sodium phosphate, 0.15 M NaCl). The supernatant was discarded by placing the beads on a magnet and beads resuspended in 250 µl 5 mM BS^3 (bis[sulfosuccinimidyl] suberate) [Thermo Scientific] at rt, for 30 min with rotation. 12.5 µl Quenching buffer (1 M Tris HCl pH 7.5) was added for 15 min at rt with rotation, before washing beads 3x with 200 µl PBS-T; beads were placed on the magnet and the supernatant discarded each time. Antigen samples: 10 µl HeLa S100 extract or 1 µg Recombinant Human La protein [Prospec-Tany Technogene Ltd] in 200 µl PBS were added to the beads and incubated at rt for 30 min to allow antigen-antibody binding. The bead-Ab-Ag complex was washed 3x in 200 µl PBS; the supernatant was separated by magnet and discarded between

each wash. 100 µl PBS was added to each sample, which was removed to a clean Eppendorf for elution. After discarding the supernatant, 20 µl 2x SDS sample buffer was added to samples which were heated to 100°C for 5 min. Eluted protein samples were separated from beads using magnetism and resolved by SDS-PAGE.

Additionally, UV cross-linking reaction samples were used for La immunoprecipitation. Following UV cross-linking, and prior to the addition of SDS, samples were, instead, diluted in 200 µl PBS and added as antigen samples to this stage of the immunoprecipitation protocol.

2.2.38 RNA affinity chromatography (RAC)

Magnetic Dynabeads® M-280 Streptavidin [Invitrogen] were vortexed and placed on a MagnaRack^{TM} [Invitrogen] to allow aspiration of the supernatant. Beads were prepared for RNA binding by washing in twice the bead volume of Binding & Washing buffer (10 mM Tris HCl pH 7.5, 1 mM EDTA, 2 M NaCl) for a total of 3 washes, Solution A (0.1 M NaOH, 0.05 M NaCl) for a total of 2 washes and Solution B (0.1 M NaCl) for 2 washes. Solution B was removed from the beads which were then resuspended in twice the bead volume of Binding & Washing buffer. Beads were incubated with an equal volume of diluted biotin RNA (2 pmol RNA/µl beads) for 1 h at rt on a Spiramix 5 tube rotator [Denley]. The supernatant was removed by placing the sample on the magnet. Biotinylated RNA coated beads were washed 2 times with Binding & Washing buffer and added to a protein binding reaction containing 2 µl HeLa extract S100, Binding buffer (at a final concentration of 10 mM HEPES pH 7.5, 3 mM $MgCl_2$, 5% glycerol, 1 mM DTT), 1 mg/ml tRNA and 0.1 M KCl. Protein binding was carried out for 1 h at 30°C. Beads were washed with increasing concentrations of NaCl in PBS to elute RNA-bound proteins. After each wash, biotin RNA-bead-protein complexes were isolated by placing samples on the magnet and the supernatant wash fraction removed to a clean tube. After several washes, the beads were resuspended in 20 µl 2x SDS sample buffer to elute any remaining RNA-bound proteins. 10 µl wash fractions were added to 10 µl SDS, heated at 100°C for 5 min, and resolved

by SDS-PAGE, or fractions were used in UV cross linking to identify RNA binding proteins.

CHAPTER 3: TRANSCRIPTION AND NUCLEAR EXPORT OF HIV GAG-POL MRNA

3.1 Introduction

Various stages of the viral life cycle may differ between HIV-1 and HIV-2 and thus contribute to the lower rate of replication witnessed for HIV-2. This chapter addresses the potential differences in HIV-1/2 transcription and the export of full-length viral RNA from the nucleus to the cytoplasm. Both of these steps, if attenuated, may prove rate-limiting for the production of viral particles; lowered mRNA synthesis and inefficient mRNA export would result in a limited supply of viral RNA in the cytoplasm for the translation of viral proteins and genome packaging. Consequently, we wanted to address whether HIV-2 has a reduced transcription rate or inefficient export when compared to HIV-1.

Firstly, this chapter discusses already noted differences between the HIV-1 and HIV-2 viruses which may account for transcriptional or export variations. Considerations of potential HIV RNA degradation pathways, affecting both nuclear and cytoplasmic viral RNA levels, are made. Actinomycin D and leptomycin B are introduced as investigative tools to shutdown transcription and RNA export respectively, to examine HIV-1/2 RNA degradation rates. Finally, quantitative real-time RT-PCR results are presented showing a comparison of HIV-1/2 mRNA levels in total cell lysate, nuclear and cytoplasmic fractions in order to assess the level of HIV-1/2 mRNA transcription and export.

3.1.1 HIV-1/2 transcription

Although it is recognized that individuals infected with the HIV-2 virus exhibit significantly slower disease progression, the mechanisms responsible for this attenuated pathogenicity remain unclear. The level of viral RNA in the blood is much lower during a HIV-2 infection compared to HIV-1. However, both HIV-1 and HIV-2 are able to establish stable integration of proviral DNA. Consequently, this suggests that the production of viral mRNA may be attenuated for HIV-2 (MacNeil *et al.*, 2007).

There are several features of HIV-2, which differ from HIV-1 and, moreover, which could potentially affect the way in which it undergoes transcription. The HIV-1 long terminal repeat (LTR) contains two binding sites for the transcriptional enhancer NFκB (nuclear factor kappa B) whereas the equivalent region of the HIV-2 LTR contains only one conserved NFκB binding site. T-cell activation signals were shown to initiate a better response from the HIV-1 LTR than for HIV-2 due to the qualitative difference in LTR transcriptional enhancer regions (Tong-Starksen *et al.*, 1990). Thus the immediacy of transcriptional activation may differ between HIV-1 and HIV-2.

HIV transcription is regulated by both the interaction of cellular factors with the HIV LTR and binding of the viral *trans*-activator protein Tat to the TAR structure, also found within the HIV LTR. HIV-1 and HIV-2 Tat bind with similar efficiency to their respective TAR structures. Additionally, both HIV-1/2 Tat proteins have been shown to bind interchangeably with HIV-1/2 TAR structures (Dillon *et al.*, 1990). However, HIV-2 Tat is a weaker activator of the HIV-1 TAR than HIV-1 Tat. Consequently, the binding properties of HIV-1 and HIV-2 TAR may differ, and thus their interactions with cellular transcription factors may also differ. Subsequently, there are apparent differences in the mechanisms by which HIV-1 and HIV-2 Tat assert their *trans*-activation functions (García-Martínez *et al.*, 1995).

HIV-1 TAR extends from nucleotides 1-59 of the HIV-1 5’ UTR whereas HIV-2 TAR presents an extended structure which occupies nucleotides 1-123 of the HIV-2 5’ UTR. Essentially, HIV-2 TAR appears to be a duplication of the HIV-1 TAR structure; each HIV-2 TAR stem-loop consists of a bulge and 6 nucleotide conserved loop similar to the HIV-1 TAR [figure 28] (García-Martínez *et al.*, 1995).

Transcriptional activation of HIV-1 relies on Tat interactions with the nucleotide bulge of HIV TAR RNA, and the additional binding of cellular factors; TAK and TRP-185. The role of TAK (consisting of CyclinT_1 and CDK9 components) in Tat-activated transcription is discussed in detail in Chapter 1. TRP-185 is a TAR-RNA binding protein which regulates binding of RNA polymerase II to TAR during transcription (Wu, F. *et al.*, 1991). TRP-185

has been shown to interact with the CUGGGA loop sequence (nucleotides 30-35) of the HIV-1 TAR structure. Loop sequences (CUGGGA and CUGGGU) within the HIV-2 TAR structure closely resemble the HIV-1 CUGGGA loop sequence and therefore TRP-185 may also bind to HIV-2 TAR. Differences in the *trans*-activation of HIV-1 and HIV-2 may be further enhanced by variations in associations with TRP-185, RNA polymerase II or additional elongation factors (García-Martínez *et al.*, 1995).

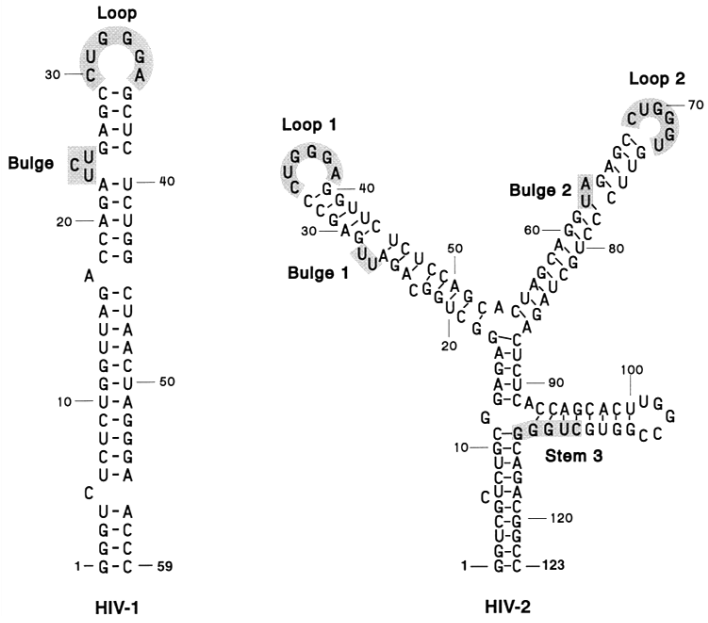

Figure 28: The stem-loop structures of HIV-1 and HIV-2 TAR showing regions of similarity regarding the loop and bulge sequences. HIV-2 TAR appears to be a duplication of the HIV-1 TAR structure (García-Martínez *et al.*, 1995).

An assessment of the transcriptional rate of both HIV-1 and HIV-2 can be undertaken by proviral transfection. This negates rate-limiting stages such as virus entry, reverse transcription and integration which occur prior to transcription in the virus life cycle and could also affect the overall rate of mRNA production post-infection. The level of viral RNA can be easily quantified using real-time RT-PCR (qPCR) which is both a sensitive and accurate means of measuring gene expression. Many qPCR detection methods have been developed, although the most commonly used non-specific detection dye is SYBR® Green. SYBR® Green intercalates with dsDNA and emits fluorescence. The amount of fluorescence from incorporated dye is directly proportional to the amount of DNA and therefore

provides an indication of the number of DNA copies. Changes in SYBR® Green fluorescence can thus be monitored using a thermocycler detector, and the number of cycles taken to reach a threshold fluorescence level provides a measure of the starting cDNA level.

To measure RNA levels a two-step reaction is required, whereby all RNA is first reverse transcribed into cDNA before carrying out qPCR using specific primers for the target gene. During each PCR cycle, the amount of DNA is doubled. Therefore an exponential increase in products is observed until one of the reaction reagents becomes limiting, whereupon a plateau is reached. Comparing the number of cycles (Ct) taken to reach a threshold level of fluorescence (within the exponential range) provides a means to compare the starting levels of cDNA. The more abundant a target is, the quicker it is amplified to the threshold level; this is reflected by a lower Ct value. As the target DNA is amplified exponentially, a cycle difference of a single Ct therefore corresponds to a two-fold difference in DNA quantity [http://www.eurogentec.com/uploads/qPCR-guide.pdf]. Overall qPCR provides a system whereby the HIV-1/2 RNA levels within cells can be quantified and compared in an environment which reflects the natural progression of gene expression during an actual infection.

3.1.2 Nuclear export of full-length HIV-1/2 mRNA

Early HIV transcripts are spliced by cellular machinery. The majority of cellular mRNAs are very efficiently spliced. However, splicing of HIV transcripts is less efficient and results in alternative splicing of viral mRNA. Many of the HIV transcripts contain introns which, for cellular mRNA, would usually be spliced. The presence of introns would normally preclude nucleocytoplasmic transport of HIV mRNA or incorrect splicing would target these mRNAs for degradation via the exosome. However, HIV expresses a regulatory factor, Rev, which functions to prevent degradation of incompletely spliced viral transcripts such as the full-length, viral RNA. Virally encoded Rev is translated from multiply-spliced viral mRNA in the cytoplasm, and imported into the cell nucleus. Here it binds to the Rev response element (RRE) which is present on all intron-containing HIV transcripts. Binding of

Rev to the RRE stabilises viral mRNA and facilitates its transport to the cytoplasm via the CRM-1 export pathway (see Chapter 1) (Blissenbach *et al.*, 2010; Malim and Cullen, 1993).

The HIV-1 RRE is a 334 nucleotide region present within the *env* coding region. A similar RNA structure is present within HIV-2 *env*. Multiply-spliced HIV mRNAs no longer contain the RRE, which is necessary for export of unspliced or partially spliced transcripts. The HIV-1 Rev protein is able to interact with both the HIV-1 and HIV-2 RRE. However, the same is not true for HIV-2 Rev which can only function with the HIV-2 RRE. Nonreciprocal Rev-RRE binding results from the HIV-2 Rev protein, which is unable to stably interact with the HIV-1 RRE. The phosphorylation level of HIV-1 Rev is higher than for HIV-2 Rev although it remains unclear as to whether this influences the Rev-RRE interaction as Rev phosphorylation is not thought to correlate with Rev function (Dillon *et al.*, 1990). Consequently, differences in the HIV-1/2 Rev-RRE interaction may affect the efficiency with which viral mRNAs are exported from the nucleus.

3.1.3 HIV-1/2 mRNA degradation

The level of viral RNA within the cell is not merely a product of mRNA synthesis. In order to assess the level of HIV transcript synthesis it is important to consider other factors which may alter mRNA levels such as RNA degradation. mRNA degradation is important in regulating gene expression and therefore is a prevalent part of normal gene expression. Transcribed precursor mRNA is subject to processing and extensive quality control checks before nucleus-cytoplasm transport occurs. Both viral and cellular mRNA undergoes capping, polyadenylation and splicing to remove introns; if any of these stages produce erroneous mRNA, the mRNA is degraded.

The nucleus contains an exosome which is responsible for inducing the degradation of mRNAs (Raijmakers *et al.*, 2004). Additionally, spliceosome associated mRNAs which have failed to splice correctly are retained in the nucleus by Mlp1 and subsequently degraded by the nuclear exosome. Furthermore, the exosome core, in conjunction with Rrp6p, prevents mRNAs

lacking, or with an excessive poly(A) tail from undergoing nuclear export (Raijmakers *et al.*, 2004).

In the cytoplasm, incorrectly spliced mRNAs may contain a premature stop codon and therefore undergo nonsense mediated decay (NMD); Upf1 recruits these mRNAs to the cytoplasmic exosome where they are sequestered into mRNA turnover pathways in order to inhibit their translation. Successfully produced mRNAs are translated several times before they, too, are directed for degradation (Raijmakers *et al.*, 2004). The normal mRNA turnover pathway induces 3'-5' removal of the mRNA poly(A), which stabilises mRNA, and degradation by exoribonucleases within the exosome. Additionally, removal of the 5' cap structure by hydrolysis permits subsequent 5'-3' mRNA degradation by the exoribonuclease hXrn1. Lsm1 is also important in transcript degradation following shortening of the poly(A) tail, and recruitment of the decapping enzyme (Slomovic *et al.*, 2010).

HIV-1 infection also stimulates cellular mRNA degradation although it is unknown whether HIV proteins directly function as nucleases or whether they induce degradation through activation of cellular ribonucleases. SIV infected cells do not activate cellular mRNA degradation. As HIV-2 is more closely related to SIV, it is therefore possible that this feature of HIV-1 infection is not present during a HIV-2 infection. Thus HIV-1 infection may promote preferential translation of its own, viral mRNA by inducing degradation of competitive, cellular mRNAs whereas HIV-2 may not be able to enhance translation of its own mRNA via the same mechanism (Agy *et al.*, 1996).

The transcriptional inhibitor, actinomycin D (actD), provides an approach to studying mRNA degradation. ActD is an antibiotic typically used in the treatment of cancer. It non-specifically inhibits cellular proliferation by binding to deoxyguanosine within dsDNA. DNA-actD complexes prevent transcription by inhibiting DNA-primed RNA synthesis by RNA polymerase (Imamichi *et al.*, 2005). It has also been reported that actD can produce single-strand breaks within DNA which disrupts transcription (Kang and Park, 2009). The inhibitory activities of actD make it a useful tool for observing the cellular effects of transcriptional shutdown. Likewise, it provides a means to quantify

RNA degradation levels without interference from continued mRNA synthesis.

Previous experiments have utilised actD to assess the effect of this drug on HIV virion mRNA levels. Treating HIV-1 infected Jurkat (T-lymphocyte) cells with actD results in a decrease in the level of virion RNA, reflecting the decline in cytoplasmic mRNA levels resulting from transcriptional shutdown. Following HIV-2 infection of Jurkat cells, viral mRNA levels were shown to be more stable even at higher concentrations of actD although the level of virion mRNA still reflected the cytoplasmic level of viral mRNA. This suggests that HIV-2 mRNA may be more stable than HIV-1 mRNA (Dorman and Lever, 2000).

Shutting down CRM-1 dependent nuclear export also provides a means to assess viral RNA degradation. Leptomycin B (lepB) is often used as a means to do this. LepB is an antibiotic metabolite derived from *Streptomyces*. Typically, lepB is used in the treatment of tumours. It was shown that treating HIV-1 infected Jurkat cells with lepB lowered the levels of both viral and cellular cytoplasmic mRNA. However, HIV-2 infected cells treated with lepB maintained a relatively constant level of cytoplasmic mRNA, even when the dosage of lepB was doubled. Consequently, HIV-2 Rev-dependent export may not be susceptible to inhibition by lepB (Dorman and Lever, 2000). Further work is necessary to quantify and characterise the potential differences between the export of HIV-1/2 RNA.

It remains unknown as to the extent to which HIV-1/2 mRNA degradation influences the life cycles of these viruses. Any differences in mRNA stability, or the inadvertent activation of mRNA degradation machinery, may have a substantial impact on gene expression. With regard to this, any differences in transcript stability and consequential degradation may, therefore, contribute to the differing replicative capacity of these viruses. Likewise, to effectively compare the transcription rates of the HIV-1 and HIV-2 viruses, it is necessary to control for mRNA degradation.

3.2 Results

3.2.1 Primer testing: Gag primers

Primers targeting HIV gag genes were designed by Cyril Barbezange. HIV-1 gag forward (1077-1096n) and HIV-1 gag reverse (1230-1249n) primers amplified a 172n region of gag. HIV-2 gag forward (912-931n) and HIV-2 gag reverse (1087-1106n) primers amplified a 194n gag product. To test these primers, HeLa cells were transfected with 580 ng HIV-1/2 provirus in a 6-well plate and total, cytoplasmic and nuclear RNA extracted at 24 h post-transfection. cDNA was produced from reverse transcription of extracted RNA, and used in a PCR with HIV-1 gag (primer #22, 23) and HIV-2 gag (primer #24, 25) primers. PCR products were run on an agarose gel [figure 29].

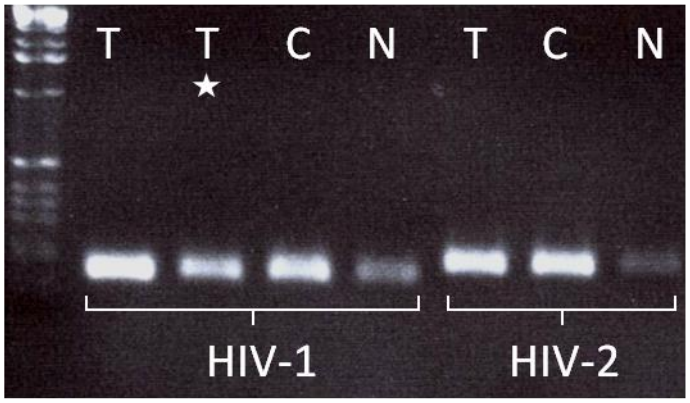

Figure 29: PCR to test HIV gag primers. HIV gag was amplified by RT-PCR from RNA extracted from HIV-1, HIV-2 and HIV-1 MA2 provirus transfections. HIV-1 MA2 is a chimeric provirus with the HIV-1 5' UTR/Gag coding region and the matrix region of HIV-2 (marked with a *). Primers to HIV-1 and HIV-2 gag were used on cDNA samples produced from total (T), cytoplasmic (C) and nuclear (N) RNA.

HIV-1 and HIV-2 gag primers produced the expected fragment sizes (172n and 194n) following RT-PCR. Gag mRNA could be detected in total, nucleus and cytoplasmic RNA samples for both primer sets. Furthermore, HIV-1/2 gag primers did not amplify product from a negative control of untransfected HeLa cell RNA (data not shown). This indicates that these primers are, firstly, amplifying the correct products and, secondly, are sensitive enough to use in a comparison of HIV-1 and HIV-2 gag RNA expression levels following sub-cellular fractionation.

3.2.2 Primer testing: housekeeping primers

Detection of differential gene expression can be accurately determined by qPCR. However, it is necessary to control for any experimental variations which may arise from reagent disparities, dissimilar RNA extraction levels or pipetting error. Consequently, control 'housekeeping' (HK) genes are frequently used to normalize the expression levels of qPCR gene expression data (Barber *et al.*, 2005). Cellular GAPDH (glyceraldehyde-3-phosphate dehydrogenase) is frequently used as a housekeeping gene. Spliced GAPDH mRNA can act as an endogenous, cytoplasmic marker within the cell. Additionally, the unprocessed precursor to GAPDH (pre-GAPDH) provides a nuclear marker (Blissenbach *et al.*, 2010). qPCR results were thus normalised to housekeeping genes; pre-GAPDH for nuclear samples and GAPDH as a cytoplasmic control.

Primers were initially designed by Cyril Barbezange. Forward (947-969n) and reverse (1051-1072n) primers targeting cytoplasmic GAPDH produced a 126n GAPDH fragment. Forward (2833-2851n) and reverse (3019-3039n) primers targeting pre-GAPDH (the unspliced precursor to GAPDH) produced a PCR product of 207n. It was necessary to, firstly, ensure that the housekeeping genes in the nucleus and cytoplasm did not overlap in their detection and, secondly, ensure that the primers were only amplifying the target gene in the correct cell fractions. The expression of GAPDH and pre-GAPDH in total, nuclear and cytoplasmic RNA samples was thus compared. HeLa cells were subjected to sub-cellular fractionation and RNA extracted from total, nucleus and cytoplasm samples. cDNA, produced from extracted RNA, was amplified by PCR using primers to GAPDH (primer #18, 19) and pre-GAPDH (primer #20, 21) and gene expression detected by running PCR samples on an agarose gel [figure 30].

GAPDH was only detected in the cytoplasm and pre-GAPDH was only detected in the nucleus [figure 30]. This indicates that the targets of GAPDH and pre-GAPDH primers were distinct and therefore the primers did not cross-react. These results also confirmed successful sub-cellular fractionation and isolation of separate nuclear and cytoplasmic RNA pools.

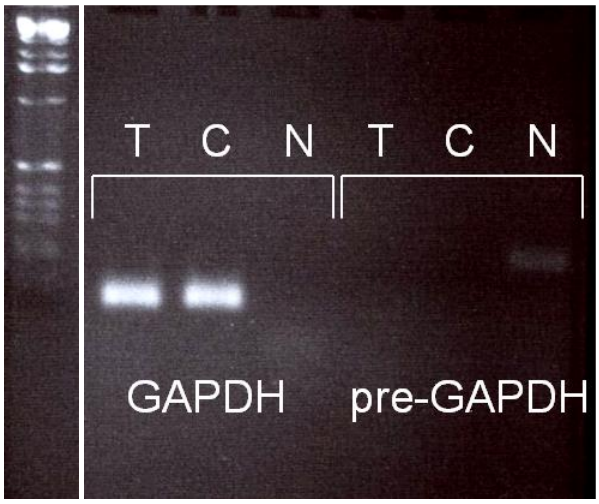

Figure 30: An agarose gel of PCR products showing the expression of GAPDH and pre-GAPDH in RNA extracted from total (T), cytoplasmic (C) and nuclear (N) HeLa cell fractions.

Pre-GAPDH primers did not detect pre-mRNA from total RNA samples. This may be because the levels of pre-mRNA, as a percentage of the total RNA fraction, may be below the detection threshold.

Since GAPDH and pre-GAPDH primers successfully amplified discrete products from the nucleus and cytoplasm, they were suitable for using as housekeeping gene controls for subsequent qPCR experiments.

3.2.3 Optimisation: RT negative samples

For a comparison of HIV-1 and HIV-2 gene expression, cells were transfected with HIV provirus and cellular RNA extracted for qPCR. To accurately compare HIV-1 and HIV-2 transcription, it was necessary to ensure that HIV primers were only detecting cDNA reverse transcribed from viral RNA, and not amplifying the transfected provirus DNA template.

DNase treatment of extracted RNA was optimised to ensure that template DNA was not amplified by PCR. 2-4 µg of total, nuclear or cytoplasmic HIV-1 RNA samples were treated with DNase prior to reverse transcription. This ensured removal of contaminating, transfected proviral DNA. A PCR was carried out using RT+ve and RT-ve (made with/without reverse transcriptase) cDNA samples and primers to HIV-1 gag. Products were run on an agarose gel [figure 31].

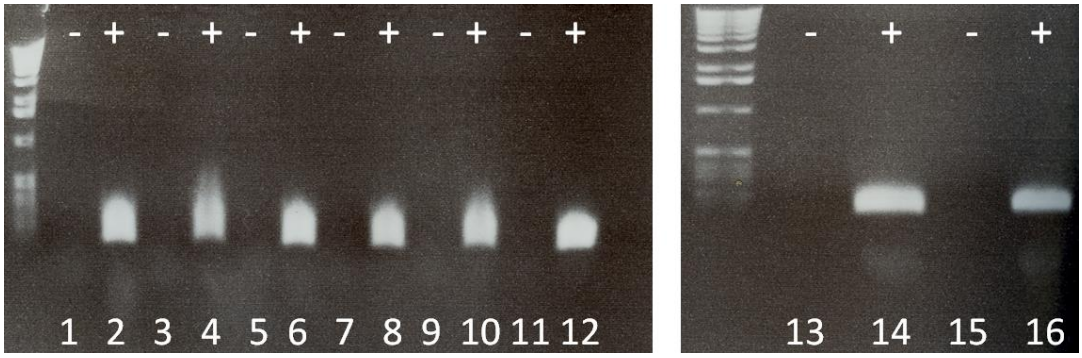

Figure 31: An agarose gel showing pairs of alternate RT–ve (odd # lanes) and RT+ve (even # lanes) cDNA from an RT-PCR of HIV-1 transfection RNA. RNA cellular fractions were used from an actD HeLa cell transfection timecourse. T=0 represents 24 h post-proviral transfection when some cells were treated with actD. Only lanes 1+2 shown were treated with actD. Lanes 1+2: T=0, total RNA (actD), lanes 3+4: T=0, total RNA, lanes 5+6: T=0 cytoplasmic RNA, lanes 7+8: T=0 nuclear RNA, lanes 9+10: T=2 total RNA, lanes 11+12: T=4 total RNA, lanes 13+14: T=6 total RNA, lanes 15+16: T=8 total RNA.

Bands were not detected from RT-ve samples indicating that DNase treatment of extracted RNA was effective at removing transfected plasmid templates. Thus only synthesised RNA was detected in subsequent qPCR experiments.

3.2.4 A comparison of HIV-1 and HIV-2 total RNA levels

HIV-1 and HIV-2 transcription was compared by quantifying the amount of HIV-1/2 gag RNA transcribed from transfected proviral DNA over a time course. HeLa cells were transfected with 580 ng of HIV-1 or HIV-2 provirus for 6, 12, 24 and 48 h and total RNA harvested. Following DNase treatment and reverse transcription, the same quantity of cDNA was used in a qPCR with primers to HIV-1 or HIV-2 gag, in triplicate. Gene expression was normalised to the GAPDH housekeeping gene. qPCR data was analysed by calculating ΔCt. This was done by subtracting the sample Ct from the housekeeping gene Ct produced from the same cDNA (ΔCt = Ct sample – Ct HK). Results were subsequently plotted by raising 2 to the power of ΔCt ($2^{\Delta Ct}$) which accounts for the 2-fold increase in RNA quantity relative to each decrease in Ct. Experiments were repeated twice and graphs were plotted in Excel showing relative HIV-1 and HIV-2 gag RNA levels (as $2^{\Delta Ct}$) in total RNA

for 6, 12, 24 and 48 h time points [figure 32]. Error bars were calculated as the standard error.

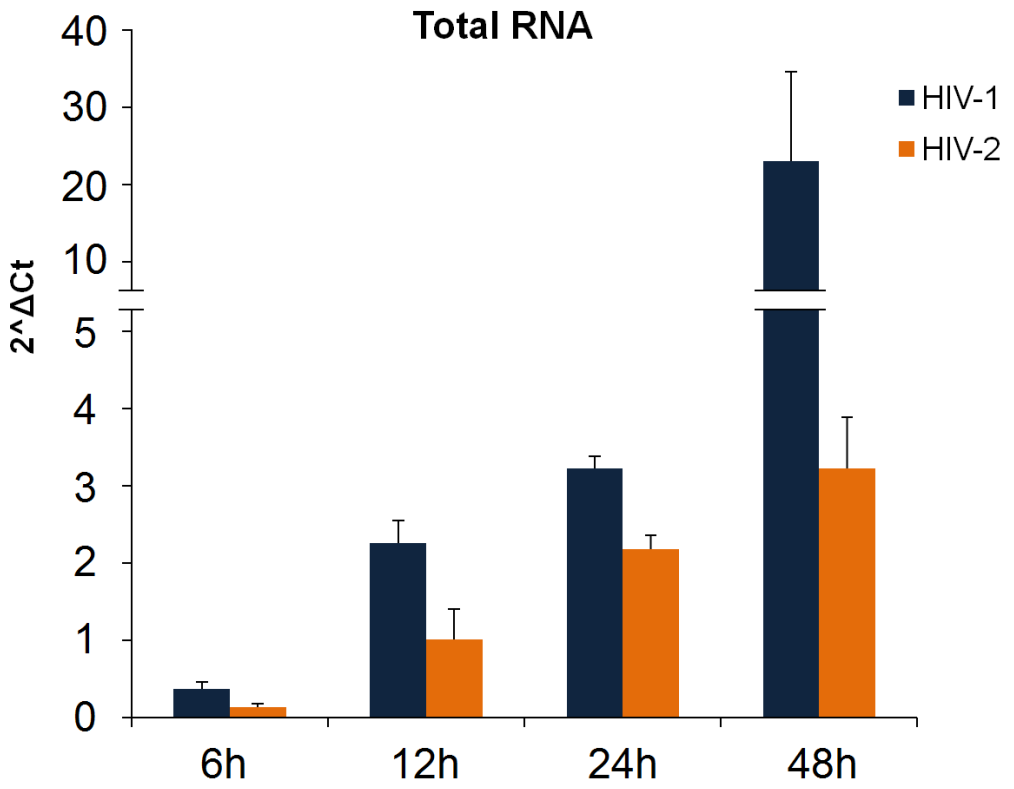

Figure 32: The relative expression levels of HIV-1 gag (blue) and HIV-2 gag (orange) in total RNA (expressed as $2^{\Delta Ct}$) quantified by qPCR from samples extracted following 6, 12, 24 and 48 h HIV-1/2 provirus transfection. Error bars represent the standard error of the mean (SEM)

Both HIV-1 and HIV-2 gag levels steadily increased between 6 and 48 h although HIV-1 gag total RNA levels were higher than HIV-2 gag RNA across the time course. The difference in HIV-1/2 gag RNA levels was particularly noticeable by 48 h where HIV-1 gag RNA levels were 7-fold higher than HIV-2 gag RNA levels, indicating a much higher level of HIV-1 gag mRNA synthesis. These results suggest that HIV-1 transcription is more efficient than HIV-2 as gag mRNA was produced more quickly from transfected HIV-1 provirus.

3.2.5 A comparison of HIV-1 and HIV-2 gag RNA levels in the nucleus and cytoplasm

The level of HIV-1 and HIV-2 gag RNA in the nucleus and cytoplasm was compared at various times post-transfection to assess how quickly gag

mRNA is exported from the nucleus for HIV-1 and HIV-2. HeLa cells were transfected with 580 ng HIV-1 or HIV-2 provirus for 6, 12, 24 and 48 h. After sub-cellular fractionation of harvested cells, RNA was isolated from the nuclear and cytoplasmic fractions. The level of HIV-1/2 gag RNA in each fraction was quantified, in duplicate, by qPCR using primers to HIV-1/2 gag RNA. Results were normalised to a GAPDH housekeeping gene for cytoplasmic fractions and pre-GAPDH for nuclear fractions and RNA levels expressed as $2^{\Delta Ct}$ [figure 33]. Experiments were repeated twice and error bars plotted as the standard error.

There was a noticeable difference in the scale of results from the nucleus and cytoplasm [figure 33]. This is due to expressing viral RNA levels relative to different housekeeping genes; pre-GAPDH RNA (at very low levels) in the nucleus and GAPDH RNA levels (at levels comparable to viral RNA) in the cytoplasm.

In the nucleus, HIV-1 gag RNA levels increased rapidly between 6 h and 12 h post-transfection, before decreasing between 12 h and 48 h [figure 33]. This indicates efficient transcription of HIV-1 mRNA before nuclear export commences to reduce nuclear gag mRNA levels at 12 h post-transfection. HIV-2 gag RNA levels in the nucleus increased more slowly between 6 and 12 h, before decreasing slightly after this time. The 12 h peak in nuclear HIV-2 gag RNA levels was also noticeably lower (by 3.5-fold) than for HIV-1 gag RNA. This suggests that HIV-2 exhibits a slower rate of gag mRNA transcription. In the cytoplasm, HIV-1 gag RNA levels increased steadily across the time course and were consistently higher (by up to 3.8-fold) than HIV-2 gag RNA levels. HIV-2 RNA levels steadily increased in the cytoplasm, although not as rapidly as HIV-1 gag RNA levels. Consequently, HIV-2 mRNA export may be slower than for HIV-1.

Overall, these results suggest that HIV-1 gag RNA builds up more rapidly in the nucleus, and then transitions more quickly from the nucleus to the cytoplasm than HIV-2 gag RNA i.e. HIV-1 transcription and export is more efficient than for HIV-2.

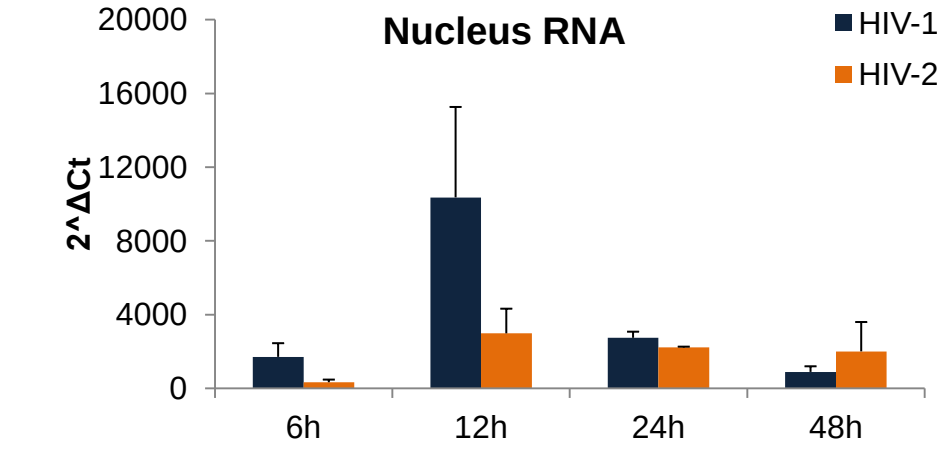

(A)

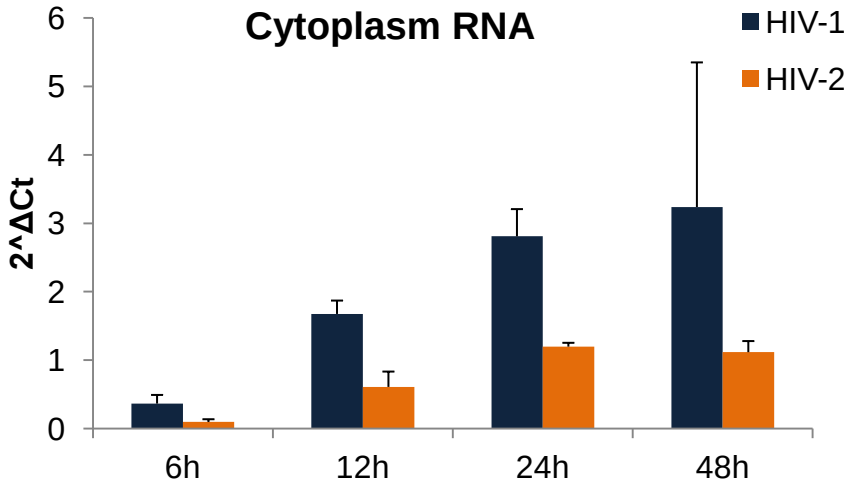

(B)

Figure 33: qPCR data showing the relative expression of HIV-1 (blue) and HIV-2 (orange) gag RNA (expressed as $2^{\Delta Ct}$) in the nucleus (A) and cytoplasm (B) at 6, 12, 24 and 48 h post-proviral transfection. Gag RNA levels are expressed as $2^{\Delta Ct}$ with results normalised to pre-GAPDH (nucleus) and GAPDH (cytoplasm) housekeeping genes. Error bars represent the SEM.

The nucleus:cytoplasm ratio of HIV-1/2 RNA was calculated using the following method:

- *ΔCt* : sample data was normalised to housekeeping genes by calculating ΔCt; the nucleus/cytoplasm Ct value was subtracted from the pre-GAPDH/GAPDH housekeeping gene Ct (ΔCt = Ct sample – Ct HK)
- *ΔΔCt*: calculated by subtracting the cytoplasm ΔΔCt from the nucleus ΔΔCt (ΔΔCt = ΔCt nucleus – ΔCt Cytoplasm)
- Ratio N:C *($2^{\Delta\Delta Ct}$)*: the nucleus to cytoplasm ratio (N:C ratio) was calculated by raising 2 to the power of ΔΔCt ($2^{\Delta\Delta Ct}$) which accounts for the 2-fold increase in RNA quantity relative to each decrease in Ct.

Comparing the N:C ratio of HIV-1 and HIV-2 over time provides an indication of the rate of RNA export from the nucleus to the cytoplasm [figure 34]. A higher N:C ratio value reflects a larger level of HIV RNA in the nucleus and a lower RNA level in the cytoplasm. A decrease in the N:C value represents less RNA in the nucleus and an increase in RNA in the cytoplasm.

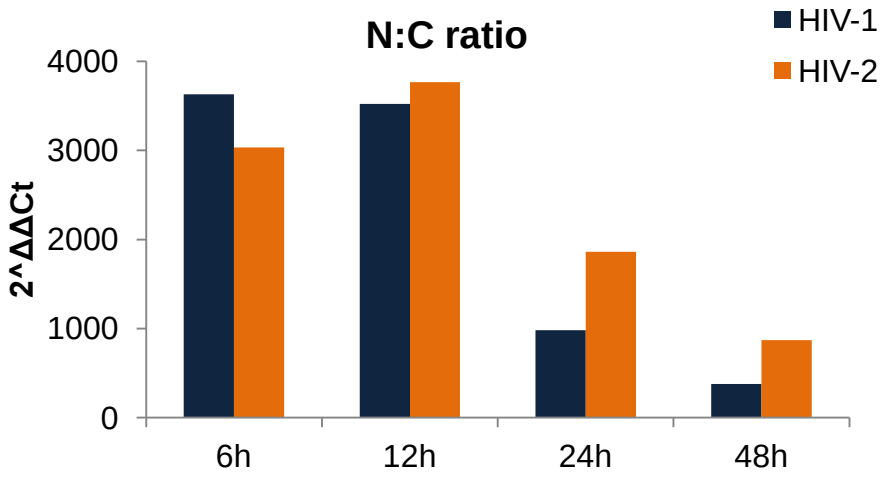

Figure 34: The N:C ratio (expressed as $2^{\Delta\Delta Ct}$) of HIV-1 and HIV-2 gag RNA at 6, 12, 24 and 48h post-proviral transfection of HeLa cells.

The HIV-1 N:C ratio decreased very slightly between 6 and 12 h before dropping dramatically after 12 h. This suggests that initially HIV-1 mRNA was slowly exported from the nucleus. However, after 12 h, HIV-1 mRNA export was more rapid resulting in the dramatic decrease in N:C ratio. Alternatively,

the HIV-2 N:C ratio increased between 6 and 12 h, suggesting nuclear export was slow to initiate. After 12 h the HIV-2 N:C ratio decreased, indicating nuclear export of mRNA, albeit less rapidly than HIV-1. The N:C ratio of HIV-2 did not drop to the same level as HIV-1 even by 48 h. This suggests that HIV-1 gag RNA is exported more quickly to the cytoplasm than HIV-2 gag RNA.

3.2.6 A comparison of HIV-1 and HIV-2 Gag RNA stability

A lower level of HIV-2 RNA in total cell lysate may have been caused by less efficient transcription, increased mRNA degradation, or a combination of the two. Similarly, a lower level of HIV-2 RNA in the cytoplasm may have been caused by inefficient export or an enhanced rate of mRNA degradation. To assess whether differences in RNA stability contribute to lower total and cytoplasmic levels of HIV-2 RNA, a comparison of HIV-1/2 gag RNA stability was made using actD. ActD inhibits mRNA synthesis and therefore provides a means to assess the decline in existing RNA pools due to degradation. HeLa cells were transfected with 580 ng HIV-1/2 provirus and, after 24 h, transcription was shut down by treating cells with 5 µg/ml actD. HIV gag RNA levels from total cell lysate were assayed over a time course 0, 2, 4, 6 and 8 h post-actD treatment (T=0) to assess the rate at which HIV gag RNA levels dropped (i.e. RNA was degraded) in the absence of ongoing RNA synthesis. cDNA was produced from RNA extracted at various time points and qPCR was carried out to quantify viral RNA levels using primers to HIV-1/2 gag and HK genes. Data was normalised to HK genes and $2^{\Delta Ct}$ was calculated for each sample [figure 35].

In the absence of actD, HIV-1 gag RNA levels increased slightly over the time course whereas HIV-2 gag RNA levels remained constant over the 8 h time course [figure 35]. This reflects the enhanced transcriptional rate of HIV-1. Shutdown of transcription using actD resulted in a decrease, after 2 h, of both HIV-1 and HIV-2 gag RNA levels over the time course as existing RNA was degraded.

For the 2 h period after actD treatment (T=0), HIV-1 and HIV-2 Gag RNA levels did not change significantly [figure 35]. During this period it is likely that

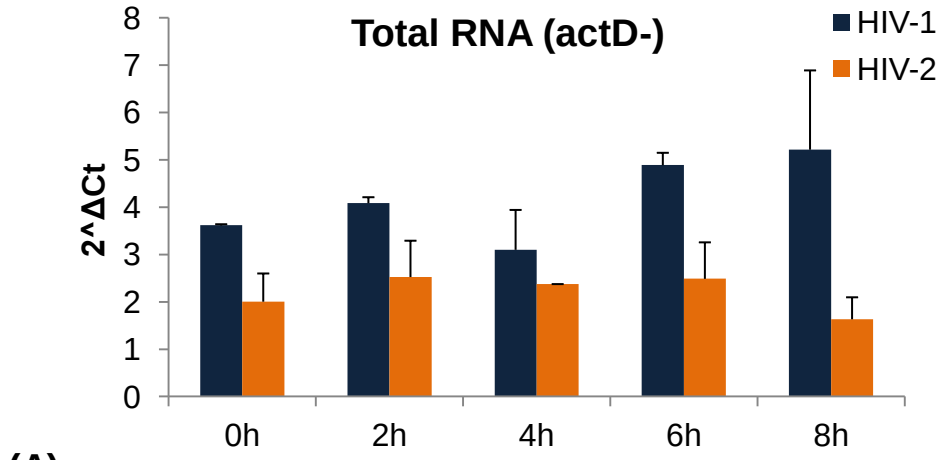

(A)

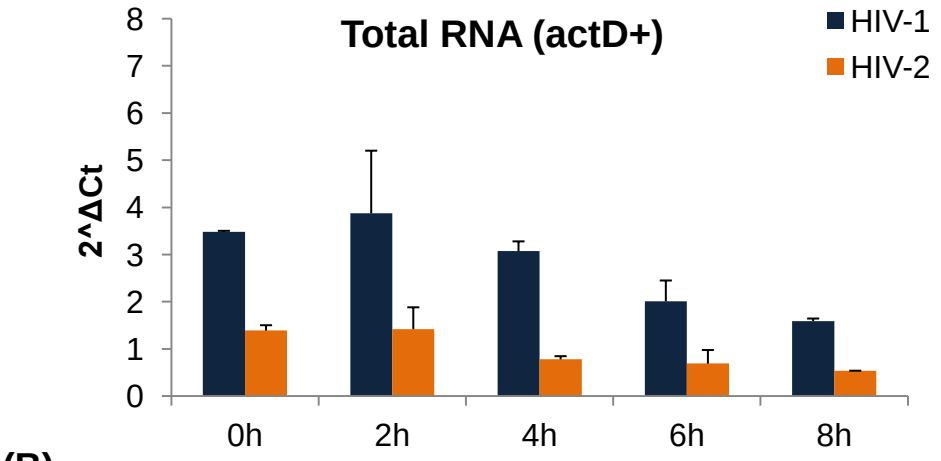

(B)

Figure 35: qPCR results quantifying HIV-1/2 total gag RNA levels (expressed as $2^{\Delta Ct}$) over a time course (0, 2, 4, 6, 8 h) starting 24 h post-provirus transfection (T=0) in the absence (A) or presence (B) of 5 µg/ml actD. Error bars represent the SEM.

transcription was still occurring and the cells were transitioning from a state of being transcriptionally active to transcriptional shutdown. Thus it appears that actD takes a while to exert its effect on the cells resulting in this lag phase.

To compare the decline in HIV-1/2 RNA levels relative to starting levels of RNA, the results were expressed as a percentage of 2 h data [figure 36]. This was because prior to 2 h, when actD treatment was still taking effect, RNA may still have been synthesised.

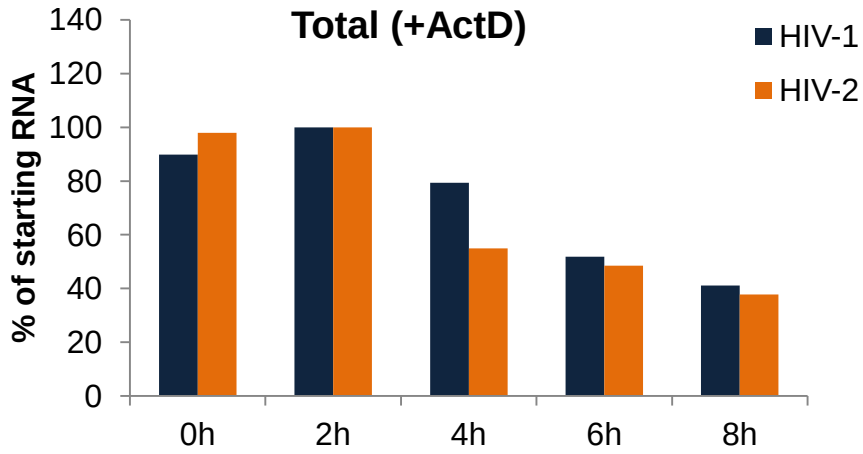

Figure 36: A comparison of total HIV-1/2 RNA levels at each time point after actD treatment expressed as a percentage of the 2 h value.

Both HIV-1 and HIV-2 gag RNA levels declined at a similar rate by 8 h relative to the starting level of RNA. This suggests that HIV-2 RNA is not degraded more rapidly and therefore the higher level of HIV-1 RNA is likely due to more efficient transcription.

The degradation rate of HIV-1/2 gag RNA in the cytoplasmic fraction was also studied to determine whether export differences or degradation rates were responsible for the slower accumulation of HIV-2 gag RNA in the cytoplasm. HIV-1/2 provirus (580 ng) was transfected into HeLa cells for 24 h, prior to the addition of actD. Cells were harvested and fractionated at 0, 2, 4, 6 and 8 h after actD treatment. The level of cytoplasmic HIV gag RNA at each time point, with and without actD treatment, was examined by qPCR.

Data were normalised to the GAPDH HK gene and RNA expression levels calculated as $2^{\Delta Ct}$ [figure 37].

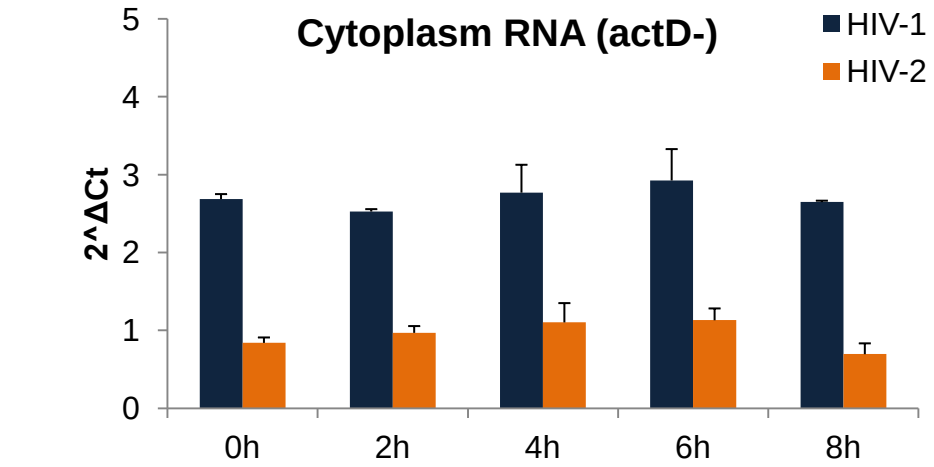

(A)

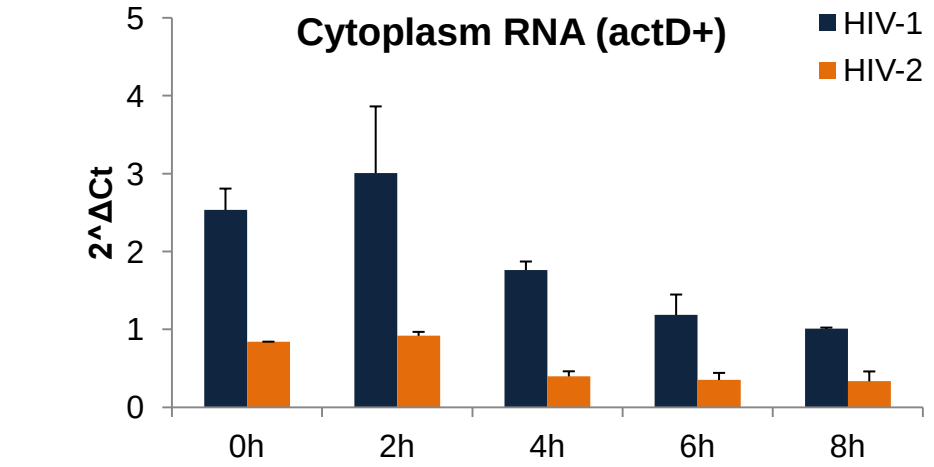

(B)

Figure 37: qPCR results quantifying HIV-1/2 cytoplasmic RNA levels (expressed as $2^{\Delta Ct}$) over a time course (0, 2, 4, 6, 8 h) starting 24 h post-provirus transfection (T=0) in the absence (A) or presence (B) of 5 µg/ml actD. Error bars represent the SEM.

Cytoplasmic HIV-1/2 gag RNA levels did not change significantly over the time course in HeLa cells without actD treatment [figure 37A] although HIV-1 gag RNA levels were consistently higher than HIV-2 gag RNA levels. When transcription was shutdown via actD treatment, both HIV-1 and HIV-2 cytoplasmic gag RNA levels decreased steadily after an initial delay of 2 h [figure 37B]. This suggests that following transcriptional shutdown, both HIV-1 and HIV-2 RNA levels were not maintained (i.e. were degraded) in the cytoplasm.

A comparison of the rate of HIV-1/2 RNA degradation was made by comparing the level of gag RNA, at each time point after actD treatment, to the starting value of HIV-1/2 RNA [figure 38].

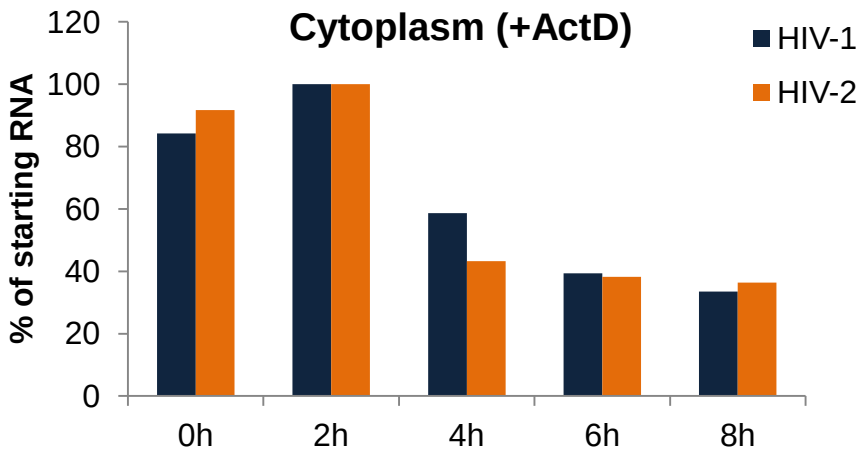

Figure 38: A comparison of the HIV-1/2 cytoplasmic RNA levels at each time point after actD treatment expressed as a percentage of the 2 h value.

Both HIV-1 and HIV-2 RNA levels dropped at an equivalent rate over the time course comparative to their respective starting RNA levels. These results suggest that the rate of HIV-1/2 mRNA degradation is similar, and, consequently, that the slower accumulation of HIV-2 gag RNA in the cytoplasm is due to slower export from the nucleus rather than faster degradation in the cytoplasm.

Leptomycin B (lepB) was also used as a tool to investigate the effect of export shutdown on the stability of cytoplasmic HIV-1/2 gag RNA levels (data not shown). HeLa cells were transfected with HIV-1/2 provirus for 24 h before treating cells with lepB (T=0) to shutdown export. Cells were subsequently harvested at 0, 2, 4, 6, and 8 h post-lepB treatment and total and cytoplasmic RNA isolated. Real-time RT-PCR was carried out using primers to HIV-1 and HIV-2 gag. However, there was very little effect of lepB on cytoplasmic HIV-2 gag RNA levels suggesting that lepB was unable to shut down HIV-2 gag RNA export from the nucleus. HIV-1 gag RNA levels in the cytoplasm did decrease over the time course as expected (Dorman and Lever, 2000). Due to the discrepancy of the effect of lepB on HIV-1/2 gag RNA export, it was not

possible to compare the rate of RNA degradation between these viruses using lepB.

3.3 Discussion

3.3.1 HIV-1 and HIV-2 transcription

Following HIV-1/2 provirus transfection into HeLa cells, the level of cellular HIV-1 gag mRNA produced was greater than for HIV-2 at all time points. This suggests that HIV-1 provirus DNA was transcribed into gag mRNA more efficiently than for HIV-2. Consequently, a reduced availability of HIV-2 mRNA during infection may limit the rate of HIV gene expression and therefore contribute to the lower rate of particle production observed during a HIV-2 infection.

Transcription was shut down using actD to assess the stability of existing HIV-1/2 gag RNA in total pools after this time. The levels of HIV-1/2 gag mRNA, relative to each starting level, decreased comparably indicating that the degradation rates of HIV-1/2 mRNA were equivalent. Therefore the higher level of cellular HIV-1 gag mRNA observed is most likely due to a higher rate of HIV-1 transcription rather than a result of accelerated HIV-2 gag mRNA degradation.

3.3.2 HIV-1 and HIV-2 gag RNA export

To investigate the rate at which HIV-1/2 gag mRNA is synthesised and transitions from the nucleus to the cytoplasm, the level of HIV-1/2 gag mRNA in the nucleus and cytoplasm was compared by sub-cellular fractionation post-provirus transfection. At 6 h and 12 h post-transfection HIV-1 gag RNA levels in the nucleus were higher than HIV-2, reflecting the faster rate of transcription seen for HIV-1. Between 12 and 48 h, the level of HIV-1 gag RNA decreased. Expression of the viral Rev protein promotes increased export of unspliced HIV-1 gag mRNA by enhancing Rev/RRE dependent export of HIV RNA from the nucleus. Consequently, as more Rev is expressed during the viral life cycle, gag mRNA is more efficiently exported from the nucleus. Therefore the decrease in HIV-1 gag mRNA in the nucleus after 12 h likely reflects efficient export of full-length HIV-1 gag RNA to the

cytoplasm via the Rev-RRE pathway. To complement this, the level of HIV-1 viral RNA in the cytoplasm increased over the time course, reflecting the export of synthesised HIV-1 gag RNA from the nucleus.

The amount of HIV mRNA remaining in the nucleus is relative to both the rate of transcription (producing nascent mRNA) and the rate of mRNA export from the nucleus to the cytoplasm (removing mRNA from the nucleus). Assuming the rate of transcription and mRNA degradation are constant over time, if the rate of export is lower than the rate of mRNA transcription (T>E), then mRNA levels in the nucleus will increase, albeit at a lower rate than previous to export commencing. If the rate of mRNA synthesis is equivalent to the rate at which it is exported (T=E), the level of mRNA in the nucleus will remain relatively constant, whereas if the rate of mRNA export exceeds the rate of mRNA transcription (T<E), RNA levels in the nucleus will drop (summarised in figure 39).

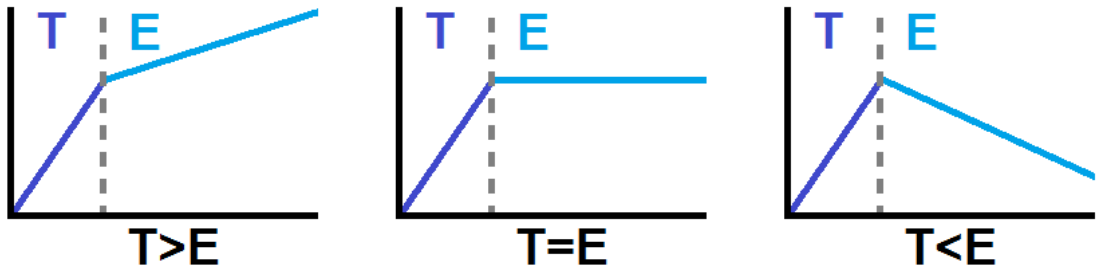

Figure 39: The effect of differing export rates (E) on the level of RNA in the nucleus (blue line) assuming a constant level of transcription (T).

Thus HIV-1 export appears to have been occurring very efficiently as the level of overall RNA in the nucleus dropped after 12 h indicating that HIV-1 Gag RNA export was occurring at a greater rate than Gag RNA synthesis (T<E).

HIV-2 Gag mRNA accumulated much more slowly in the nucleus indicating less efficient transcription. After 12 h, the level of HIV-2 RNA in the nucleus only decreased slightly, rather than decreasing rapidly like HIV-1. This suggests that HIV-2 mRNA was undergoing export at a similar, or only slightly higher, rate to the rate at which it was being synthesised (T=E). The level of HIV-2 transcription was shown to be less efficient than HIV-1.

Therefore, as the export rate was not vastly different to the transcription rate for HIV-2, this suggests that export is equally inefficient for HIV-2 and, additionally, less efficient than for HIV-1.

The N:C ratios for HIV-1 and HIV-2 support these observations. The HIV-1 N:C ratio remained similar 6-12 h post-transfection. During this period the rate of mRNA increase in the nucleus and cytoplasm was the same i.e. mRNA synthesised matched the mRNA export rate (T=E). As HIV-1 transcription was shown to be very efficient, HIV-1 mRNA export must have been reasonably efficient to match the mRNA synthesis rate during this time. The N:C rate for HIV-1 dropped rapidly after 12 h indicating that HIV-1 mRNA was exported more efficiently from the nucleus after this time (T>E). As replication progressed, the presence of more Rev RNA in the nucleus may have served to accelerate the rate of HIV-1 gag mRNA export producing the observed drop in N:C ratio.

The HIV-2 N:C ratio increased initially from 6-12 h indicating that mRNA levels were increasing in the nucleus (via synthesis) but the rate of HIV-2 gag mRNA in the cytoplasm was not increasing by an equivalent amount. This suggests that HIV-2 export was slow to initiate as mRNA transcription levels were greater than the mRNA export rate (T>E). As overall HIV-2 transcription was shown to be inefficient, HIV-2 mRNA export must have been very inefficient (or not occurring) between 6-12 h to result in an increase in HIV-2 mRNA in the nucleus during this time. By 24 h, the HIV-2 N:C ratio started to decrease (T<E), but not to the same extent as for HIV-1, indicating that cytoplasmic HIV-2 RNA levels were not increasing as quickly for HIV-2 as for HIV-1. Consequently, these results suggest that the rate of gag RNA export appears to be much slower for HIV-2.

Increased HIV-2 mRNA instability in the cytoplasm could have resulted in the lower levels of HIV-2 gag mRNA observed. ActD was successfully used to shut down mRNA synthesis and thereby compare the rate at which existing HIV-1/2 mRNA in the cytoplasm was degraded. There was a detectable decrease in the level of both HIV-1/2 viral mRNA in the cytoplasm post-actD treatment indicating degradation. However, following the shutdown of mRNA

synthesis, HIV-1/2 cytoplasmic gag mRNA levels fell by an equivalent rate suggesting that the rate of gag mRNA degradation was the same for both viruses.

It is likely that depletion of nuclear viral RNA occurred via transport to the cytoplasm following transcription shutdown. This may account for the increase in cytoplasmic RNA levels for both HIV-1 and HIV-2 in the 2 h post-actD treatment. As HIV-1 transcription is more efficient than HIV-2, one can hypothesise that more HIV-1 RNA may have been present in the nucleus at the point of transcriptional shutdown. This is reflected by the greater peak in HIV-1 RNA appearing in the cytoplasm at T=2; potentially due to export of a larger quantity of HIV-1 RNA from the nucleus. If anything, these results therefore suggest that HIV-1 RNA may be degraded more quickly in the cytoplasm than HIV-2 to result in more similar levels by 8 h. Either way, these findings indicate that a greater rate of HIV-2 gag RNA degradation does not cause the lowered cytoplasmic levels of HIV-2 gag RNA seen in the cytoplasm. Consequently, we put forward the idea that HIV-2 export is much less efficient than HIV-1 export and, in conjunction with a lowered rate of HIV-2 transcription, accounts for the reduced levels of HIV-2 gag RNA found in the cytoplasm.

Overall, results indicate that both HIV gag mRNA transcription and export are less efficient for HIV-2 than for HIV-1. Inefficiencies within mRNA transcription and export may thus contribute to the lower rate of viral particle production observed for HIV-2 infected individuals by limiting the rate of gene expression and thus the availability of components required for virion assembly.

3.3.3 Controls and drawbacks

Despite normalising qPCR data to a generic control, even common housekeeping genes such as GAPDH show variations in expression levels. As a result, although normalising to housekeeping genes can improve the accuracy of gene expression date, no perfect control to validate data exists (Barber *et al.*, 2005).

However, further work could be carried out to improve the accuracy of current experiments. The actual number of HIV-1/2 RNA copies could be calculated by comparing qPCR values to a standard curve of known RNA concentration. This would provide a more accurate reading of differences in HIV-1/2 RNA levels in sub-cellular fractions and thereby provide a means to quantify differences in HIV-1/2 transcription and export rates. Better controls are also required to affirm that HIV-1/2 gag mRNA primers bind with equal efficiency to their target RNAs.

qPCR is highly sensitive and therefore results are susceptible to contamination. A study by Blissenbach *et al.* (2010) was carried out to compare pre-mRNA levels in nuclear and cytoplasmic extracts following sub-cellular fractionation. Extracted cytoplasmic RNA was shown to contain 3% of RNA derived from the nucleus. Assuming that pre-mRNA is exclusively present in the nucleus, this indicates that, during processing, cytoplasmic RNA fractions can be contaminated with nuclear RNA. This highlights a possible factor which may affect the consistency of qPCR data from samples which have undergone sub-cellular fractionation (Blissenbach *et al.*, 2010). Measuring the level of pre-mRNA expression in nuclear RNA samples and comparing this to the level of pre-mRNA in cytoplasmic RNA samples by qPCR would identify the extent of this error.

Furthermore, difficulties in normalising qPCR results occur when cells are treated with inhibitory agents such as actD or lepB. Shutting down cellular transcription or export not only affects the target genes of interest, but also alters cellular mechanisms. This could prove detrimental to the cell and also alter the expression of housekeeping genes which are used as controls for these experiments. For example, inhibiting cellular transcription can block GAPDH synthesis and, additionally, interfere with the production of spliceosome, export or exosome-associated proteins necessary for the successful nuclear processing and export of GAPDH mRNA. All of these additional factors will affect the qPCR data produced concerning overall viral RNA levels. Consequently, it is very difficult to precisely isolate one stage of gene expression within a biological system without inadvertent consequence to other processes.

As an alternative to RNA degradation, viral RNA may, additionally, have been removed from the cytoplasm by packaging of gag mRNA into viral particles as genomic RNA. Our assay does not account for the deficit of viral RNA in the cytoplasm which may be induced by RNA incorporation into viral particles. However, Dorman et al. (2000) reported that the amount of viral RNA in the cytoplasm is proportional to the rate at which it is packaged (Dorman and Lever, 2000). HIV-2 does not demonstrate more efficient particle production than HIV-1 (Popper *et al.*, 2000) and our experiments have shown that HIV-2 RNA is inefficiently transcribed (limiting the supply of cytoplasmic RNA). In view of this, it is unlikely that enhanced packaging of viral RNA contributes to the lower HIV-2 cytoplasmic RNA levels observed.

3.3.4 Future work

Overall, the results presented in this chapter suggest that HIV-1 gag RNA is transcribed with greater efficiency than HIV-2 gag RNA. Additionally, the export of HIV-2 gag RNA is less efficient than HIV-1 gag RNA export. The culmination of these results is that a lower level of HIV-2 gag RNA is observed in both the nucleus and cytoplasm following proviral transcription. The factors prompting more efficient HIV-1 transcription and mRNA export remain unclear. Future work will look to elucidate the factors enhancing HIV-1 or restricting HIV-2 transcription. Likewise, inhibition of export by leptomycin B appeared to affect HIV-1 export to a greater extent than HIV-2 export. This suggests that HIV-2 gag RNA export may require alternative pathways to HIV-1 gag RNA or, instead, may rely on factors that are not affected by leptomycin B-induced export inhibition. Therefore, further work is required to determine the mechanisms of HIV-1/2 export and examine how these differ to limit the rate of HIV-2 mRNA export.

Recent research has shown that the HIV-2 5’ UTR contains a 142 nucleotide intron which, when spliced, removes part of the 5’ UTR spanning from halfway through TAR to the C-box region and including the entire poly (A) signal [figure 40] (Strong *et al.*, 2009). HIV-2 transcripts lacking the 5’ UTR intron showed a 5’ fold increase in translation efficiency. Spliced mRNA was not found to be incorporated into virus particles as it lacks a packaging

signal. The transition between translation and packaging may therefore be controlled by the presentation of the packaging signal on unspliced 5' UTR mRNA (Strong *et al.*, 2009).

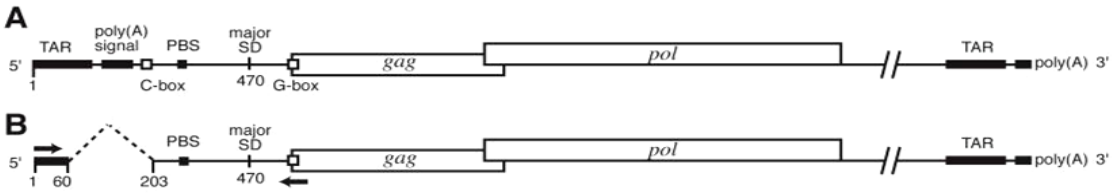

Figure 40: The HIV-2 5' UTR (A) can undergo splicing to remove a 142 nucleotide intron which includes part of TAR, all of the poly(A) signal and the C-box region (B) (Strong *et al.*, 2009).

Although both spliced and unspliced HIV-2 mRNA variants have been identified within infected cells, the sub-cellular localisation and relative abundance of these transcript variants has not been determined. Identifying whether HIV-2 spliced transcripts are exported more quickly from the nucleus may provide an indication of the temporal regulation of gene expression for HIV-2. Furthermore, quantifying the contribution of spliced HIV-2 mRNA to the overall mRNA pool in both the nucleus and cell cytoplasm may suggest a role for these variants in the regulation of HIV-2 gene expression.

Future work will therefore look to quantify the contribution of spliced and unspliced HIV-2 mRNAs in total, nuclear and cytoplasmic cellular fractions, as well as assessing the stability of spliced and unspliced transcripts. Quantifying the relative level of HIV-2 mRNAs in sub-cellular fractions will allow us to see whether there is any difference in the export of spliced and unspliced transcripts. We detected both spliced and unspliced variants of HIV-2 gag RNA in a PCR of cDNA from HIV-2 provirus transfections [figure 41].

Using a primer spanning the splice site, or primers solely within the intron, would allow specific detection of spliced or unspliced HIV-2 gag transcripts respectively. Work is underway to design and verify such primers, and use

them in qPCR experiments to assess the levels of spliced and unspliced HIV-2 gag RNAs in provirus-transfected cells.

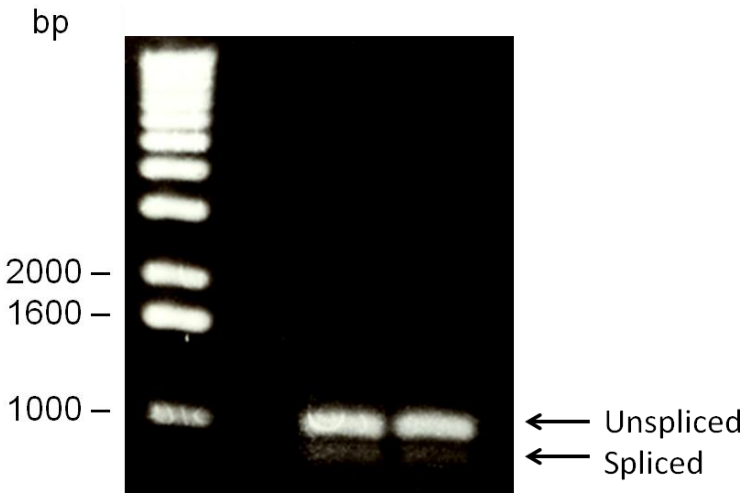

Figure 41: RT-PCR of total RNA extracted from HIV-2 provirus transfected HeLa cells. Primers at the start of the HIV-2 5' UTR and within *gag* were used to amplify both spliced and unspliced HIV-2 transcript variants. The sample was halved and run in duplicate on the gel.

CHAPTER 4: HIV GAG TRANSLATION

4.1 Introduction

In this chapter an overview of eukaryotic translation is presented. Cap-dependent and IRES-driven translation are introduced, followed by a discussion on how the 5' UTR structure affects translation, and an overview of the translational attributes of HIV-1 and HIV-2. Finally, the factors regulating HIV translation are discussed before presenting results. My work establishes translational differences between HIV-1 and HIV-2 both *in vitro* and in cells. Translation of both HIV-1 and HIV-2 Gag is shown to be cap-dependent with little evidence of IRES activity. However, HIV-1 appears to be more reliant on cap-dependent translation than HIV-2, indicating that differences in translational initiation mechanisms may effect variations in the rate of HIV-1/2 translation. Based on the composition of Gag, we propose that elongation rates between HIV-1/2 Gag are likely to be similar. We suggest that the extended HIV-2 5' UTR, and the intrinsic level of structure, is likely to contribute to translational initiation differences between HIV-1/2. Attempts to characterise the origins of translational differences between HIV-1 and HIV-2 are discussed.

4.1.1 Eukaryotic translation: cap-dependent initiation

HIV mRNA hijacks the host translational machinery and is therefore translated in the same way as eukaryotic cellular mRNA. Translation can be separated into three stages: initiation, elongation and termination. The efficiency with which eukaryotic mRNA is translated is dependent on the rate of translation initiation. mRNA has several structural features, including a 5' cap and a 50-300 nucleotide 3' poly(A) tail, which enhance translation initiation (Mathews *et al.*, 2007). Additionally, at least 12 initiation factors (eIFs) are involved in translation initiation in eukaryotes (Mathews *et al.*, 2007). Although important for translation initiation, in the absence of a 5' cap structure, translation initiation can still commence in a 5' end dependent manner and, like cap-dependent translation, is reliant on the scanning mechanism of the 40S ribosomal subunit. Highly stable secondary structures,

such as those found within the HIV 5' UTR, can impair ribosomal scanning and thus decrease the rate of translation initiation (Mathews *et al.*, 2007).

During translation initiation, the mRNA poly(A) tail is bound by poly(A) binding protein (PABP) which interacts with the eIF4F cap-binding complex [figure 42] (Mathews *et al.*, 2007). Binding of eIF4F (a eukaryotic initiation factor composed of eIF4E, eIF4A and eIF4G) to the m^7GpppN cap structure located at the 5' end of mRNA initiates formation of an mRNA complex (Mathews *et al.*, 2007). eIF4E is the cap-binding component of the eIF4F complex and is therefore necessary for cap-dependent translation (López-Lastra *et al.*, 2005). eIF4A is a member of the DEAD-box family and functions as an ATPase and RNA helicase to unwind RNA secondary structure. This requires ATP (Lamphear *et al.*, 1993). The RNA helicase activity of eIF4A is enhanced more than 20-fold by its incorporation into the eIF4F complex (Mathews *et al.*, 2007). Both eIF4G and a RNA-binding protein, eIF4B, can stimulate the weak helicase activity eIF4A. Scaffold proteins eIF4GI and eIF4GII (referred to commonly as eIF4G) direct construction of the translation initiation complex which culminates in associating mRNA with the translational machinery (López-Lastra *et al.*, 2005).

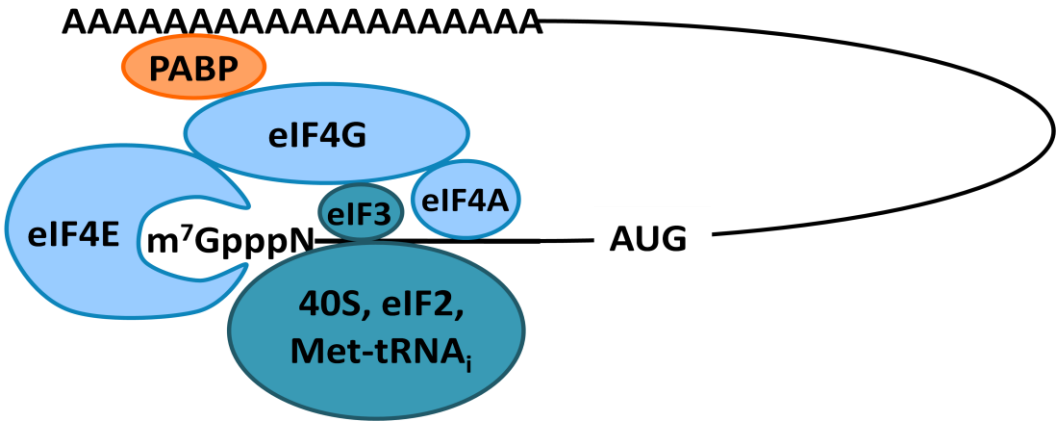

Figure 42: A (closed loop) model of translation initiation. The eIF4F complex (comprised of eIF4G, eIF4A and eIF4E) associates with the 5' mRNA cap (m^7GpppN) via eIF4E, the poly(A) tail via PABP and the 40S ribosomal subunit via eIF3 [adapted from (López-Lastra *et al.*, 2005)].

Formation of a 43S pre-initiation complex occurs when eIF2 recruits Met-$tRNA_i^{Met}$ to the P site located on the 40S ribosomal subunit. Thus the P site

of the 40S ribosomal subunit carries a methionyl-transfer RNA (Met-$tRNA_i^{Met}$)-eIF2-GTP complex to start translation (López-Lastra *et al.*, 2005). The 43S complex associates with the 5' end of the mRNA with the help of eIF2 and eIF3 (Lapointe and Brakier-Gingras, 2003). The 40S ribosomal subunit associates with eIF3, which in turn interacts with the eIF4G subunit of eIF4F, and facilitates attachment of 40S to the 5' end of the mRNA. Binding of the 43S pre-initiation complex to mRNA results in a 43S-mRNA complex which is ready to undergo ribosomal scanning [figure 43].

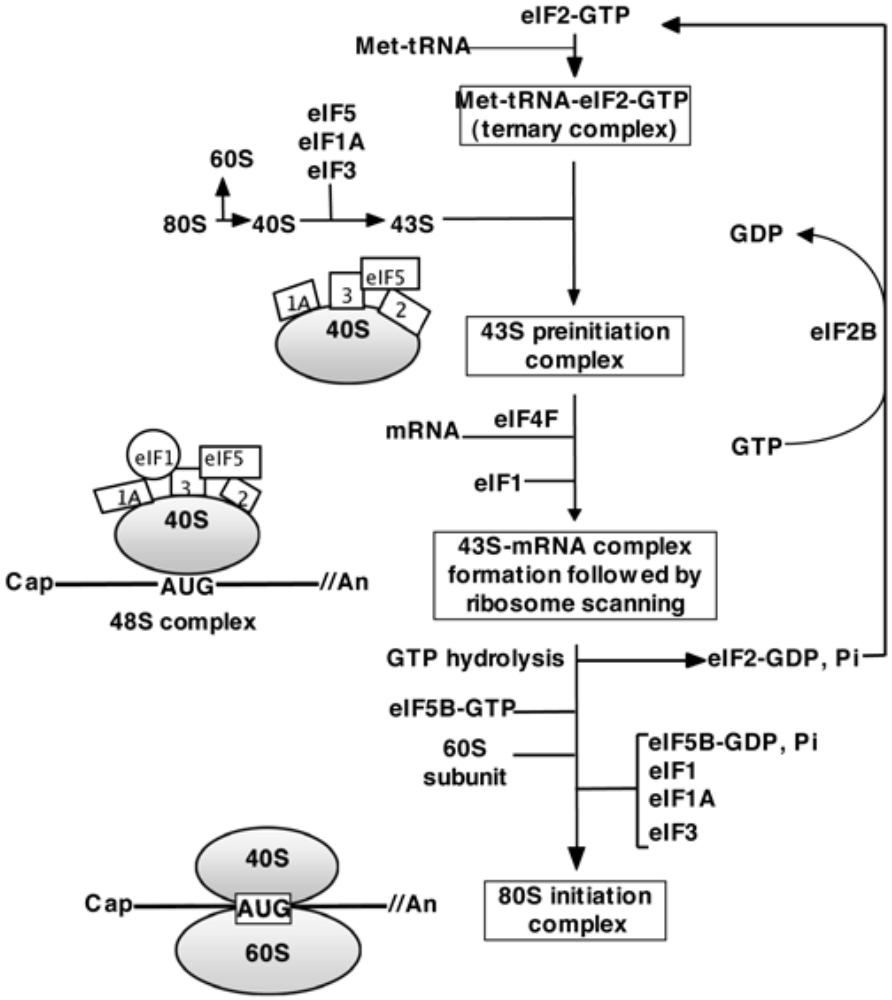

Figure 43: Initiation of translation in eukaryotes (López-Lastra *et al.*, 2005).

Further factors, eIF1 and eIF1A, bind to mRNA and facilitate 5'-3' directional transport of the 43S complex along the mRNA to the initiation codon. eIF4F-dependent binding of mRNA to the 43S pre-initiation complex is enhanced by eIF1A. Subsequently, 40S commences scanning along the mRNA until it

reaches an AUG start codon. This requires energy provided by ATP. Translation initiation is optimal when the AUG start codon is in the context of a flanking Kozak sequence: GCC**(A/G)**CCAUG**G** (with key nucleotides shown in bold). Deviations at the -3 and +4 positions can result in leaky scanning and the use of alternative, suboptimal start codons. Lower efficiency initiation can occur at codons CUG, GUG and UUG, and is reliant on flanking sequences (Weill *et al.*, 2010). Additionally, the presence of a downstream 12-15 nucleotide hairpin structure can enhance translation initiation by stalling scanning of the 40S ribosomal subunit (Mathews *et al.*, 2007).

Once the 43S complex encounters an initiation codon, eIF1 promotes base-pairing of the initiator tRNA anticodon to the AUG start codon, forming a 48S complex which primes translation. The initiator tRNA anticodon is usually the CAU anticodon of eIF2-associated Met-$tRNA_i^{Met}$ located in the 40S ribosome P site (López-Lastra *et al.*, 2005). Following base-pairing of Met-$tRNA_i^{Met}$ and the AUG start codon, eIF5 promotes the hydrolysis of GTP within the initiation complex. This facilitates the release of eIF2 and other associated initiation factors from the ribosomal 40S subunit; a necessary step to allow joining of the ribosomal subunits (Das, S. and Maitra, 2001). eIF5B is a GTPase which promotes binding of the 60S ribosomal subunit to 40S (Lee *et al.*, 2002). The resulting 80S ribosome forms an active translation complex which can undergo elongation (Mathews *et al.*, 2007).

4.1.2 IRES-driven translation initiation

An alternative to cap-dependent translation is internal initiation. Ribosomes may be recruited to an internal site in the 5’ UTR of mRNA, independently of the 5’ end, usually by a structured RNA element called an internal ribosome entry site (IRES) (Buck *et al.*, 2001; Lapointe and Brakier-Gingras, 2003). IRES were first discovered in picornaviruses (Jang *et al.*, 1988; Pelletier and Sonenberg, 1988) and subsequently in a number of other viruses such as cricket paralysis virus, hepatitis C virus and classical swine fever virus (Pestova *et al.*, 1998; Wilson *et al.*, 2000) as well as retroviruses (Brasey *et*

al., 2003; Buck *et al.*, 2001; Herbreteau *et al.*, 2005; Miele *et al.*, 1996; Ohlmann *et al.*, 2000) and cellular mRNAs (Komar and Hatzoglou, 2005).

An IRES is thought to form a stable structure that is recognised by the 40S ribosomal subunit and/or associated initiation factors. Binding of IRES *trans*-acting factors (ITAFs) may stabilise the IRES structure or provide protein interaction sites for 40S or initiation factors (Vallejos *et al.*, 2011). It has been shown that mutations which disrupt the IRES structure dramatically reduce IRES function (Mathews *et al.*, 2007).

Internal initiation allows ribosomes to by-pass some of the requirements for cap-dependent translation, such as components of the eIF4F complex, enabling translation of mRNAs with long, structured 5' UTRs, or upstream AUG codons (Mathews *et al.*, 2007). Several viruses shut down cellular, cap-dependent translation e.g. by cleavage of eIF4G (Glaser *et al.*, 2003) but maintain viral protein synthesis via internal initiation. Similarly, many of the cellular IRES-containing mRNAs are expressed under conditions where cap-dependent translation is unfavourable such as during the G_2/M phase of the cell cycle (Buck *et al.*, 2001) during nutrient limitation, apoptosis, mitosis or hypoxia (Komar and Hatzoglou, 2011).

4.1.3 Eukaryotic translation: elongation

During translation, the ribosome functions to decode genetic information into a polypeptide chain. This process occurs in a 5'-3' direction along the mRNA and requires continual processing of amino-acyl tRNAs by the ribosome active site, which catalyses the formation of a peptide bond between associated peptides [figure 44]. Amino-acyl tRNAs carry amino acids defined by the anticodon they present. The order of amino acids incorporated into the nascent polypeptide chain is defined by the sequence of triplet nucleotide codons within the mRNA (Rospert *et al.*, 2005).

The accuracy of translation is important to limit errors in the synthesised protein product. Events such as amino acid misincorporation (Zaher and Green, 2009), frameshifting, and read through of stop codons can lead to errors in translation (Proud, 1994). Cellular factors such as elongation factor-

1 (eEF1) assist translation. eEF1 is composed of two subunits; eEF1α and eEF1β. In the presence of GTP, eEF1α binds to amino-acyl tRNAs forming a ternary complex of eEF1α-GTP and amino-acetyl tRNA.

Initially, a tRNA carrying methionine (initiator Met-tRNA$_i^{Met}$) binds loosely to the mRNA start codon (AUG) in the ribosome P site [figure 44A].

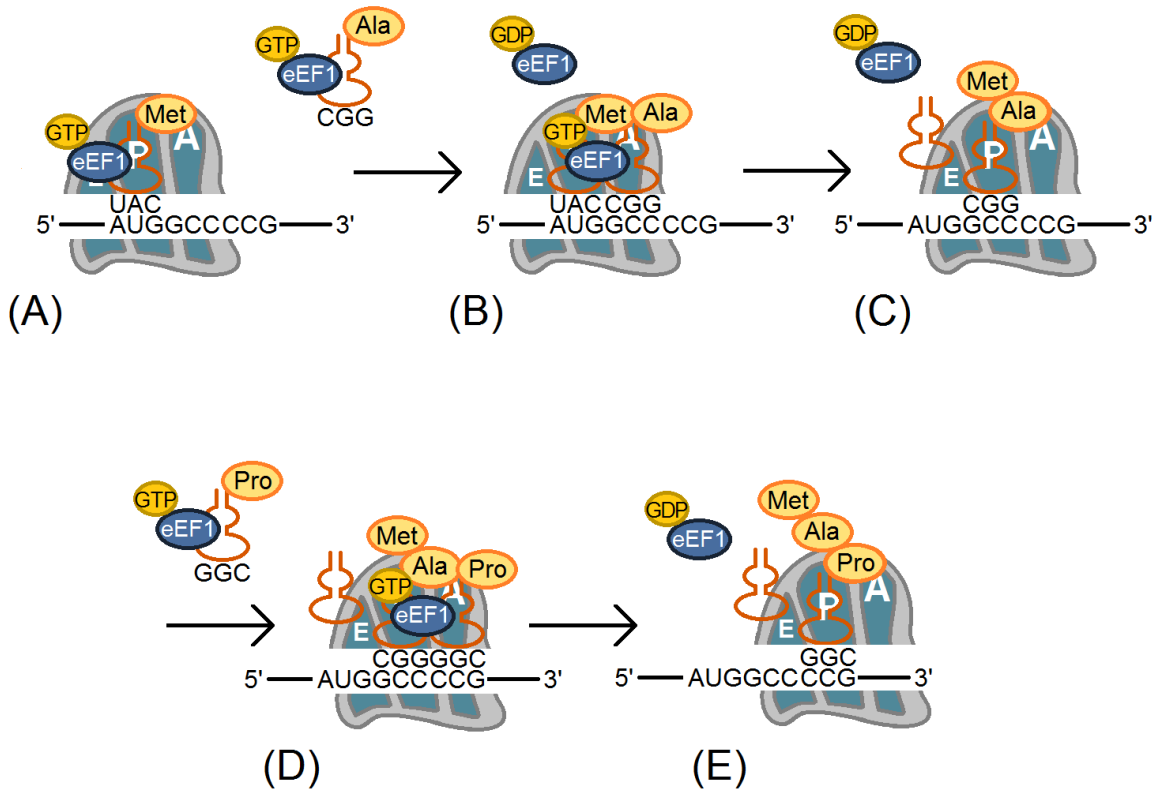

Figure 44: An overview of translation initiation and elongation [Image adapted from http://www.nobelprize.org/educational/medicine/dna/a/translation/elongation.html].

Subsequently, amino-acyl tRNAs, carrying specific anticodon-determined amino acids enter the ribosome A site [figure 44B]. If the amino-acyl tRNA anticodon is complementary to the mRNA codon, a peptide bond is catalysed between the amino acid on the incoming peptidyl tRNA and the amino acid of the previous peptidyl tRNA now in the ribosome P site [figure 44C]. The peptidyl transferase activity of the ribosome catalyses this reaction. Once the peptide it is carrying has been incorporated into the nascent polypeptide chain, the empty tRNA relocates to the ribosome P site, freeing the A site for incoming peptidyl tRNAs. This occurs simultaneously with the ribosome advancing 3 nucleotides (one codon) along the mRNA each time, moving the

uncharged tRNA out of the P site into the E site (Proud, 1994). Cyclical repetition of amino-acyl tRNA positioning at the A site [figure 44D], peptide bond formation and ribosome shifting along the mRNA results in stepwise addition of amino acids to the emerging polypeptide chain [figure 44E]. eEF1α-GTP is hydrolysed during elongation resulting in eEF1α-GDP. Consequently, a guanine nucleotide exchange factor converts eEF1α-GDP to eEF1α-GTP to allow recycling of eEF1α-GTP for continued elongation.

4.1.4 Eukaryotic translation: termination

The final stage of translation, termination, is triggered by the presence of an in-frame stop codon (UAA, UAG or UGA) in the ribosome A site (Sund *et al.*, 2010). Eukaryotic release factors (eRF) and GTP are important in termination. eRF1 recognises stop codons within mRNA and induces activation of the ribosome peptidyl centre (RPC). The RPC triggers release of the newly synthesised peptide by hydrolysing the ester bond linking it to the terminal tRNA. As part of this mechanism, eRF1 occupies the A site of the ribosome where it functions as a tRNA. A GTPase, eRF3, enhances eRF1 function (Moreira *et al.*, 2002). Termination is catalysed by ribosomal RNA and results in the release of the completed, nascent peptide (Rospert *et al.*, 2005). Following termination, the translational machinery disassembles and can reform to initiate translation on other mRNAs. Several ribosomes can simultaneously synthesise protein from the same mRNA by temporal binding and initiation. Multiple ribosomes translating the same mRNA are called polysomes; the number of bound ribosomes determines the polysome size (Zouridis and Hatzimanikatis, 2007).

4.1.5 Eukaryotic translation: regulation

The rate of translation can be regulated by many factors such as the availability of nutrients, stress, cell cycle adjustments and viral infection (Gale *et al.*, 2000). Control of gene expression is achieved on a cellular level by modulating the assembly of components involved in the mRNA cap-binding complex. Thus, the expression of mRNAs can be regulated by phosphorylation or dephosphorylation of translation factors (Lapointe and Brakier-Gingras, 2003). Likewise, binding of eukaryotic mRNAs to various

cytoplasmic proteins can mediate nuclear export, alter mRNA stability, promote sub-cellular localisation or bring about translational repression (Mathews *et al.*, 2007). Changes to the cellular environment can also affect the mechanism of translation utilised, and thus cause a switch between translation initiation mechanisms (Ricci *et al.*, 2008). For example, during infection viral proteins produced may alter translation rates. The human rhinovirus 2 (HRV-2) genome encodes a cysteine protease, 2A, which is self-processed by autocatalytic cleavage from the HRV-2 viral polyprotein VP1. 2A has been shown to cleave both isoforms of eIF4G in rabbit reticulocyte lysate (RRL). Since eIF4G forms part of the eIF4F complex which is involved in recruiting capped mRNAs to the 40S ribosomal subunit, HRV-2 infection shuts down cap-dependent translation. Likewise, poliovirus also encodes a 2A protease which cleaves eIF4G directly, as well as indirectly via the activation of cellular proteases (Glaser *et al.*, 2003).

Non-standard translation events such as alternative initiation events (IRES-driven translation, ribosomal shunting and leaky scanning), frameshifting, stop codon read-through and re-initiation can also regulate protein synthesis. Secondary structure within mRNA can affect ribosomal scanning and induce non-standard translation events thus reducing the rate of protein synthesis.

The intrinsic properties of translated genes can also affect the rate of elongation. The genetic code is degenerate therefore amino acids can be encoded by more than one codon. However, within the human genome, some codons are rarer than others resulting in the concept of codon bias. The presence of rare codons can cause ribosomal stalling due to the low abundance of corresponding amino-acyl tRNAs. Likewise, translation elongation is also affected by the orientation of codons. Adjacent amino acids can be encoded by up to 36 synonymous codon pairs, with some codon pairs being more frequently used than others. This is called the codon pair bias. It is unknown why some codons are represented more frequently than others, although the fact that some codon pairings are more common means that codon, and codon pair, arrangements within a gene may also affect translational rates (Coleman *et al.*, 2008).

The structural features of RNA affecting translation are summarised in table 7.

Structural feature	Effect on translation
5' UTR length	Influences scanning. A long 5' UTR may impede translation.
5' UTR and coding region secondary structure	Complex 5' UTR structures may impede scanning. IRES structures promote cap-independence and allow the ribosome to largely avoid scanning. Pseudoknot structures promote frameshifting and recoding. Structure may also mediate binding with *trans*-acting factors.
Sequence context of the initiation codon	Imparts ribosome selectivity for first AUG codon. 'Weak' AUG codons promote leaky scanning.
M^7G Cap	Promotes mRNA stability and interaction with eIF4F. Facilitates the translation of most cellular mRNAs. Accessibility to initiation factors may influence translational efficiency.
uORF	Upstream open reading frames (uORFs) may impede ribosome scanning to downstream cistrons.
Poly(A) tail	Length imparts stability and translational efficiency to mRNA. Interaction with PABP mediates association with cap-binding complex on the mRNA.
3' UTR	Mediates the closed-loop translation complex via PABP interaction. Structural complexity may influence translational efficiency and interaction with *trans*-acting factors.
Codon usage	Use of non-abundant tRNAs may impede elongation. Influences frameshifting and recoding.
Trans-acting factors	Specific RNA sequence and/or structural motifs promote interaction with RNA-binding proteins, which may influence translational efficiency.

Table 7: The structural features of mRNA which influence translational control (Gale *et al.*, 2000).

4.1.6 HIV translation

4.1.6.1 Structure within the HIV 5' UTR

Transcribed HIV mRNA contains a considerable level of RNA structure which can affect translation. The presence of pseudoknots, frameshift elements, packaging signals, IRES and other regulatory motifs provides a means for the ssRNA genome to direct multiple aspects of the viral life cycle. Due to its extensive structure, HIV RNA therefore plays a role in initiating reverse transcription and transcription, directing nuclear export, altering reading

frame usage, promoting genome dimerization and regulating packaging. However, although evolutionarily conserved, many structural components of the HIV genome remain uncharacterised (Watts *et al.*, 2009).

Transcription of the HIV provirus produces capped and polyadenylated RNA with terminal 5' and 3' untranslated regions (UTR) [figure 45]. The 5' UTR is the most conserved region of the HIV genome and is responsible for directing various stages of the HIV life cycle (Abbink and Berkhout, 2003).

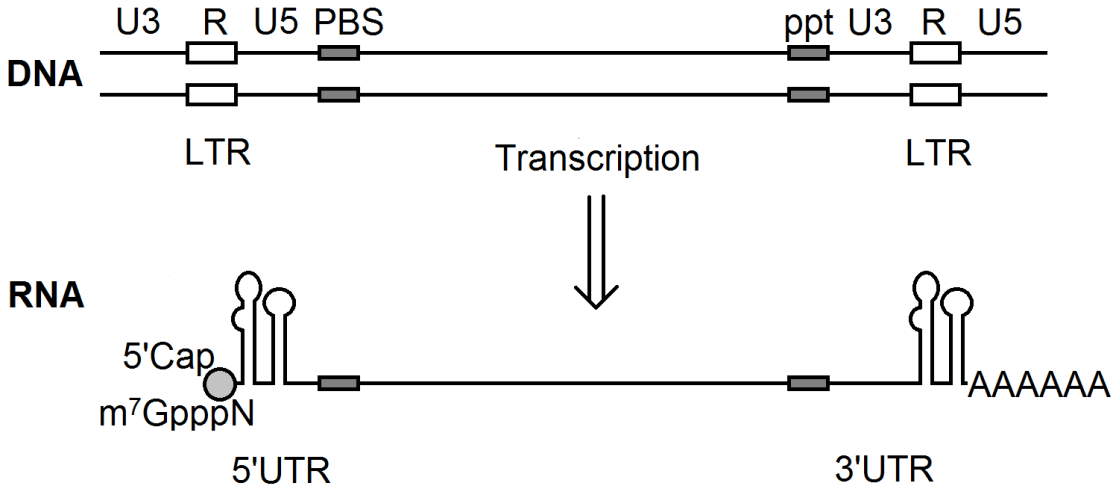

Figure 45: HIV proviral DNA is flanked by long terminal repeats (LTR) containing U3, R and U5 regions and reverse transcription signals: the primer binding site (PBS) and polypurine tract (ppt). Transcription of HIV DNA produces capped and polyadenylated RNA with terminal 5' and 3' untranslated regions (UTR). The TAR and poly(A) hairpin are present in both the 5' and 3' UTRs (Das, A.T. *et al.*, 1997).

Several structural features within the HIV 5' UTR play an important role in directing gene expression and viral assembly [figure 46]. *Trans*-activation response element (TAR) is a highly conserved, secondary (stem-loop) structured region comprised of a loop of 6 unpaired nucleotides, and a partially base-paired stem containing a tripyrimidine bulge (Braddock *et al.*, 1993; Strong *et al.*, 2009). The HIV-1 TAR structure is 59 nucleotides long and contains 1 stem-loop, compared to a 123 nucleotide TAR, with 3 stem-loops, for HIV-2 (Strong *et al.*, 2009). TAR interacts with the viral protein Tat to up-regulate transcription of viral genes (see Chapter 1).

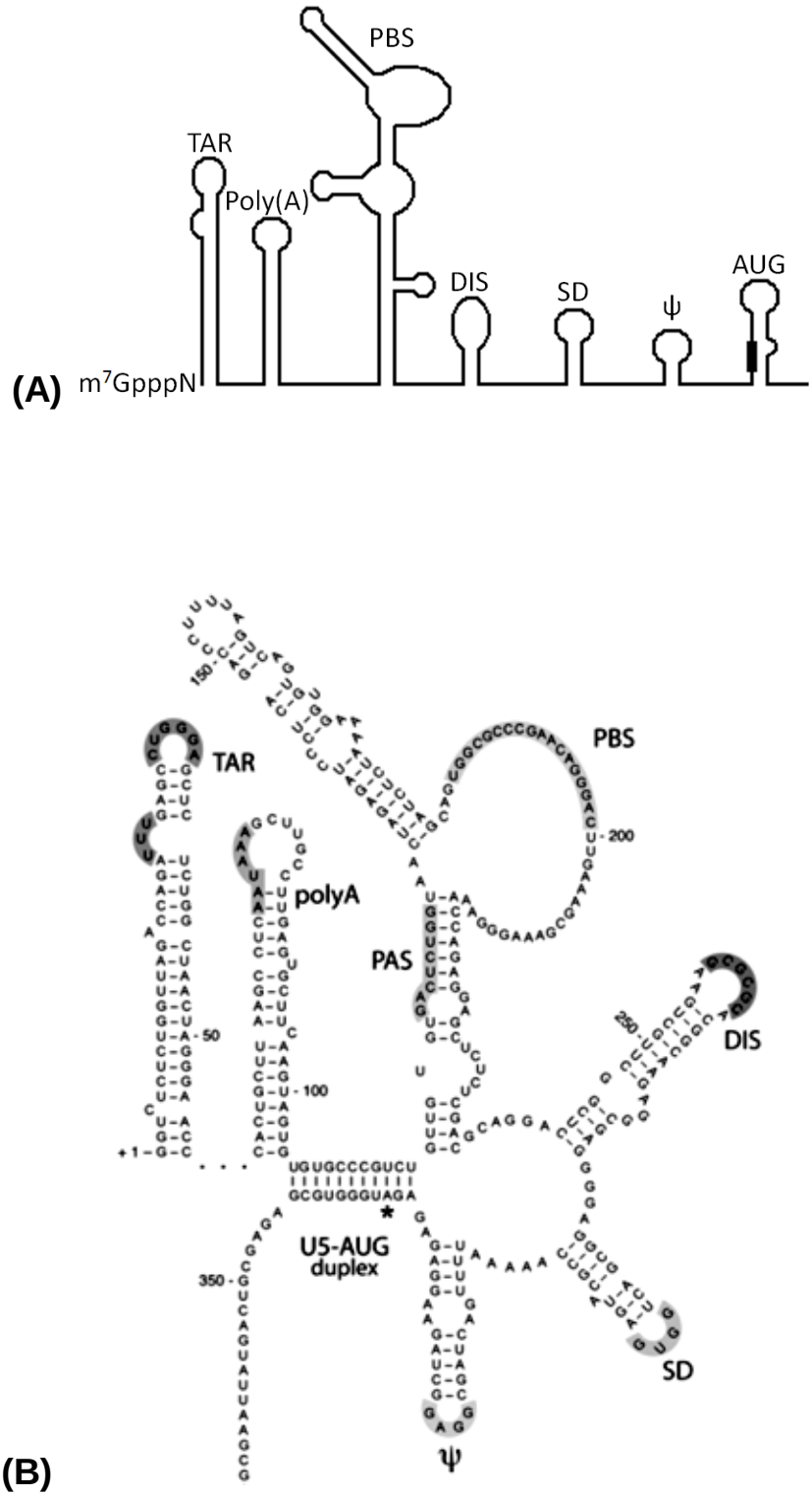

Figure 46: The functional domains of the HIV-1 5' leader showing TAR, the poly(A) hairpin, the primer binding site (PBS), the dimer initiation site (DIS), the major splice donor (SD), the RNA packaging signal (ψ) and the AUG hairpin loop (with the start codon shown as a black box) (A) and the folded structure of the HIV-1 5' UTR (B) [adapted from (Berkhout *et al.*, 2011; Brasey *et al.*, 2003)].

The HIV 5' UTR has been shown to inhibit translation from downstream cistrons as a result of the TAR stem-loop structure it contains. In HeLa cells, TAR stem-loop translational inhibition was less than in RRL. This suggests that a factor present in HeLa cell extracts (and missing from RRL) may mitigate translational inhibition by TAR. The La autoantigen is a possible candidate as it is abundant in HeLa cell extracts (Svitkin, Y.V *et al.*, 1994). Cellular TAR binding proteins have been identified in extracts from mammalian cells. These include loop binding proteins (LBP); p68, TRP-1 and TRP-185 and bulge binding proteins (TRP-2) (Braddock *et al.*, 1993; Svitkin, Y.V *et al.*, 1994). Other proteins binding to the TAR stem have been reported; PKR, SBP and TAR RNA-binding protein (TRBP) (Svitkin, Y.V *et al.*, 1994).

TAR also alters the rate of translation initiation by inhibiting or activating PKR (a dsRNA-dependent protein kinase). At low concentrations, HIV TAR can activate PKR which phosphorylates eIF2α to decrease translation initiation. At higher TAR concentrations, TAR inhibits PKR by blocking PKR dimerization (important for functional PKR). Inactivated PKR cannot phosphorylate eIF2α therefore permitting translation initiation (Cole, 2007).

Downstream of TAR is the poly(A) hairpin. A polyadenylation signal (AAUAAA) within the single-stranded loop of the poly(A) hairpin is responsible for production of a poly(A) tail at the 3' end of HIV genomic RNA (Berkhout and van Wamel, 2000). The stem-loop structure of poly(A) in the 5' UTR obstructs the polyadenylation signal and therefore suppresses its function (Kasprzak *et al.*, 2005). Two important reverse transcription signals; the PAS (primer activation signal) and PBS (primer binding site), are located in U5 - a structural domain downstream of the R region (Abbink and Berkhout, 2003). Newly synthesised RNA is single-stranded, although within viral particles genomic HIV RNA exists as a non-covalent dimer (Watts *et al.*, 2009). Dimerization of genomic RNA is a unique feature of retroviruses and is coordinated by the DIS (dimer initiation site) found adjacent to the PBS. A 6 nucleotide complementary sequence (usually GCGCGC or GUGCAC) self-anneals to make a hairpin DIS loop. A base pairing interaction between the DIS structure of two adjacent HIV mRNAs results in the formation of a

'kissing loop' complex which initiates dimerization (Kasprzak *et al.*, 2005). Only unspliced, genomic RNA retains the dimerization element and therefore only full-length, genomic RNA undergoes dimerization (Baudin *et al.*, 1993). The major splice donor site (SD), the packaging signal (Psi, ψ) and the start codon (AUG) hairpin are equally essential downstream structures within the HIV 5' UTR (Abbink and Berkhout, 2003).

During translation of newly synthesised viral mRNA, the highly structured 5' UTR is the first region encountered by scanning ribosomes. Consequently, the length and structure of the HIV-1 5' UTR have been shown to limit the rate of HIV-1 translation by impeding ribosomal scanning and cap accessibility (Svitkin, Y.V. and Sonenberg, 2004). The organisation of the HIV-1 5' UTR resembles that of HIV-2. Therefore, it is likely that the rate of HIV-2 translation is also regulated by its 5' UTR. However, the HIV-2 5' UTR (545 nucleotides) is significantly longer than the HIV-1 5' UTR (335 nucleotides) and contains a higher level of structure (Strong *et al.*, 2009).

4.1.6.2 Evidence for cap-dependent translation

Current literature on the mechanism of HIV-1/2 translation initiation remains controversial. Both ribosomal scanning and internal initiation have been observed in different experimental settings. Consequently, cap-dependent translation and IRES-driven translation have both been proposed to account for Gag translation (Berkhout *et al.*, 2011).

HIV Gag is translated from viral mRNA which is produced analogously to host cell mRNA. Consequently, HIV viral mRNA is both capped and polyadenylated and proposed to undergo cap-dependent translation in an equivalent manner to cellular mRNA. Several experiments have highlighted the role of cap-dependence in HIV Gag translation. Insertion of additional, upstream AUG codons within the HIV-1 5' UTR resulted in a decrease in translation from the native HIV-1 AUG codon and translation, instead, of the introduced ORF. These results confirmed the presence of ribosomal scanning throughout the HIV-1 5' UTR. Likewise, a putative HIV-1 5' UTR IRES did not disrupt translation from upstream AUGs suggesting that internal initiation was not occurring (Berkhout *et al.*, 2011).

A high level of RNA secondary structure within the HIV-1/2 5' UTR has been shown to be inhibitory to ribosomal scanning and therefore limits the efficiency of cap-dependent translation. Nevertheless, the presence of a 5' cap structure and evidence for the involvement of ribosomal scanning in Gag translation are both consistent with cap-dependent translation (Miele *et al.*, 1996). Furthermore, the HIV-1 5' leader sequence was unable to promote translation when it was cloned into a dicistronic construct with a downstream reporter gene. This suggests that the HIV-1 5' UTR is unable to undergo internal initiation via an IRES, also favouring cap-dependent translation from the Gag AUG (Miele *et al.*, 1996).

Recent work by Ricci *et al.* (2008) suggests that translation of full-length, HIV-1 p55 Gag occurs via a cap-dependent mechanism. Ricci *et al.* (2008) used a cap-analogue, which competes for eIF4E, and FMDV-encoded L-protease, which cleaves eIF4G, to shut-down cap-dependent translation in an *in vitro* RRL system. Translation of HIV-1 p55 was inhibited within this system whereas HIV-2 p57 translation was not. Thus Ricci *et al*. (2008) propose that HIV-1 p55 Gag relies on cap-dependent translation whereas HIV-2 p57 Gag may employ alternative translation initiation mechanisms.

4.1.6.3 Evidence for IRES-dependent translation

Evidence for HIV-1 IRES activity:

Brasey *et al.* (2003) used foot and mouth disease virus (FMDV) L-protease to shut down cap-dependent translation in an *in vitro* RRL system. Surprisingly, and in contrast to the work by Ricci *et al.* (2008), HIV-1 mRNA translation was able to continue within this system. A potential IRES element was identified within the 5' leader of HIV-1, spanning 232 nucleotides (between nucleotides 104 to 336) and overlapping with the RNA packaging signal (ψ) (Brasey *et al.*, 2003).

An additional IRES within the *gag* ORF has also been suggested for HIV-1. Buck *et al.* (2001) report the finding of an IRES region within the HIV-1 *gag* ORF which allows translation of the Gag precursor ($Pr55^{gag}$) and a 40 kDa N-terminally truncated Gag isoform. Experiments were carried out using

poliovirus-infected cells to shut down cap-dependent translation by viral 2A protease cleavage of eIF4G and cleavage of PABP by viral 2A and 3C. HIV Gag translation was not severely impacted when cap-dependent translation was inhibited whereas translation of a cap-dependent control was greatly reduced. The *gag* 5' UTR was also shown to be dispensable for IRES activity within the *gag* ORF. Furthermore, Buck *et al.* (2001) suggest the presence of the HIV-1 5' UTR is unnecessary, and even slightly detrimental to the translational capability of the *gag* ORF.

The data presented by Buck *et al.* (2001) and Brasey *et al.* (2003) suggest the presence of two HIV-1 IRESs; one within the 5' leader sequence and another within the *gag* ORF. Subsequent to IRES binding, 5' to 3' ribosomal scanning would be expected to occur although this may not be necessary depending on the location of the IRES. One of the reported HIV-1 IRESs is located downstream of the *gag* ORF and therefore translocation of the 40S ribosomal subunit, in a 3'-5' direction would need to occur in order for recognition of the upstream *gag* start codon (Brasey *et al.*, 2003). It remains unclear, however, as to whether 40S ribosomal recruitment to the gag mRNA can occur from backscanning in a 3'-5' direction from the *gag* ORF IRES (Buck *et al.*, 2001), or whether traditional 5'-3' scanning can promote translation initiation from the 5' leader IRES (Brasey *et al.*, 2003). The HIV-1 5' UTR contains secondary structures which can inhibit cap-dependent translation by blocking access of the translation initiation complex (eIF4F) to the 5' cap. Thus, the presence of HIV-1 IRESs may provide a mechanism by which the ribosome can bypass the structural obstacles hindering cap-dependent translation, and allow translation to proceed via direct ribosome recruitment to the *gag* ORF (Buck *et al.*, 2001).

Ventoso *et al.* (2001) observed that HIV-1 Protease can cleave eIF4G, thus shutting down cap-dependent translation. However, *in vitro* translation of HIV-1 mRNA was increased by 4-fold when eIF4G was cleaved by HIV-1 Protease. This suggests not only that eIF4G cleavage enhances the rate of HIV-1 mRNA translation, but that HIV-1 mRNA is also able to undergo translation in a cap-independent manner. Consequently, HIV-1 IRES activity

is proposed to permit translation of HIV mRNAs when cap-dependent translation is shut down (Ventoso *et al.*, 2001).

Evidence for HIV-2 IRES activity:

Herbreteau *et al.* (2005) demonstrated IRES activity in the HIV-2 *gag* ORF in a dicistronic assay in both RRL and HeLa cells. Translation from the HIV-2 Gag AUG, and two internal AUG codons, occurred when the matrix region of the *gag* ORF was present in the intercistronic region of reporter constructs. However, the presence of the HIV-2 5' UTR reduced IRES activity.

Weill *et al.* (2010) and Locker *et al*. (2011) have extended this work to show that transcripts containing the first 420 nt of the HIV-2 *gag* ORF without the 5' UTR are able to recruit translation initiation complexes directly (Locker *et al.*, 2011).

SIV_{mac}, which is closely related to HIV-2, has been reported to contain an IRES in its 5' UTR (Ohlmann *et al.*, 2000). However, it has also been postulated to contain an IRES similar to HIV-2 in its *gag* ORF (Weill *et al.*, 2010).

Compelling arguments exist for both cap-dependent and IRES initiated translation. Ostensibly, HIV mRNA is structured to undergo translation in a cap-dependent fashion alongside cellular mRNA. However, several stages of the viral life cycle appear to result in unfavourable conditions for cap-dependent translation. Cleavage of eIF4G by HIV PR, or cellular arrest at the G2/M stage of the cell cycle by viral Vpr, both inhibit cap-dependent translation. Likewise, during assembly, the HIV 5' UTR may become blocked by binding of Gag proteins to the HIV genome, inhibiting cap-dependent translation (Anderson and Lever, 2006). Although cap-dependent translation of viral mRNA may be favourable, more complex initiation mechanisms may have developed to ensure that the important step of translation initiation is not disregarded due to cellular circumstance. It may be that under certain conditions IRES activity permits HIV translation or, alternatively, other regulatory factors or pathways may serve to sustain cellular HIV translation.

Currently the manner and conditions under which HIV Gag translation is initiated are not fully understood and further work is required to elucidate HIV translational mechanisms. Likewise, it remains unknown whether HIV-1 and the less studied HIV-2 virus use comparative or distinctive translational methods.

4.1.6.4 Regulation of translation of HIV Gag

The mechanism of switching between cap-dependent and IRES-driven translation, and what determines this switch, are unknown, but an involvement of the Gag protein has been suggested (Ricci *et al.*, 2008). Investigation into the effect of Gag concentration on protein synthesis has shown that at high concentrations, p55 Gag inhibits protein synthesis of viral RNA, whereas at low concentrations, p55 Gag stimulates synthesis (Anderson and Lever, 2006). Binding of p55 Gag protein to the 5' UTR of its mRNA following synthesis may prevent adherence of scanning ribosomes thus triggering a switch to IRES driven translation (Ricci *et al.*, 2008). Consequently, an additional role for the Gag protein may be to control the rate of viral translation.

Additionally, two variant HIV-2 Gag transcripts have been identified which are translated with differing efficiencies. The removal of a 142 nucleotide intron from the HIV-2 5' UTR results in a spliced version of HIV-2 Gag RNA which is translated with a 5-fold increased efficiency. It is thought that the removal of secondary structure by splicing may promote more efficient ribosome scanning (Strong *et al.*, 2009). Likewise, splicing removes a C-box/G-box long range interaction within the HIV-2 RNA; removal of the C-box region has been shown to enhance translation rates (Brasey *et al.*, 2003). Thus different HIV-2 transcripts may facilitate regulation of HIV-2 Gag translation.

Further work is necessary to assess whether translation differs between HIV-1 and HIV-2 and, moreover, develop a clearer picture as to the translational mechanisms employed by these viruses. As translation is such an important regulatory step within the HIV life cycle, variations in translational efficiency may thus impart differences in the overall replicative capacity of these viruses

and provide an answer as to why HIV-1 is a more voracious pathogen than HIV-2.

4.2 HIV-1/2 Gag translation

4.2.1 HIV Gag RNA reporters

Initial work focused on comparing Gag translation between HIV-1 and -2. The binding affinity of HIV-1 and HIV-2 Gag-specific antibodies may vary, so western blotting or immunoprecipitation cannot be used to compare Gag protein synthesis directly. Consequently, capped and polyadenylated RNA reporters were generated from T7 promoter-driven transcription of HIV Gag-Luc reporter plasmids. RNA reporters contained the 5' UTR and *gag* coding region from HIV-1 or HIV-2 linked to the coding sequence for firefly luciferase to provide a common basis for assay [figure 47].

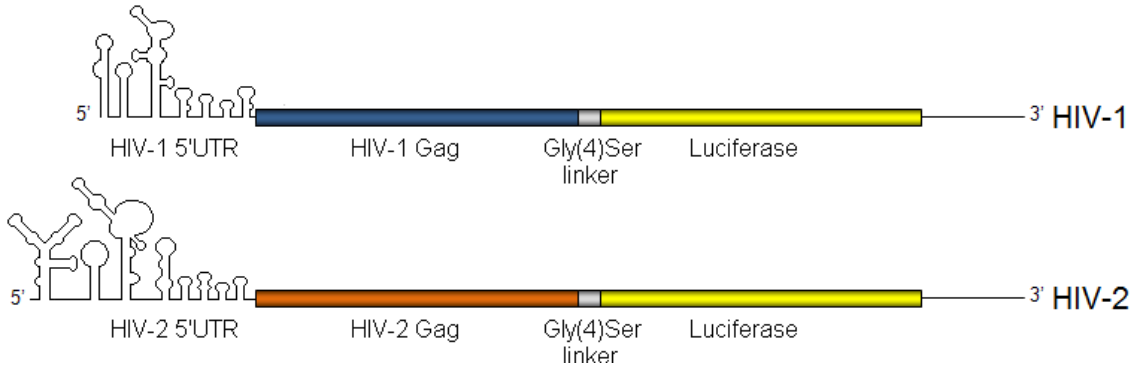

Figure 47: Capped and polyadenylated RNA reporters produced from T7-driven transcription of reporter plasmids. Reporter RNA contained the 5' UTR and *gag* coding region from HIV-1 or -2 linked, via a Gly(4)Ser linker, to a gene encoding firefly luciferase.

Translation of these RNA reporters produces a fusion protein of Gag and luciferase, detectable by luciferase assay. In this way, translation is isolated from transcription and splicing. Consequently, the luciferase activity of the HIV-1/2 RNA reporters can be used as a measure of Gag translation and, thus, these reporters can be used to compare the rate of translation between HIV-1 and HIV-2.

4.2.2 *In vitro* HIV-1/2 Gag-Luc expression

The size and functionality of the Gag-Luc fusion protein was tested by *in vitro* transcription and translation of HIV-1/2 Gag-Luc reporter plasmids in a TnT

rabbit reticulocyte lysate (RRL) system [Promega] using radioactively labelled ^{35}S-methionine. The proteins produced were detected by SDS-PAGE and autoradiography [figure 48A] or by luciferase assay [figure 48B].

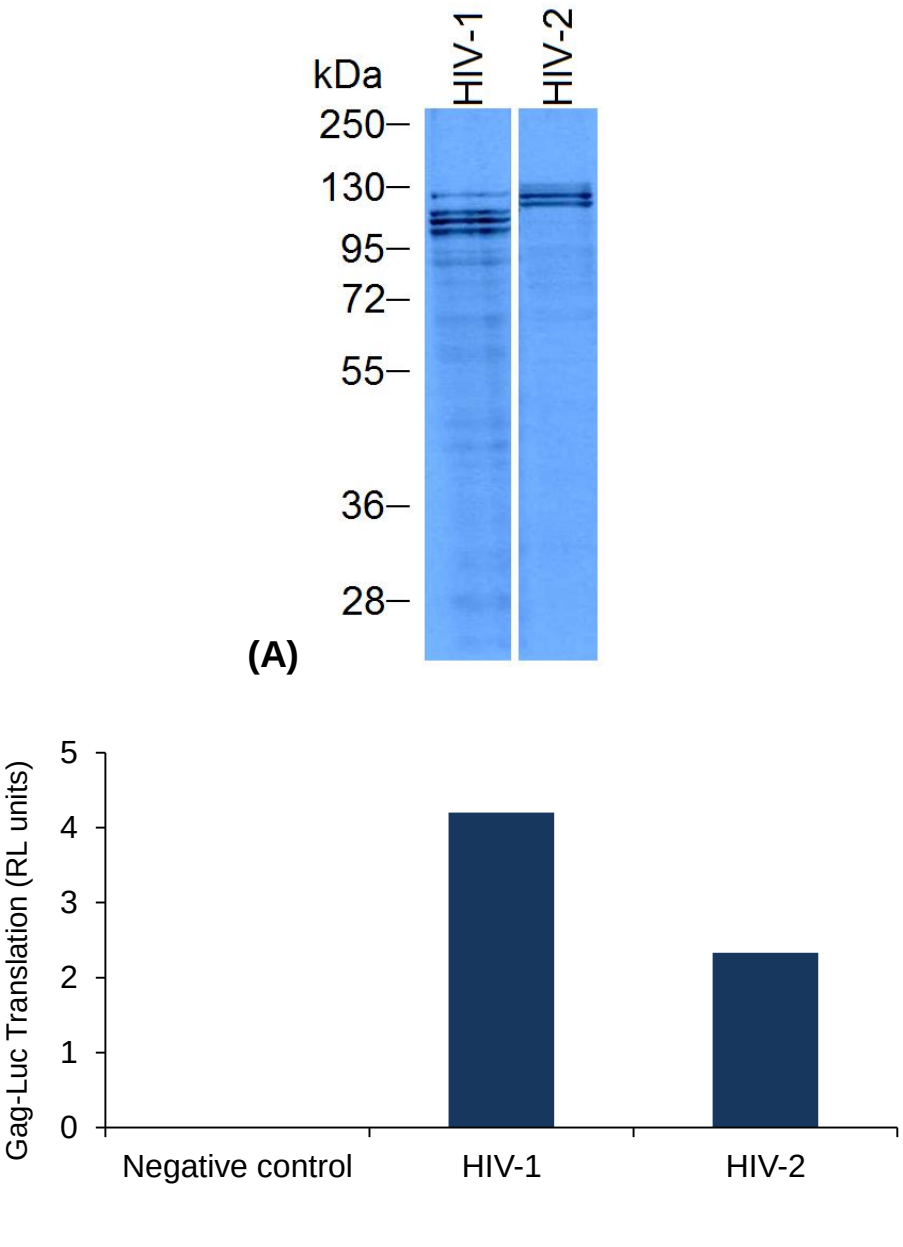

Figure 48: *In vitro* transcription and translation of ^{35}S-methionine labelled HIV-1/2 Gag-Luc DNA SDS-PAGE and autoradiography (A) and luciferase assay results to verify luciferase functionality (B). Fluorescence of Gag-Luc in terms of relative light (RL) units was used as a measure Gag translation.

The size of proteins produced from HIV-1 and 2 Gag-Luc reporters was shown to be ~120 kDa, which is the expected size of the Gag-Luc fusion proteins (HIV-1 Gag = 55 kDa, HIV-2 Gag = 57 kDa, Luc = 65 kDa). Several

bands were produced from translation of reporters. This is likely to be due to alternative translation initiation at internal Gag AUG codons producing different Gag isoforms. Previously identified Gag isoforms include two HIV-2 Gag isoforms (p50 and p44) which would produce Gag-Luc fusion proteins of 115 kDa and 109 kDa, and a single HIV-1 isoform (p40) which would result in a fusion protein of 105 kDa (Ricci *et al.*, 2008). As expected, the HIV-2 Gag-Luc fusion proteins have a larger MW than HIV-1 Gag-Luc fusion proteins. However, several additional HIV-1 bands were produced potentially representing unknown N-terminally or C-terminally truncated HIV-1 Gag isoforms.

The functionality of the Gag-Luc fusion protein was tested by carrying out a luciferase assay [figure 48B]. This showed that firefly luciferase within the Gag-Luc fusion protein was functional and, furthermore, could be detected by this method. Consequently, the Gag-Luc fusion proteins could be used as a suitable means to assess the level of HIV-1/2 Gag translation. *In vitro* transcription and translation from HIV-1/2 Gag-Luc reporter plasmids suggested that HIV-1 Gag was expressed 1.8-fold better than HIV-2 Gag. However, this may have been due to more efficient HIV-1 transcription (see Chapter 3) so it was necessary to isolate translation by using RNA reporters in order to directly compare HIV-1/2 translation rates.

4.2.3 HIV-1/2 Gag translation in cells

Comparing the rate of translation between HIV-1/2 may indicate whether this is a rate limiting stage of replication responsible for the lower level of viral particle production observed during a HIV-2 infection. HIV-1 and HIV-2 Gag translation was compared in several cell types; HeLa (human cervical carcinoma cell line), COS-1 (African green monkey kidney cell line) and Jurkat (human T-lymphocyte cell line). All these cell lines support HIV replication, with Jurkat cells being the most closely related to the cells infected in a natural HIV infection.

Capped and polyadenylated HIV-1/2 Gag-Luc reporter RNAs [figure 47] were generated by *in vitro* transcription and varying concentrations of RNA were used to transfect HeLa [figure 49], COS-1 [figure 50] and Jurkat [figure 51]

cells before harvesting protein after 6 h. *Renilla* luciferase RNA was co-transfected as a control for transfection efficiency. The quantity of Gag-Luc fusion protein translated from HIV-1/2 reporters was measured using a Dual-Luciferase® Reporter Assay System [Promega] and normalised to *Renilla* luciferase. Each transfection was conducted in duplicate and results shown are the average of 3 experiments. Error bars represent the SEM.

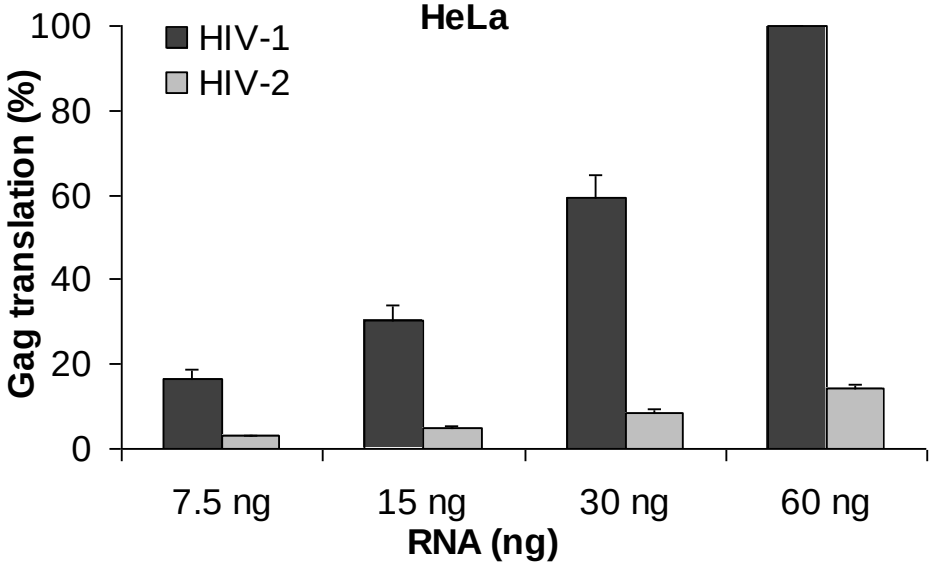

Figure 49: Translation of HIV-1/2 RNA reporter constructs in HeLa cells. Fluorescence of Gag-Luc in terms of relative light (RL) units was used as a measure Gag translation. Results were normalised to the *Renilla* transfection control.

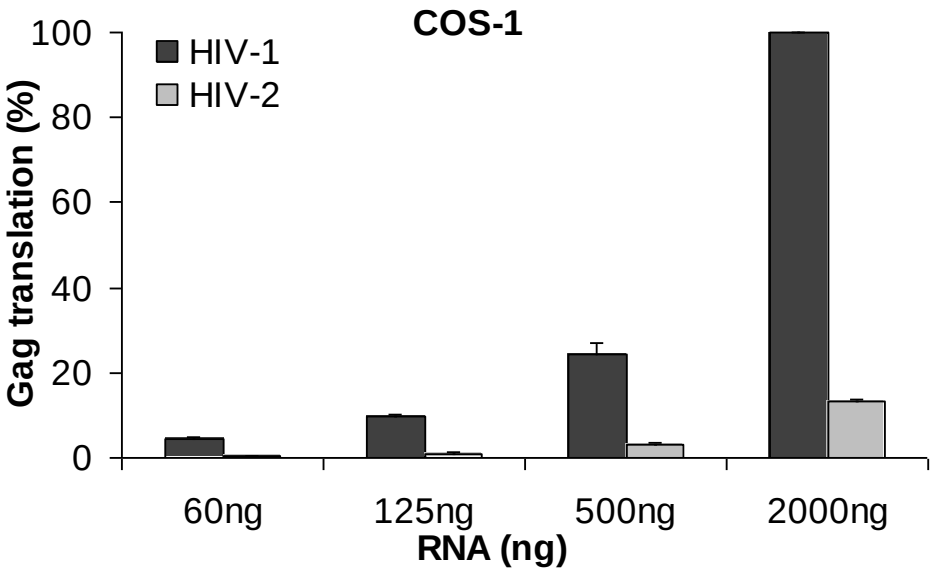

Figure 50: Translation of HIV-1/2 RNA reporter constructs in COS-1 cells. Fluorescence of Gag-Luc in terms of relative light (RL) units was used as a measure Gag translation. Results were normalised to the *Renilla* transfection control.

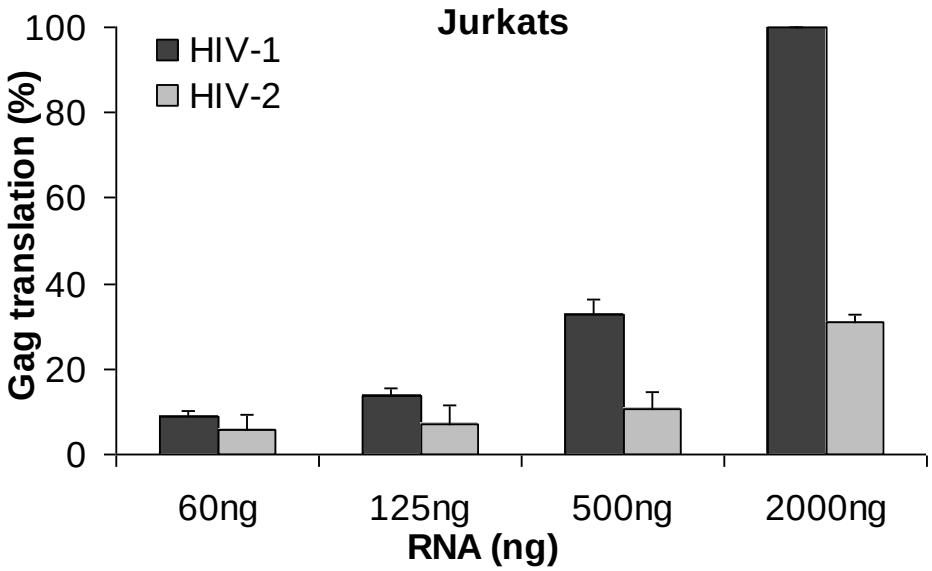

Figure 51: Translation of HIV-1/2 RNA reporter constructs in Jurkat cells. Fluorescence of Gag-Luc in terms of relative light (RL) units was used as a measure Gag translation. Results were normalised to the *Renilla* transfection control.

HIV-2 Gag was translated to a much lower level than HIV-1 for varying concentrations of RNA and in several different cell lines. In HeLa cells, HIV-1 Gag was translated up to 6.9-fold more efficiently than HIV-2 Gag [figure 49]; in COS-1 cells HIV-1 Gag was translated up to 11.9-fold more efficiently than HIV-2 Gag [figure 50] and in Jurkat cells HIV-1 Gag was translated up to 3.2-fold more efficiently than HIV-2 Gag [figure 51]. Overall, these data indicates that HIV-2 Gag translation is much less efficient than HIV-1 Gag translation in a variety of cell types. It is interesting to note that in Jurkat cells, the most physiologically relevant cell type, the lowest fold difference in HIV-1/2 translation rates occurred.

4.2.4 HIV-1/2 RNA reporter stability

In cells, HIV-1 Gag RNA is translated more efficiently than HIV-2 Gag RNA. However, HIV-1/2 translation rates may be altered by differences in HIV-1/2 RNA stability. Thus it was necessary to confirm that the observed differences in HIV-1/2 Gag-Luc fusion protein production were due to translational differences rather than RNA degradation. HeLa cells were transfected with 60 ng of HIV-1/2 Gag-Luc reporter RNA and the level of RNA remaining in the cells after 3 h and 6 h was quantified by harvesting total cell RNA and

carrying out real-time RT-PCR (qPCR). Primers to HIV-1 (primer #22, 23) and HIV-2 (primer #24, 25) Gag were used for the qPCR, with results normalised to a GAPDH housekeeping gene (amplified using primers #18, 19). Reactions were carried out in duplicate. $2^{\Delta Ct}$ was calculated for each sample and expressed as a percentage of the largest $2^{\Delta Ct}$ RNA value to permit scaled averaging of results from two experiments [figure 52].

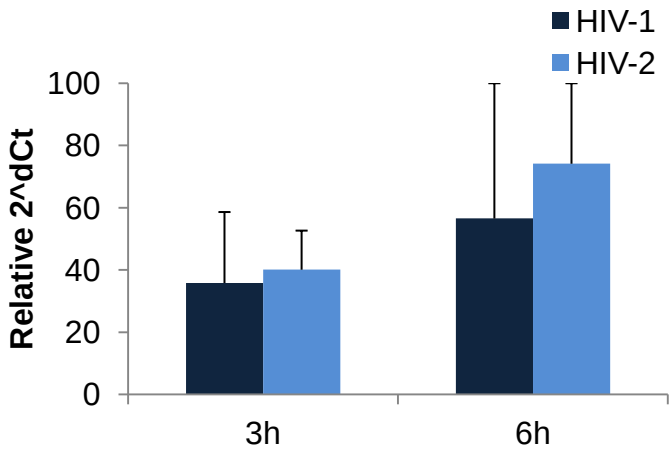

Figure 52: A comparison of HIV-1/2 Gag-Luc reporter RNA stability at 3 h and 6 h post-transfection. Gag RNA levels were quantified by qPCR and normalised to a GAPDH housekeeping gene. To compensate for scale, RNA levels are shown as $2^{\Delta Ct}$ expressed as a percentage of the largest $2^{\Delta Ct}$ RNA value, averaged for two experiments. Error bars represent the SEM.

Transfected HIV-1 and HIV-2 reporter RNA levels were similar at 3 h and 6 h. Neither HIV-1 nor HIV-2 Gag-Luc RNA levels decreased between 3 h and 6 h indicating that no observable RNA degradation occurred during the experiment. Therefore the reporter RNAs were reasonably stable following transfection and enhanced HIV-2 reporter RNA degradation was not responsible for the lower rate of HIV-2 Gag translation observed in cells.

4.2.5 HIV-1/2 Gag translation in the presence of proviral DNA

The presence of viral proteins may affect the level of HIV-1 or HIV-2 translation differently. Consequently, HeLa cells were transfected with 30 ng of HIV-1 or HIV-2 provirus for 24 h to produce viral proteins, before transfection of 60 ng of HIV-1/2 reporter RNAs [figure 47] for 6 h. Gag translation in the presence/absence of provirus (and thus viral proteins) was

assayed by a luciferase assay of harvested protein [figure 53]. 60 ng of *Renilla* luciferase RNA was co-transfected as a control for translation efficiency. 30 ng of two DNA controls was also used: pcDNA GFP expressing GFP protein was used as a control for non-specific translation competition, and pJHRV (containing a non-mammalian promoter) was used to control for any effect of plasmid presence on translation levels. Reactions were carried out in duplicate and the results shown are the average of 3 experiments.

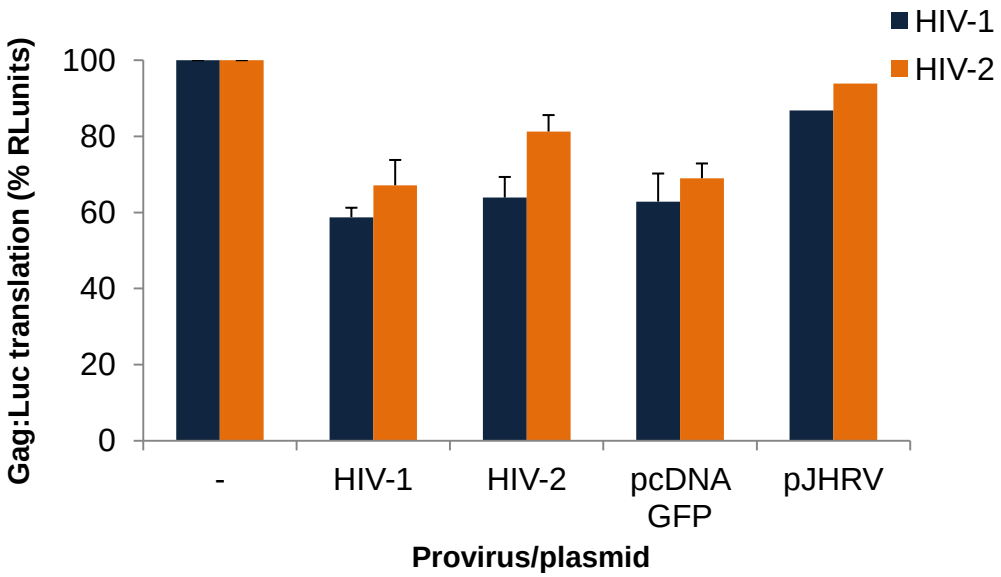

Figure 53: Luciferase assay results showing the translation of HIV-1/2 Gag-Luc RNA reporters in the presence of HIV-1 provirus, HIV-2 provirus, pcDNA GFP plasmid or pJHRV plasmid co-transfections. Gag translation is expressed in relative light (RL) units as a percentage of Gag translation levels from isolated HIV-1/2 RNA reporter transfections. Error bars represent the SEM.

In the presence of either HIV-1 or HIV-2 viral proteins, HIV-1/2 Gag translation decreased by a similar level. A comparable effect was observed when HIV-1/2 Gag translation was monitored in the presence of non-specific GFP translation (from pcDNA GFP). This indicates that, in the presence of proviral plasmids, competition for translational machinery was likely effecting a reduction in the levels of HIV-1/2 Gag translation. For this reason, it is unlikely that proviral plasmids effected a specific reduction in translation attributable to the presence of translated viral proteins.

The presence of a generic plasmid, pJHRV, did not alter HIV-1/2 Gag translation levels significantly. As a similar decrease in HIV-1/2 Gag

translation was observed in the presence of HIV-1/2 provirus, it appears that viral proteins do not differently affect HIV-1/2 translation rates.

4.3 HIV-1/2 Gag translation initiation: cap-dependent or IRES-dependent?

4.3.1 Transfection of HRV-2 RNA

HIV-1/2 translation initiation strategies may differ. This may account for the lowered HIV-2 Gag translation rate observed *in vitro* and in cells. We therefore wanted to assess the reliance of HIV-1/2 gag mRNA on cap-dependent translation initiation. Inhibition of cap-dependent translation can be achieved using human rhinovirus (HRV-2) which encodes a 2A protease. 2A cleaves eIF4G, an initiation factor involved in cap-mediated translation initiation, thus inhibiting cap-dependent translation. HRV-2 can therefore be used as a tool to specifically inhibit cap-dependent translation.

HeLa cells were transfected with 250 ng HRV-2 RNA (encoding 2A) for 16 h to shut down cap-dependent translation, before transfection for 6 h with 60 ng either HIV-1 or HIV-2 reporter RNA constructs [figure 47]. All reactions were carried out in duplicate. Further dicistronic RNA controls [figure 54] were transfected alongside reporter RNAs to assess whether HRV-2 RNA transfections had an effect on IRES-dependent translation.

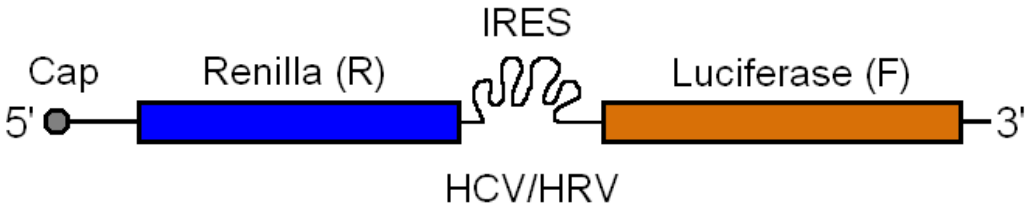

Figure 54: Cap-dependent *Renilla* luciferase and (HCV/HRV) IRES-dependent firefly luciferase dicistronic RNA controls.

The dicistronic RNAs have an upstream cap-dependent region encoding *Renilla* luciferase and a downstream region expressing firefly luciferase under the control of an internal ribosome entry site (IRES) from either hepatitis C virus (HCV) or human rhinovirus (HRV). Thus *Renilla* luciferase translation is cap-dependent whereas firefly luciferase translation is IRES-

dependent. Consequently, these dicistronic controls were used as a positive control for both IRES activity and to assess the inhibition of cap-dependent translation by HRV-2 2A. After 6 h transfection, cells were harvested and total cell protein extracted before carrying out a luciferase assay to quantify the levels of HIV-1/2 translation and that of the dicistronic controls [figure 55]. Results shown are the average of 3 experiments.

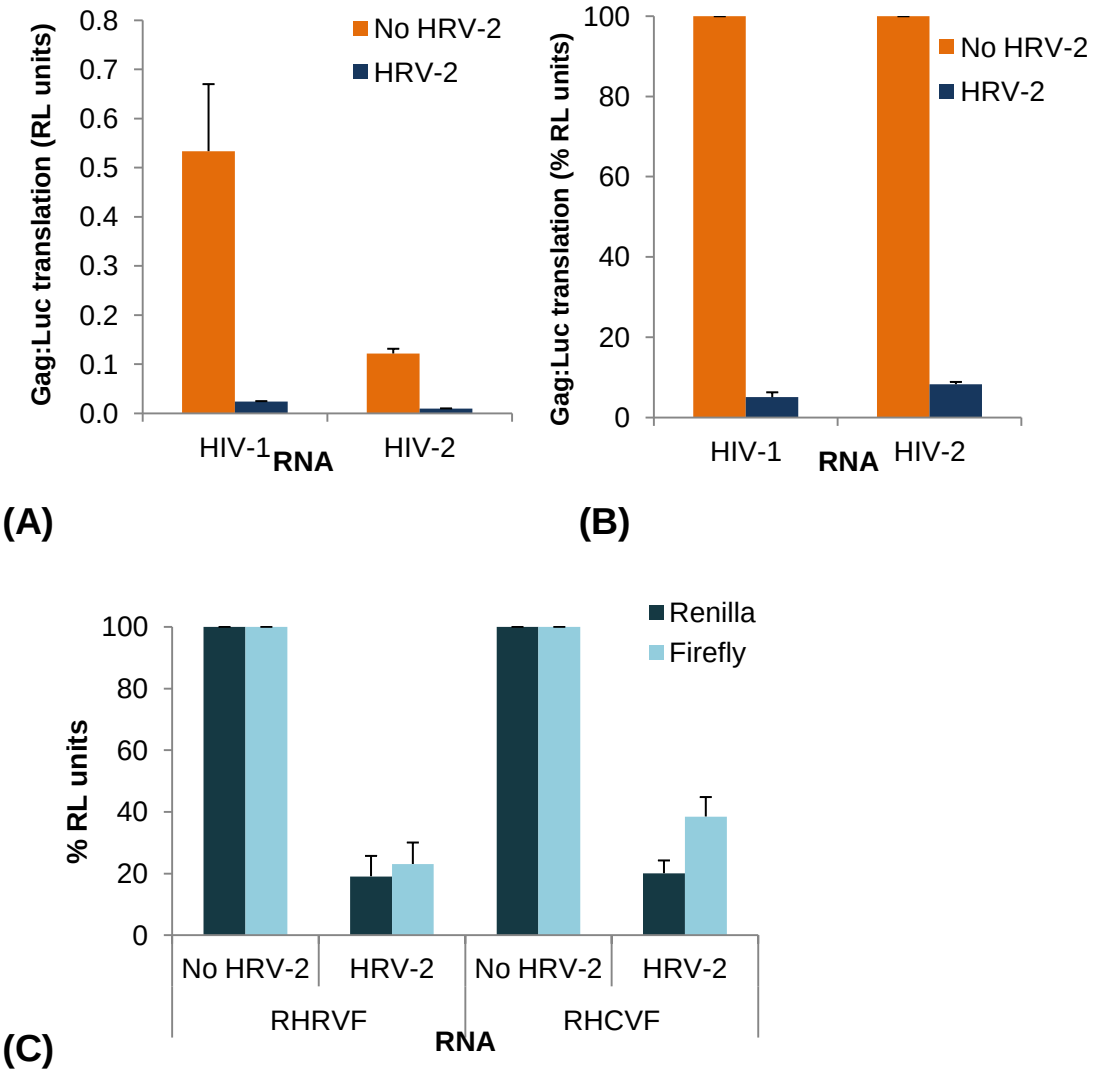

Figure 55: Translation of HIV-1 and HIV-2 RNA reporters in the presence and absence of HRV-2. Gag-Luc fusion protein translation was quantified by firefly luciferase fluorescence measured in terms of relative light (RL) units (A) and expressed as a percentage of 'No HRV-2' values (B). Translation of cap-dependent *Renilla* luciferase and IRES-driven firefly luciferase from RHRVF and RHCVF were compared in the presence and absence of HRV-2. *Renilla* and firefly luciferase translation was measured in RL units and expressed as a percentage of 'No HRV-2' values (C). Error bars represent the SEM.

In the presence of HRV-2 RNA a significant decrease in HIV-1 Gag translation, by 22.5-fold, and HIV-2 Gag translation, by 12.2-fold, was observed [figure 55]. This suggests that both HIV-1 and HIV-2 Gag translation relies on cap-dependent initiation.

Translation of cap-dependent *Renilla* within the dicistronic controls decreased by 5.2-fold for RHRVF and 5.0-fold for RHCVF in the presence of HRV-2. This suggests that HRV-2 RNA transfections shut down cap-dependent translation. However, IRES-driven firefly translation also decreased by 4.3-fold for RHRVF and 2.6-fold for RHCVF in the presence of HRV-2. Although this decrease was not to the same extent as for *Renilla*, it was expected that eIF4G cleavage would stimulate IRES activity within the dicistronic controls. As this was not the case, eIF4G may not have been fully cleaved and therefore cap-dependent translation may not have been fully shut down. If eIF4G was not fully cleaved, ongoing cap-dependent translation may have competed for translational machinery and therefore prevented an increase in IRES-driven translation. Alternatively, the transfection of lots of HRV-2 RNA may have had a cytopathic effect on the cells, thus also effecting a reduction in IRES-dependent translation.

4.3.2 Expression of 2A protease

Non-specific effects of the HRV-2 virus may have been contributing to translational inhibition of HIV-1 and HIV-2 Gag. To isolate 2A induced shut down of cap-dependent translation, HRV-2 2A, rather than the full-length HRV-2 genome, was cloned into pcDNA3. However, expression of pcDNA3-2A did not inhibit cap-dependent translation of a *Renilla* RNA control *in vitro* or in HeLa cells [not shown].

It was thought that HRV-2 2A may have been inhibiting its own cap-dependent translation through eIF4G cleavage. Consequently, HRV-2 2A was cloned into pcDNA3 downstream of an encephalomyocarditis virus (EMCV) IRES to promote better 2A protein expression. Both IRES-driven 2A expression (from pcDNA3-2A IRES) and cap-dependent 2A expression (from pcDNA3-2A) were tested in an *in vitro* transcription/translation TnT system [Promega] [figure 56].

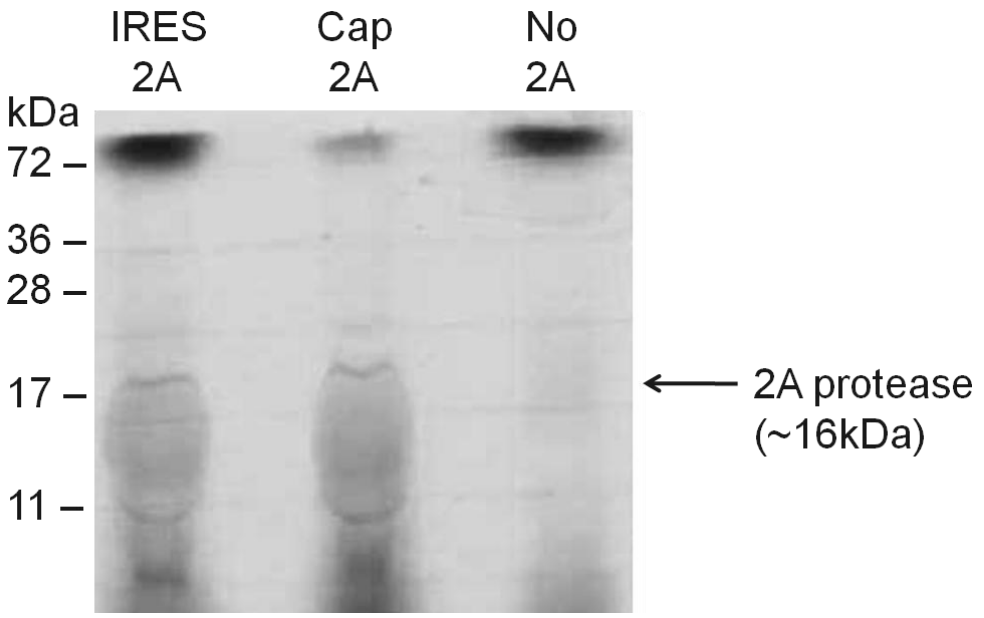

Figure 56: An SDS-PAGE of ^{35}S-methionine labelled 2A from an *in vitro* transcription/translation in a TnT system. Lane 1: IRES-driven 2A expression from pcDNA3-2A IRES, Lane 2: Cap-dependent 2A expression from pcDNA3-2A, Lane 3: protein expression from a pcDNA3 control plasmid (with no 2A).

Expression of 2A from both pcDNA3-2A and pcDNA3-2A-IRES was low, only producing a faint band at around 16 kDa following an *in vitro* transcription/translation [lanes 1+2, figure 56].

To verify whether cap-dependent or IRES-dependent expression of 2A affected HIV-1/2 Gag translation, 1.5 µg of pcDNA3-2A or pcDNA-2A-IRES DNA was used to transfect HeLa cells for 16 h to express 2A. Reactions were carried out in duplicate. As a comparison, cells were also not transfected, mock transfected or transfected with pcDNA3 (which does not encode 2A). After 16 h, 60 ng of HIV-1/2 reporter RNA reporters was transfected into HeLa cells for 6 h before harvesting total cellular protein for use in a luciferase assay [figure 57]. *Renilla* luciferase RNA was co-transfected with HIV-1/2 RNA reporters as a control for 2A inhibition of cap-dependent translation, and to account for variations in transfection efficiency. Results shown are the average of 2 experiments.

Both cap-dependent and IRES-driven 2A expression had very little effect on the translation rate of the cap-dependent *Renilla* luciferase control [not shown]. This suggests that cap-dependent translation was not efficiently shut

down. Unsurprisingly, the very low level of 2A expressed therefore had little effect on either HIV-1 or HIV-2 Gag translation levels [figure 57].

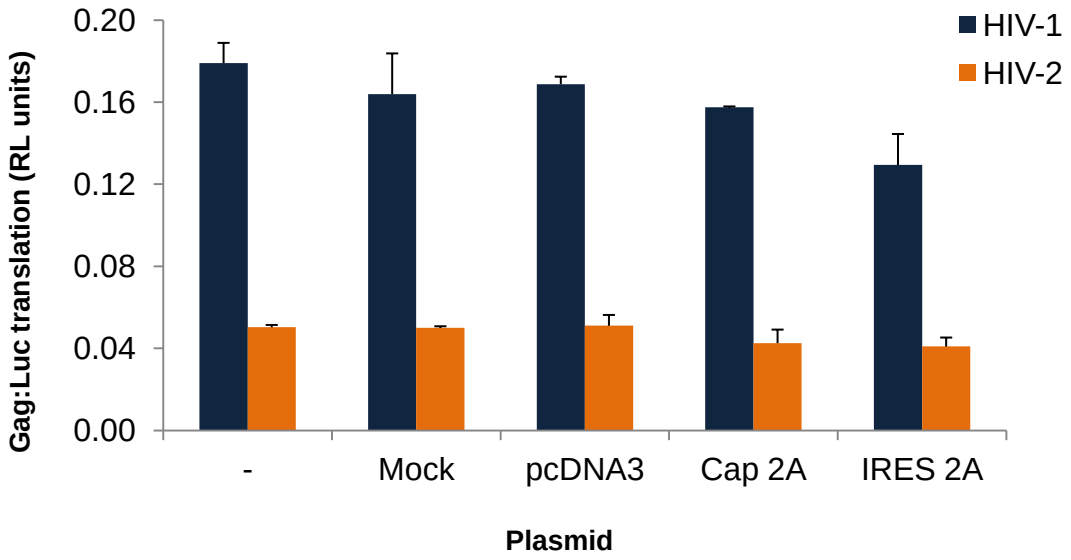

Figure 57: Luciferase assay results from HeLa transfection of 2A plasmids (pcDNA3-2A and pcDNA3-IRES-2A) for 16 h, followed by HIV-1/2 RNA reporters for 6 h. Gag-Luc translation is expressed in relative light (RL units), normalised to the *Renilla* control. HIV-1/2 Gag translation was compared in the presence of no transfection, mock transfection and pcDNA3 transfection controls. Error bars represent the SEM.

To check whether 2A protein expressed from either pcDNA3 2A or pcDNA3-2A IRES was cleaving eIF4G, protein samples were used in a western blot with an antibody to eIF4G [figure 58].

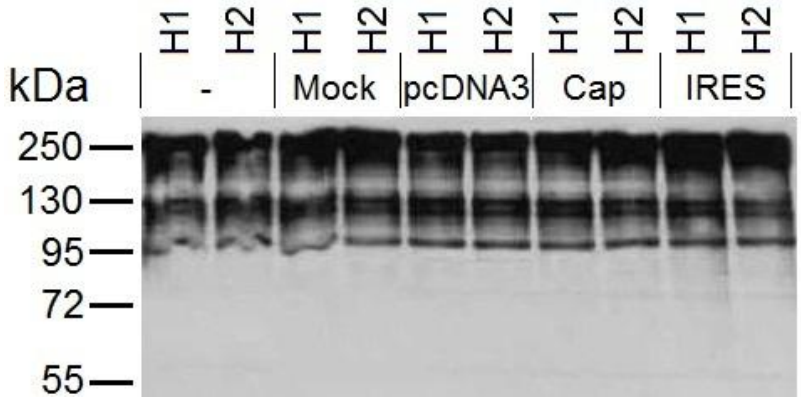

Figure 58: A western blot of HIV-1 (H1) and HIV-2 (H2) transfection protein with an antibody to eIF4G. Harvested protein was used from cells not transfected (-), mock transfected, transfected with pcDNA3 (without 2A), pcDNA3-2A (with cap-dependent 2A) and pcDNA3-IRES-2A (with IRES-driven 2A).

As expected, no transfection, mock transfection and pcDNA3 transfection controls showed inact eIF4G. There was also no difference in 2A expression between the controls and cap-dependent 2A (expressed from pcDNA3-2A) transfection cell protein [lanes 8+9, figure 58]. Likewise, IRES-driven 2A expression (from pcDNA3-2A IRES) did not affect the cleavage pattern of eIF4G [lanes 9+10, figure 58]. As neither cap-dependent HRV-2 2A nor IRES-driven HRV-2 2A was able to promote complete cleavage of eIF4G, cap-dependent translation was, therefore, not shut down.

As an alternative approach, pT7EV7ΔP1, which encodes a poliovirus 2A protease, was tested as a means to inhibit cap-dependent translation via eIF4G cleavage. 5 µg of poliovirus 2A RNA (transcribed from pT7EV7ΔP1) was used to transfect HeLa cells for 18 h in duplicate. 5 µg of HRV-2 2A RNA (produced from both pcDNA3-2A and pcDNA3-IRES-2A) was also used to transfect HeLa cells for 18 h as a comparison. After 18 h, HeLa were transfected with 120 ng of cap-dependent *Renilla* luciferase RNA for 6 h and total cell protein harvested. *Renilla* luciferase translation was quantified by luciferase assay to see whether poliovirus 2A was able to shut down cap-dependent translation [figure 59].

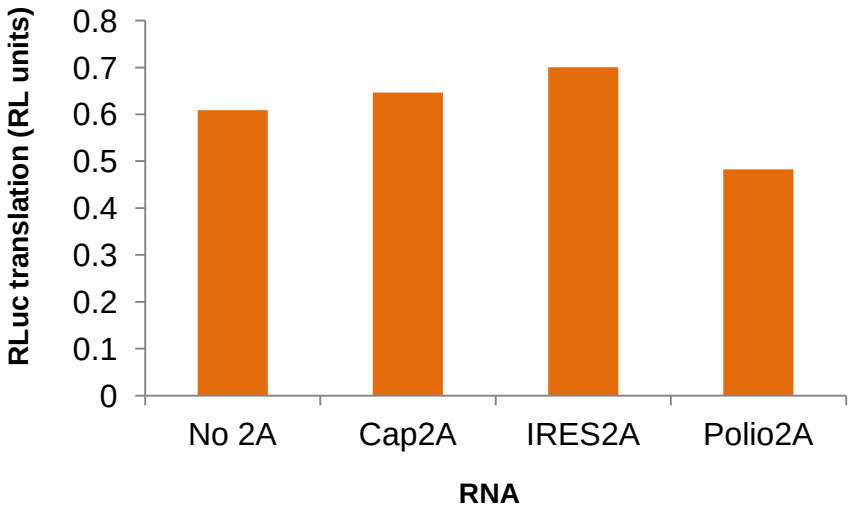

Figure 59: A luciferase assay of protein harvested from cap-dependent *Renilla* luciferase RNA transfections in mock (no 2A), pcDNA3-2A (cap-dependent 2A), pcDNA3-IRES-2A (IRES-driven 2A), and pT7EV7ΔP1 RNA (poliovirus 2A) transfected cells.

Whereas cap-dependent and IRES-driven HRV-2 2A failed to shut down cap-dependent translation, expression of poliovirus 2A reduced the level of cap-dependent translation. Although the reduction in cap-dependent translation was fairly small, poliovirus 2A RNA transfection also resulted in some cleavage of eIF4G [figure 60].

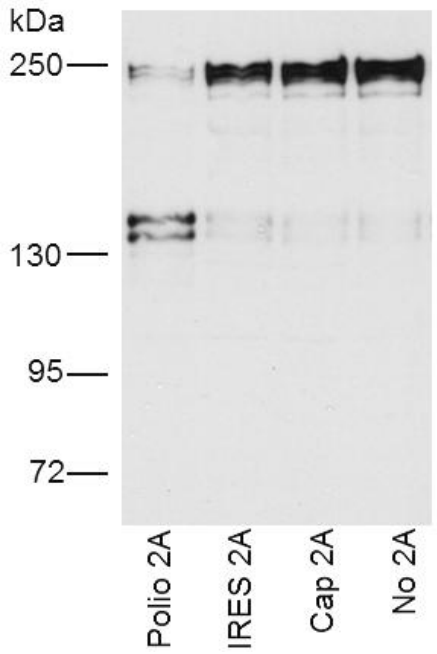

Figure 60: Western blot showing eIF4G cleavage in protein cell extracts from poliovirus 2A (polio 2A) transfections. Cells were transfected with: poliovirus 2A RNA (lane 1) from pT7EV7ΔP1, IRES-driven 2A RNA (lane 2) from pcDNA3-IRES-2A, cap-dependent 2A RNA (lane 3) from pcDNA3-2A and no RNA (lane 4).

Partial eIF4G cleavage was detected in cells transfected with poliovirus 2A RNA, shown by a band at 140 kDa [figure 60, lane 1], in contrast to cells transfected with cap-dependent or IRES-driven HRV-2 2A [figure 60, lane 2+3] where no eIF4G cleavage was detected. However, eIF4G cleavage with pT7EV7ΔP1 was incomplete, shown by a residual band at 220 kDa [figure 60, lane 1] signifying uncleaved eIF4G. Consequently, cap-dependent translation may not have been completely inhibited. However, it appeared that poliovirus 2A was more efficient than HRV-2 2A at cleaving eIF4G and knocking down cap-dependent translation.

4.3.3 HIV-1/2 Gag translation initiation: cap-dependence (poliovirus infections)

As poliovirus appeared to be more efficient at inhibiting cap-dependent translation, HeLa cells were infected with poliovirus (PV) type 1 at a multiplicity of infection (m.o.i) of 10 to shut down cap-dependent translation. PV infection was carried out, rather than using the less reliable transfection method, to ensure that each cell was targeted with PV. After 1 h, infected cells were transfected with 60 ng HIV-1/2 RNA reporters and controls (dicistronic RHCVF, RHRVF and *Renilla* RNA) for 6 h before harvesting protein to quantify expression of the controls [figures 61 and 62] and Gag [figure 64] via a luciferase assay. Transfections were carried out in duplicate with the results shown as the average of 3 experiments.

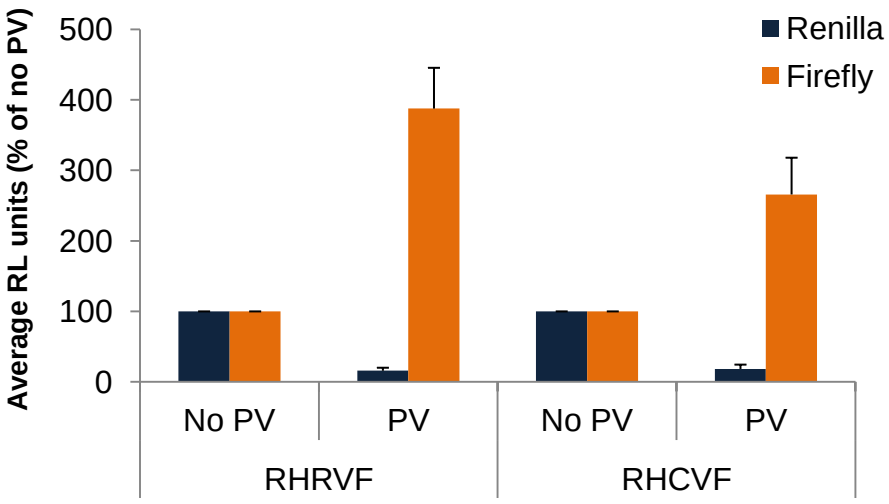

Figure 61: Translation of *Renilla* and firefly luciferase from dicistronic controls (RHRVF and RHCVF) in the presence/absence of poliovirus (PV) infection. The level of *Renilla* (blue) and firefly (orange) luciferase translation is expressed in relative light (RL) units as a percentage of 'no PV' transfections. Error bars represent the SEM.

Dicistronic poliovirus infection controls behaved as expected in the presence and absence of poliovirus 2A. When poliovirus was present, 2A cleavage of eIF4G resulted in a decrease in the level of upstream cap-dependent *Renilla* translation (by 88% for RHRVF and 87% for RHCVF), whilst downstream IRES-driven firefly luciferase translation was strongly enhanced; 4-fold for RHRVF and 2.2-fold for RHCVF [figure 61] (López de Quinto *et al.*, 2002).

The cap-dependent *Renilla* RNA control also showed a 77% decrease in translation in the presence of poliovirus infection [figure 62].

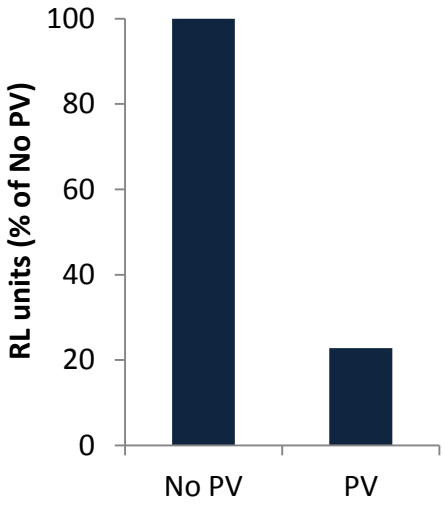

Figure 62: Translation of cap-dependent *Renilla* luciferase RNA in the presence/absence of poliovirus (PV) infection. *Renilla* translation is expressed in RL units as a percentage of translation levels in the absence of poliovirus (no PV).

Furthermore, a western blot of transfection protein with an eIF4G antibody showed that complete cleavage of eIF4G occurred in poliovirus infected cells [figure 63].

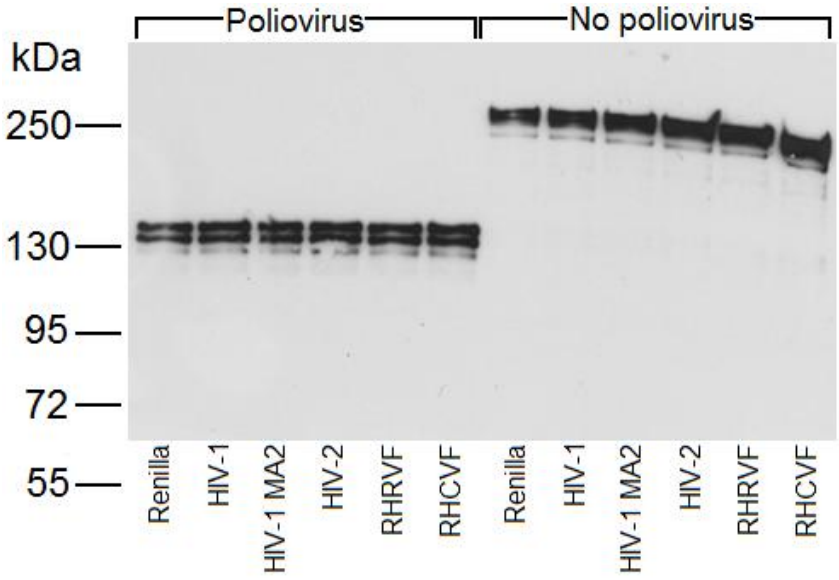

Figure 63: A western blot of protein extracts from poliovirus infected and mock infected (no poliovirus) cells. Cells were infected with poliovirus (or mock) for 1 h followed by 6 h transfection of RNA: *Renilla* luciferase, HIV-1/2 Gag-Luc RNA reporters, a HIV-1 MA2 chimera reporter (containing HIV-1 Gag with the matrix domain from HIV-2) and dicistronic RHRVF/RHCVF RNA controls. eIF4G cleavage, shown by a band ~140 kDa is seen in poliovirus infected cells but not in the mock infected (control) cells.

HeLa cells infected with poliovirus were shown to have complete cleavage of eIF4G, producing a band of around 140 kDa [lanes 1-6, figure 63], in contrast to uninfected cells where intact eIF4G, producing a band around 220 kDa [lanes 7-12, figure 63], was detected.

Poliovirus infection resulted in complete cleavage of eIF4G and thus allowed a comparison of the rate of HIV-1/2 Gag RNA translation when cap-dependent translation was shutdown [figure 64].

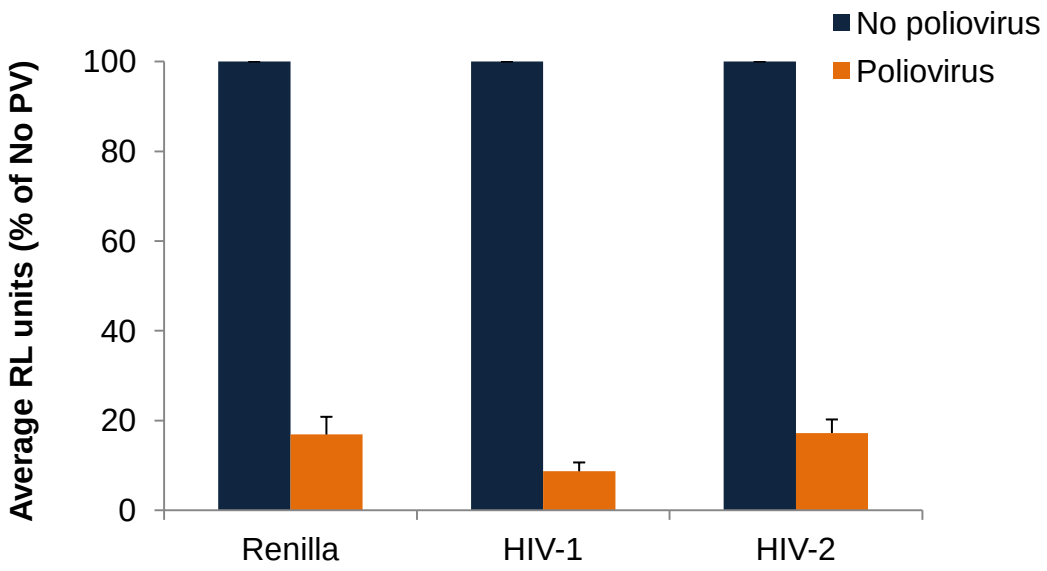

Figure 64: Translation of *Renilla* RNA and HIV-1/2 Gag-Luc RNA reporters in the presence and absence of poliovirus (PV) infection. Reactions were carried out in duplicate and averaged over 3 experiments. Values are normalised to 'no poliovirus' for each reporter to allow for a direct comparison of translation knockdown. Error bars represent the SEM.

In the presence of poliovirus infection, when cap-dependent translation was shut down by eIF4G cleavage, translation of both HIV-1 Gag and HIV-2 Gag RNAs decreased significantly by 91% and 83% respectively [figure 64]. Likewise, translation of the cap-dependent *Renilla* RNA control also decreased by 83% in poliovirus transfected cells. These results strongly suggest that both HIV-1 and HIV-2 Gag translation rely on cap-dependent initiation. Both of these RNAs are poorly translated when cap-dependent translation is shut down and, additionally, both RNAs behave comparably to the cap-dependent *Renilla* RNA control. The *Renilla* control solely relies on

cap-dependent translation; both HIV-1/2 Gag RNA translation decreased by a similar level to the cap-dependent *Renilla* RNA control suggesting that alternative translation initiation mechanisms are also inefficient under these conditions. This suggests that any cap-independent mechanism of translation that HIV-1/2 Gag RNAs may undergo is not able to compete with the poliovirus IRES for translational machinery.

4.3.4 HIV-1/2 Gag translation initiation: cap-dependence (uncapped RNA)

Inhibiting cap-dependent translation may have resulted in off-target cellular effects. As an alternative method to determine the importance of the 5' cap to HIV-1/2 Gag translation, uncapped HIV-1/2 reporter RNAs [figure 47] were produced. Transfection of 60 ng of both capped and uncapped HIV-1/2 RNA reporters, in duplicate, alongside a *Renilla* RNA control was carried out for 6 h in HeLa. Total cell protein was extracted and used in a luciferase assay to quantify translation of the Gag-Luc fusion protein from HIV-1/2 capped/uncapped RNA reporters [figure 65].

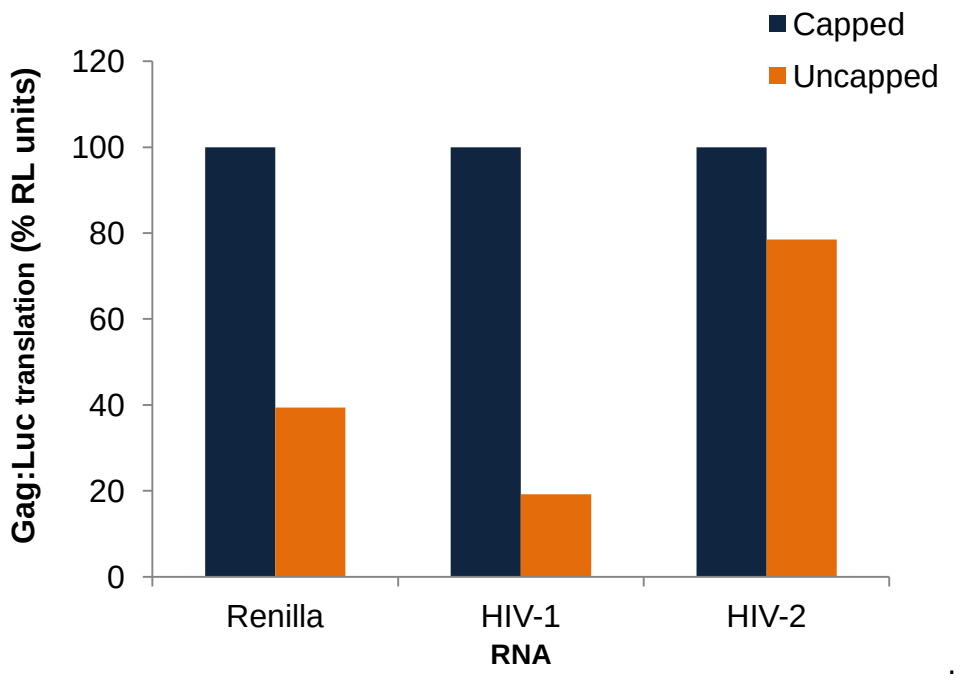

Figure 65: Luciferase assay of HIV-1/2 Gag translation expressed in relative light (RL) units from capped and uncapped RNA reporters. Results are normalised to a co-transfected *Renilla* luciferase RNA control and expressed as a percentage of 'capped RNA' data.

Removal of the 5' cap structure resulted in a considerable decrease in both the level of HIV-1 Gag translation (81%) as well as translation of the cap-dependent *Renilla* control (61%). Uncapped HIV-2 RNA showed a slight decrease (21%) in translation although not to the same extent as HIV-1 [figure 65]. These results suggest that translation of HIV-1 Gag is highly cap-dependent. Alternatively, whilst HIV-2 Gag translation still requires intact eIF4G, it depends less on the presence of a cap structure than for HIV-1 translation. However, these results could also mean that uncapped HIV-2 RNA is more stable in cells than uncapped HIV-1 RNA. Further work is required to check the stability of uncapped HIV-1/2 RNA and determine whether a greater degradation rate of uncapped HIV-1 RNA may have contributed to the lower HIV-1 translation level.

4.3.5 Use of internal AUG codons

Full-length Gag is reportedly produced from cap-dependent translation, whereas internal initiation from additional AUG sites is proposed to produce Gag isoforms (Ricci *et al.*, 2008). To determine whether alternative translational strategies are employed by HIV-1/2, the use of internal AUG codons was examined. However, the anti-capsid antibody typically used to visualise HIV-1/2 Gag detects capsid-containing products from the proteolytic cleavage of Gag, and not primarily full-length Gag. Consequently, to observe full-length Gag and thus visualise translational isoforms of the Gag precursor, it was necessary to prevent HIV Protease cleavage of Gag. Saquinavir (SQ) is a HIV Protease inhibitor and was therefore used to specifically inhibit HIV Protease cleavage of Gag.

HeLa cells were transfected with 580 ng of HIV-1/2 provirus DNA for 24 h in the presence/absence of saquinavir (+/- SQ) before harvesting cellular proteins. Western blotting and immunoprobing with antibodies to the HIV Gag capsid region (p24 for HIV-1, p27 for HIV-2) allowed visualisation of Gag precursors and cleavage products [figure 66].

In the absence of SQ, HIV-1 full-length p55 Gag and Gag cleavage products: the processing intermediate p41 (Matrix/Capsid, p17/p24) and p24 Capsid protein, were identified [lane 1, figure 66]. In the presence of SQ, an

additional 160 kDa band was identified [lane 2, figure 66] representing HIV-1 Gag-Pol in addition to full-length p55 Gag, whereas the p41 processing intermediate and Capsid p24 were no longer detectable. Likewise, both HIV-2 p57 Gag and cleaved p27 Capsid were detectable in the absence of SQ [lane 3, figure 66] whereas only full-length p57 Gag was detected when SQ was present [lane 4, figure 66]. This indicates that SQ successfully inhibited HIV-1/2 Protease cleavage.

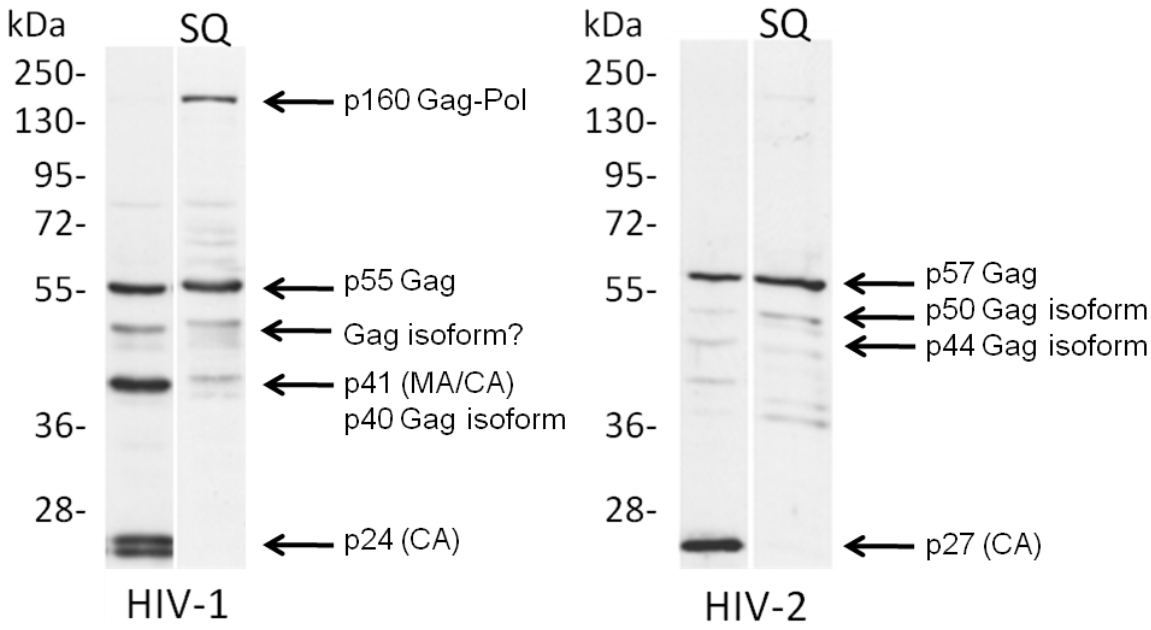

Figure 66: Western blot with antibodies to the capsid region of HIV-1/2 Gag. Expression of HIV-1 and HIV-2 Gag (p55/p57) precursors, the HIV-1 p41 Matrix/Capsid (MA/CA) processing intermediate and both HIV-1/2 Capsid (p24/p27) proteins are shown from transfected provirus in the presence/absence of saquinavir (SQ).

Furthermore, the p40 HIV-1 Gag isoform and a potentially new HIV-1 Gag isoform around 48 kDa were detected [lanes 1+2, figure 66] in addition to the HIV-2 p50 and p44 Gag isoforms [lanes 3+4, figure 66].

Ricci *et al.* (2008) have suggested that translation of these Gag isoforms may be driven by internal initiation from one or several HIV IRES. PV infection was therefore used to shut down cap-dependent translation (via eIF4G cleavage) and monitor whether internal AUG translation initiation was able to promote translation of the Gag isoforms. HeLa cells were transfected with 580 ng of HIV-1/2 provirus DNA for 24 h in the presence/absence of saquinavir (+/- SQ) before infecting cells with poliovirus (PV) for 1 h (+/-

saquinavir). Cells were subsequently left for 6 h (+/- saquinavir) before harvesting cellular protein for use in a western blot with antibodies to HIV-1/2 Gag p24/p27 [figure 67].

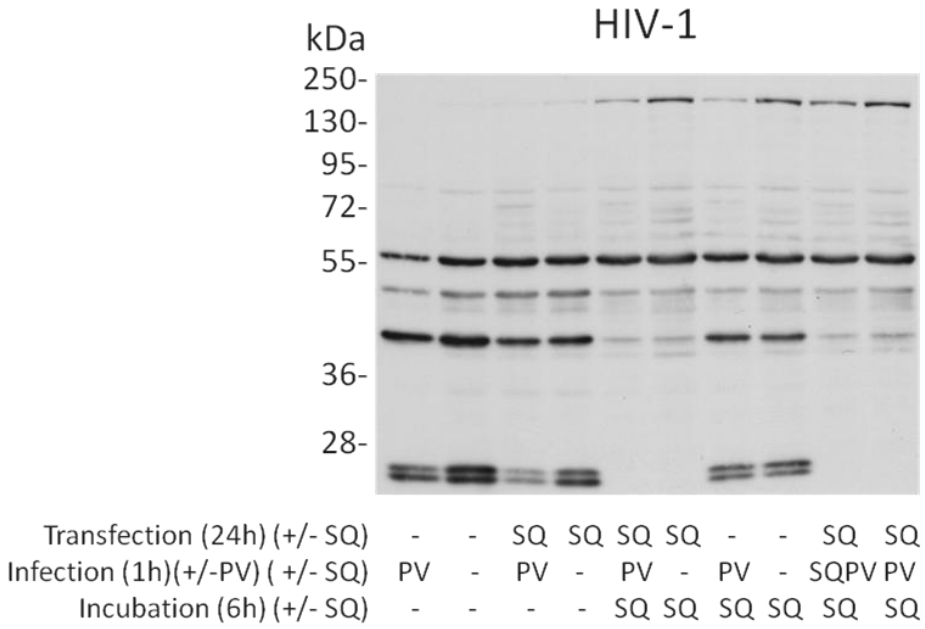

(A)

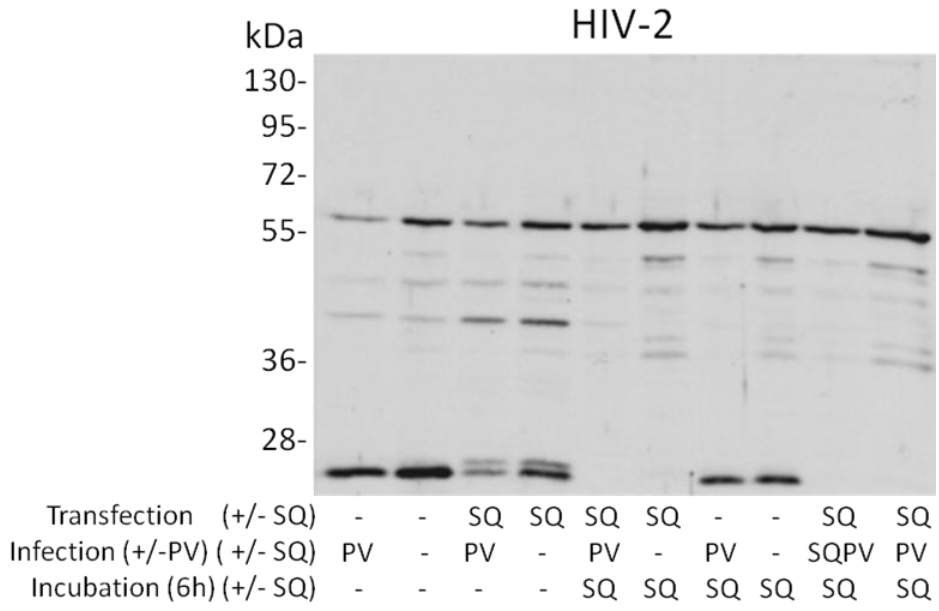

(B)

Figure 67: Western blot of transfection protein with antibodies for HIV-1 Gag (p24) (A) and HIV-2 Gag (p27) (B). Provirus transfections were carried out for 24 h with/without saquinavir (+/- SQ). Cells were then infected with/without poliovirus (+/- PV) for 1 h (+/- SQ) and then incubated for 6 h (+/- SQ) before harvesting total cell protein.

In cells infected with poliovirus, the level of HIV-1/2 Gag precursors, p41 processing intermediates and Capsid proteins were lower than for uninfected cells. This was represented by fainter bands on the gel [lanes 1+2 for HIV-

1/2, figure 67] indicating that the shutdown of cap-dependent translation via eIF4G cleavage was preventing HIV Gag translation. A western blot of samples with an antibody to eIF4G showed that complete eIF4G cleavage was detected in all samples infected with poliovirus (+/- SQ) (data not shown). This indicates that cap-dependent translation was shut down in poliovirus infected cells. Likewise, this confirmed that SQ was not inhibiting the activity of the poliovirus 2A protease and its activity was therefore specific to the HIV Protease.

It was unknown whether SQ treatment was necessary at every stage of the experiment to prevent Gag precursor cleavage, or whether SQ treatment would interfere with the success of PV infection on shutting down cap-dependent translation. The presence of SQ throughout the experiment successfully prevented cleavage of the Gag precursor into either processing intermediates or Capsid. This was evident from the lack of lower molecular weight bands and an increase in the intensity of the Gag precursor band for samples fully treated with SQ [lanes 5, 6, 9+10 for HIV-1/2, figure 67]. Samples which were only treated with SQ for partial stages of the experiment produced some Gag cleavage products [lanes 3, 4, 7+8 for HIV-1/2, figure 67], albeit to a lesser extent than cells not treated with saquinavir. This indicates that some Gag cleavage was able to occur at stages of the experiment where SQ was not present.

It was thought that when cap-dependent translation was shut down, IRES-driven translation, utilising internal Gag AUG codons, may have been enhanced due to reduced competition for translational machinery by cap-dependent RNAs. However, in cells treated with both PV and SQ, whereby cap-dependent translation was inhibited and Gag precursor cleavage prevented, no additional translation of HIV-1/2 Gag isoforms was identified [lanes 5, 9+10 for HIV-1/2, figure 67].

Furthermore, eIF4G cleavage has been shown to enhance IRES activity (Dobrikova *et al.*, 2006). Therefore, if IRES-driven activity from internal Gag AUG codons was stimulated by eIF4G cleavage (in PV infected cells) it was expected that stronger bands around 40 kDa (HIV-1) and 44 kDa/50 kDa

(HIV-2) would be apparent for protein samples from PV infected and SQ treated cells [lanes 5, 9+10 for HIV-1/2, figure 67]. However this was not the case; PV infection did not alter the ratio of Gag isoforms produced. This suggests that hypothesised IRES elements linked to internal AUG sites are non-functional and unable to compensate for the shutdown of cap-dependent translation under these conditions. The expression of Gag isoforms may therefore be a result of alternative translation events such as leaky scanning.

4.4 HIV-1/2 Gag translation initiation: 5' UTR secondary structure

4.4.1 Folding energy

4.4.1.1 Full HIV-1/2 5' UTR folding energies

The 5' UTR folding energy of HIV-1 and HIV-2 may affect translation. A high folding energy indicates a higher level of secondary structure which may inhibit ribosomal scanning or spatially impede formation of a translation initiation complex. The average 5' UTR folding energy of HIV-1/2 strains, referenced from the Los Alamos Database, were compared (http://www.hiv.lanl.gov/content/sequence/HIV/mainpage.html) and the folding energy calculated for HIV-1 sequences >300 nt and HIV-2 sequences >500 nt using UNAfold (http://www.bioinfo.rpi.edu/applications/hybrid/download.php). Additionally, the average folding energy per nucleotide for each 5' UTR was calculated [table 8].

	Kcal (AVG)	Kcal/nt (AVG)
HIV-1	-113.6	-0.320
HIV-2	-191.0	-0.356

Table 8: The average folding energy (Kcal) and folding energy per nucleotide (Kcal/nt) for the 5' UTR of several HIV-1 and HIV-2 strains. A greater negative energy value represents a more stable RNA structure.

The HIV-2 5' UTR has a more negative folding energy (-191.0 Kcal) than HIV-1 (-113.6 Kcal) suggesting it has a more stable RNA structure. The folding energy per nucleotide of the HIV-2 5' UTR (-0.356 Kcal/nt) is also

more negative than for HIV-1 (-0.320 Kcal/nt). Given that the HIV-2 5' UTR is also longer (545 nt compared to 335 nt for HIV-1), this suggests that the HIV-2 5' UTR is intrinsically more structured than the HIV-1 5' UTR. Thus impeded ribosomal scanning of the HIV-2 5' UTR may hinder the rate of HIV-2 Gag translation to a greater extent than for HIV-1.

4.4.1.2 ΔTAR HIV-1/2 5' UTR folding energies

Specific sequences or structures within HIV RNA may affect translation efficiency, especially those at the very 5' end of the RNA where initial ribosome recruitment may occur. The 5' terminus of the HIV 5' UTR contains a highly conserved, secondary stem-loop TAR structure [figure 68].

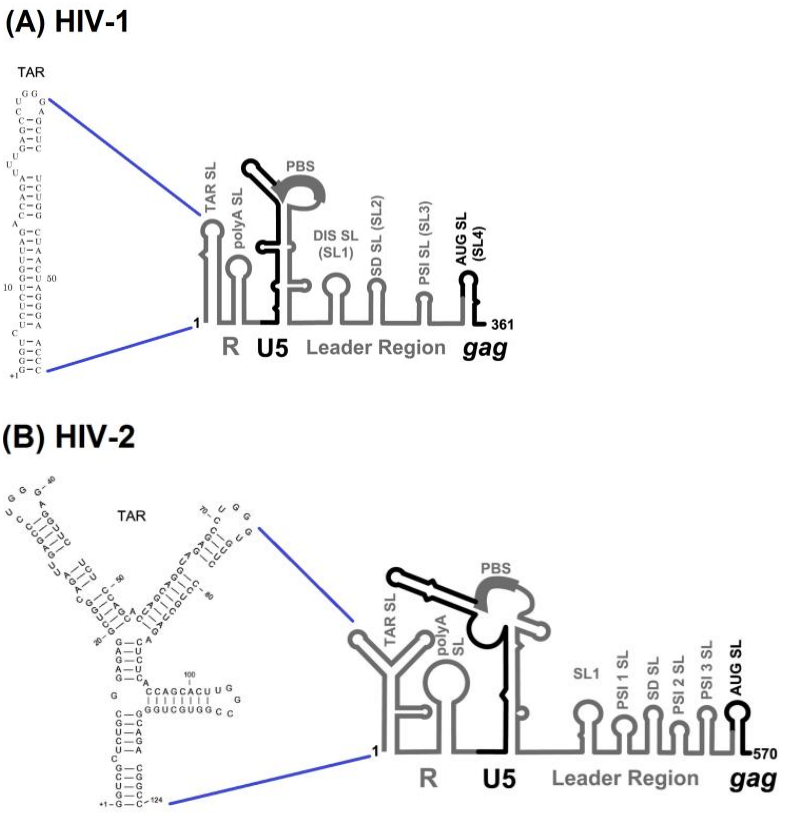

Figure 68: The HIV TAR structures found at the start of the HIV-1/2 5' UTR. HIV-1 TAR consists of a 59 nucleotide structure whereas HIV-2 has an extended, 123 nucleotide structure (Dirac *et al.*, 2001; Jossinet *et al.*, 2001; Purzycka and Adamiak, 2008; Strong *et al.*, 2009).

TAR RNA has a different structure in HIV-1 and HIV-2 (Brady and Kashanchi, 2005). The HIV-2 TAR consists of an extended 123 nucleotide structure compared to 59 nucleotides for HIV-1. HIV-2 TAR may therefore obstruct

ribosomal scanning to a greater extent than HIV-1 TAR, contributing to the lower HIV-2 translation rate.

The folding energy (Kcal) and folding energy per nucleotide (Kcal/nt) were calculated following removal of the TAR structure from HIV-1/2 5' UTR sequences to see if this resulted in more equivalent 5' UTR folding energies [table 9].

	Kcal (AVG)	Kcal/nt (AVG)
HIV-1 ΔTAR	-85.8	-0.295
HIV-2 ΔTAR	-135.1	-0.326

Table 9: The average folding energy (Kcal) and folding energy per nucleotide (Kcal/nt) for ΔTAR HIV-1/2 5' UTRs. A greater negative energy value represents a more stable RNA structure.

The HIV-2 ΔTAR 5' UTR still had a more negative folding energy (-85.8 Kcal) than the HIV-1 ΔTAR 5' UTR (-135.1 Kcal) indicating that there are further structural differences between the HIV-1/2 5' UTRs than just those observed within the TAR region. Removal of the TAR structure slightly reduced the difference between the HIV-1/2 folding energies, from a difference of 77.4 Kcal with TAR, to 49.3 Kcal without TAR. Therefore, although TAR is not solely responsible for folding energy differences between HIV-1/2, it partly contributes to the greater negative score, and thus greater level of structure, for the HIV-2 5' UTR.

4.4.1.3 TAR G-C content

The folding energy of RNA is dependent on the level of G-C and A-U base pairing within the RNA sequence. G-C base pairing contributes a higher level of stability, thus indicating the presence of more structure and contributing to a higher folding energy. The G-C nucleotide pair content of the HIV-1 and HIV-2 TAR structures was compared to see if introducing base pairing mutations could reduce the folding energy of HIV-2 TAR to a similar level to the HIV-1 TAR folding energy. HIV-1 TAR contains 12 G-C pairs, whereas HIV-2 TAR contains 30 G-C pairs [figure 69].

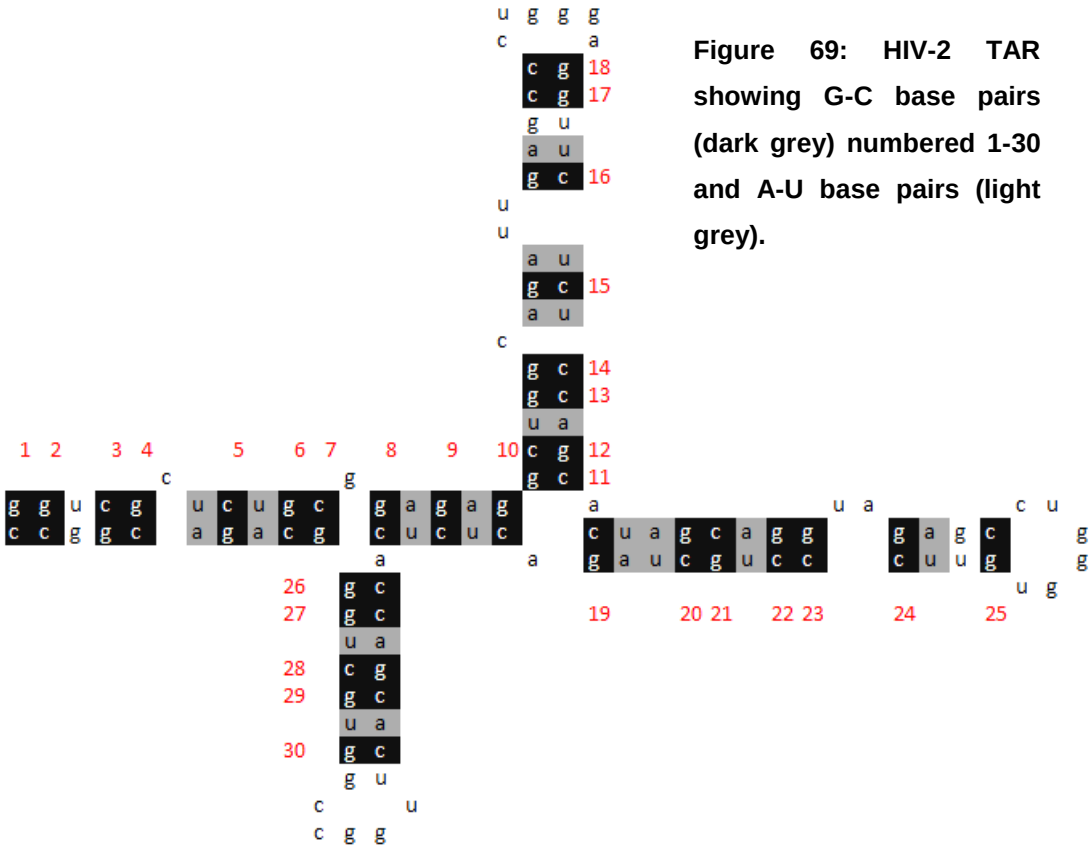

Figure 69: HIV-2 TAR showing G-C base pairs (dark grey) numbered 1-30 and A-U base pairs (light grey).

The TAR folding energy of HIV-1/2 TAR was calculated using MFOLD [http://bibiserv.techfak.uni-bielefeld.de/mfold]. The folding energy of HIV-1 TAR is -29.6 Kcal and HIV-2 TAR is -65.5 Kcal. A-U base pairs are less stable than G-C base pairs and thus reduce folding energy (Yakovchuk *et al.*, 2006). G-C to A-U exchanges were therefore introduced into the TAR base pairs of the HIV-2 5' UTR sequence and the folding energy calculated using MFOLD. The effect of reducing G-C concentration on the overall TAR folding energy was analyzed [Table 10].

A single G-C to A-U substitution within HIV-2 TAR had little impact on the MFOLD folding energy of HIV-2 TAR. This suggests that there is not a single G-C base pair that contributes a significant amount to the high folding energy of HIV-2 TAR. Therefore, a greater number of G-C to A-U substitutions were made to HIV-2 TAR to see how many G-C substitutions were necessary to reduce the HIV-2 TAR folding energy (-65.5 Kcal) to a similar folding energy as HIV-1 TAR (-29.6 Kcal). The folding energies for differing numbers of G-C to A-U substitutions, whilst still retaining the original HIV-2 TAR structure, were calculated using MFOLD and plotted in Excel [figure 70].

GC-AU substitution #	Folding energy (Kcal)	Energy difference to wt (Kcal)
26	-64.60	-0.9
3	-64.30	-1.2
4,23	-64.10	-1.4
10	-64.00	-1.5
1	-63.80	-1.7
25,30	-63.60	-1.9
2, 6, 13, 16, 17, 18, 19, 21,	-63.50	-2
12,14, 20, 22, 28	-63.10	-2.4
5, 7, 9, 11, 15	-62.80	-2.7
8	-62.50	-3.0
27	-60.60	-4.9

Table 10: The folding energy of HIV-2 TAR for individual G-C to A-U substitutions. G-C pair numbers are based on the position of G-C [figure 69]. Energy difference is shown as the deviation in folding energy from the wild type HIV-2 TAR structure (-65.6 Kcal).

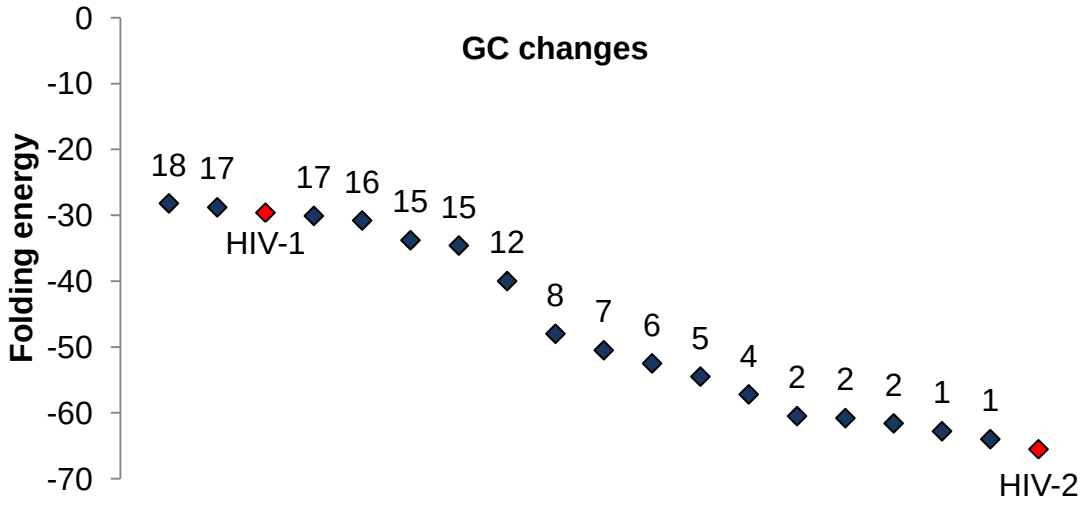

Figure 70: G-C to A-U substitutions within HIV-2 TAR. The number of G-C to A-U substitutions (shown above each data point) is plotted alongside the corresponding TAR folding energy. The folding energy of both HIV-1 and HIV-2 TAR are indicated in red.

The introduction of G-C to A-U substitutions reduced the folding energy of HIV-2 TAR relative to the number of substitutions introduced. To achieve a HIV-2 TAR structure with a similar folding energy to that of the HIV-1 TAR structure it is necessary to introduce between 17 and 18 G-C to A-U substitutions to HIV-2 TAR. Future work could include synthesis of an HIV-2 reporter with these substitutions to test its translation efficiency.

4.4.2 Deletion of the HIV-1/2 TAR structure

4.4.2.1 *In vitro* ΔTAR translation

To investigate the translational effect of deleting TAR, and ascertain whether this results in more equivalent HIV-1/2 Gag translation levels, 60 ng of HIV-1/2 RNA reporters [figure 47] with or without TAR deletions (ΔTAR) were used in an *in vitro* RRL translation system. Translated proteins were visualised by SDS-PAGE and autoradiography [figure 71] and used in a luciferase assay [figure 72].

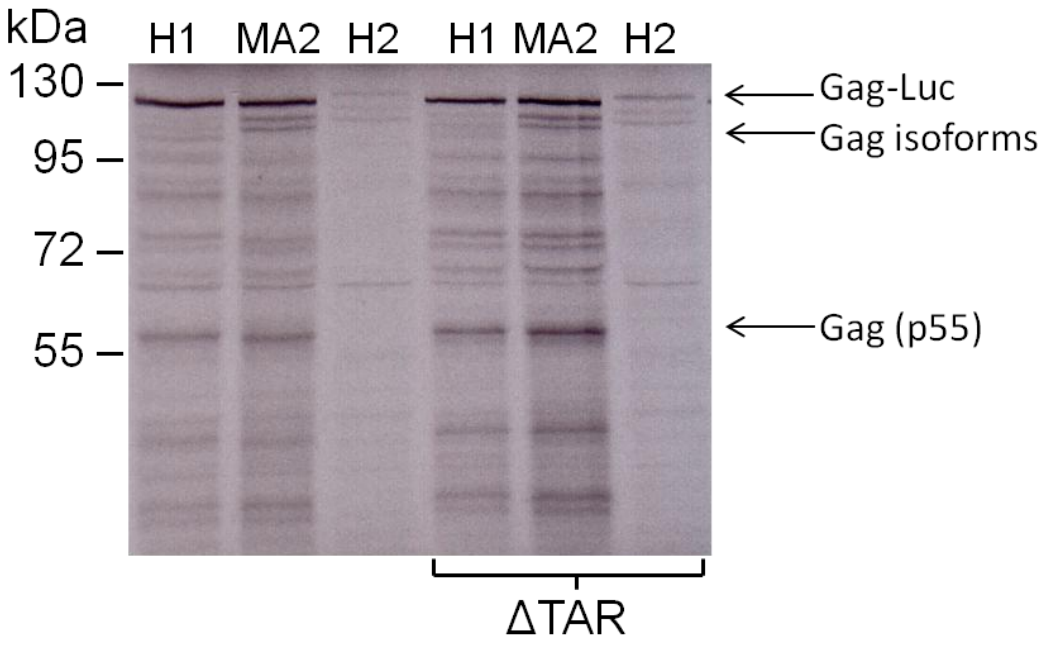

Figure 71: Expression of ^{35}S-methionine labelled proteins from HIV-1/2 RNA reporters (with/without TAR deletions) during an *in vitro* RRL translation.

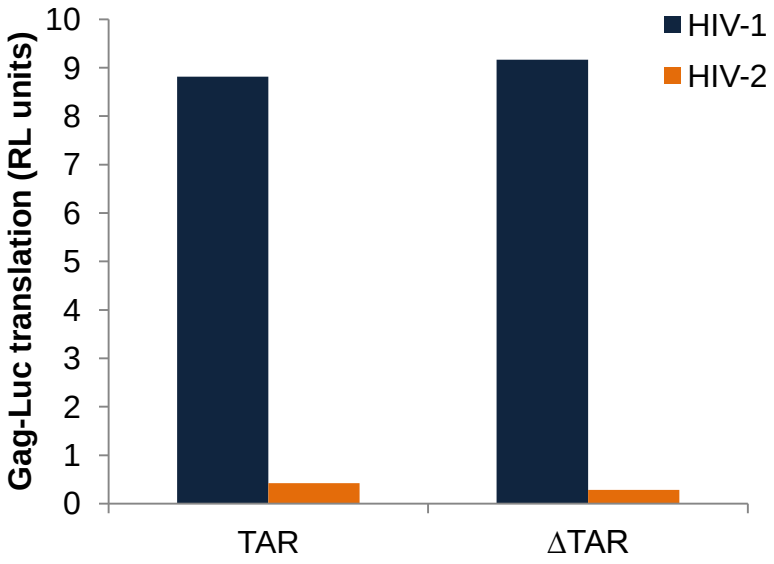

Figure 72: A luciferase assay of ^{35}S-methionine labelled proteins translated from HIV-1/2 RNA reporters (with/without TAR deletions) during an *in vitro* RRL translation.

Both HIV-1 and HIV-2 Gag translation levels appeared to be similar in the presence and absence of TAR when visualised by autoradiography [figure 71] or used in a luciferase assay [figure 72]. Therefore deleting TAR appeared to have relatively little effect on the translation level of either HIV-1 or HIV-2 Gag. HIV-1 Gag translation remained more efficient than HIV-2 whether TAR was present or not. These results were surprising considering the contribution of HIV-2 TAR to a higher 5' UTR folding energy. However, additional translational factors may negate the structural impediment imposed by HIV-2 TAR. As deleting HIV TAR did not produce equivalent translation rates for HIV-1/2, it is likely that the presence of a different TAR structure in HIV-2 is not accountable for the lower HIV-2 Gag translation rate *in vitro*.

4.4.2.2 Cellular ΔTAR translation

The contribution of HIV-1/2 TAR to the translation efficiency of HIV-1/2 Gag was also compared in cells. 50 ng, 500 ng or 1000 ng of HIV-1/2 reporter RNA (with/without TAR) was used to transfect HeLa cells for 6 h and the rate of Gag translation measured by a luciferase assay of harvested protein. Results were normalised to a co-transfected *Renilla* luciferase RNA control

[figure 73]. Transfections were carried out in duplicate and results shown are the average of 2 experiments.

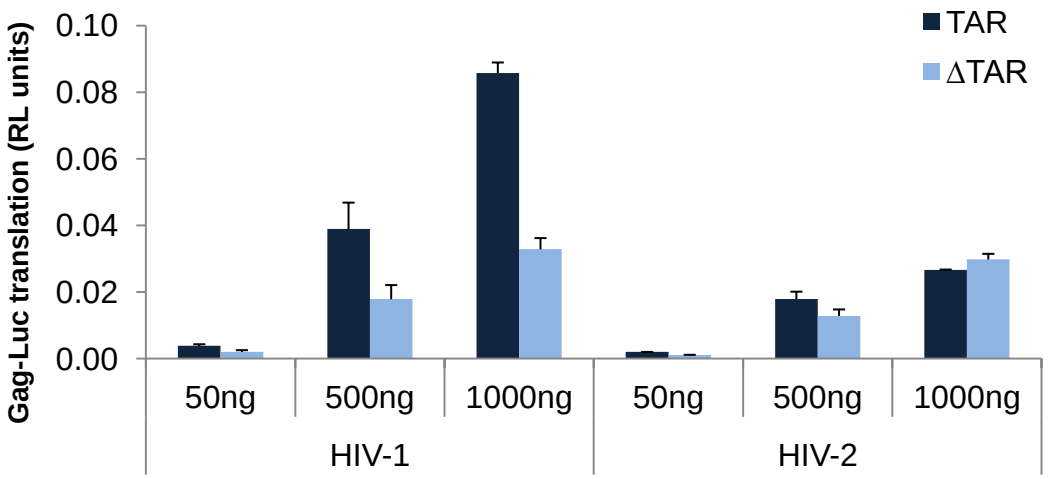

Figure 73: Luciferase assay results from HeLa cell translation of varying concentrations of HIV-1/2 Gag-Luc RNA reporters (with and without TAR) for 6 h. Error bars represent the SEM.

Surprisingly, both HIV-1 and HIV-2 gag RNA was translated less efficiently when TAR was deleted. In the absence of TAR, translation of gag RNA was up to 62% (for HIV-1) and up to 45% (for HIV-2) less efficient. Interestingly, at higher concentrations of HIV-2 gag RNA, TAR deletions were less detrimental, and for 1000 ng even beneficial, to HIV-2 gag translation levels. At lower concentrations, HIV-2 ΔTAR RNA may not have been able to compete with naturally occurring cellular translation. However, at higher concentrations, the abundance of HIV-2 ΔTAR RNA may overwhelm translational machinery allowing this normally inefficient RNA to be preferentially translated.

Although removing TAR did not enhance HIV-2 Gag translation levels equivalent to wild type HIV-1 Gag translation levels, when TAR was deleted HIV-1 and HIV-2 Gag translation was more equivalent. HIV-1 TAR suppresses PKR, thus enhancing translation. Removing HIV-1 TAR may therefore effect a decrease in translation as active PKR is able to phosphorylate eIF2; this inhibits translation (Cole, 2007). A similar mechanism may not be present for HIV-2 TAR; this may contribute to the

lower rate of HIV-2 Gag translation and explain why deleting TAR does not further reduce HIV-2 Gag translation to the same extent as for HIV-1.

Additionally, BSRT7 cells were transfected with 250 ng or 1000 ng of the same HIV-1/2 Gag-Luc RNA reporters (with/without TAR), in duplicate, for 6 h and total cellular protein harvested. Again, a luciferase assay was carried out to determine the rate of Gag-Luc translation from reporter RNAs [figure 74].

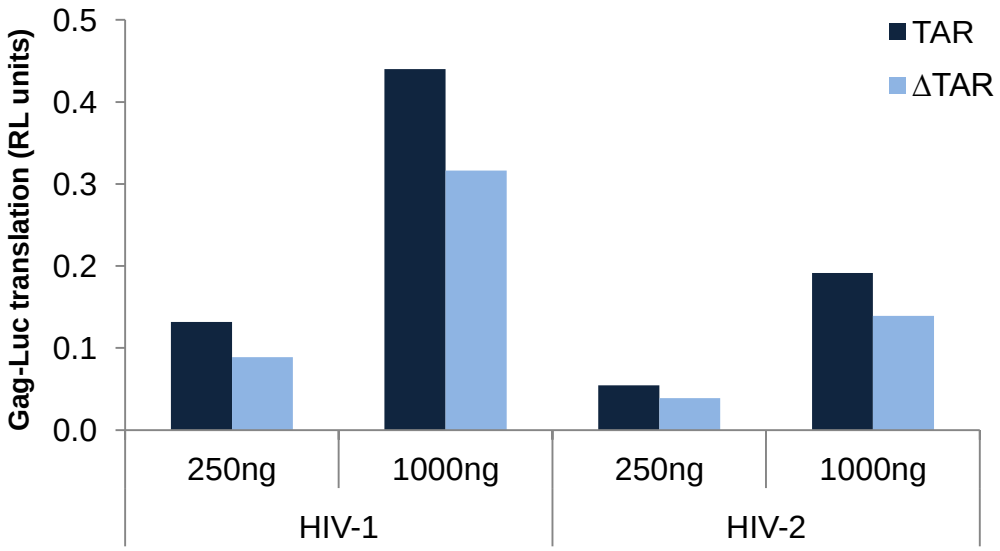

Figure 74: BSRT7 translation of HIV-1/2 Gag-Luc RNA reporters (with and without TAR) for 6 h for varying concentrations of RNA. Gag-Luc expression is shown in relative light (RL) units and is normalised to a co-transfected *Renilla* luciferase RNA control. Error bars represent the SEM.

As for HeLa cell transfections, HIV-1 Gag-Luc translation levels were consistently higher than HIV-2 Gag-Luc translation levels, even in the absence of TAR. Additionally, deleting TAR reduced the translation levels of HIV-1 (by up to 33%) and HIV-2 (by up to 29%). However, unlike with HeLa cell transfections, when both HIV-1 and HIV-2 TAR elements were deleted HIV-2 ΔTAR Gag-Luc RNA translation remained much lower than for HIV-1.

BSRT7 cells stably express T7 RNA polymerase allowing for transfection of reporter plasmids containing a T7 promoter. Consequently, 1 µg of HIV-1/2 Gag-Luc plasmids (with and without TAR deletions) were used to transfect BSRT7 cells for 24 h. Total cell protein was harvested and a luciferase assay

carried out to measure the level of HIV-1/2 Gag-Luc expression in the presence and absence of TAR. Gag-Luc expression was normalised to *Renilla* luciferase protein levels expressed from co-transfection of a *Renilla* luciferase plasmid (pTK *Renilla*) [figure 75]. Transfections were carried out in duplicate and results shown are the average of 2 experiments.

(A)

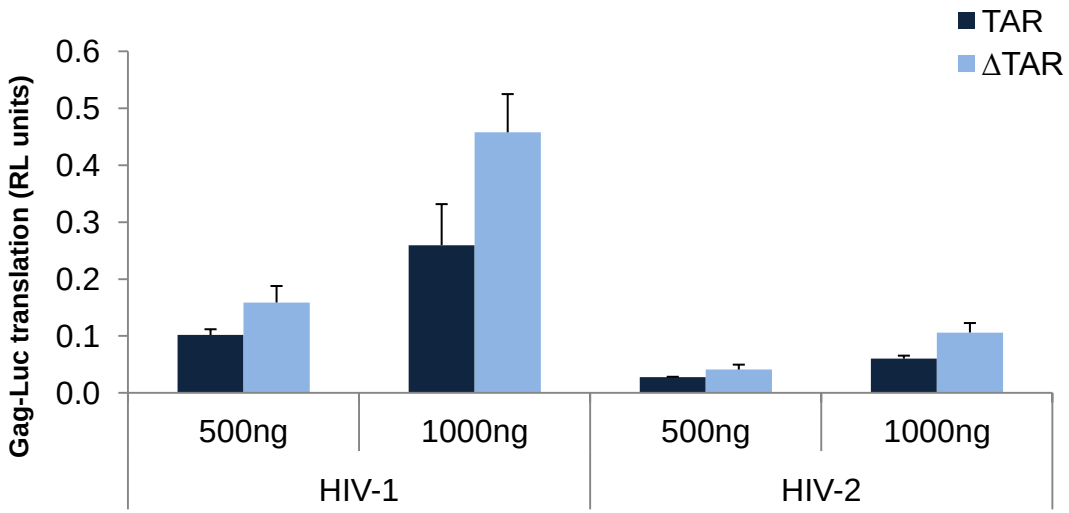

(B)

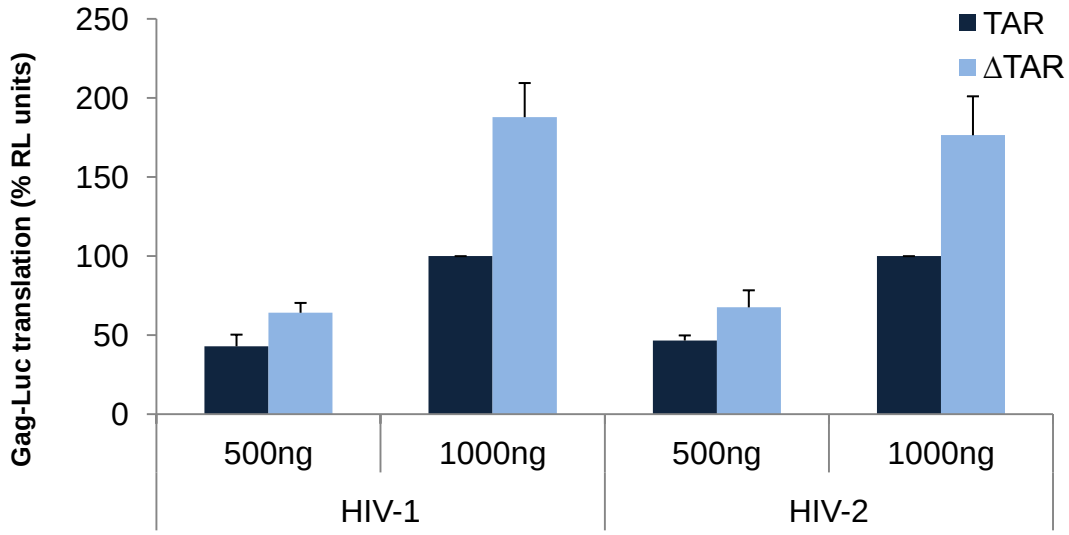

Figure 75: Transfection of BSRT7 cells with 500 ng and 1000 ng of HIV-1/2 Gag-Luc plasmids (with and without TAR) for 24 h. Gag-Luc translation is measured in relative light (RL) units. Gag-Luc expression was normalised to *Renilla* luciferase expressed from a co-transfected *Renilla* luciferase plasmid (A). Results are expressed as a percentage of 1000 ng TAR RNA reporter values to compare the HIV-1/2 percentage change in Gag-Luc expression levels (B). Error bars represent the SEM.

When Gag levels were quantified following reporter plasmid transfections, deleting TAR appeared to increase the level of Gag expression by up to 1.8-fold for both HIV-1 and HIV-2 Gag [figure 75]. This is directly opposed to the results shown for RNA reporter transfections where deleting TAR decreased Gag translation. This effect is not an artefact caused by cell type as both reporter RNA [figure 74] and reporter plasmid DNA [figure 75] were transfected into BSRT7 cells. Thus it appears that when Gag is transcribed and translated from a DNA plasmid, deleting TAR enhances expression whereas when Gag is translated from reporter RNA, deleting TAR reduces Gag translation.

4.4.2.3 ΔTAR RNA stability

To determine whether ΔTAR affects reporter RNA stability, a comparison of TAR/ΔTAR RNA reporter degradation rates was carried out using qPCR. 60 ng HIV-1/2 (TAR/ΔTAR) RNA reporters were used to transfect HeLa cells and total RNA harvested at 3 h and 6 h post-transfection. Following the production of cDNA, qPCR was carried out in duplicate using primers to HIV-1 Gag (primer # 22, 23) and HIV-2 Gag (primer # 23, 24). Gag gene expression was normalised to a GAPDH housekeeping gene (primer #18, 19) and expressed as $2^{\Delta Ct}$ [figure 76].

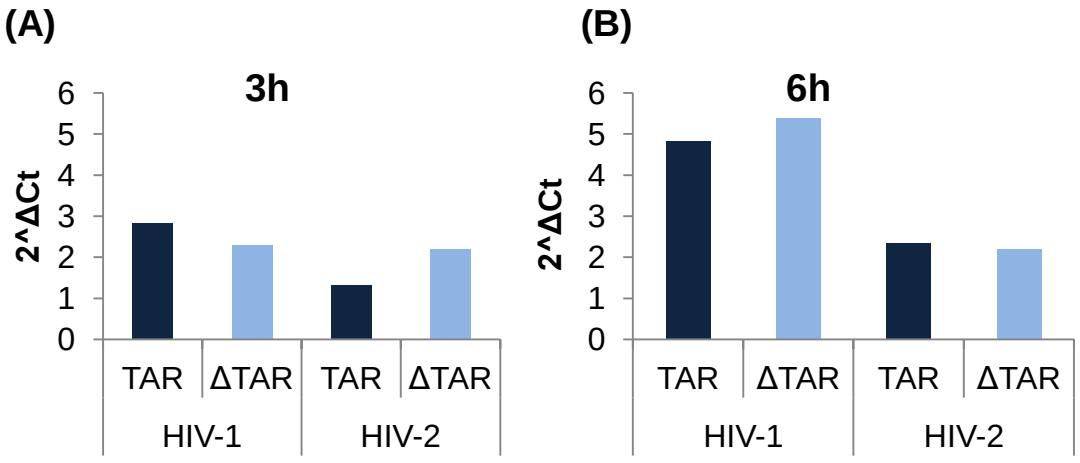

Figure 76: Luciferase assay showing the level of HIV-1/2 (TAR/ΔTAR) RNA 3 h (A) and 6 h (B) post-transfection. RNA levels are normalised to GAPDH and expressed as $2^{\Delta Ct}$.

A comparison of HIV TAR and ΔTAR RNA levels for both HIV-1 and HIV-2 at 3 h and 6 h post-transfection revealed that deleting TAR did not reduce the

stability of reporter RNA. By 6 h HIV-1 TAR/ΔTAR RNA levels were equivalent as were HIV-2 TAR/ΔTAR RNA levels. Consequently, HIV-1/2 ΔTAR/TAR RNA reporter stability does not differentially affect translation rates.

4.5 HIV-1/2 Gag translation: elongation

4.5.1 A comparison of HIV-1/2 Gag codon bias

The translation elongation rate can be reduced by the presence of rare codons. Within the human genome, 20 amino acids are encoded by 61 codons. The cellular concentration of amino-acyl tRNAs, which recognise these codons, is asymmetric and can vary by up to 10-fold. Therefore the rate of codon translation can vary dependent on the availability of the cognate amino-acyl tRNA. Codons that are recognised by abundant tRNA maximise translation efficiency, whereas rare tRNAs can cause stalling of the ribosome whilst it waits to encounter a cognate tRNA. Some synonymous codons are more commonly used and therefore dominate in genes which are frequently expressed, introducing the concept of codon bias (Zhang *et al.*, 2009).

The human codon usage table was used to calculate the frequency of each codon within the HIV-1 and HIV-2 Gag ORFs [http://genome.imim.es/courses/Lisboa01/slide3.8.html]. The average codon bias of the entire HIV-1/2 Gag ORF was calculated to see if elongation rates may contribute to differences in the translation efficiencies of these two viruses [table 11].

	HIV-1	HIV-2
Codon Bias (Average)	0.364	0.379

Table 11: The average codon usage within the HIV-1/2 Gag ORF. A lower value reflects the occurrence of more rare codons.

The average frequency of codon usage, and therefore the average codon bias, does not appear to differ greatly between HIV-1 (0.364) and HIV-2 (0.379) considering the range of codon bias within human genes (from 0.06

to 1). Moreover, the HIV-2 frequency of codon usage is actually marginally higher than HIV-1; therefore fewer rare codons are present within HIV-2 Gag. This would result in more efficient elongation for HIV-2. Consequently, overall, codon bias is unlikely to reduce HIV-2 elongation sufficiently to cause the observed reduction in HIV-2 Gag translation levels.

The average codon bias as a continuous window of 10 codons was plotted to indicate regions of high or low codon bias within the HIV-1/2 Gag ORF. The results were plotted as a line graph to compare the peaks and troughs in codon bias throughout HIV-1 and HIV-2 Gag [figure 77].

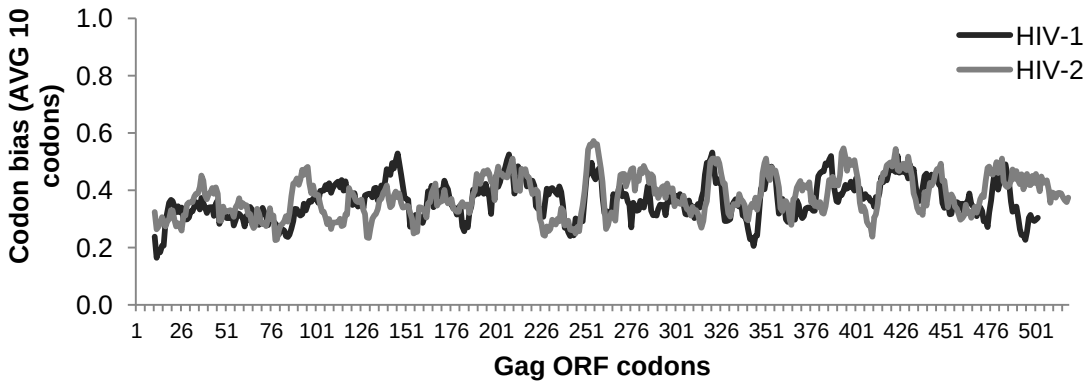

Figure 77: The codon bias throughout the HIV-1/2 Gag ORF. The average codon bias of a sliding 10 codon window is plotted along the length of the Gag ORF.

The HIV-1/2 average codon bias graphs are reasonably equivalent, with peaks and troughs in rare codon usage at similar locations in Gag. This further demonstrates that it is unlikely that rare codon use differentially alters HIV-1/2 elongation rates to contribute to the lower rate of HIV-2 Gag translation.

4.5.2 A comparison of HIV-1/2 Gag codon pair bias (CPB)

Translation efficiency can also be affected by the combination of adjacent codon pairs. Under-represented codon pairs have poor translatability. This is known as the codon pair bias (CPB). CPB was compared in the HIV-1/2 Gag ORF using codon pair scores (CPS) from the human ORFeome (Coleman *et al.,* 2008; supplementary online material) [table 12].

	HIV-1	HIV-2
Codon Pair Bias (Average)	0.029	0.021

Table 12: The average codon pair usage within the HIV-1/2 Gag ORF. A lower value reflects the occurrence of more rare codon pairs.

The average CPB is 0.029 for HIV-1 and 0.021 for HIV-2 compared to an average of 0.07 (and a range of -2.191 to 1.516) for all annotated human genes [figure 78].

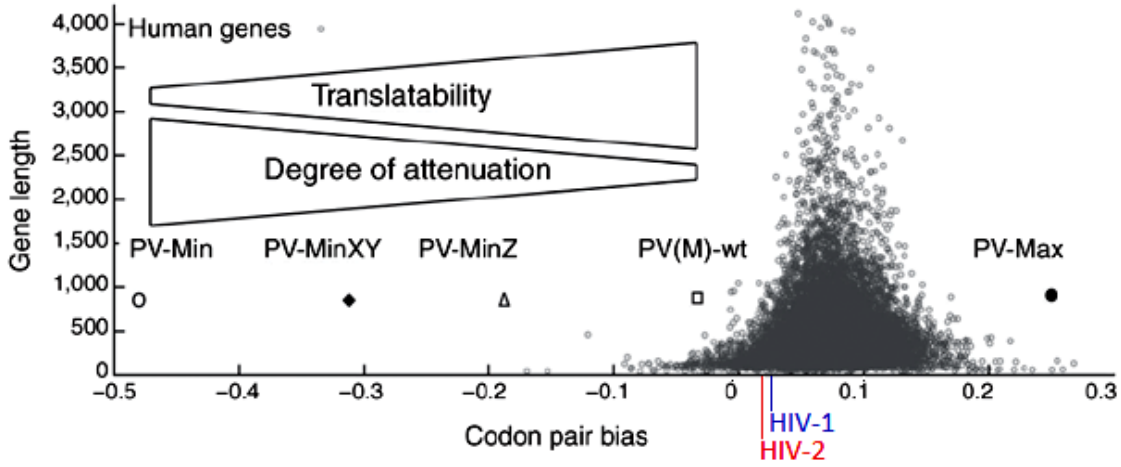

Figure 78: The CPB score of genes within the human genome. Each dot represents the CPB score of one gene plotted against the gene length (in amino acids). Genes containing increasing numbers of rare amino acids yield a more negative score and show decreased translatability (Coleman *et al.*, 2008).

Given the range of CPB scores within the human genome, it is apparent that the HIV-1/2 average CPB do not differ significantly from each other within the distribution. An increased prevalence of rare codon pairs does not, therefore, account for the reduced translatability of HIV-2 Gag.

The average CPB was plotted as a continuous window of 10 codons along the HIV-1/2 Gag ORF to compare the distribution of high or low regions of codon pair bias [figure 79].

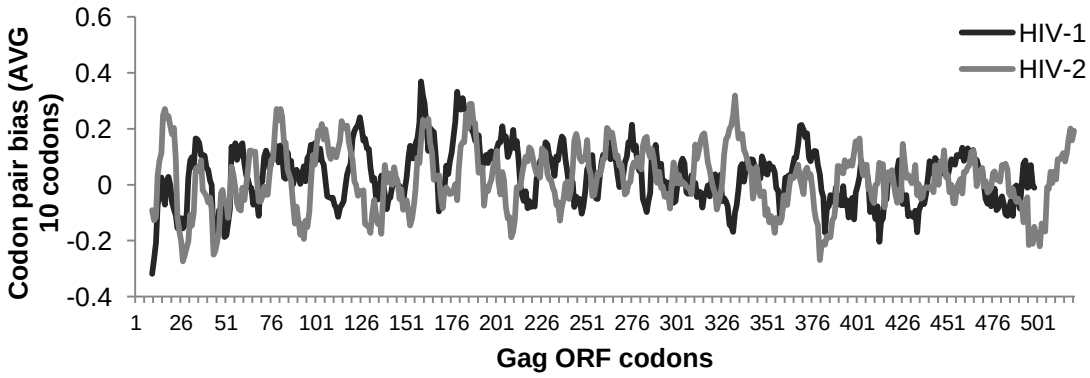

Figure 79: Codon pair usage within the HIV-1/2 Gag ORF. The average CPS for continuous groups of 10 codons is plotted along the length of the Gag ORF.

The distribution of rare codon pairs does not differ significantly throughout the HIV-1/2 Gag ORF, suggesting the presence of rare codon pairs is unlikely to differentially affect HIV-1/2 elongation or translation. Overall, codon bias and codon pair bias do not differ significantly between HIV-1 and HIV-2 Gag. Therefore, translational differences between HIV-1/2 are not likely to be due to elongation.

4.6 Discussion

4.6.1 A comparison of HIV-1/2 Gag translation

HIV-1/2 Gag translation from reporter RNA was compared *in vitro* and in several cell types. In all cases, HIV-1 Gag was translated much more efficiently than HIV-2 Gag; by 20.8-fold *in vitro* [figure 72], by 6.9-fold in HeLa, 11.9-fold in COS-1 and 3.2-fold in Jurkat cells. HeLa were chosen as these are a robust cell line well documented for their transfectability. HIV is a virus of primate origin and therefore COS-1 monkey cells are representative of a natural SIV host cell. Likewise, Jurkat cells are physiologically relevant cells to HIV infection as T-lymphocytes are targets of HIV infection *in vivo*.

HIV-1/2 RNA stability was not shown to differ, therefore differences in the level of Gag produced from HIV-1/2 RNA reporters were due to translation efficiency. Thus translation of HIV-2 may be a limiting factor during its replication, potentially accounting for, or contributing to, the reduced viral load attributed to infection with HIV-2.

It was noticeable that HIV-2 transfection in Jurkat cells showed the lowest fold change in Gag translation from HIV-1. This suggests that factors within the Jurkat cell line may enhance HIV-2 translation thereby reducing the HIV-2 Gag translation deficit observed in other cell types. Potentially, these factors could contribute to HIV-1/2 cell tropism; T-lymphocytes may support more efficient translation than other cell types *in vivo*.

The presence of viral proteins expressed from HIV-1/2 provirus did not differently affect the rate of either HIV-1/2 Gag translation. Simultaneous provirus transfections resulted in a reduction in RNA reporter translation, but this is likely due to translational competition as the same effect was observed with a pcDNA GFP control. The presence of high levels of Gag protein has previously been shown to alter Gag translation levels (Anderson and Lever, 2006). However, it may have been that insufficient Gag was translated from HIV-1/2 proviruses, due to competition from reporter RNA, to specifically observe this effect. Likewise, during the 6 h reporter transfection, enough Gag may not have been produced to observe the start of translational inhibition via this mechanism. Alternatively, Gag expressed from the proviruses may not have localised to where the transfected reporter RNAs were being translated.

4.6.2 A comparison of HIV-1/2 Gag translation initiation

Literary evidence suggests both ribosomal scanning and IRES activity as a means for HIV translation initiation. In order to clarify how HIV translation is initiated we investigated the effect of shutting down cap-dependent initiation on HIV-1/2 Gag translation levels. Several experiments were undertaken to shutdown cap-dependent translation by eIF4G cleavage; poliovirus infection was shown to be the most effective method. Poliovirus infection resulted in complete cleavage of eIF4G and significantly reduced the translation of cap-dependent controls. Likewise, eIF4G cleavage by poliovirus was shown to stimulate IRES-driven translation in our experimental system, in accordance with the literature (Svitkin, Y.V. *et al.*, 2001). In addition to eIF4G cleavage, infection with poliovirus provides additional RNAs to the cell which compete

for translational apparatus. Consequently, this assay provided a stringent environment in which to test for true IRES activity. An efficient IRES would be able to convincingly compete for translation within this environment, whereas inefficient IRES activity would remain undetected.

When HIV-1/2 Gag translation was monitored in cells where cap-dependent translation was shut down using poliovirus, both HIV-1 and HIV-2 Gag translation levels were significantly impaired. This strongly confirms that both HIV-1 and HIV-2 Gag translation is reliant on cap-dependent initiation. Furthermore, whereas IRES-driven controls showed stimulated translation under conditions of eIF4G cleavage, neither HIV-1 nor HIV-2 Gag translation was enhanced. Instead, the decrease in HIV-1 and HIV-2 Gag translation, following shut down of cap-dependent translation, mirrored that of a solely cap-dependent RNA control. Taken together, these results conclude that both HIV-1 and HIV-2 translation is primarily cap-dependent with little evidence of IRES activity.

Experimental results from Buck *et al.* (2001) reported little decrease in HIV translation in poliovirus infected cells and therefore they concluded that HIV-1 translation was not cap-dependent. This is in direct contrast to our results which show HIV-1 translation is significantly decreased in poliovirus infected cells, thus indicating a cap-dependent translation mechanism. However, the experiments carried out by Buck *et al.* (2001) looked at Gag translation from the transfection of plasmids encoding Gag linked to a CAT reporter. Consequently, these experiments do not isolate translation in the same way as our RNA reporter transfections because plasmid transfection necessitates both transcription and translation to synthesise proteins. Importantly, the entire HIV-1 5' UTR was also not included in the plasmids used for Gag expression in the experiments by Buck *et al* 2001. Consequently, expression of Gag would not occur under the natural circumstances for Gag translation. This experiment therefore lacks the qualities necessary for comparing changes in natural Gag translation levels in the presence of poliovirus. Additionally, Buck *et al.* (2001) measured the level of Gag produced by anti-HIV-anti-CAT antibody immunoprecipitation which is a less sensitive method of detection than a direct luciferase assay of harvested proteins.

We also inhibited cap-dependent translation by removal of the 5' cap structure from HIV-1/2 Gag RNA reporters. In the absence of a 5' cap, both HIV-1 and HIV-2 Gag translation was decreased, again highlighting the importance of cap-dependence for HIV-1/2 translation. However, HIV-2 translation was not decreased to the same extent as HIV-1. This may indicate that HIV-2 RNA is less dependent on its 5' cap structure for translation. However, within the cell HIV RNAs produced are always capped as they are produced by the same process that makes capped cellular mRNA. Subsequent removal of the 5' cap structure from HIV-1/2 RNA does not imitate a naturally occurring event and therefore these RNAs may be subject to enhanced degradation by the exosome (Hocine *et al.*, 2010). Uncapped HIV-1 RNA may, therefore, have been less stable than uncapped HIV-2 RNA, resulting in the lower rate of translation from uncapped HIV-1 RNA. Despite this, these results still highlight the importance of the cap structure to HIV-1/2 translation.

Although full-length HIV-1 and HIV-2 Gag RNA was primarily shown to undergo cap-dependent translation initiation, we wanted to investigate reports of IRES-activity resulting in the translation of Gag isoforms. It was necessary to prevent Gag cleavage to detect only full-length Gag (and potential isoforms) in a western blot using an antibody to the capsid region of Gag. When cleavage of Gag was inhibited, using the HIV Protease inhibitor saquinavir, full-length Gag proteins (p55 for HIV-1 and p57 for HIV-2) were observed without subsequent cleavage products. Additionally, HIV-1 p40 and HIV-2 p44 and p50 Gag isoforms were detected. Ricci *et al.* (2008) proposed that IRES-driven translation from internal AUGs produces these Gag isoforms. However, when poliovirus infection was used to shut down cap-dependent translation in the presence of saquinavir, the levels of Gag isoform translation were not affected. If the translation of internal Gag isoforms was IRES-driven, it would be expected that in the presence of cleaved eIF4G (which stimulates IRES activity) a greater level of isoform translation would occur. Likewise, shut down of cap-dependent translation would limit competition for translational machinery, facilitating more efficient IRES-driven translation. However, this was not the case. Increased

translational products from HIV-1/2 internal Gag AUG codons were not observed during this experiment. Consequently, neither HIV-1 nor HIV-2 Gag isoforms appear to undergo expression via IRES-activity. An alternative proposal, that HIV-1/2 IRES-driven translation compensates for the shutdown of cap-dependent translation, was also not evident from our experiments. The function of Gag isoforms is currently unknown. It may be that Gag isoforms are merely a product of aberrant translational events, such as leaky scanning, and are as such inconsequential to the life cycle of HIV. Further work is necessary to assess whether Gag isoforms are found in HIV particles.

Brasey *et al.* (2003) found that HIV-1 translation was increased when cap-dependent translation was shut down and proposed IRES-activity from the 5' UTR to be responsible for continued translation under these conditions. However, we observed the opposite; HIV-1/2 Gag translation decreased in poliovirus infected cells where cap-dependent translation was shut down. The experiment by Brasey *et al.* (2003) used FMDV L-protease to inhibit cap-dependent translation in an *in vitro* RRL system. This may have been less effective than using poliovirus infection in a cellular environment. Likewise, Brasey *et al.* (2003) monitored HIV translation by SDS-PAGE. This may be a less sensitive, and therefore less accurate, method of determining translational efficiency than the luciferase assays of harvested lysates which we used in our experiments.

Furthermore, the work of Brasey *et al.* (2003) contradicts the work of Buck *et al.* (2001). Whereas Brasey *et al.* (2003) detect no IRES activity within the HIV-1 *gag* ORF, Buck *et al.* (2001) reported no IRES-activity within the HIV-1 5' UTR and, instead, propose that the ribosome scans backwards from an IRES within the *gag* ORF to the upstream *gag* start codon. This is an unorthodox translational event and has not yet been proven. Currently, the data from either Buck *et al.* (2001) or Brasey *et al.* (2003) have not been confirmed by other groups and it remains unclear as to whether HIV-1 demonstrates IRES activity during infection.

Similarly, Herbreteau *et al.* (2005) and Weill *et al.* (2010) suggest that HIV-2 Gag isoforms are a product of IRES-activity. This contrasts with our findings that HIV-2 Gag isoform translation did not show enhanced translation under conditions favourable for IRES activity. However, the experiments by Herbreteau *et al.* (2005) and Weill *et al.* (2010) are not physiologically relevant as they were carried out using HIV-2 RNA without the 5' UTR which is not how it is present within the cell. This may account for why we did not observe IRES activity from our HIV-2 RNA; inclusion of the HIV-2 5' UTR appears to promote cap-dependent translation which negates IRES-activity occurring otherwise. Although, alike to HIV-1, HIV-2 translation is predominantly cap-dependent, more work is necessary to determine whether HIV-2 translation can also operate under an IRES. Further work requires the demonstration of HIV-2 IRES activity in a setting more reflective of natural infection.

HIV Gag is produced via cellular transcription mechanisms and likewise translated via cellular machinery. Consequently, it is unlikely that cap-dependent translation does not contribute to Gag translation at all as this would suggest a redundancy of function. In view of this, a preferable model of Gag translation is one where IRES activity does not occur consistently, rather providing a means to facilitate Gag translation during unfavourable conditions for cap-dependent translation. HIV IRES activity has been proposed to result from cellular proteins available during the G2/M transition phase, providing further evidence for temporal HIV IRES activity (Vallejos *et al.*, 2011)

We conclude that HIV-1/2 Gag translation is primarily cap-dependent. This is in compliance with the work of Miele *et al.* (1996) which shows that the HIV leader cannot function as an IRES, and in accordance with the evidence of ribosomal scanning throughout the HIV 5' UTR put forward by Berkhout *et al.* (2011). Despite reported findings of HIV-1/2 IRES structures, IRES-driven translation does not compensate when cap-dependent translation is shut down and we could find no evidence of IRES activity for either HIV-1 or HIV-2. Furthermore, enhanced IRES-driven translation from internal Gag AUGs was not observed when cap-dependent translation was shut down. Thus, at least in our system, the HIV-1/2 IRESs appear to be non-functional or,

alternatively, are an artefact of experiments that do not mirror typical translational events from naturally occurring capped and 5' UTR containing viral mRNA.

4.6.3 A comparison of HIV-1/2 5' UTR secondary structure

Extensive structure within the 5' UTR can slow the rate of translation by impeding ribosomal scanning. RNA folding energy is a measure of secondary structure. The folding energy and folding energy per nucleotide of the HIV-2 5' UTR were both found to be more negative than for the HIV-1 5' UTR. Consequently, the HIV-2 5' UTR, with its greater length, is intrinsically more structured. The extensive structure of the HIV-2 5' UTR may hinder the rate of translation by inhibiting ribosomal scanning or spatially impeding the formation of a translation initiation complex on the Gag AUG within the HIV-2 5' UTR.

TAR was investigated as a specific structure responsible for the high folding energy of the HIV-2 5' UTR. When TAR was deleted from both the HIV-1 and HIV-2 5' UTR, the difference in folding energy was slightly reduced but not abolished. Therefore TAR alone is not responsible for the enhanced folding energy of the HIV-2 5' UTR, although it is a contributor. Consequently, it is possible that HIV-2 TAR may obstruct ribosomal scanning to a greater extent than the HIV-1 TAR and partly factor in the lower translation rate of HIV-2.

A high number of G-C base pairings within HIV-2 TAR contributes to its folding energy. The high folding energy of HIV-2 TAR was shown to be a consequence of a high number of G-C base pairs, rather than one or two critical base pairs contributing to the overall folding energy. It is, however, not surprising that the number of G-C bonds corresponded to the TAR sequence folding energy as the MFOLD programme (used to calculate folding energy) is reliant on G-C content for its calculation. Thus, this correlation seen within our results may be an artefact of this. 17 G-C to A-U mutations would be necessary to reduce the folding energy of the HIV-2 TAR to an equivalent value to the HIV-1 TAR. Future work could introduce these mutations to HIV-2 TAR and assess whether this enhances the translatability of HIV-2 Gag by reducing the structural hindrance imposed by HIV-2 TAR.

4.6.4 A comparison of HIV-1/2 Gag translation in the absence of TAR

HIV-1 TAR was shown to be inhibitory to translation of heterologous transcripts *in vitro* (Svitkin, Y.V *et al.*, 1994). Likewise, mutating HIV-1 TAR to disrupt its structure increased the efficiency of HIV-1 translation 190-fold (Parkin *et al.*, 1988). In view of these results, it was thought that TAR might be inhibitory to HIV-1/2 translation and that HIV-2 TAR, with its extended structure and increased folding energy, may have been more inhibitory and contribute to the lower translation rate of HIV-2 Gag. Consequently, the translation of HIV-1/2 in the absence of TAR was monitored to see whether deleting the HIV-2 TAR structure would alleviate translational repression, resulting in translational levels more similar to HIV-1 Gag. Surprisingly, this was not the case; deleting TAR decreased the translation of both HIV-1/2 Gag RNA reporters in HeLa cells, particularly for HIV-1.

HIV-1 TAR binds to and down-regulates the activity of cellular PKR. If HIV-1 TAR is deleted, PKR is not down-regulated so functions to phosphorylate eIF2, inhibiting translation (Cole, 2007). This may account for the decrease in HIV-1 Gag translation observed when HIV-1 TAR was deleted. It was interesting to note that, although HIV-2 translation was not equivalent to HIV-1 wild type Gag translation, in the absence of TAR HIV-1 and HIV-2 levels of translation were equivalent. HIV-1 TAR may, therefore, function to enhance HIV-1 translation such that when it is deleted, translation efficiency is reduced. It is possible that a corresponding function is not present for HIV-2 TAR. However, in BSRT7 cells, HIV-2 Gag RNA translation remained below the level of HIV-1 translation for TAR and ΔTAR RNA reporters. Likewise, in BSRT7 cells, deleting TAR reduced the translatability of both HIV-1 and HIV-2 Gag RNA. The stability of HIV-1/2 ΔTAR RNA was shown to be equivalent, and additionally comparable to the stability of TAR RNA. Thus RNA stability was not responsible for changes in translational rates.

BSRT7 cells were also transfected with HIV-1/2 reporter plasmids to compare HIV-1/2 TAR/ΔTAR transcription/translation rates. Deleting TAR appeared to increase the levels of Gag-Luc expressed from reporter plasmids. This is the opposite effect observed from RNA transfection results.

Reporter plasmids rely on a T7 promoter for Gag mRNA transcription. This is not the natural means of wild type Gag transcription from integrated provirus. Likewise, expression of Gag from reporter plasmids involves two stages of expression: both transcription and translation. Thus this assay does not directly monitor the effect of TAR deletions on translation alone. These factors may partly explain why such conflicting results were produced from RNA and DNA transfections of ΔTAR reporters.

Overall, results suggest that HIV TAR may have several functions in translation. Deleting TAR does not enhance HIV-2 translation to the levels of wild type HIV-1. However, deleting TAR from both HIV-1 and HIV-2 may result in more analogous levels of HIV-1/2 translation, possibly by decreasing HIV-1 TAR enhancement of translation via PKR suppression and, additionally, removing excessive structure from the HIV-2 5' UTR. Thus TAR may serve to enhance HIV-1 translation via a mechanism which is not accessible to HIV-2 due to its differing TAR structure. However, HIV-2 TAR alone is not responsible for the lower rates of translation in HIV-2. It would be interesting to note whether adding HIV-1 TAR to HIV-2 reporters would enhance HIV-2 translation via interactions with PKR. Investigations into the phosphorylation status of eIF2α (a measure of PKR activity) within these experiments might shed some light on the effect of TAR and PKR on HIV-1/2 translation rates. Further investigation into the effect of TAR deletions on both transcription and translation are therefore necessary in order to elucidate the role of TAR for HIV-1 and HIV-2 translation.

4.6.5 A comparison of HIV-1/2 Gag elongation

Additional factors such as codon bias may contribute differently to the rate of HIV-1/2 Gag translation. The presence of rare codons or codon pairs can reduce gene translatability by causing the ribosome to stall. Thus the composition of Gag can affect the rate of translational elongation via the presence of rare codons or codon pairs. A higher level of rare codons or codon pairs incorporated into Gag may differentially affect the rate of Gag translation between HIV-1/2 by slowing ribosomal elongation. Consequently,

the codon bias and codon pair bias were compared for both HIV-1 and HIV-2 Gag.

The average frequency of Gag codons, and thus the average codon bias, was calculated to be similar for HIV-1 and HIV-2. Likewise, the HIV-1/2 codon pair bias was calculated as 0.029 for HIV-1 Gag and 0.021 for HIV-2 Gag, compared to an average of 0.07 for all annotated human genes. Although the HIV-1 and HIV-2 codon pair bias is slightly lower than that of the average human gene, suggesting a greater presence of rare codon pairs, the HIV-1/2 values are fairly similar. Overall, codon bias and codon pair bias do not differ significantly between HIV-1 and HIV-2 Gag. Therefore, translational differences between HIV-1/2 are not likely to be due to elongation.

4.6.6 Future work

Various avenues of future work could proceed from work on HIV-1/2 translation. Although we have established that the rate of HIV-1 translation is more efficient than HIV-2, more work is necessary to define the origins of this translational difference.

With regard to RNA structure, we could investigate other notable sequences or structured components of the HIV-1/2 genome which may prove important to the rate of HIV-1/2 translation. Various structures within the HIV-2 5' UTR could be swapped with equivalent HIV-1 structures to see whether this equalises the rate of translation between HIV-1 and HIV-2. Additionally, the HIV-2 5' UTR contains a recently identified splice site (Strong *et al.*, 2009); removal of the putative 142 nt 5' UTR intron has been reported to increase the translation efficiency of HIV-2 Gag. Comparing translation of the spliced HIV-2 variant to HIV-1 translation levels could indicate whether the HIV-2 spliced region contributes to the reduced HIV-2 Gag translation levels.

Cellular helicases are required to unwind HIV RNA structure during replication. As the 5' UTR of HIV-1/2 differs in size and structure, the efficiency with which the 5' UTR interacts with cellular helicases may differ, subsequently affecting the rate of replication. Investigation into which cellular helicases interact with HIV-1 and HIV-2 RNA, and the rate at which they

unwind the HIV-1/2 5' UTRs could, therefore, reveal a mechanism which causes translation of HIV-2 to proceed less efficiently than HIV-1.

Finally, establishing whether IRES activity contributes to HIV translation during infection, and evaluating the importance of IRES activity to HIV-1/2 translation, could provide a clearer picture of how HIV translation is regulated. In order to do this, more work is necessary to understand the cellular conditions and viral components governing cap-dependent or IRES-driven HIV-1/2 translation.

CHAPTER 5: HIV RNA-PROTEIN INTERACTIONS

5.1 Introduction

RNA-protein interactions take place throughout the HIV RNA genome. In particular, the highly structured HIV 5' UTR is important in regulating many stages of the viral replication cycle and this, predominantly, occurs through interactions with both cellular and viral proteins. The roles of viral RNA-binding proteins, such as Tat, Rev, Gag, and RT have been well characterised within the life cycle of the HIV virus. However, a greater variety of cellular proteins also interact with HIV RNA. Consequently, there are potentially numerous interactions between the HIV genome and cellular RNA-binding proteins which remain unexplored.

This chapter examines the cellular RNA-binding proteins interacting primarily with the HIV-1/2 5' UTR. Initial discussion focuses on the recognised cellular proteins binding to the HIV 5' UTR and Gag, before results are presented identifying 5' UTR/Gag HIV binding proteins from cross-linking reactions with proteins from cellular extracts. Differential protein binding patterns are recognised between the HIV-1/2 5' UTRs and attempts to characterise the nature of these unknown proteins are outlined.

5.1.1 RNA binding proteins

Cellular proteins are important functional contributors to every post-transcriptional process within the cell. As the HIV virus hijacks cellular processes to coordinate its own gene expression, cellular proteins are, therefore, essential components of the HIV life cycle. Several types of protein RNA-binding domains with different properties permit RNA-protein interactions. Cellular proteins can recognise and bind to both nucleotide sequences or secondary structure within single-stranded RNA (ssRNA) or double-stranded (dsRNA). Moreover, protein binding may be determined either by a single RNA domain or the interactions of multiple protein-binding domains. Likewise, the RNA structure consists of several features: ribose sugars, phosphate groups and RNA bases - all of which can act as binding points for cellular proteins (Elliott and Ladomery, 2010).

5.1.2 Cellular proteins binding to HIV

The 5' UTRs of HIV-1 and HIV-2 are long (335 nt and 545 nt respectively) and heavily structured with numerous structures and sequences that have the capacity to interact with cellular RNA-binding proteins [figure 80].

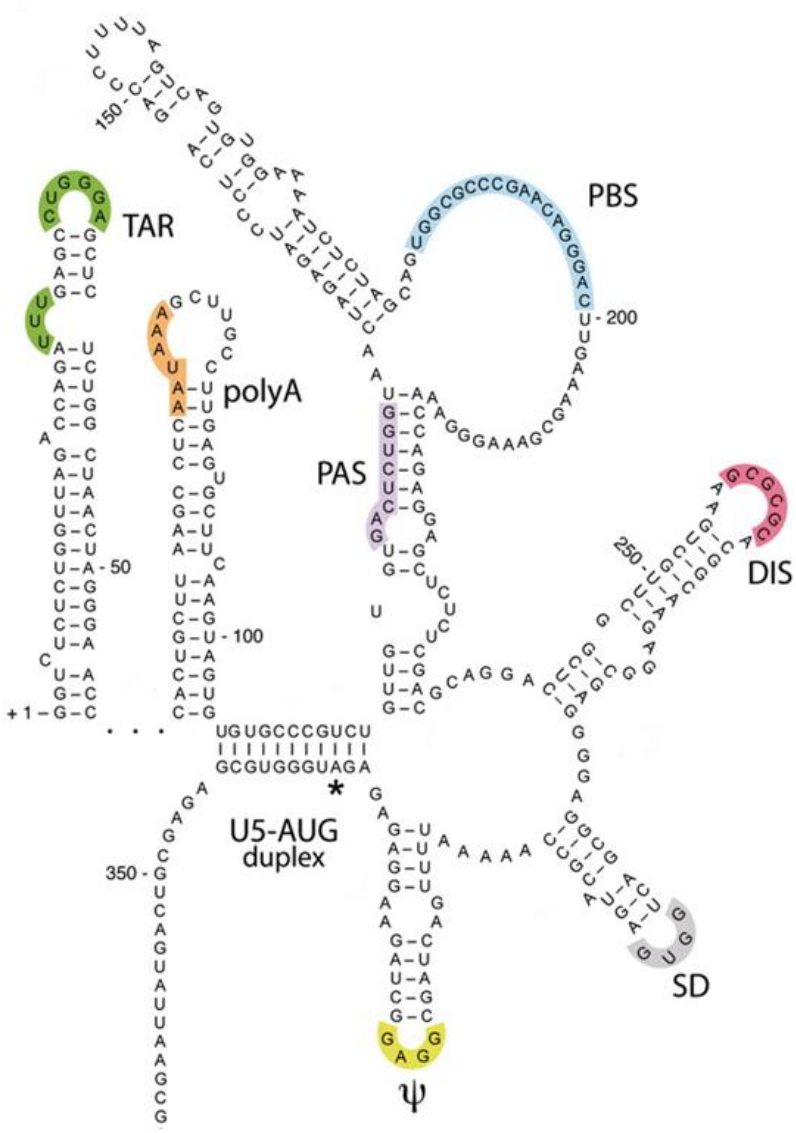

Figure 80: Structures within the HIV-1 5' UTR which may present binding sites for cellular proteins. The unpaired 6 nt and tripyrimidine bulge of TAR (green), the AAUAAA polyadenylation signal (orange), the primer activation site (PAS) (purple), the primer binding site (PBS) (blue), the 6 nt GCGCGC dimer initiation site (DIS) (pink), the major splice donor (SD) (grey) and the GGAG tetraloop packaging signal (ψ) (yellow) are all highlighted. The Gag AUG start codon is also indicated (*).

Several stages of the HIV replication cycle entail the involvement of cellular RNA-binding proteins. These are outlined below and summarised in table 13.

RNA-binding proteins	Function
P-TEFb (Cyclin T1, Cyclin T2a, Cyclin T2b, CDK9), SBP	Transcription regulation (via HIV TAR)
La autoantigen	Transcription, promoting IRES-driven translation, alleviating translation repression
hnRNP A1, hnRNP H, hnRNP F, PTB, SR proteins	mRNA splicing
hnRNP C1/C2	mRNA nuclear localisation and packaging
hnRNP A2/B1	Cellular RNA trafficking
HuR	RNA stability
DDX3	Nuclear Export (unwinding RNA)
PABP, eIF1, eIF1A, eIF2, eIF3, eIF4B, eIF4F (eIF4A, eIF4GI, eIF4GII, eIF4E)	Cap-dependent translation initiation
PKR, TRBP	Translation regulation
Staufen1	Assembly (genomic RNA)

Table 13: Cellular RNA-binding proteins implicated in the HIV lifecycle.

The viral protein Tat binds to the HIV-1 TAR RNA structure. Human Cyclin T1 facilitates this via interactions with the TAR central loop and the activation domain of viral Tat. Additional factors Cyclin T2a, Cyclin T2b and CDK9 (cyclin-dependent kinase 9) together with Cyclin T1 produce a complex termed the positive transcription elongation factor b (P-TEFb) complex. P-TEFb functions to hyperphosphorylate RNA polymerase II resulting in *trans*-activation of Tat (Fujinaga *et al.*, 1999).

La autoantigen is a 48 kDa human cellular protein which is involved in the termination of RNA polymerase III transcription. Cleavage of La can produce a 43 kDa protein (Ayukawa *et al.*, 2000). La autoantigen is predominantly a nuclear protein, but is also found in the cytoplasm. For example, during poliovirus infection it is transported from the nucleus to the cytoplasm (Svitkin, Y.V *et al.*, 1994). La has been shown to bind HIV-1 TAR RNA (Chang *et al.*, 1994) and to stimulate translation of TAR-containing transcripts *in vitro* (Svitkin, Y.V *et al.*, 1994). During HIV infection, La could potentially be translocated from the nucleus to the cytoplasm as a ribonucleoprotein by

binding to TAR on HIV transcripts. Cheung *et al*. (2002) propose a model whereby La-HIV ribonucleoproteins (RNPs) are transported from the nucleus into the cytoplasm. La-bound HIV mRNAs are subsequently preferentially translated over mRNAs which do not have La bound to them (Cheung *et al.*, 2002). A role for La in the initiation of IRES-dependent translation has also been suggested following UV cross-linking studies which showed that La binds to the 5' UTR of coxsackievirus B3 RNA. Furthermore, La was the first identified ITAF which was shown to stimulate cap-independent translation from the poliovirus IRES (Meerovitch *et al.*, 1993). An additional TAR-binding protein, TRBP, has been shown to increase the rate of translation from HIV RNA by repressing cellular PKR (Gatignol *et al.*, 2005).

Post-transcription, cellular proteins are involved in modifying RNA and coordinating nuclear export. HnRNPs (heterogenous nuclear ribonucleoproteins) are a well-characterised and abundant group of cellular, multi-functional RNA-binding proteins. Many post-transcriptional processes involve hnRNPs; splicing (hnRNP A1, hnRNP H, hnRNP F), nuclear localisation and packaging of pre-mRNA (hnRNP C1/C2), RNA trafficking (hnRNPA2/B1) and RNA stability (HuR). Around 20 hnRNP proteins have been identified and have been shown to direct a diverse array of activities from RNA processing, folding and nucleocytoplasmic export (Cullen, 2000). In conjunction with their role in modulating processing, hnRNP complexes have also been shown to form the main components of the spliceosome. In particular, hnRNPs function to maintain single-stranded RNA for splicing (Elliott and Ladomery, 2010). Additional cellular proteins PTB and members of the SR protein family have also been shown to play a role in cellular splicing (Asai *et al.*, 2003). Following RNA processing, cellular DDX3 helicase has been shown to interact with HIV-1 viral mRNA, facilitating CRM-1 dependent nuclear export by unwinding RNA secondary structure (Yedavalli *et al.*, 2004).

In the cytoplasm, numerous RNA-binding proteins are involved in translation and are therefore likely to bind HIV RNA. During translation initiation, PABP binds to the mRNA poly(A) tail. Several proteins of the eIF4F cap-binding complex: eIF4A, eIf4G (eIF4GI and eIF4GII) and eIF4E, interact with the 5'

cap structure of viral mRNA (Mathews *et al.*, 2007). An additional RNA-binding protein, eIF4B, stimulates activity from the eIF4A helicase (López-Lastra *et al.*, 2005). Furthermore, proteins eIF2, eIF3 and the 40S ribosomal subunit form a 43S initiation complex which binds to mRNA during translation initiation (Lapointe and Brakier-Gingras, 2003). Factors eIF1 and eIF1A bind to mRNA to coordinate 5'-3' transport of the 43S complex to the initiation codon. Consequently, an array of cellular proteins combine with both cellular and viral mRNA to allow it to undergo translation (López-Lastra *et al.*, 2005).

HIV RNA functions both as a template for translation and as genomic RNA incorporated into virions. To facilitate packaging, HIV genomic RNA associates with host RNA-binding proteins to form a ribonucleoprotein complex which is incorporated into immature virions. Staufen 1 is a dsRNA-binding protein which binds to the Gag nucleocapsid region and modulates RNA inclusion into assembling virions (Milev *et al.*, 2010). Staufen 1 has also been reported to stimulate translation of TAR-containing transcripts (Dugré-Brisson *et al.*, 2005).

Structural and sequential differences between the HIV-1/2 genome may result in variations in cellular protein binding. Thus the coordination of HIV-1/2 gene expression could vary as a result of differences in RNA-protein binding interactions. Consequently, the aim of the work in this chapter is to identify any differences in cellular protein binding to the HIV-1/2 RNA.

5.2 Results

5.2.1 A comparison of protein binding to HIV-1/2 5' UTR-gag RNA.

Binding of cellular proteins to HIV-1 and HIV-2 gag RNA may differ, and thus provide an explanation for the differing rates of gene expression observed for HIV-1 and HIV-2. UV cross-linking was used to investigate HIV-1 and HIV-2 RNA-protein interactions. Cellular proteins were extracted from HeLa cells (S100 extracts) and used in a cross-linking reaction with 1 mg/ml tRNA and α-^{32}P UTP radioactively labelled HIV-1 and HIV-2 RNA reporters [figure 81].

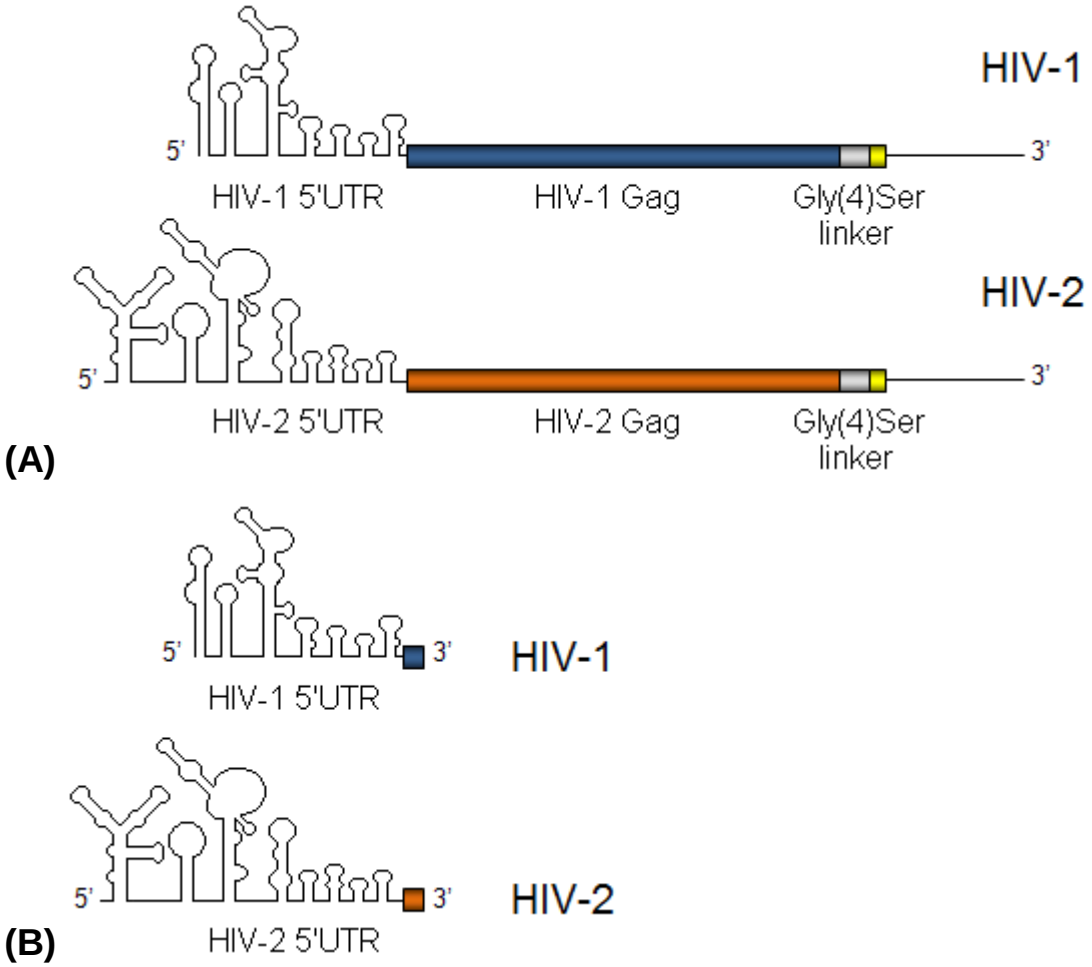

Figure 81: Truncated HIV-1/2 UTR-Gag RNA reporters (A) and HIV-1/2 5' UTR RNA reporters (B).

Proteins associated with radioactively labelled HIV-1 or HIV-2 RNA were visualised by SDS-PAGE and autoradiography [figure 82]. Unradiolabelled 'cold' RNA was used in UV cross-linking binding reactions to act as a competitor for protein binding. This permitted identification of RNA-specific competition for protein binding.

Several proteins of differing sizes were shown to bind to HIV-1/2 UTR-gag RNAs although no qualitative differences in protein binding were identified [figure 82A]. However, when UV cross-linking was carried out with the HIV-1/2 5' UTRs [figure 82B] several bands of differing intensities were produced. In particular, a band of around 45 kDa was identified binding to the HIV-1 5' UTR but not to the HIV-2 5' UTR. The tRNA non-specific competitor did not remove binding of the 45 kDa protein to the HIV-1 5' UTR [lane 1, figure

82B]. In contrast, when an unlabelled, HIV-1 5' UTR competitor was present, it competed for the same protein thereby removing the band at 45 kDa [lane 2, figure 82B]. Equally, the presence of an unlabelled HIV-2 5' UTR competitor did not compete away this band, confirming that the 45 kDa protein does not bind to the HIV-2 5' UTR [lane 3, figure 82B]. Therefore the 45 kDa band represents a protein which binds uniquely to the HIV-1 5' UTR and not the HIV-2 5' UTR.

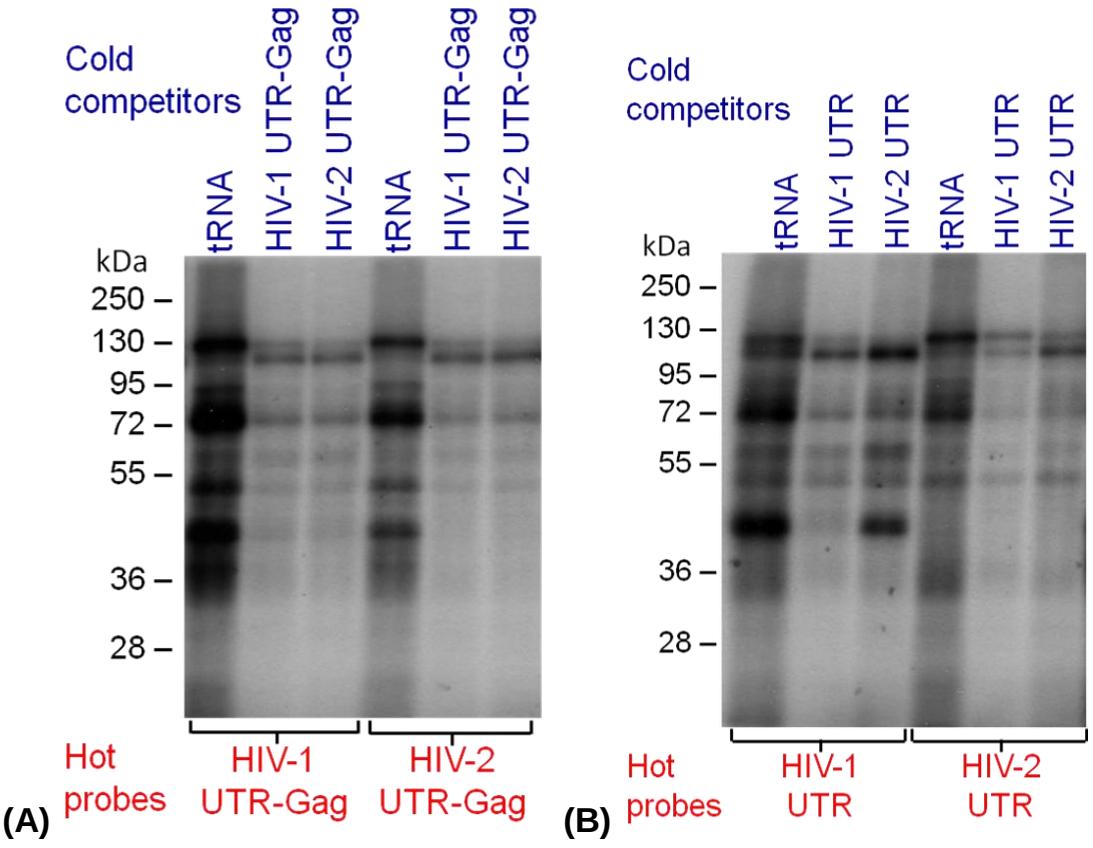

Figure 82: UV cross-linking of HeLa cell proteins binding to 'hot probes': HIV-1/2 UTR-gag (A) and HIV-1/2 UTR radiolabelled RNA reporters (B). Binding reactions included either unradiolabelled 'cold' tRNA, HIV-1/2 5' UTR-gag or HIV-1/2 5' UTR competitor RNA.

Binding of the 45 kDa protein to the HIV-1, but not the HIV-2, 5' UTR was also shown to occur in the presence of additional non-specific 'cold' competitors: the human rhinovirus 2 (HRV-2) 5' UTR RNA and *Renilla* RNA (data not shown).

The 45 kDa protein appears to bind weakly to HIV-2 5' UTR-gag RNA [lane 4, figure 82A] but not to HIV-2 5' UTR RNA alone [lane 4, figure 82B].

Consequently, an additional binding reaction requiring part of gag may be necessary for binding of this protein to HIV-2 RNA. Alternatively, the conformation of the HIV-2 5' UTR may be altered when gag is present, allowing binding of the 45 kDa protein.

Further bands of interest migrated between 95-130 kDa [figure 82]. The binding profile of these proteins is less obvious; they both appear to bind to the HIV-1 and HIV-2 5' UTR albeit with differing binding affinities. The top band (~130 kDa) appeared to bind better to the HIV-2 5' UTR, producing a strong band [lane 4, figure 82B]. This protein is also present binding to the HIV-1 5' UTR but the band is fainter [lane 1, figure 82B]. The presence of a HIV-2 5' UTR unlabelled competitor [lanes 3+6, figure 82B] competes away the 130 kDa band better than the HIV-1 5' UTR competitor does [lanes 2+5, figure 82B] confirming that this protein has a stronger binding affinity for the HIV-2 5' UTR. Alternatively, the slightly smaller protein band migrating at ~120 kDa appears to bind more strongly to the HIV-1 5' UTR [lane 1, figure 82B] with a fainter band present at this size for the HIV-2 5' UTR [lane 4, figure 82B]. In the presence of a HIV-1 5' UTR competitor [lanes 2+5, figure 82B], the 120 kDa band is reduced more than in the presence of the HIV-2 5' UTR competitors [lanes 3+6, figure 82B]. This confirms that the 120 kDa protein binds more strongly to the HIV-1 5' UTR.

5.2.2 La protein binding to the HIV-1/2 5' UTR

A number of experiments were carried out to test whether the ~45 kDa protein was La, which has been shown to bind to the HIV-1 5' UTR. Recombinant La protein was purchased [Prospec-Tany Technogene Ltd] and used in a UV cross-linking assay alongside HeLa extract and ^{32}P-labelled HIV-1/2 5' UTR [figure 83].

1 µg La bound both HIV-1 and HIV-2 5' UTRs (whereas 100 ng La bound neither), although stronger labelling was observed with the HIV-1 5' UTR [figure 83]. However, the size of the band representing recombinant La [lane 3, figure 83] was larger than the ~45 kDa band in HeLa extract [lane 1, figure 83], suggesting it may not be La.

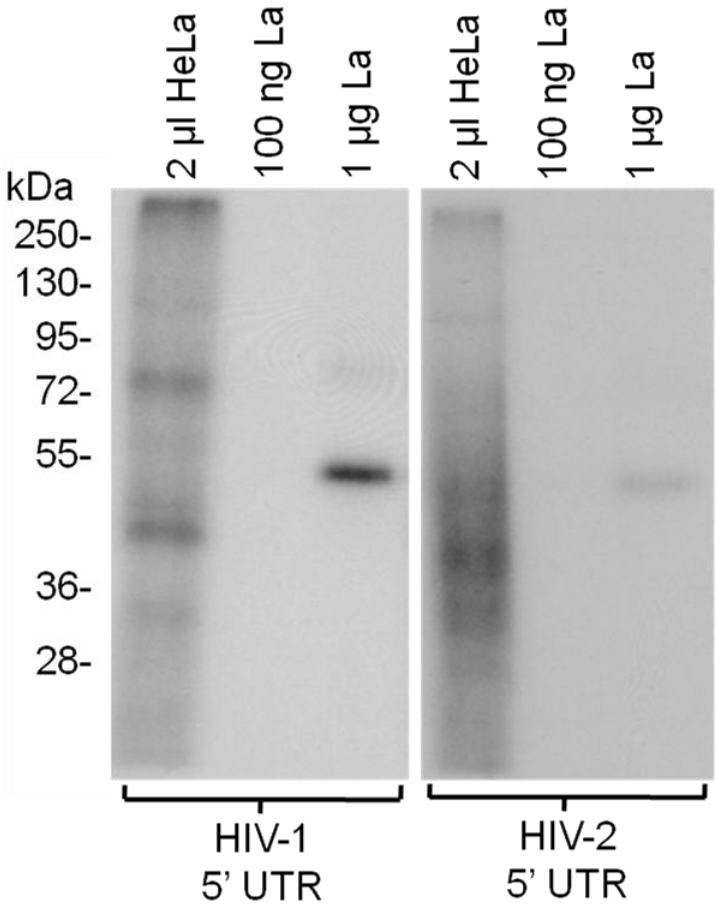

Figure 83: UV cross-linking of 2 µl HeLa extract or 100 ng/1 µg recombinant La with the HIV-1/2 5' UTR.

Anti-La antibody was used to immunoprecipitate La from UV cross-linking reactions. However, despite a number of attempts, using protein G agarose beads and magnetic Dynabeads, La could not be detected following immunoprecipitation of UV cross-linking reactions (data not shown).

Western blotting showed that the anti-La antibody could detect recombinant La and native La from HeLa extract [figure 84, lanes 4+3 respectively].

Immunoprecipitation of recombinant La [lane 1, figure 84] demonstrated that La could be immunoprecipitated, however the band was very weak. La was unable to be immunoprecipitated from HeLa extract (data not shown), therefore it was not surprising that La immunoprecipitation from HeLa extract UV cross-linking reactions was unsuccessful.

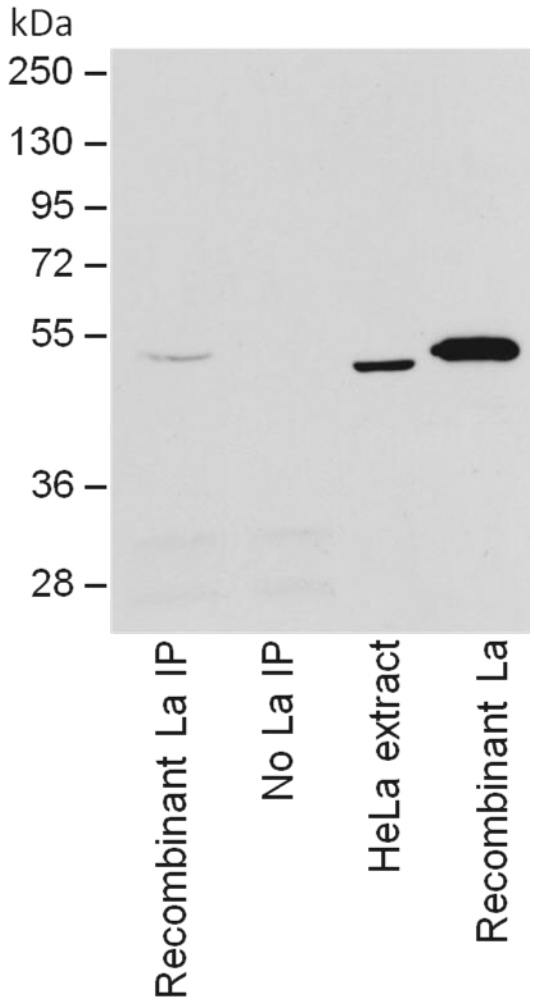

Figure 84: A western blot with an antibody to La. Lanes 1+2: La immunoprecipitation in the presence and absence of recombinant La. Lane 3: 2 µl HeLa extract. Lane 4: 100 ng recombinant La.

An alternative approach was used to test whether the ~45 kDa protein was La. It is reported that La interacts with the poliovirus IRES (Meerovitch *et al.*, 1993) so poliovirus (PV1) IRES RNA was used as a competitor in UV cross-linking assays with HIV-1/2 5' UTR RNAs [figure 85].

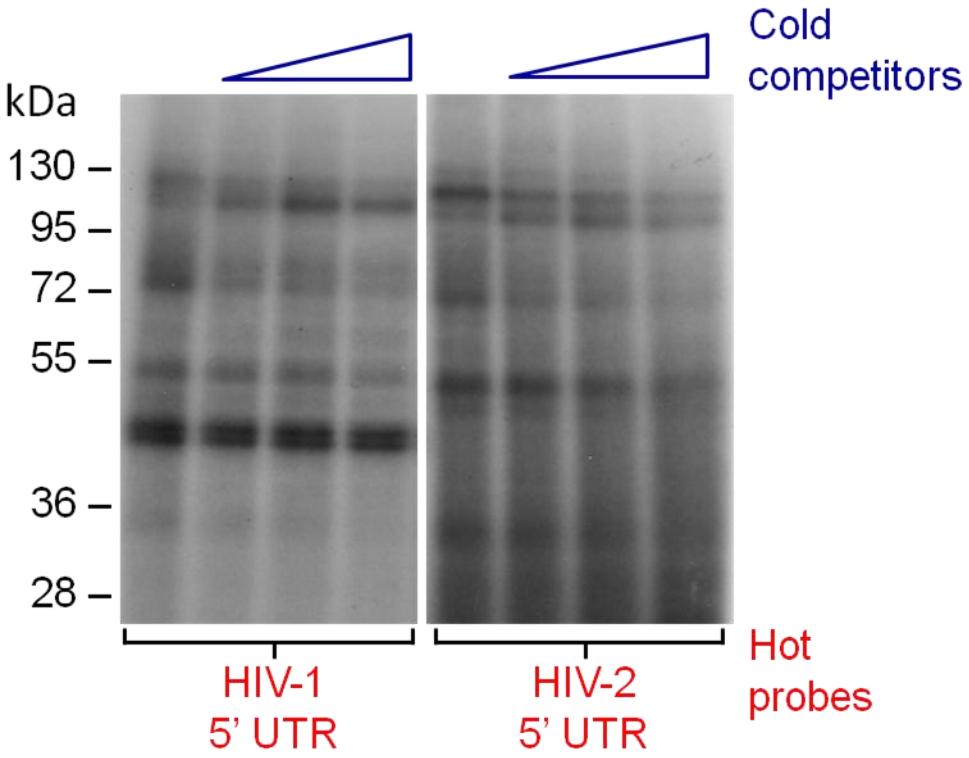

Figure 85: UV cross-linking of HeLa proteins to radiolabelled HIV-1/2 5' UTR RNA (hot probes) in the presence of unlabelled PV1 IRES RNA competitor (cold competitors) at various concentrations.

A 45 kDa protein was present binding to the HIV-1 5' UTR but not to the HIV-2 5' UTR [figure 85]. However, the PV1 IRES RNA competitor did not compete for binding of the 45 kDa protein band. This suggests that the 45 kDa protein is not La. Additionally, PV1 IRES RNA competes for binding of other proteins at 72 kDa, 55 kDa and 36 kDa. It also appears that the 45 kDa band may be a duplet, possibly representative of two proteins, or different forms of the same protein.

La is reported to bind to the TAR structure within the HIV-1 5' UTR (Chang *et al.*, 1994). HIV-1 ΔTAR 5' UTR RNA was used as a probe in a UV cross-linking assay to see whether the 45 kDa protein was able to bind to the HIV-1 5' UTR in the absence of TAR [figure 86].

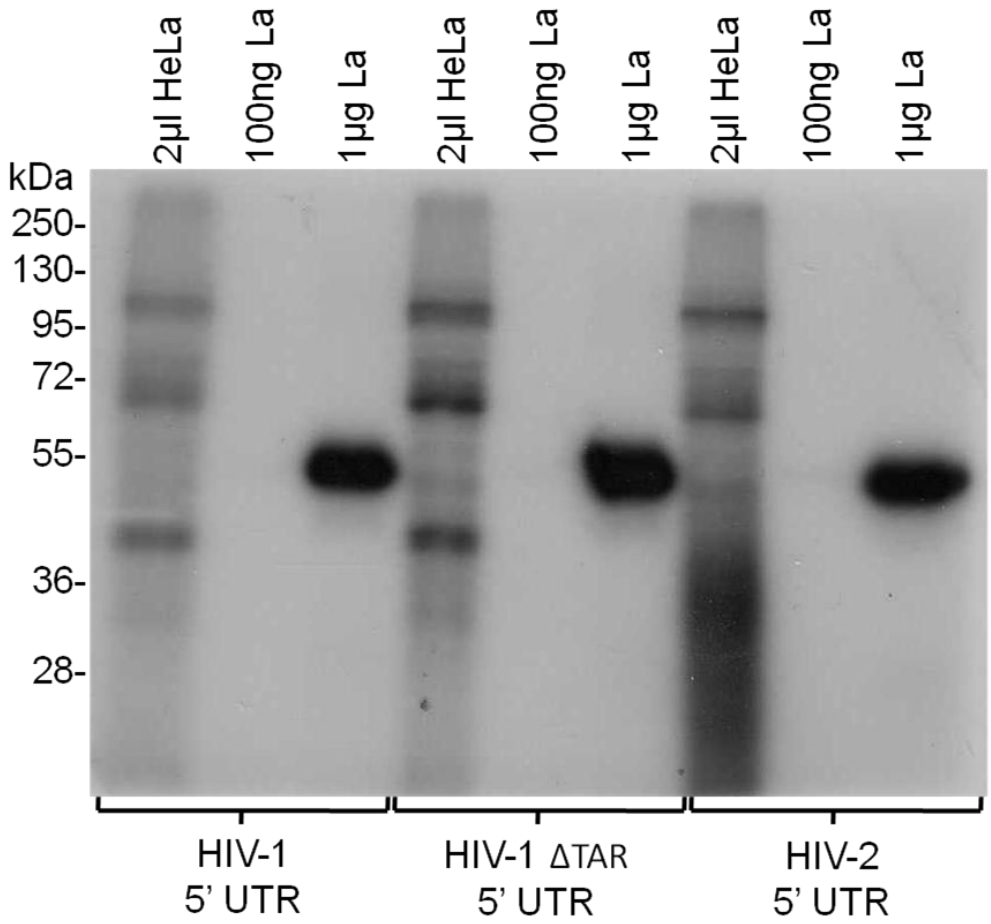

Figure 86: UV cross-linking of HeLa cell proteins, 100 ng or 1 µg recombinant La to labelled HIV-1, HIV-1 ΔTAR or HIV-2 5' UTR RNAs.

The 45 kDa protein from HeLa extract was still able to bind to HIV-1 ΔTAR RNA [lane 4, figure 86]. However, 1 µg recombinant La also bound to HIV-1 ΔTAR RNA [lane 6, figure 86]. La is known to bind TAR, but it may also have additional binding sites within the HIV-1 5' UTR. Interestingly, whereas recombinant La bound to both the HIV-1 and HIV-2 5' UTRs, the 45 kDa protein from HeLa extract was only able to bind to the HIV-1 5' UTR suggesting it is not La. Although this experiment doesn't rule out La as a candidate for the 45 kDa protein, together with other experiments results suggests that the 45 kDa protein is not La.

5.2.3 RNA affinity chromatography

To isolate the 45 kDa unknown protein binding to the HIV-1 5' UTR, RNA affinity chromatography was carried out using biotinylated RNA pulled down by Magnetic Dynabeads® M-280 Streptavidin [Invitrogen]. To assess

whether the unknown protein would still bind to biotinylated HIV-1 5' UTR RNA, a UV cross-linking assay was carried out. ^{32}P-labelled biotinylated or non-biotinylated RNA was UV cross-linked to HeLa S100 extract [figure 87].

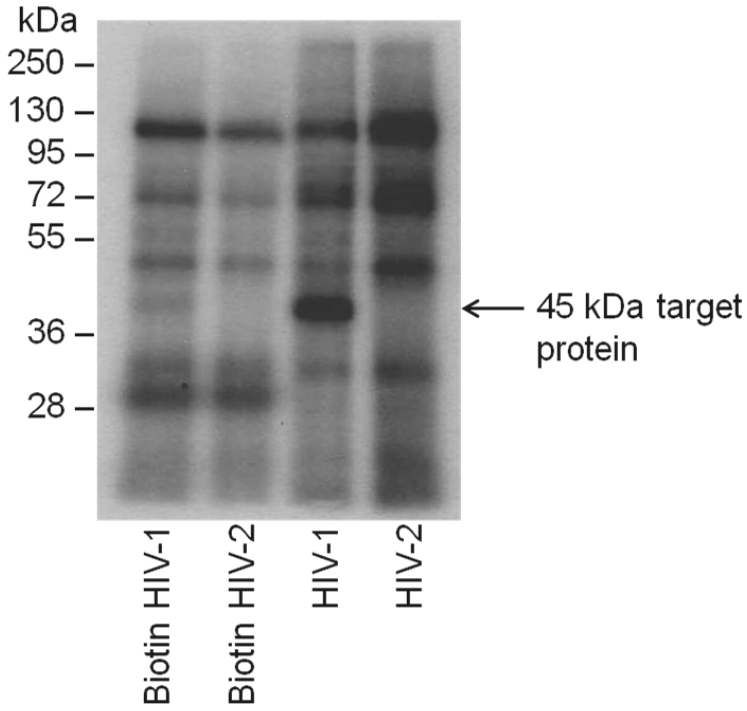

Figure 87: UV cross-link of biotinylated (lanes 1+2) and non-biotinylated (lanes 3+4) ^{32}P-labelled HIV-1/2 5' UTR RNA with HeLa extract.

Lanes 3 and 4 showed the usual cross-linking pattern of HeLa extract proteins to HIV-1 and HIV-2 5' UTR RNA. The biotinylated RNAs [lanes 1 and 2, figure 87] gave a similar cross-linking pattern; the 45 kDa target protein bound to biotinylated HIV-1 5' UTR RNA but not HIV-2. However, the binding of this protein to (or labelling of) biotinylated RNA was less efficient than to non-biotinylated RNA resulting in a fainter band.

To assess the binding capacity of biotinylated HIV-1/2 RNA to Magnetic Dynabeads® M-280 Streptavidin, a known quantity of HIV-1/2 biotinylated 5' UTR RNA was added to a binding reaction with the beads. When beads were placed on a magnet, the subsequent level of RNA remaining in the supernatant was quantified by Nanodrop. This provided an indication of how much RNA was bound to the beads as a percentage of the starting quantity [table 14]. Comparisons were made to an unbiotinylated HIV-1 5' UTR RNA control.

RNA	RNA added to beads (ng)	RNA in supernatant (ng)	RNA bound to beads (%)
Biotin HIV-1	6660	4160	37.5
Biotin HIV-2	7335	4920	32.9
Control	4748	4365	8.1

Table 14: The binding capacity of biotinylated HIV-1/2 5' UTR RNAs to streptavidin beads.

Both HIV-1/2 biotinylated 5' UTR RNAs bound much better to beads than the control. HIV-1 biotinylated RNA appeared to bind marginally better to the beads, although both HIV-1 and HIV-2 biotinylated RNA showed a reasonable level of binding for RNA affinity chromatography to continue.

RNA affinity chromatography was carried out using 2 µg biotinylated HIV-1 5' UTR RNA bound to 10 µl of Magnetic Dynabeads® M-280 Streptavidin [Invitrogen] followed by protein binding of 2 µl HeLa S100 extract in a total volume of 30 µl. Beads were washed 3 times in B&W buffer and bound products eluted by boiling in 20 µl SDS. Products were separated by SDS-PAGE and protein bands identified by silver stain [figure 88].

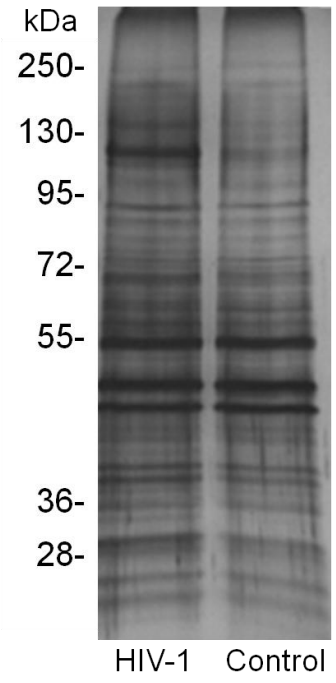

Figure 88: RNA affinity chromatography of 2 µl HeLa S100 extract and either HIV-1 5' UTR biotinylated RNA or a control with no RNA.

A lot of non-specific protein bands were detected binding to the magnetic beads when no biotinylated RNA was present [lane 2, figure 88]. RNA affinity

chromatography was repeated using HIV-1/2 5' UTR biotinylated RNA and a *Renilla* RNA control. Varying salt concentration washes (100-1000 mM NaCl) were used to elute RNA-binding proteins, followed by final elution: boiling beads in SDS buffer. 10 µl of each wash was used for SDS-PAGE and the gel silver stained to identify the proteins in each fraction [figure 89].

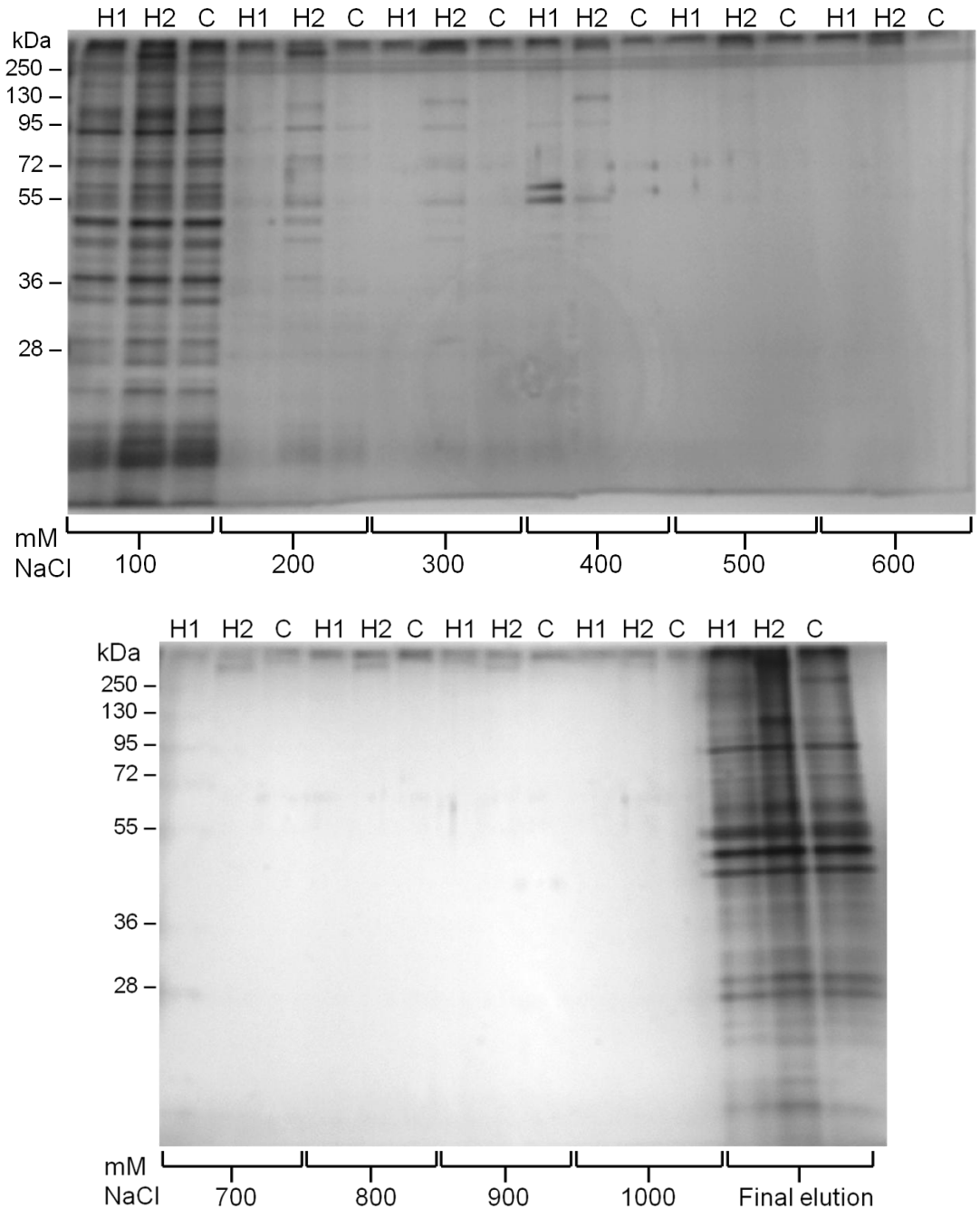

Figure 89: Silver stain of RNA affinity chromatography washes. Wash fractions at varying salt concentrations (100-1000 mM NaCl) were used to elute RNA-binding proteins from HIV-1 (H1) and HIV-2 (H2) 5' UTR RNAs and a control reaction (C) containing *Renilla* RNA. A final elution was carried out by boiling beads in SDS buffer.

Many proteins were eluted in low concentration washes (100 mM) for both HIV-1 and HIV-2 [figure 89]. At higher salt washes (400 mM) proteins binding more specifically to the HIV-1 5' UTR were eluted.

We wished to use fractions in a UV cross-linking reaction with ^{32}P-labelled HIV-1/2 5' UTR RNA to see whether we could identify which fraction contained the 45 kDa protein interacting with the HIV-1 5' UTR. Firstly, it was necessary to check that the unknown protein would still bind to the HIV-1 5' UTR RNA at stronger salt concentrations. UV cross-linking was therefore carried out with ^{32}P-labelled HIV-1 5' UTR RNA and 2 µl HeLa extract at increasing salt concentrations [figure 90].

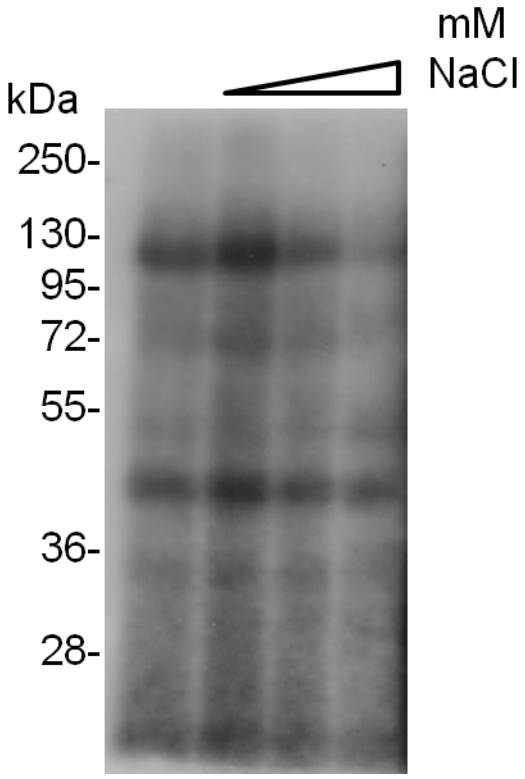

Figure 90: UV cross-linking of ^{32}P-labelled HIV-1 5' UTR RNA with 2 µl HeLa extract at varying salt concentrations; lane 1: 50 mM KCl, lane 2: 50 mM NaCl, lane 3: 100 mM NaCl, lane 4: 200 mM NaCl.

The unknown 45 kDa protein was able to bind to the HIV-1 5' UTR even at high salt concentrations although binding was decreased slightly as salt concentration increased [figure 90].

100-400 mM salt washes from the RNA affinity chromatography were used in a UV cross-linking reaction with ^{32}P-labelled HIV-1/2 5' UTR RNA to investigate whether we could isolate which wash fraction contained the unknown 45 kDa protein [figure 91].

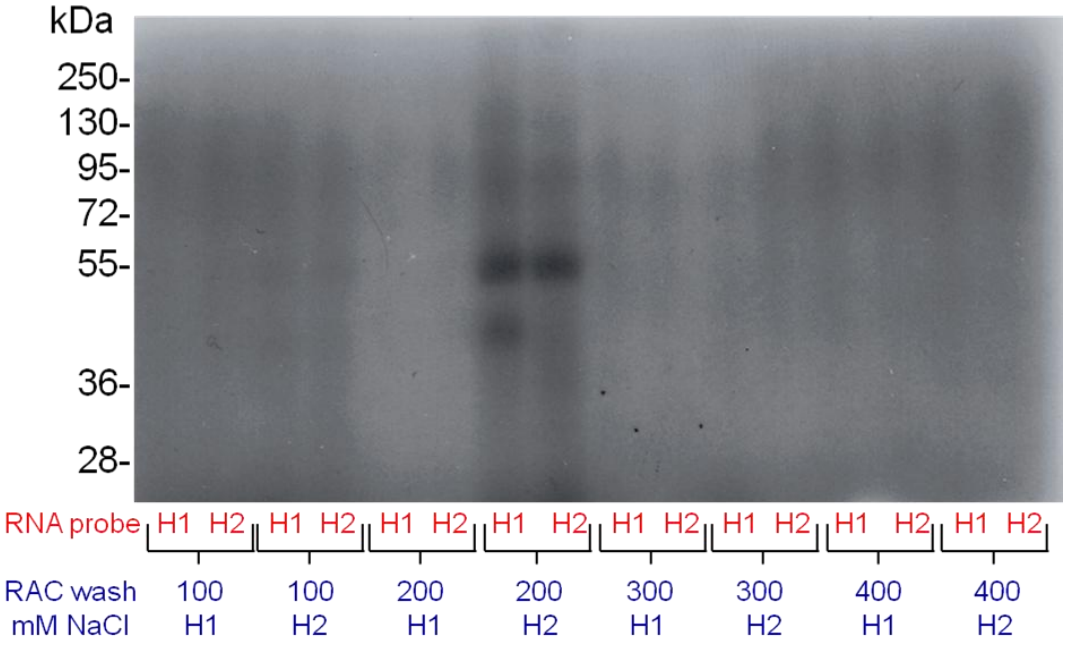

Figure 91: SDS-PAGE of UV cross-linking with the HIV-1 (H1) and HIV-2 (H2) 5' UTR and 100-400 mM NaCl salt washes from RNA affinity chromatography with HIV-1/2 5' UTRs.

Protein bands were identified at ~55 kDa binding to both the HIV-1/2 5' UTR from the HIV-2, 200 mM wash fraction [lanes 7+8, figure 91]. A further band at ~ 45 kDa binding to the HIV-1, but not the HIV-2 5' UTR [lane 7, figure 91], suggests that the unknown protein is also contained in this wash fraction.

10 µl of the same wash fractions were separated by SDS-PAGE and stained with Instant Blue [Expedeon] to see whether we could identify the same 45 kDa band for extraction and analysis by mass spectrometry [figure 92].

A faint band at ~45 kDa was observed in the H2, 200 mM wash fraction [lane 4, figure 92]. This band was excised and processed for analysis by mass spectrometry. Mass spectrometry identified seven proteins [table 15], of which three were actin and the other four metabolic enzymes.

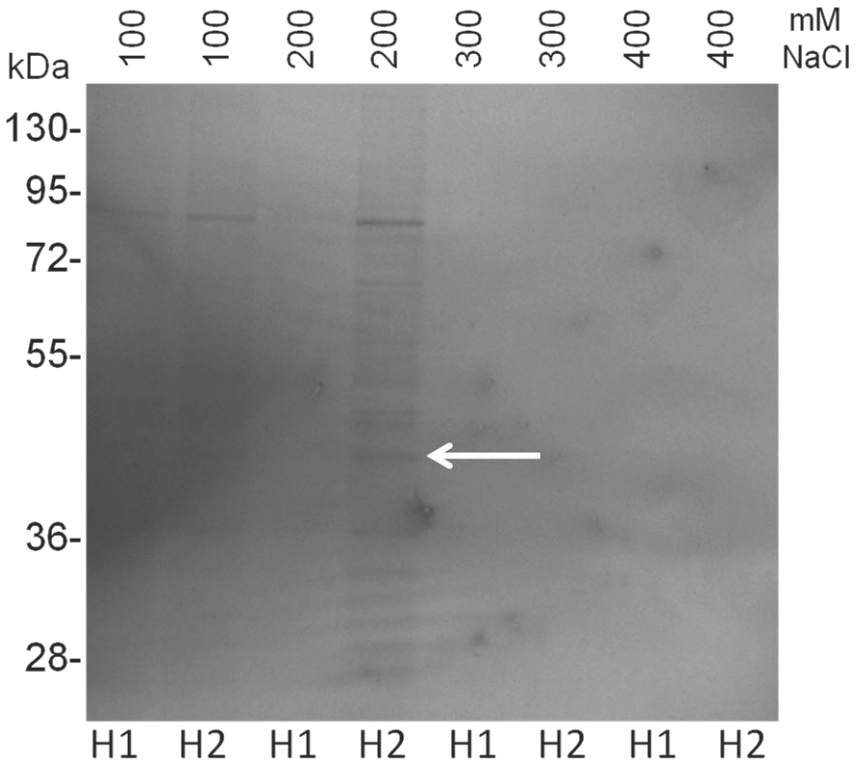

Figure 92: SDS-Page of 100-400 mM NaCl salt washes from RAC with HIV-1 (H1) and HIV-2 (H2) RNA.

Resource	Entry name	Protein name	Gene name
UniProtKB ENSEMBL	IP100894365.2	ACTG1 protein	ACTB, ACTG1
UniProtKB ENSEMBL	IP100922693.1	cDNA FU53662, highly similar to actin alpha skeletal muscle	ACTB
UniProtKB ENSEMBL	IP100027223.2	Isocitrate dehydrogenase[NADP] cytoplasmic	IDH1, PICD
UniProtKB ENSEMBL	IP1000022977.1	Creatine kinase β-type	CKB, CKBB
UniProtKB	IP100555809.3	Actin-like protein	ACT
ENSEMBL	IP100815732.1	PAICS (Phosphoribosylaminoimidazole carboxylase)	PAICS
UniProtKB ENSEMBL	IP00012007.6	Adenosylhomocysteinase	AHCY, SAHH

Table 15: Mass spectrometry results [Sources; UniProtKB: http://www.uniprot.org/uniprot, ENSEMBL: http://www.ensembl.org/Homo_sapiens/Info/Index].

None of the proteins identified by mass spectrometry are classical RNA-binding proteins or candidate proteins of known interactions with HIV-1 RNA, although actin has recently been reported to bind to respiratory syncytial virus RNA (Harpen *et al.*, 2009). It may be that an insufficient quantity of the target protein was therefore available in the sample for analysis.

5.2.4 Investigation of the binding site of the 45 kDa protein

To narrow down the binding location of the unknown 45 kDa protein, 3' truncated HIV-1 reporters were produced for UV cross-linking by digestion of the template for *in vitro* transcription with Afl II, HindIII, NarI and BssHII [figure 93].

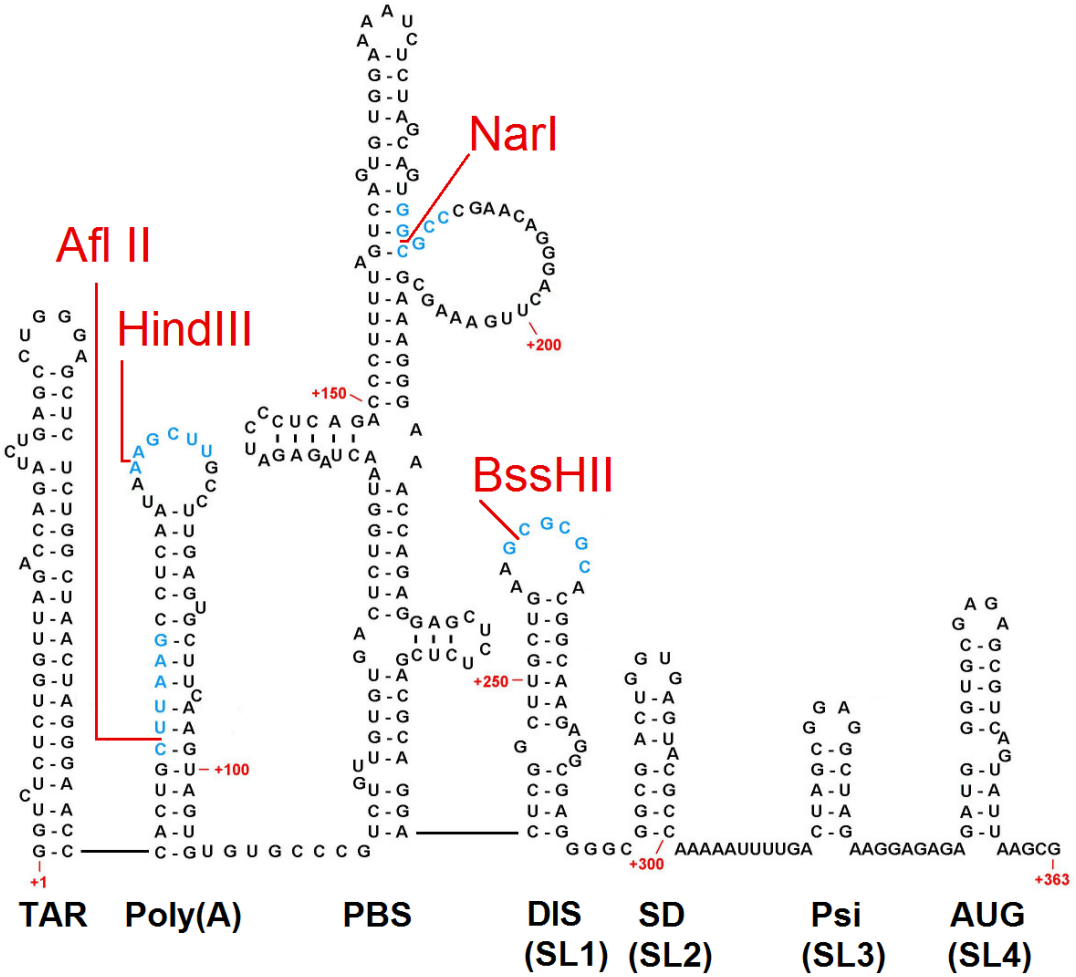

Figure 93: Restriction sites within the HIV-1 5' UTR used to linearise HIV-1 reporter plasmids to make truncated HIV-1 5' UTR RNAs [adapted from (Russell *et al.*, 2004)].

^{32}P-labelled full-length HIV-1/2 5' UTRs and the truncated HIV-1 5' UTR RNAs were used in UV cross-linking assays with HeLa S100 extract [figure 94].

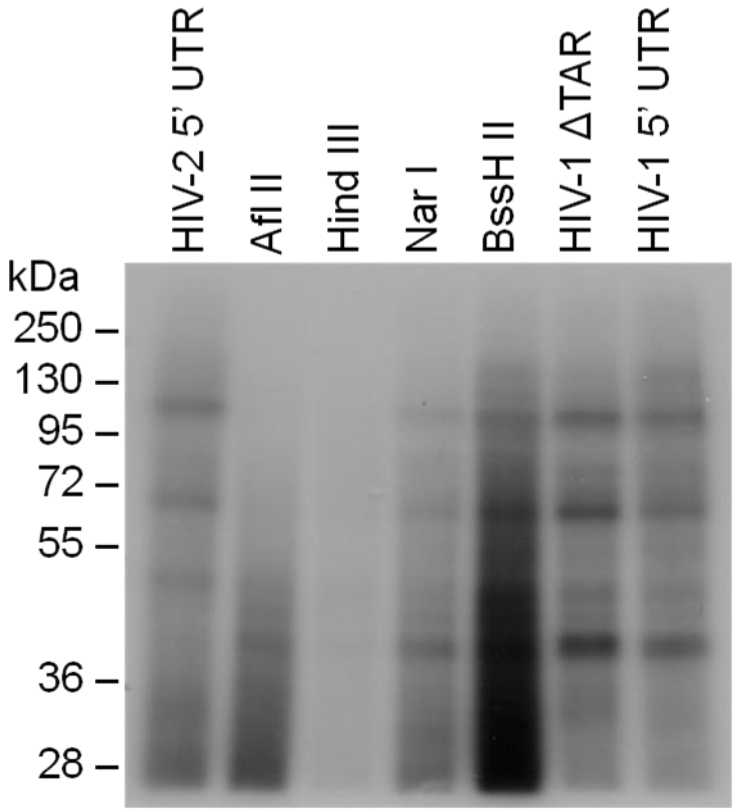

Figure 94: UV cross-linking of full-length HIV-1/2 5' UTR and truncated HIV-1 5' UTR RNAs with HeLa S100 extract.

The 45 kDa band was clearly visible bound to full-length, BssHII and NarI truncated HIV-1 RNAs [figure 94], suggesting that the binding site for this protein is in the 5' region of the 5' UTR. Weak binding of the 45 kDa protein to Afl II was also seen suggesting poor binding to the TAR structure. This is corroborated by strong protein binding to ΔTAR RNA [lane 6, figure 94]. Binding was enhanced when more of the HIV-1 5' UTR was present, suggesting multiple binding domains may be required for efficient protein binding. The HindIII lane [lane 3, figure 94] was empty, suggesting this RNA may have been unstable and therefore degraded. Lack of binding to Afl II truncated RNA [lane 2, figure 94] suggests lack of protein binding to the TAR structure.

5.3 Discussion

5.3.1 A comparison of cellular proteins binding to HIV-1/2 5' UTR-gag RNA

A 45 kDa protein from HeLa extract was shown to specifically bind to the HIV-1 5' UTR but not to the HIV-2 5' UTR. If this protein is shown to play an important role in gene expression, its enhanced binding to the HIV-1 5' UTR may indicate a mechanism by which HIV-1 gene expression is able to occur more efficiently than for HIV-2. It appears that the presence of gag is necessary to allow the 45 kDa protein to interact with HIV-2 RNA, as binding of the 45 kDa protein was only weakly detected for HIV-2 UTR-gag and not for the HIV-2 5' UTR alone. Potentially, for HIV-2, the 45 kDa binding site may be located within gag. Alternatively, the HIV-2 5' UTR may adopt a different conformation in the presence of gag. Abbink *et al.* (2003) report two different structural conformations within the HIV-1 5' UTR, highlighting the dynamic role of RNA structure for HIV-1 gene expression (Abbink and Berkhout, 2003). Although similar conformational variations have not been investigated for HIV-2, it may be that the HIV-2 5' UTR is also able to adopt different conformations and these are influenced by the presence of gag RNA. Thus the 45 kDa protein may only be able to bind to the HIV-2 5' UTR if gag is present. However, even in the presence of gag, this protein only interacts weakly with HIV-2. If the 45 kDa protein is shown to be important to HIV-1 transcription or translation, its lack of binding to the HIV-2 5' UTR may therefore account for the lower efficiency of HIV-2 gene expression.

Additional proteins of ~120 and 130 kDa showed differential binding to the HIV-1/2 5' UTRs. Although the identity of these proteins remains unknown, these results suggest that different RNA-binding proteins may interact with the HIV-1/2 5' UTRs, thus highlighting a way in which HIV-1/2 gene expression may differ.

5.3.2 La autoantigen binding to the HIV-1/2 5' UTR

La autoantigen has previously been shown to bind to the HIV-1 5' UTR. La was therefore considered as a candidate protein for the 45 kDa protein we identified binding to the HIV-1 5' UTR. A UV cross-link with recombinant La

showed that it was able to bind to the HIV-1 5' UTR, although the size of recombinant La was larger than that of the unknown 45 kDa protein from HeLa extract. Attempts to immunoprecipitate native La from UV cross-linking reactions with HeLa extract were unsuccessful. However, this was unsurprising given that even recombinant La could only be weakly immunoprecipitated. Binding of the 45 kDa protein to the HIV-1 5' UTR was not reduced in the presence of a poliovirus IRES competitor, which is known to bind La. Furthermore, the 45 kDa protein was shown to bind to the HIV-1 5' UTR in the absence of TAR indicating that TAR is not the binding site for this protein. Recombinant La also bound to the HIV-2 5' UTR whilst the 45 kDa protein does not. Given these results, we therefore conclude that the unknown 45 kDa protein is unlikely to be La autoantigen.

Interestingly, during cross-linking of HIV-1 5' UTR RNA to HeLa extract in the presence of poliovirus IRES RNA, it appeared that the 45 kDa protein band interacting with the HIV-1 5' UTR may, in fact be a duplet band representative of more than one RNA-binding protein of similar size. Alternatively, the dual bands could be representative of isoforms or post-translational modifications of the same protein.

5.3.3 Isolating the 45 kDa binding protein

Initial attempts to isolate the 45 kDa protein by RNA affinity chromatography resulted in a lot of non-specific binding. This masked attempts to specifically extract the protein of interest. Several variations in the RNA affinity chromatography protocol were consequently investigated, to see whether we could reduce background levels of protein binding and enhance the level of specific protein binding. These included pre-absorption of HeLa extract with magnetic beads to remove non-specific binding proteins prior to use in the RNA affinity chromatography, blocking beads in 5% Marvel TBS-T for 1 h before use to inhibit non-specific protein binding to beads, and increasing the RNA concentration used to saturate the beads and prevent non-specific protein binding. Additionally, following protein-RNA binding, beads were washed in increasing concentrations of salt washes to remove non-specific or weak protein interactions prior to elution of bead-bound proteins. Varying the

order of the RNA affinity chromatography stages, to initially bind proteins to RNA before carrying out the pull-down using magnetic beads, was also tried. Despite the numerous approaches undertaken, a lot of non-specific protein binding to the beads was still observed. Furthermore, very little specific protein binding was detected. This may have been because only a fraction of the specifically bound proteins were isolated, or that the proteins of interest were masked by non-specific protein binding.

Introducing increasing salt concentration washes as part of the protein elution stage resulted in fewer proteins eluted in later washes. These possibly represented more specific HIV RNA-protein interactions. After confirming that UV cross-linking experiments would still function at increasing salt concentrations, wash fractions were used in a UV cross-link with HIV-1/2 5' UTR RNA to analyse which fraction contained the unknown 45 kDa protein. The HIV-2 RNA, 200 mM wash fraction yielded an interesting band at 45 kDa binding solely to the HIV-1 5' UTR. This fraction was separated by SDS-PAGE and the gel stained to excise the resulting 45 kDa band. Analysis of this fraction was carried out by mass spectrometry. However, the 45 kDa band was only faintly present following staining, and mass spectrometry results did not yield any well-known RNA-binding proteins. Thus it is likely that there was not sufficient protein in this band fraction to produce an accurate assessment of the 45 kDa protein (or proteins) present.

However, the most abundant protein identified by mass spectrometry was an actin isoform: Beta-actin (ACTB). Although not well-known as an RNA-binding protein, actin was shown to be important for the transcription of the negative-strand RNA virus: respiratory syncytial virus (RSV). Direct binding of actin to the RSV genome is mediated by the actin divalent-cation-binding domain. Thus actin is proposed to act as a transcription factor for RSV replication (Harpen *et al.*, 2009). Although no interaction between actin and the HIV genome has been reported, these findings could be of relevance to HIV if actin is shown to be the 45 kDa protein binding to the HIV-1 5' UTR. If actin is able to enhance HIV-1 transcription by binding to the 5' UTR, but the same is not true for HIV-2, this may provide a rationale for the less efficient transcription rate of HIV-2 evidenced in chapter 3.

Further work is necessary to validate the identity of this unknown 45 kDa protein. Optimisation of the RNA affinity chromatography protocol requires scaling up the production of HeLa S100 extract and biotinylated RNA, using a greater quantity of magnetic streptavidin beads, including larger volumes for initial salt washes and tailoring washes to a smaller quantity for expected protein elution fractions. Likewise, additional considerations, including carrying out protein precipitation to concentrate proteins in wash fractions and dialysis of fractions prior to testing in UV cross-linking assays, will allow easier detection and isolation of protein bands by SDS-PAGE. It is hoped that a coordinated scale-up and optimisation of this protocol may permit isolation of the unknown HIV-1 5' UTR RNA-binding protein in sufficient quantity for better identification by mass spectrometry.

Alternative approaches could also be investigated as a means to isolate the unknown HIV-1 5' UTR binding protein in greater abundance. One method, called the MS2:MBP pull down, involves fusing the HIV-1 5' UTR to multiple copies of the 3' UTR stem loop of bacteriophage MS2 [figure 95].

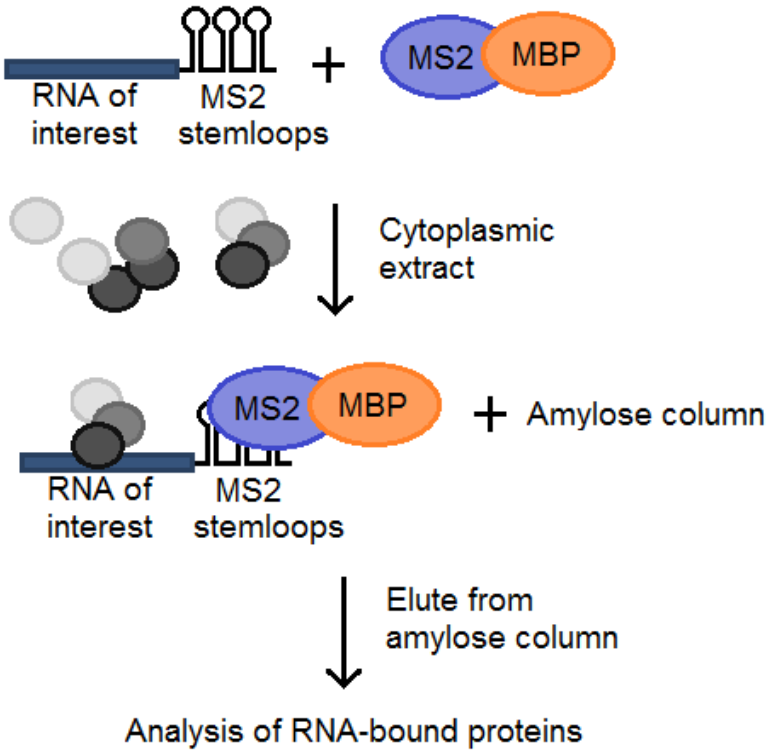

Figure 95: Isolation of specific RNA-binding proteins using the MS2: MBP RNA pull down method.

MS2 coat protein is an RNA-binding protein which binds efficiently to the MS2 stem loops. MS2 coat protein can be fused to a maltose binding protein (MBP) forming MS2:MBP. When cellular extract is added to a reaction with the RNA-stem loops, RNA-binding proteins specifically interact with the RNA of interest. The RNA-bound proteins attached to the MS2 stem loops can form a complex with MS2:MBP which is all extracted via MBP binding to an amylose column. In this way, specific RNA-binding proteins can be isolated from non-specific proteins and identified (Elliott and Ladomery, 2010).

5.3.4 Identifying the 45 kDa protein binding site

Despite the unknown identity of the protein binding to the HIV-1 5' UTR, it was hoped that narrowing down the binding location of this protein within the 5' UTR might provide an indication of its function. Furthermore, this could potentially facilitate isolation of the protein by RNA affinity chromatography by reducing the non-specific binding associated with excess RNA. This would only be possible, however, assuming that just a specific region of the HIV-1 5' UTR was implicated in binding to this protein. The 45 kDa protein bound strongly to more complete, lengthier HIV-1 5' UTR RNAs. This suggests that perhaps multiple protein binding domains within the HIV-1 5' UTR enhance binding of the unknown protein rather than a small, specific motif. Conversely, the RNA-binding site of this protein may be located at the 5' end of the HIV-1 5' UTR. Further work is consequently necessary to isolate the exact binding position of the unknown 45 kDa protein.

Future work will endeavour to uncover the identity of the unknown 45 kDa protein binding to the HIV-1 5' UTR and, moreover, elucidate a potential role for this RNA-protein interaction in the life cycle of HIV-1. After optimising the methods necessary to achieve this, the identity of other HIV-1/2 RNA-binding proteins, such as the 120/130 kDa proteins binding with opposing strengths to the HIV-1/2 5' UTR, will be investigated.

Future work could also look to isolate protein extracts from HIV-infected HeLa cells for use in cross-linking. This will determine whether viral proteins bind differently to HIV-1 and HIV-2 RNA or whether cellular proteins bind differently in the presence of viral proteins. If cross-linking results show

differences in viral or cellular proteins binding to HIV-1/2 RNA, RNA-affinity chromatography and proteomics will be necessary to identify those proteins.

CHAPTER 6: THE EFFECT OF AP-1 ON GAG PROTEIN LEVELS

6.1 Introduction

This chapter explores the role of the clathrin adaptor protein AP-1 in HIV Gag expression and trafficking. In the introduction, the roles of adaptor proteins in facilitating vesicular transport are discussed alongside the relevance of this to HIV Gag transport to, and assembly at, the plasma membrane. Results are presented showing that specific knockdown of AP-1 effects a reduction in the cellular levels of both HIV-1 and HIV-2 Gag. The role of AP-1 in both HIV-1 and HIV-2 Gag expression and cellular transport was explored by inhibiting this adaptor protein and visually assessing the effect on HIV-1/2 Gag protein levels within the cell by confocal microscopy.

6.1.1 Gag trafficking

Genomic RNA, Gag and Env proteins are transported on endosomes to the plasma membrane during virus assembly to form immature virions. Although progress has been made in determining the components of viral assembly and budding, the pathways used to traffic HIV Gag to assembly sites at the plasma membrane have not yet been clearly defined (Gousset *et al.*, 2008). Gag interactions with endosomal sorting proteins are fundamental to retroviral assembly and virus-like particles (VLPs) have been shown to assemble when only the HIV Gag protein is expressed (Camus *et al.*, 2007). Gag has been shown to localize to the plasma membrane and is also found associated with internal, cellular components which bear a resemblance to multi-vesicular bodies (MVBs) (Gousset *et al.*, 2008). Two groups of proteins associated with cellular trafficking have been linked to HIV Gag; MVB proteins and clathrin adaptor (AP) proteins. Within the cell, ESCRT (endosomal sorting complexes required for transport) protein complexes recognise and sort ubiquitinated cargo proteins into the intralumenal vesicles of MVBs, and clathrin APs sort target proteins into clathrin coated transport vesicles (Camus *et al.*, 2007). The mechanism of clathrin coated vesicular transport is outlined in figure 96. Clathrin and adaptor proteins are essential components of clathrin coated vesicles (Orzech *et al.*, 2001).

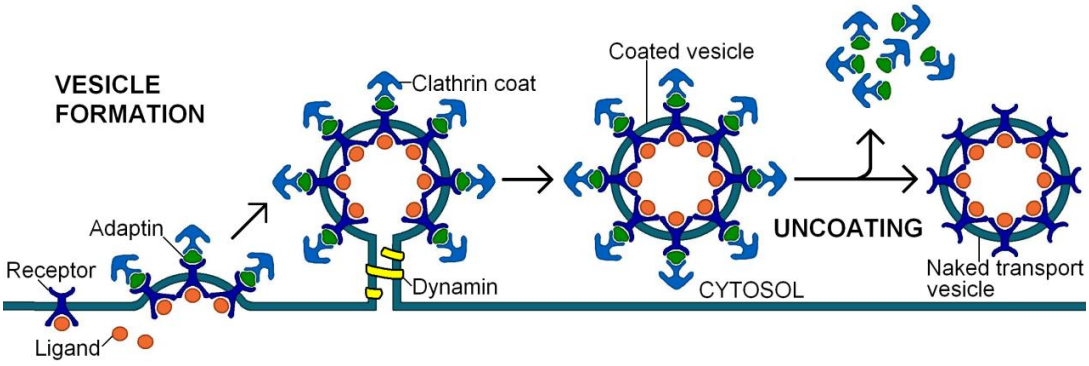

Figure 96: During the formation of a clathrin coated vesicle, ligands bind to, and activate, their cognate receptors. Clathrin and adaptor proteins subsequently bind to activated receptors forming a coated pit which, in turn, becomes a vesicle. Dynamin mediates the separation and release of coated vesicles from the lipid membrane [http://www.zoology.ubc.ca/~berger/B200sample/unit_8_protein_processing/images_unit8/14_19.jpg].

Eukaryotic protein transport relies on the movement of vesicles between celllular, membrane-bound compartments. Both endocytic and exocytic protein pathways involve budding of vesicles from a donor compartment and subsequent fusion with an acceptor compartment (Orzech *et al.*, 2001).

6.1.2 The adaptor proteins and AP-1

Heterotetrameric adaptin protein complexes are important in vesicular transport where they have a duality of function; selecting cargo proteins for vesicle incorporation through specific receptor binding, and providing an anchor for clathrin coat formation [figure 97].

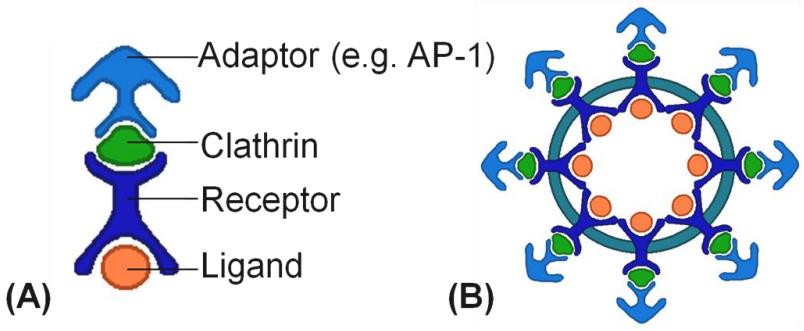

Figure 97: AP complexes form a link between receptor-ligand complexes and clathrin triskelions (A). A peptide recognition sequence within the receptor specifically binds to adaptin to mediate this interaction. The assembly of many receptor-ligand complexes bound to clathrin results in the formation a clathrin-coated vesicle (B) [adapted from http://www.erin.utoronto.ca/~w3bio315/lecture17.htm].

Four AP complexes (AP-1-4) exist in eukaryotes. Transport between the t*rans*-Golgi network (TGN) and endosomes relies on AP-1 and AP-3; AP-1 facilitates the formation of exocytic vesicles whereas AP-3 is involved in anterograde transport to endosomes and lysosomes (Odorizzi *et al.*, 1998). AP-2 permits the formation of endocytic vesicles at the plasma membrane and AP-4 functions during transport between the TGN and cell surface (Nevin and Dacks, 2009; Orzech *et al.*, 2001). AP complexes are composed of a small subunit (σ1-4), a medium subunit (μ1-4) and two large subunits (γ/β1, /β2, δ/β3, ε/β4) (Camus *et al.*, 2007). The composition of AP-1 is shown in table 16.

Component	Size
B1-adaptin	~100 kDa
γ-adaptin	~100 kDa
μ1	47 kDa
σ1	19 kDa

Table 16: Components of the mammalian adaptor protein AP-1 and their molecular weights.

6.1.3 The role of AP in Gag trafficking

Retroviral release relies on AP-1. Camus *et al.* (2007) showed that the HIV-1 Gag matrix region interacts specifically with the μ1A medium chain of AP-1μ (but not with AP-2 and AP-3 homologous μ2 and μ3 subunits). Mutation or knockdown of AP-1 significantly decreases Gag trafficking, viral replication and the number of budding virions (shown by an 80% decrease in the release of Gag p24) (Camus *et al.*, 2007). It is plausible that HIV-1 may exploit the interaction of AP-1 with clathrin (and its role in forming coating vesicles) as a scaffold for the production of virus particles (Camus *et al.*, 2007).

Binding of HIV-1 Gag to AP-2 was shown to regulate the release and assembly of HIV-1 virions. However, disruption of the interaction between Gag and AP-2 enhances viral budding (Batonick *et al.*, 2005) The matrix region (N-terminus) of HIV-1 Gag has also been shown to bind to the δ

subunit of the AP-3 complex, which enhanced Gag budding by directing Gag to late endosomal compartments (Dong *et al.*, 2005). This indicates that the Gag assembly pathway involves late endosomal trafficking.

Camus *et al*. (2007) suggest that AP-1 and AP-3 are involved in two different steps of the Gag budding pathway as mutations in AP-1 and AP-3 did not have an additive effect on HIV-1 Gag release. Alternatively, targeting of Gag to the plasma membrane for budding may preferentially use AP-1 or AP-3 (Camus *et al.*, 2007).

In addition to the effect on budding, preliminary results from our group (E.Anderson, unpublished) suggested that AP-1 knockdown may also result in a reduction in cellular HIV-1 Gag levels. However, the finer details of HIV Gag interactions with adaptor proteins, and in particular AP-1, have yet to be resolved.

6.2 Results

6.2.1 AP-1 knockdown in cells

To confirm whether we could successfully knock down the expression of AP-1 in cells, HeLa cells were transfected with siRNA to AP-1, a siRNA negative control and a mock transfection control. Total cellular protein was harvested at 48 h and 72 h post-transfection, separated by SDS-PAGE and western blotted with an antibody to the gamma subunit of AP-1 (AP-1γ) [figure 98].

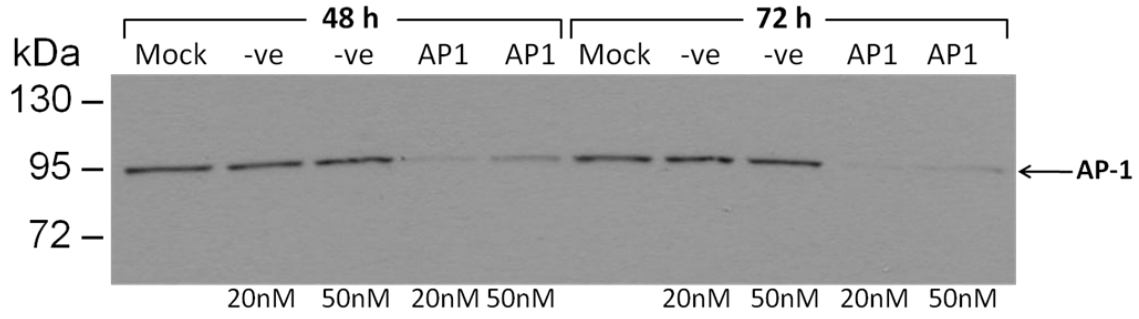

Figure 98: Western blot with an antibody to AP-1γ showing AP-1 knockdown in mock, negative siRNA and AP-1 siRNA (either 20 nM or 50 nM) treated cells at 48 h or 72 h post-transfection.

AP-1 appears as a 104 kDa protein [figure 98]. Results showed that AP-1 knockdown was achieved using 20 nM siRNA. AP-1 knockdown was better after 72 h, but still detectable after 48 h. Knockdown was specific as the negative control siRNA had no effect on AP-1 levels.

6.2.2 A comparison of AP-1 knockdown on HIV-1/2 Gag levels

We then tested the effect of AP-1 knockdown on the cellular levels of HIV-1/2 Gag. HeLa cells were transfected with AP-1 siRNA (or a negative siRNA control) for 24 h followed by transfection with HIV-1 or HIV-2 provirus for a further 24 h to produce viral proteins. After this time, total protein was harvested from cells and analysed by western blotting with an antibody to HIV-1 Gag p24 (Capsid) or HIV-2 Gag p27 (Capsid) [figure 99].

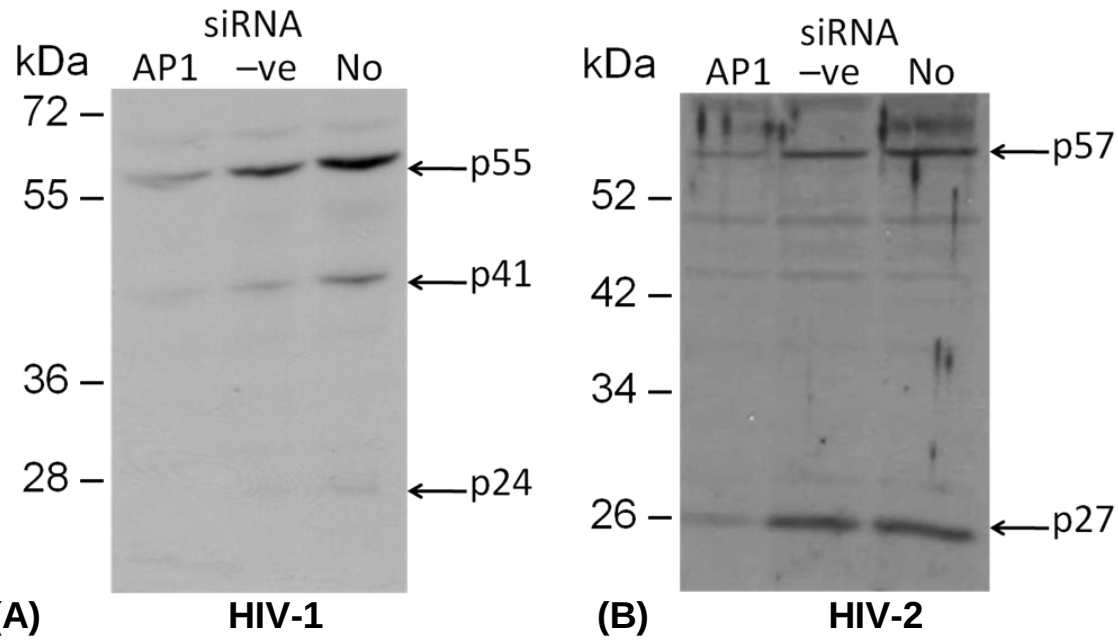

Figure 99: Western blot of AP-1 transfection protein using antibodies to HIV-1 Gag (p24) and HIV-2 Gag (p27). HIV-1/2 Gag expression from transfected provirus is shown in the presence [lane 1] or absence [lane 3] of AP-1 siRNA or with a negative control siRNA [lane 2].

AP-1 siRNA knockdown reduced the level of full-length p55 (HIV-1) and p57 (HIV-2) Gag products, the HIV-1 p41 Gag processing intermediate, and both p24 (HIV-1) and p27 (HIV-2) Capsid proteins, when compared to a negative control siRNA or no siRNA. This suggests that specific knockdown of AP-1 reduces the cellular levels of both HIV-1 and HIV-2 Gag.

6.2.3 Visualisation of AP-1 knockdown in cells

Confocal microscopy was then used to visualise AP-1 knockdown within cells. HeLa cells were transfected with AP-1 siRNA, negative control siRNA or no siRNA for 48 h, fixed, and stained with an antibody to AP-1 and secondary Alexaflour antibody. Cellular nucleic acid was stained using DAPI and cells were visualised at different magnifications using a confocal microscope [figures 100+101].

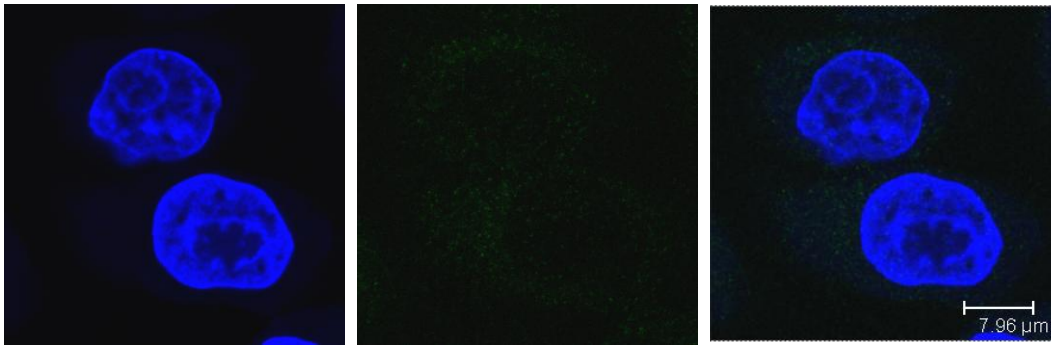

(A) AP-1 siRNA

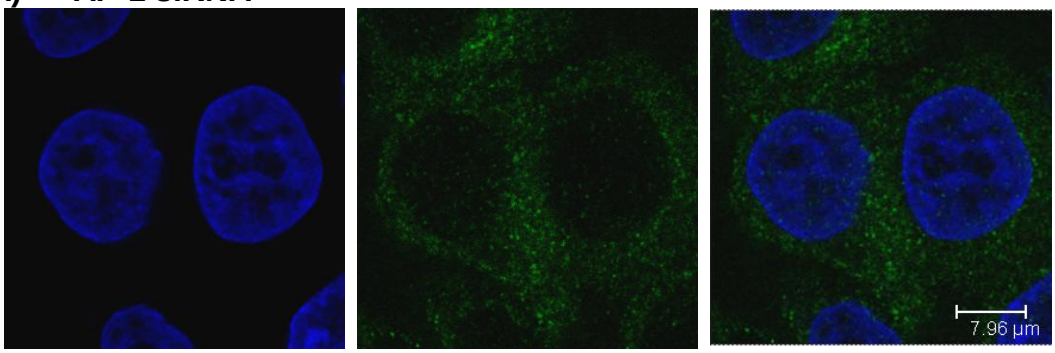

(B) Negative control siRNA

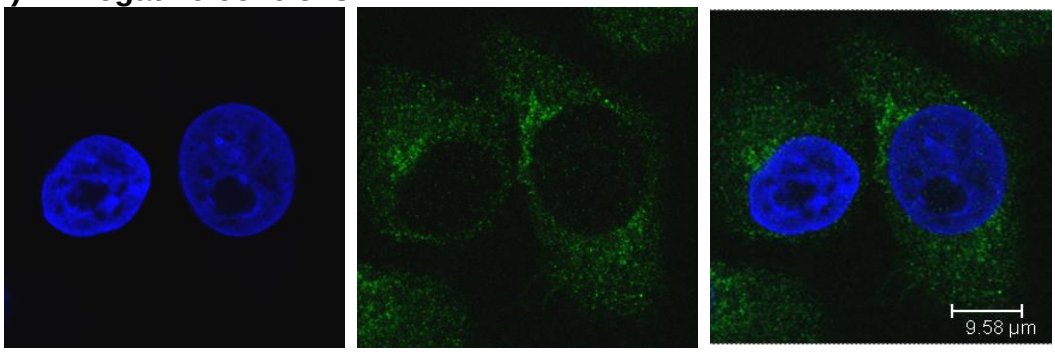

(C) No siRNA

Figure 100: Confocal microscopy images showing blue DAPI staining of the nucleus and green AP-1 fluorescence in AP-1 siRNA (A), negative control siRNA (B) and mock 'no siRNA' (C) transfected HeLa cells.

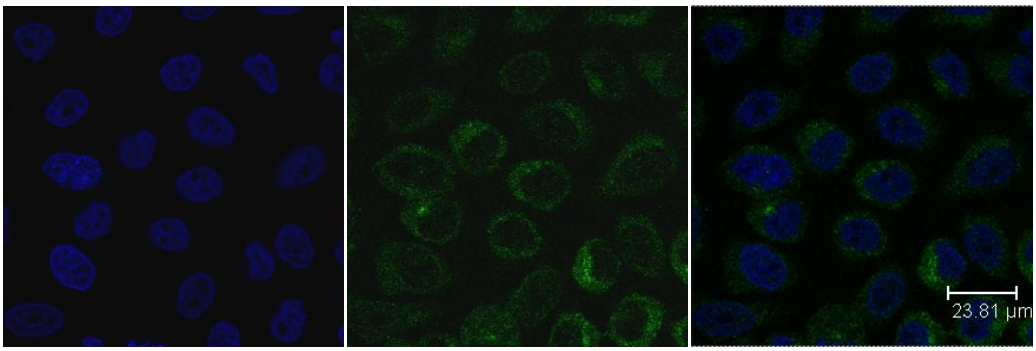

(A) AP-1 siRNA

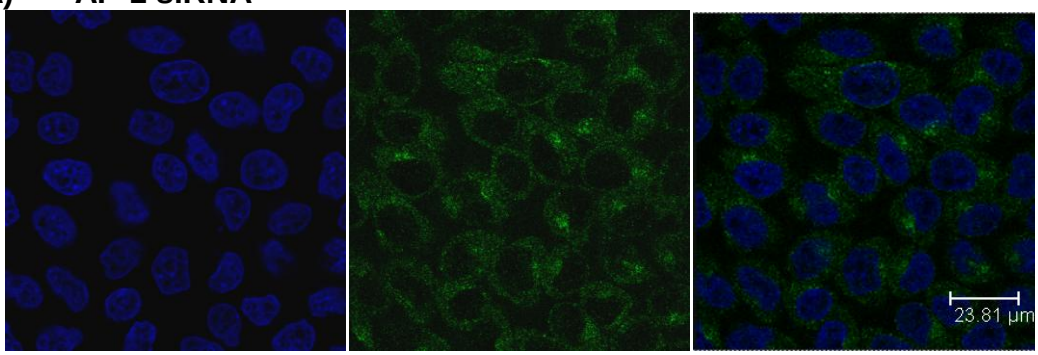

(B) Negative control siRNA

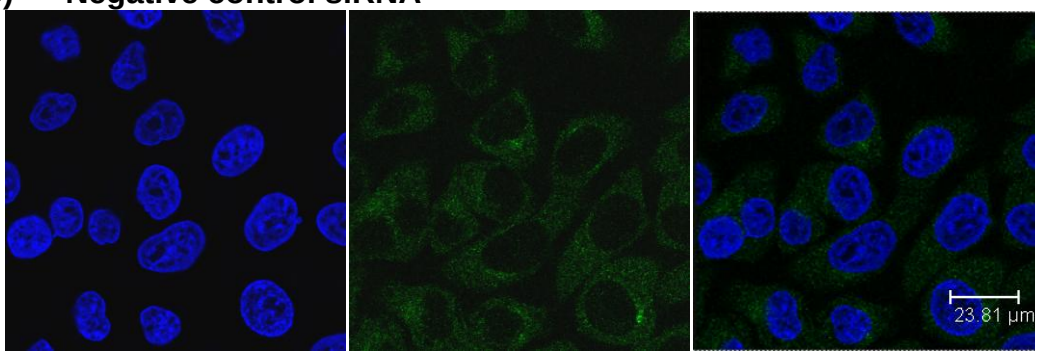

(C) No siRNA

Figure 101: Confocal microscopy images showing blue DAPI staining of the nucleus and green AP-1 in AP-1 siRNA (A), negative control siRNA (B) and mock 'no siRNA' (C) transfected HeLa cells.

AP-1 could be detected in cells mock transfected or treated with negative control siRNA. AP-1 staining localised to perinuclear structures, likely corresponding with the *trans*-Golgi network (TGN). Additionally, punctate AP-1 staining throughout the cell was suggestive of cytoplasmic vesicles and likely represents AP-1 bound to endosomes. AP-1 clathrin coats are principally located at the TGN and mediate endosomal transport (Odorizzi *et al.*, 1998). The specific AP-1 staining pattern we visualised correlates with both AP-1 function and, furthermore, matches other literary reports of AP-1 staining (Meyer *et al.*, 2000). We were thus able to successfully visualise AP-

1 within the cell. siRNA knockdown of AP-1 was also successful. Although not every cell treated with siRNA showed knockdown, there was a significant reduction in AP-1 immunofluorescence in most of the cells treated with AP-1 siRNA.

6.2.4 Visualisation of HIV-1/2 Gag in cells

To verify whether Gag p24/p27 antibodies were suitable for visualisation of HIV-1/2 Gag by confocal microscopy, HeLa cells were transfected with HIV-1/2 provirus for 24 h. Cells were subsequently fixed and stained with primary HIV-1/2 Gag antibodies and secondary Alexa Fluor antibodies [figure 102].

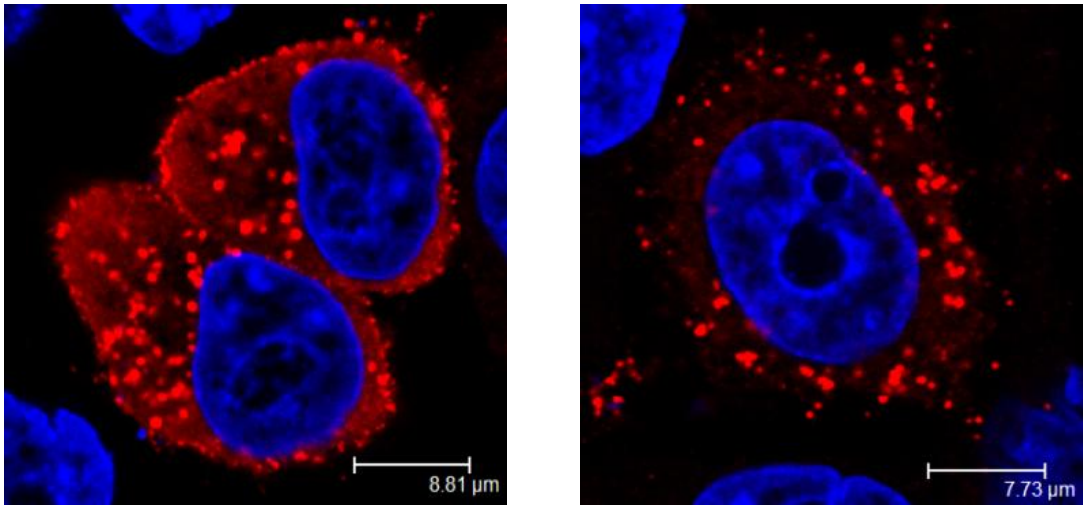

(A) HIV-1 **(B) HIV-2**

Figure 102: Confocal microscopy images showing blue DAPI staining of the nucleus and red HIV-1 (A) or HIV-2 (B) Gag expression in HeLa cells.

HIV-1/2 antibodies were able to detect Gag and allowed visualisation of the cellular localisation of HIV-1/2 Gag. Gag staining patterns differed between HIV-1/2. HIV-1 was expressed extensively throughout the cell, with localised staining at the plasma membrane. This likely represents the coordination of Gag molecules during viral particle assembly which occurs at the plasma membrane. HIV-1/2 Gag staining within the cytoplasm likely represents localisation of Gag at translation sites and Gag molecules undergoing transport to the plasma membrane via cellular endosomes or alternative mechanisms. Staining of HIV-2 Gag was diffuse within the cytoplasm, with

isolated, punctate Gag clusters and a lower overall level of Gag expression. HIV-2 Gag also showed little localisation to the plasma membrane.

The staining patterns of HIV-1/2 Gag reflect the enhanced rate of HIV-1 replication leading to an abundance of Gag within the cell, in contrast to the inefficient replication of HIV-2 reflected by slower accumulation of Gag within the cell. Likewise, HIV-1 staining represents a more advanced stage of the viral life cycle with Gag molecules undergoing assembly at the plasma membrane, whereas the HIV-2 virus appears to be much slower at progressing Gag to viral assembly. Alternatively, HIV-2 Gag may preferentially assemble at intracellular sites such as MVBs rather than at the plasma membrane.

6.2.5 Co-staining of AP-1 and HIV-1/2 Gag

Differences in the interaction of HIV-1/HIV-2 Gag proteins with AP-1, and subsequent trafficking through the cell, may indicate a mechanism by which HIV-1 and HIV-2 replication differ. Confocal microscopy was used to visualise the location of AP-1 within the cell and identify whether HIV-1/HIV-2 Gag proteins co-localised with AP-1. HeLa cells were transfected with HIV-1/2 provirus for 40 h. Cells were fixed, stained with both DAPI nuclear stain and antibodies to AP-1 and HIV-1 p24/HIV-2 p27 Gag proteins, and visualised by confocal microscopy [figure 103].

Both HIV Gag and AP-1 could be stained within the same cells and thus viewed, simultaneously, by confocal microscopy. AP-1 was localised to perinuclear structures whereas HIV-1/2 Gag staining was more diffuse within the cells. Additionally, HIV-1 Gag levels were at a greater intensity at the plasma membrane whereas HIV-2 Gag showed less localisation to the plasma membrane. Although HIV-1 Gag is reported to interact with AP-1 (Camus *et al.*, 2007), neither HIV-1 nor HIV-2 Gag showed significant co-localisation with AP-1. It may have been difficult to visualise this association due to the transient nature of the Gag trafficking interaction with AP-1.

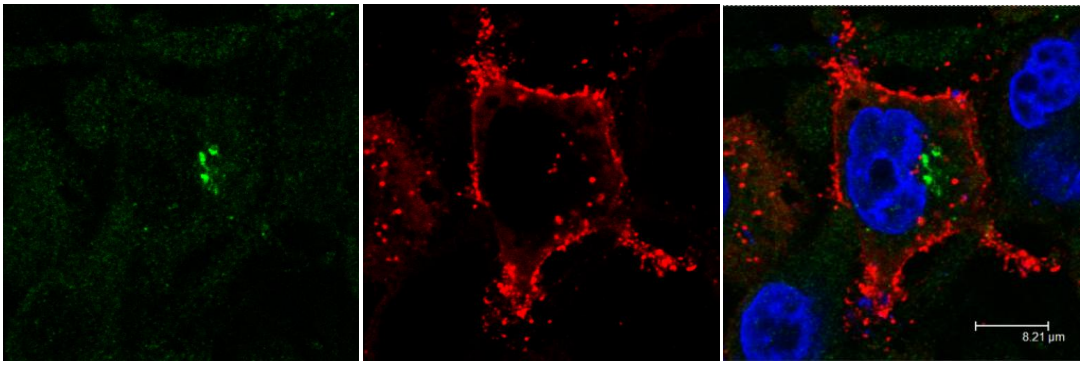

(A) HIV-1

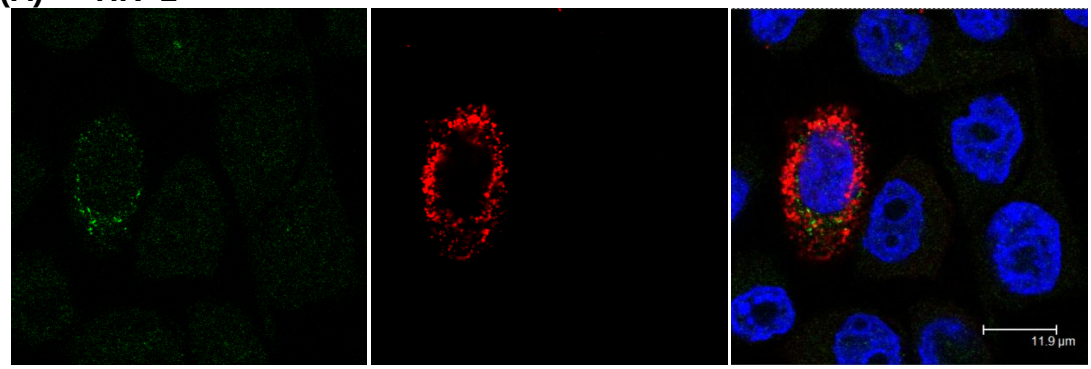

(B) HIV-2

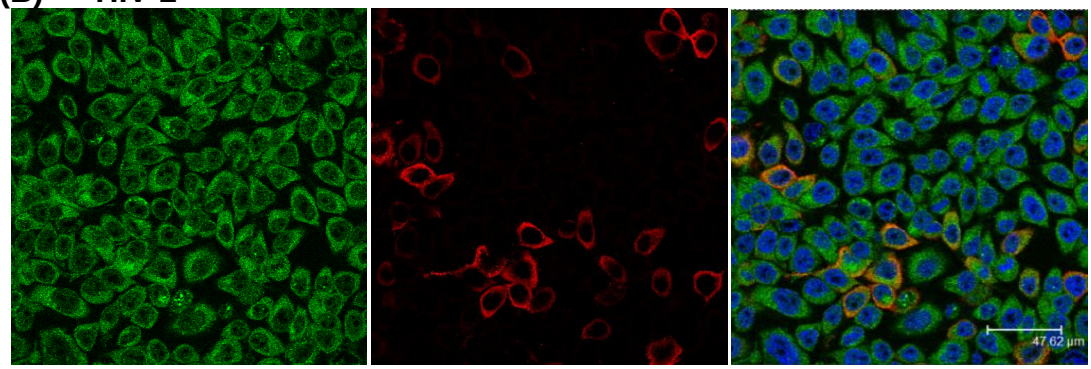

(C) HIV-1

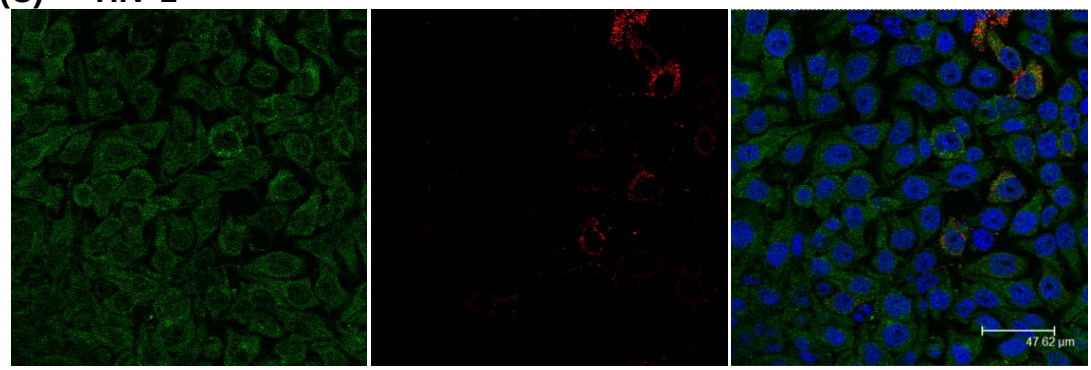

(D) HIV-2

Figure 103: Confocal microscopy images showing green AP-1 staining, red HIV-1 (A+C) and HIV-2 (B+D) Gag staining and blue DAPI staining of the HeLa cell nucleus.

6.2.6 Visualisation of the effect of AP-1 knockdown on cellular HIV-1/2 Gag levels

Knockdown of AP-1 resulted in a reduction in the level of both HIV-1 and HIV-2 Gag proteins within HeLa cells when compared by western blot. Subsequently, confocal microscopy was used to visually assess the impact of AP-1 knockdown on HIV-1 and HIV-2 Gag expression. HeLa cells were transfected with AP-1 siRNA for 24 h to knockdown AP-1, followed by HIV-1/2 provirus transfection for 24 h/40 h to allow expression of HIV-1/2 Gag with and without AP-1. Cells were fixed and stained with antibodies to AP-1 and HIV-1/2 Gag. Cell nuclei were stained with DAPI [figure 104].

AP-1 knockdown could be detected in cells transfected with AP-1 siRNA [figure 104, B+D]. For transfections in which AP-1 was knocked down, there were fewer cells expressing HIV-1 and HIV-2 Gag. Conversely, an increased number of cells were stained for HIV-1/2 Gag when AP-1 was not down-regulated. This suggests that AP-1 is important for Gag expression. Additionally, irrespective of AP-1 siRNA treatment, cells which showed good AP-1 staining (suggesting good AP-1 expression) also demonstrated a higher level of Gag expression. Consequently, results suggest that AP-1 enhances the level of HIV-1 and HIV-2 Gag expressed within the cell.

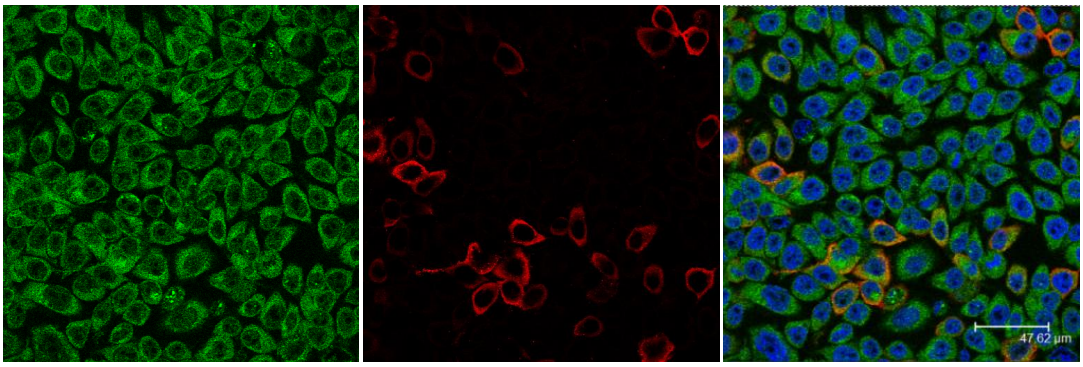

(A) HIV-1, 40 h, No siRNA

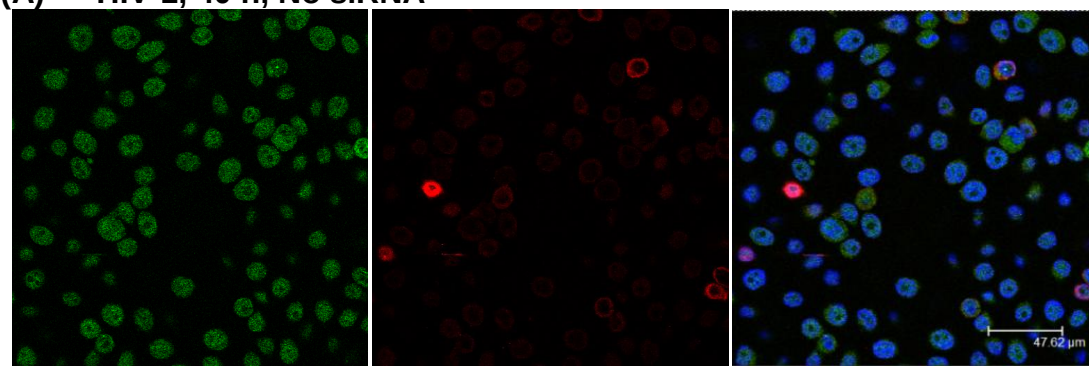

(B) HIV-1, 40 h, AP-1 siRNA

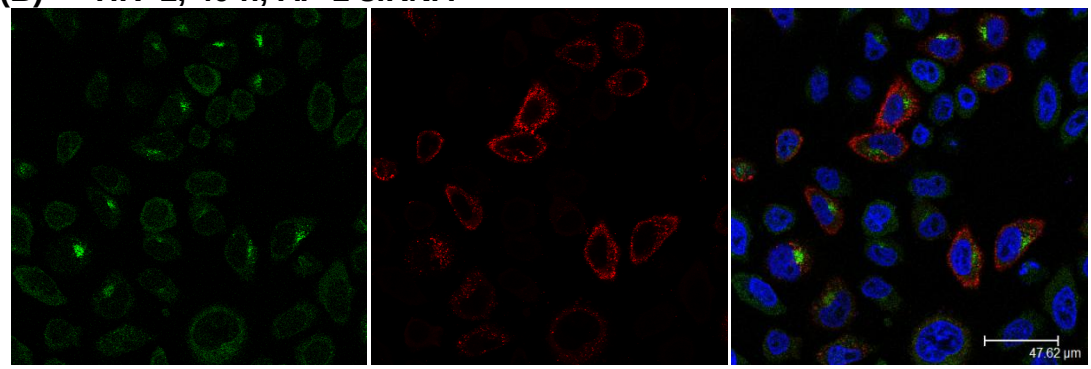

(C) HIV-2, 24 h No siRNA

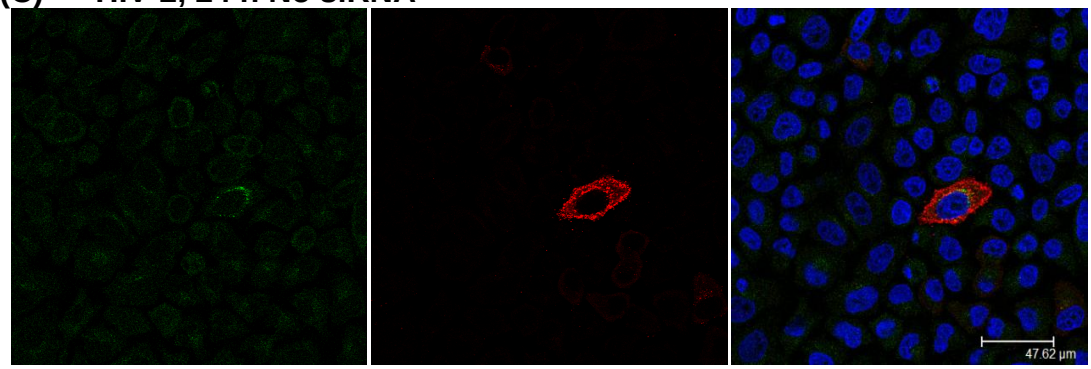

(D) HIV-2, 24 h AP1 siRNA

Figure 104: Confocal microscopy images of HIV-1/2 provirus transfected HeLa cells. Cells were transfected in the presence or absence of AP-1 siRNA. Cellular AP-1 is shown in green, HIV-1/2 Gag is shown in red and cell nuclei were stained with DAPI (blue).

6.2.7 GFP controls

To assess whether AP-1 siRNA transfections reduced gene expression and cell viability non-specifically, HeLa cells were transfected with (or without) 50 nM AP-1 siRNA and a GFP expression plasmid (pcDNA GFP) for 24 h. Cells were subsequently fixed and viewed under a confocal microscope [figure 105].

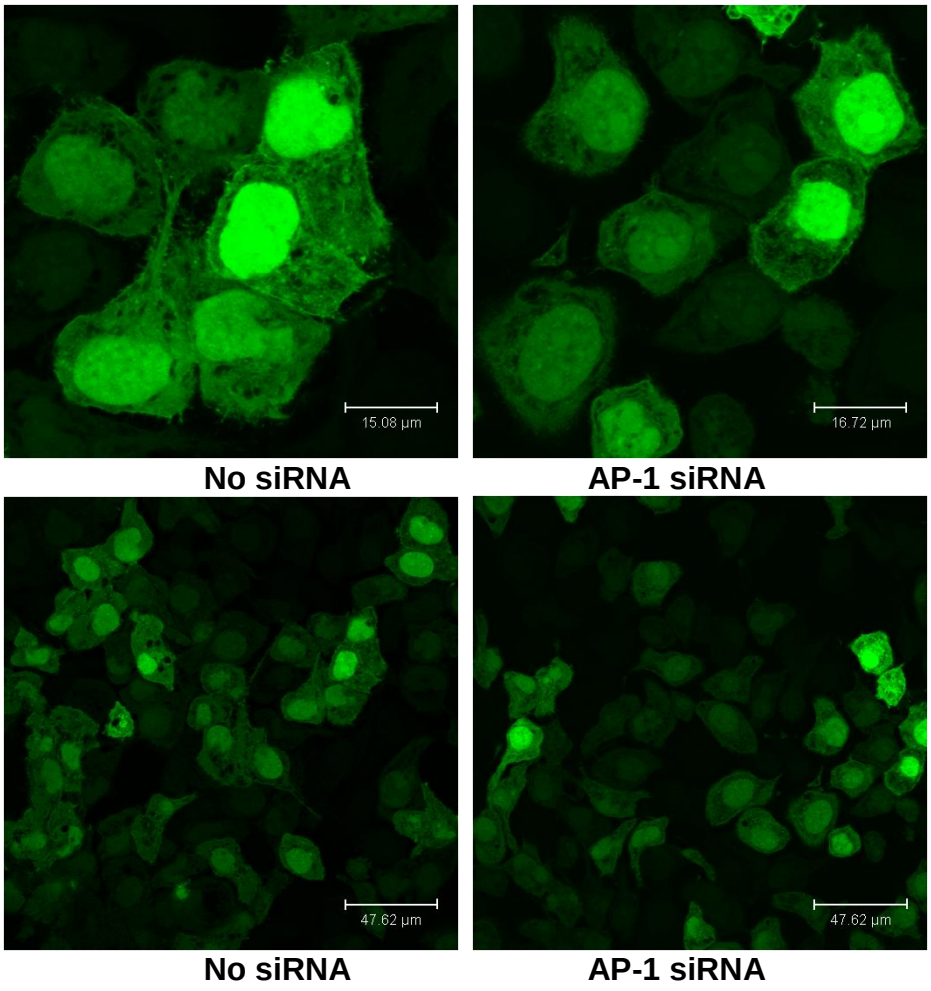

Figure 105: Confocal microscopy of HeLa cells transfected for 24 h with pcDNA GFP (green) in the presence/absence of 50 nM AP-1 siRNA.

GFP was well expressed in both mock and AP-1 siRNA co-transfected cells suggesting that AP-1 siRNA transfection did not significantly reduce non-specific gene expression or cell viability. To confirm these results in the presence of the HIV-1 provirus, the level of HIV-1 Gag was assessed in mock and AP-1 siRNA-treated cells alongside the GFP control. HeLa cells were transfected with HIV-1 provirus and a pcDNA GFP control with/without 50 nM

AP-1 siRNA for 24 h before fixing and staining with DAPI nuclear stain and antibodies to HIV-1 Gag p24 [figure106].

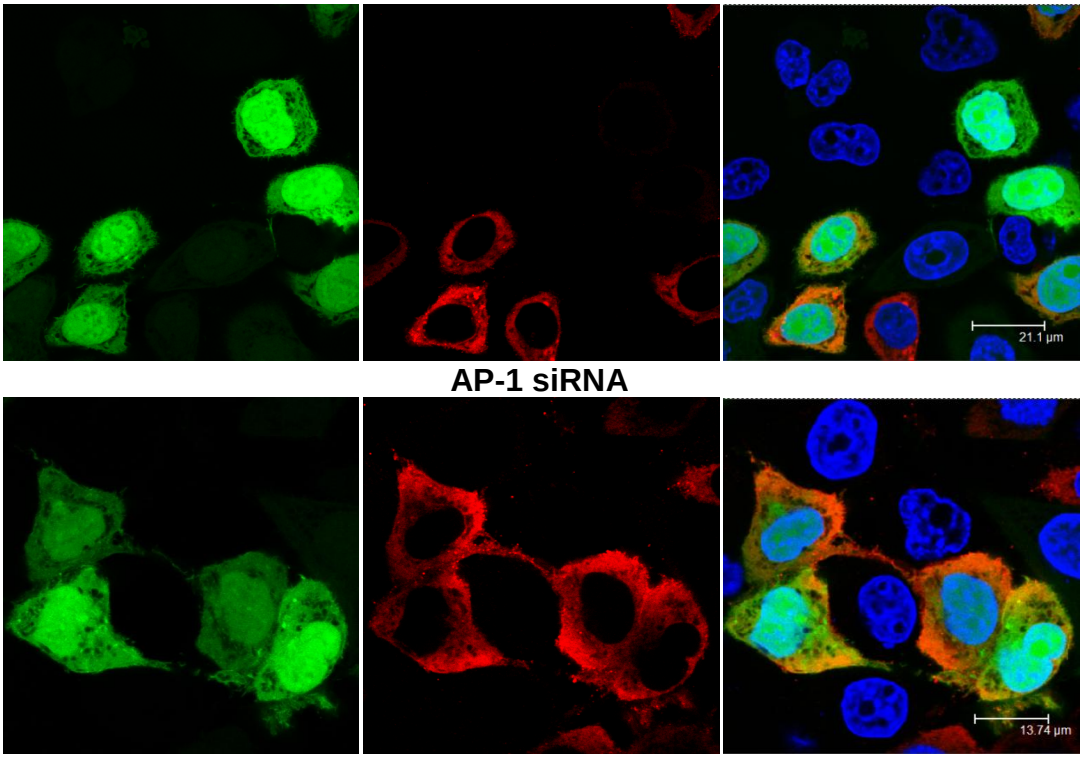

Figure 106: Confocal microscopy of HeLa cells co-transfected with HIV-1 provirus and pcDNA GFP in the presence and absence of AP-1 siRNA. GFP expression is shown in green, HIV-1 Gag is expressed in red and cell nuclei are stained with DAPI (blue).

GFP expression was similar between AP-1 siRNA and mock-treated cells, confirming that AP-1 knockdown does not affect GFP expression. However, HIV-1 Gag staining was reduced in AP-1 knockdown cells compared to mock-treated cells, indicating that AP-1 is important for HIV-1 Gag expresssion specifically.

6.2.8 Monitoring temporal Gag localisation

Confocal microscopy could be used to visualise HIV Gag expression and cellular localisation at various time points during the virus replication cycle. The expression of HIV-1/2 Gag was monitored at 24 h and 40 h post provirus transfection in HeLa cells to assess whether differences in Gag appearance could be observed at different times post-transfection. Cells were fixed,

stained with DAPI and antibodies to HIV-1 Gag p24/HIV-2 Gag p27, and viewed using a confocal microscope [figure 107].

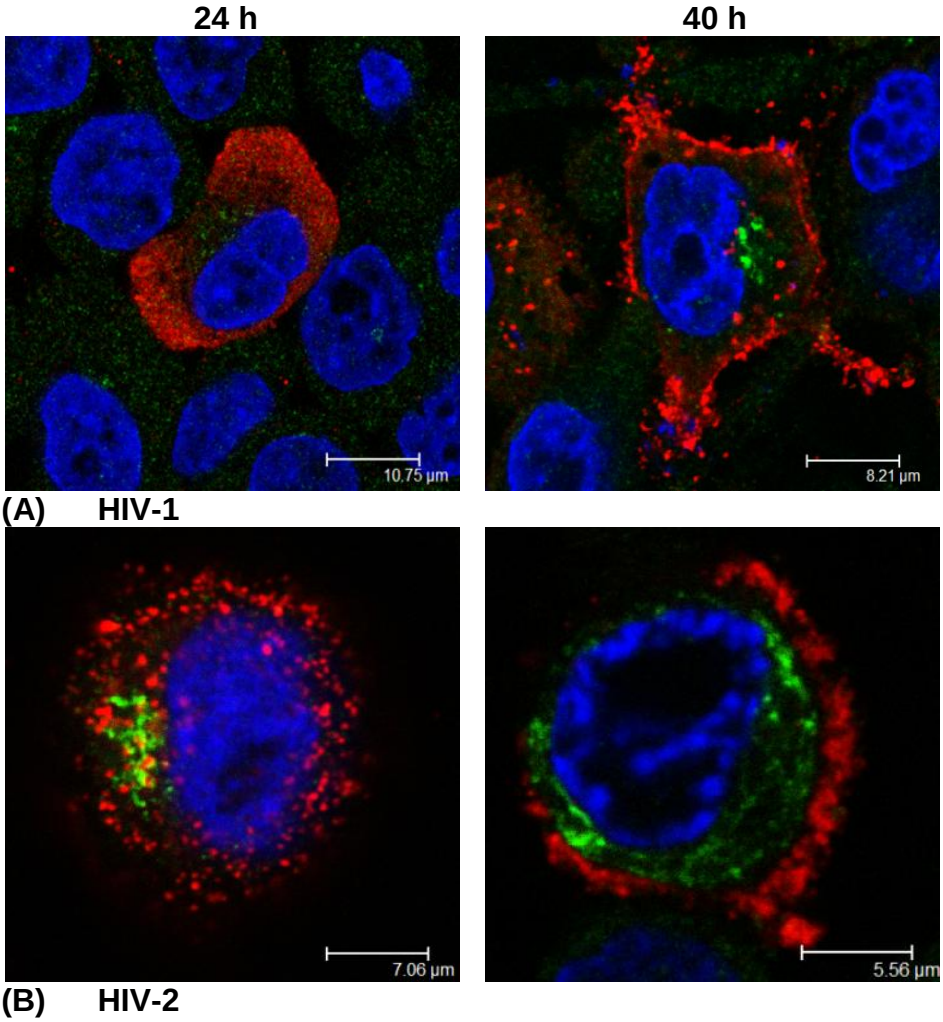

Figure 107: Confocal microscope images of HIV-1/2 Gag expressed from provirus transfection at 24 h and 40 h post-transfection. Cell nuclei are stained with DAPI (blue), cellular AP-1 is shown in green and HIV-1/2 Gag is shown in red.

Differences in HIV-1/2 Gag appearance and localisation could be seen at 24 h and 40 h post-transfection. At 24 h, extensive HIV-1 Gag expression was seen throughout the cell with some localisation to the plasma membrane. By 40 h, almost all cellular HIV-1 Gag was localised at the cellular membrane with evidence of extracellular Gag beyond the plasma membrane. This potentially represents HIV-1 Gag within budding viral particles or particles released by viral-mediated cell lysis. Initially, at 24 h, HIV-2 Gag expression was less extensive within the cell than HIV-1. By 40 h, most of the HIV-2 Gag had localised to the plasma membrane and was more reminiscent of HIV-1

Gag staining at 24 h. This may reflect the slower rate of HIV-2 Gag expression.

6.3 Discussion

Confocal microscopy was carried out to visualise the impact of AP-1 knockdown on HIV-1/2 Gag levels. Initial experiments confirmed that we were able to knock down AP-1 using siRNA and, importantly, detect AP-1 deficient cells by confocal microscopy. Knockdown of AP-1 was not complete as some cells maintained AP-1 expression. This is most likely due to less than 100% transfection efficiency. However, we were able to observe many cells in which AP-1 expression was severely reduced.

Staining of HIV-1/2 Gag produced differing patterns. Prevalent HIV-1 Gag staining was seen throughout the cell and, in particular, staining localised to the plasma membrane. Observations of HIV-1 Gag report that it accumulates both at the plasma membrane (representing sites of viral assembly) and within internal cellular compartments resembling late endosomes (Gousset *et al.*, 2008). Our observations of HIV-1 Gag support this. HIV-2 Gag produced a more punctate and dispersed staining pattern of lower intensity than HIV-1. Whereas HIV-1 Gag formed large clusters along the inside edge of the plasma membrane, HIV-2 Gag only formed isolated patches at the plasma membrane. HIV-1 transcription (Chapter 3) and Gag translation (Chapter 4) was shown to be more efficient than for HIV-2. Thus, it was expected that HIV-1 provirus transfection would result in a higher Gag expression level within the cell than HIV-2. Likewise, if the HIV-1 life cycle progresses more rapidly than HIV-2 (as suggested by results on nuclear export in Chapter 3), this may cause HIV-1 Gag to accumulate at the plasma membrane more quickly than HIV-2 Gag. Indeed, at 40 h post-transfection HIV-2 Gag staining showed more localisation to the plasma membrane and was more equivalent to the HIV-1 staining pattern evidenced at 24 h.

However, in addition to variations in transcription and translation efficiency, differences in Gag trafficking between HIV-1 and HIV-2 may also account for differences in the cellular localisation of HIV-1/2 Gag. Differences within the HIV-1 and HIV-2 Gag matrix (MA) region may alter cellular trafficking. The N-

terminus of the Gag MA region contains a myristyl group (myr) that has two conformations; exposed or sequestered. Gag binding to the plasma membrane is mediated by exposure of the myr group which engages with the interior of the plasma membrane (Waheed and Freed, 2009). The myr group of HIV-2 MA has been shown to be more tightly sequestered than the myr group of HIV-1 MA. Likewise, conformational switching of HIV-2 myr is less sensitive than for HIV-1 (Saad *et al.*, 2008). This may account for the observation that HIV-2 Gag proteins form a less stable association with the plasma membrane than HIV-1 Gag (Morikawa *et al.*, 2007). Importantly, sequestering of myr may hinder HIV-2 Gag assembly and consequently contribute to the slow and inefficient localisation of HIV-2 to the plasma membrane which we observed by confocal microscopy.

Additionally, targeting of Gag to the plasma membrane is aided by $PI(4,5)P_2$ recognition of the Gag MA domain. $PI(4,5)P_2$ binds to MA and triggers a conformational change which exposes myr, facilitating membrane binding (Saad *et al.*, 2008). Variations within HIV-1/2 MA may thus alter this interaction with $PI(4,5)P_2$, and account for the slower, less efficient HIV-2 Gag trafficking through the cell. If HIV-2 MA is unable to engage easily with $PI(4,5)P_2$, HIV-2 Gag molecules may be diverted during trafficking by loss of this association or, alternatively, may traffic via a different route to the plasma membrane. This could account for the slower localisation of HIV-2 Gag to the plasma membrane which we observed.

It was ascertained that both HIV-1/2 Gag and AP-1 could be co-stained within the cell and viewed concurrently by confocal microscopy. As expected, AP-1 staining localised to a discrete perinuclear structure, likely representing the TGN, and to cytoplasmic vesicles, most probably reflecting cytoplasmic endosomes. Although HIV-1 Gag is reported to interact with AP-1, surprisingly we did not observe co-localisation beween AP-1 and HIV-1/2 Gag by confocal microscopy. This may be due to the transient nature of this interaction. Trafficking is a dynamic cellular process; cellular vesicles are rapidly formed, transported to target membranes, and disassembled. Likewise, efficient cellular trafficking is important to ensure that this is not a rate limiting stage of cellular pathways. Consequently, movement of Gag

molecules through the cell may occur very quickly. Therefore the interaction between HIV Gag molecules and AP-1 may occur within such a short time frame that it was not easy to observe this process by confocal microscopy.

A western blot of lysates from HIV provirus transfected cells pre-treated with AP-1 siRNA showed reduced levels of both HIV-1 and HIV-2 Gag. Confocal microscopy was used to gain more insight into these results by permitting visualisation of AP-1 and Gag levels within individual cells. These experiments showed that cells in which AP-1 expression was significantly reduced by siRNA treatment also had severely reduced levels of HIV-1 or HIV-2 Gag staining. Control experiments using GFP showed that AP-1 knockdown did not affect cell viability or indeed the level of GFP expression, suggesting that the observed reduction of HIV-1/2 Gag levels was not due to non-specific effects of AP-1 siRNA on gene expression or cell growth.

Whilst AP-1 knockdown has previously been shown to affect HIV-1 budding from cells (Camus *et al.*, 2007), this experiment provides the first indication that AP-1 is required for Gag expression or stability. At this stage it is not possible to tell whether AP-1 is required for Gag synthesis or whether AP-1 knockdown results in rapid turnover of Gag. Metabolic labelling pulse-chase immunoprecipitation experiments, in which newly synthesised proteins are labelled with ^{35}S for a short time, may allow us to discern whether AP-1 siRNA treatment reduces the amount of Gag synthesised in the pulse period or increases the rate of Gag turnover in the chase period.

Following Gag synthesis, transport of Gag molecules away from their site of synthesis may be required to permit more Gag translation to occur. High concentrations of Gag have been shown to inhibit the translation of HIV-1 (Anderson and Lever, 2006). Therefore HIV-1 Gag synthesis may be reliant on the transport of Gag away from its site of synthesis to prevent the build-up of Gag in the vicinity of translating mRNA from inhibiting translation. Proteins such as AP-1, which are propsed to mediate Gag trafficking, may consequently play an additional role in the viral life cycle: regulating the rate of Gag translation.

Finally, down-regulation of AP-1 may induce the down-regulation of HIV Gag proteins via degradation. HIV Gag has been shown to localise to MVBs or late endosomes. If AP-1 is unable to faciliate the subsequent transport of Gag molecules to the plasma membrane, Gag may become sequestered into MVBs. This protein sorting failure may result in fusion of the MVB with the lysosome and subsequent degradation of Gag by lysosomal proteases. Alternatively, in the absence of AP-1, misdirected Gag may target to aberrant cellular locations resulting in subsequent degradation. Ubiquitylation provides a sorting signal for both MVB and the proteasome (Katzmann *et al.*, 2001). As HIV Gag also appears to target to MVBs, in the absence of AP-1, a similar signalling mechanism may result in Gag mistargetting to the proteasome. As a result, AP-1 may be important in ensuring Gag stability by prompting its efficient transport to viral assembly sites at the plasma membrane.

6.3.1 Future work

Previous AP-1 knockdown experiments have resulted in conflicting results. Following AP-1 shutdown, cargo proteins were shown to accumulate in the Golgi, at the plasma membrane or in endosomal/post-endosomal compartments. Additional difficulties in knockdown experiments can arise due to the longevity of AP-1 proteins. Existing AP-1 proteins may remain in the cell for several days after the knockdown event, and therefore continue to undertake cargo protein transport albeit at a reduced rate. Furthermore, removing one protein from the cellular trafficking pathways may induce compensatory measures by other trafficking proteins or pathways. Alternatively, the components of other trafficking pathways may be transported via AP-1; the resulting protein deficit may thus effect a down-regulation in other trafficking pathways as a consequence of inhibiting AP-1 transport (Robinson *et al.*, 2010).

Consequently, additional trafficking pathways may require monitoring to, firstly, see whether these compensate when AP-1 trafficking is shutdown and, secondly, assess how this impacts HIV-1/2 Gag trafficking. Further work is required to better understand the role of AP-1 in cellular transport and elucidate how this impacts HIV replication via AP-1 interactions with Gag.

Likewise, determining whether AP-1 imparts regulatory control over Gag synthesis or Gag degradation may highlight a useful inhibitory step within the life cycle of HIV.

Monitoring the cellular localisation of HIV-1/2 Gag at short intervals post-transfection would provide a more detailed, temporal assessment of Gag localisation within the cell. Combining these observations with co-localisation experiments using markers of cellular trafficking may provide a better overview of HIV-1/2 Gag trafficking mechanisms. This would allow for a more detailed comparison of HIV-1/2 Gag transport mechanisms.

Any differences in Gag trafficking mechanisms may contribute to the lower replication efficiency of HIV-2. Overall, additional work is necessary to clarify the routes of HIV-1/2 Gag transport within the cell and determine how AP-1 alters both HIV-1 and HIV-2 Gag expression levels.

CHAPTER 7: CONCLUSIONS AND FUTURE WORK

The work presented in this thesis investigates several avenues by which HIV-1 and HIV-2 Gag gene expression differ. In this last chapter, I will summarise the conclusions from these studies and highlight future work which could proceed from our conclusions. I will also describe how the work of this thesis fits in with current views and emphasize the areas in which it has expanded on our current knowledge.

7.1 HIV gag transcription and nuclear export

a) The level of HIV-1/2 gag mRNA transcribed from provirus transfections of HeLa cells was quantified by qPCR. HIV-1 transcription was shown to be more efficient than HIV-2 transcription. This resulted in higher levels of HIV-1 gag mRNA than for HIV-2. The stability of HIV-1/2 gag mRNA was not responsible for the difference in HIV-1/2 RNA levels.

b) Nuclear and cytoplasmic levels of HIV-1/2 gag mRNA were compared at several time points following provirus transfection into HeLa cells. The rate of HIV-1 gag mRNA export from the nucleus was more efficient than for HIV-2. This resulted in a quicker accumulation of HIV-1 gag mRNA in the cytoplasm and a more rapid decrease in nuclear HIV-1 gag mRNA levels following an initial period of synthesis. HIV-2 gag mRNA levels were slow to accumulate in the nucleus and equally slow at appearing in the cytoplasm indicating that both HIV-2 transcription and export were inefficient. Cytoplasmic HIV-1/2 gag mRNA was shown to have a comparable stability, affirming that differences in cytoplasmic gag mRNA levels were due to inefficient HIV-2 export.

c) Future work will look to control for additional factors affecting cellular gag mRNA levels, such as the incorporation of viral mRNA into virions. Likewise, calculating the actual number of RNA copies within sub-cellular fractions will provide a more accurate assessment of HIV-1/2 transcription rates. The factors involved in more efficient HIV-1 mRNA transcription and nuclear export remain to be uncovered, in addition to elucidating how these factors affect the mechanisms of HIV-1/2 transcription and export differently.

d) Finally, investigations are currently underway to investigate the contribution of a spliced HIV-2 gag transcript to sub-cellular mRNA pools. Identifying whether the singly-spliced HIV-2 gag transcript is preferentially exported from the nucleus over unspliced transcripts may suggest a mechanism by which HIV-2 counteracts the inefficient export of its full-length mRNA.

7.2 HIV Gag translation

a) Translation of HIV-1 gag RNA was shown to be more efficient than HIV-2 gag RNA *in vitro* and in HeLa, COS-1 and Jurkat cells. Neither the presence of viral proteins nor the stability of HIV-1/2 RNA was shown to affect HIV-1/2 translation rates differently.

b) Initiation of translation for both HIV-1 and HIV-2 was shown to be primarily cap-dependent. Shut down of cap-dependent translation by poliovirus infection severely reduced the translation of both HIV-1 and HIV-2 Gag. Uncapped HIV-1/2 RNAs also demonstrated a reduced translational capability. No additional translation of Gag isoforms was evidenced from internal AUGs to compensate for the shut-down of cap-dependent translation. IRES-driven activity was therefore not evidenced as a means to initiate translation from either HIV-1 or HIV-2 RNAs.

c) The lengthier 5’ UTR of HIV-2 was shown to be intrinsically more structured than the shorter HIV-1 5’ UTR. A more negative folding energy and folding energy per nucleotide was calculated for the HIV-2 5’ UTR when compared to the HIV-1 5’ UTR. The HIV-2 TAR structure, shown to contain a high level of G-C base pairing, was partly responsible for the higher folding energy of HIV-2. An enhanced level of structure within the HIV-2 5’ UTR is therefore thought to impair ribosomal scanning and hinder the rate of cap-dependent translation initiation for HIV-2.

d) When the TAR structure was deleted from both HIV-1 and HIV-2 5’ UTRs, surprisingly the translation rate of both HIV-1 and HIV-2 gag RNA decreased in HeLa cells and BSRT7 cells. This was not due to an enhanced ΔTAR RNA degradation rate. The down-regulation of PKR (which inhibits translation by

phosphorylating eIF2) by TAR was proposed to account for decreased translatability of RNAs in the absence of TAR. Further investigations into the phosphorylation status of eIF2 within these experiments may confirm whether this is, in fact, the case.

e) A comparison of codon bias and codon pair bias within the HIV-1 and HIV-2 Gag ORFs found that these did not vary sufficiently to cause differences in HIV-1/2 Gag elongation. Therefore the slower rate of HIV-2 translation is unlikely to be due to a reduced elongation rate relative to HIV-1.

f) The importance of cap-dependent ribosomal scanning or IRES-driven activity to the translation of HIV proteins remains a divisive issue. Although we find no evidence for IRES activity, and all of our results implicate cap-dependent translation, further work into the conditions and factors necessary to stimulate HIV translation may enable a conclusion to this debate. Deconstructing the necessary components for HIV translation therefore remains the focus of contemporary work in this field. We have shown that HIV-2 translation may be impaired by extensive 5' structure hindering ribosomal scanning. However, factors such as the efficiency of cellular helicases, additional structure within the 5' UTR, viral or cellular RNA-binding proteins, the cellular environment and the role of splicing may further contribute to the translational difference between HIV-1/2 RNAs and therefore provide areas for further investigation.

7.3 HIV RNA-protein interactions

a) UV cross-linking experiments identified a 45 kDa protein from HeLa cells which binds specifically to the HIV-1 5' UTR but not to the HIV-2 5' UTR. Non-specific competitors were unable to reduce binding of this protein whereas an unlabelled HIV-1 5' UTR competitor reduced binding. Although this protein does not bind to HIV-2 5' UTR RNA, it binds weakly to HIV-2 5' UTR-gag RNA suggesting additional binding sites within gag or a reliance on a structural conformation involving the *gag* coding region. The absence of this protein binding to the 5' UTR of HIV-2, and the weaker interaction with HIV-2 5' UTR-gag RNA, may highlight a mechanism to account for the less efficient transcription or translation reported for HIV-2 in Chapters 3 and 4

respectively. Additional proteins around 120 and 130 kDa in size were shown to bind with opposing affinities to the HIV-1/2 5' UTR. The identity and role of these RNA-protein interactions remains unknown and is therefore an avenue for future work.

b) La autoantigen was a candidate for the 45 kDa protein binding to the HIV-1 5' UTR. However, La was shown to be larger than the 45 kDa protein. Whereas La binds to the poliovirus IRES (Meerovitch *et al.*, 1993), binding of the 45 kDa protein to the HIV-1 5' UTR was not reduced in the presence of a poliovirus IRES RNA competitor. Likewise, La is reported to bind to TAR (Chang *et al.*, 1994), yet the 45 kDa protein was able to bind to the HIV-1 5' UTR when TAR was deleted. La was also able to bind to the HIV-2 5' UTR whereas the 45 kDa protein was not. The conclusion from this work is that the 45 kDa protein is not La autoantigen.

c) Several attempts were made to isolate and identify the 45 kDa protein with limited success. Initial mass spectrometry results indicate that actin may be a candidate. Although not typically recognised for its role as an RNA-binding protein, actin is reported to interact with the negative-sense RNA genome of respiratory syncytial virus and enhance transcription (Harpen *et al.*, 2009). Current research has yet to identify actin binding to the HIV RNA genome, therefore further work is required to confirm this interaction and assess the implications for HIV.

d) Truncated HIV-1 5' UTR RNAs were used to narrow down the binding site of the 45 kDa protein. Studies with La revealed that TAR is not the binding site of the 45 kDa protein and preliminary results using truncated RNAs suggests that the 45 kDa protein binds to the 5' end of the HIV-1 5' UTR. Future work will endeavour to deduce the structural binding requirements of this protein and therefore fathom the role of this protein within the life cycle of HIV-1.

e) An obvious direction for future work is the identification of the 45 kDa protein binding to the HIV-1 5' UTR and the clarification of its function. Optimisation and scaling up of the RNA affinity chromatography protocol is the initial direction future work on this topic will take. Once successful, other

RNA-binding proteins, such as the 120 and 130 kDa proteins which also bind with different affinities to the HIV-1/2 5' UTRs, could be investigated. Additionally, the protein-binding profile of the HIV-1/2 5' UTR could be examined further using protein extract from HIV-infected cells. This may enable us to detect whether the presence of viral proteins affects cellular (or viral) protein interactions with the HIV-1/2 5' UTRs.

7.4 The effect of AP-1 on Gag protein levels

a) AP-1 knockdown was achieved in cells using siRNA and shown to result in a decrease in the expression levels of HIV-1/2 Gag.

b) Confocal microscopy showed AP-1 staining localised to perinuclear structures representing the *trans*-Golgi network and to cytoplasmic vesicles likely reflecting cytoplasmic endosomes. Visualisation of cellular HIV-1/2 Gag by confocal microscopy highlighted differences in the expression level of Gag. HIV-2 Gag was present in the cell at a lower level than HIV-1 Gag (likely a result of inefficient transcription, nuclear export and translation observed in Chapters 3 and 4) and did not localise to the plasma membrane as quickly as HIV-1 Gag. Despite reports of an interaction between HIV-1 and AP-1 (Camus *et al.*, 2007), we were unable to visualise HIV-1/2 Gag staining co-localising with AP-1 by confocal microscopy.

c) When AP-1 was shut down, the level of both HIV-1/2 Gag expressed within the cell was reduced. Even when AP-1 was not knocked down, cells which showed good expression of AP-1 demonstrated higher levels of HIV-1/2 Gag staining. Results therefore indicate that either AP-1 is required for Gag synthesis or that AP-1 is important for Gag stability.

d) Further work could take several directions. Determining the involvement of AP-1 in either Gag synthesis or Gag degradation may underline a previously unknown cellular mechanism by which Gag gene expression is regulated. Alternatively, the role of AP-1, and other cellular trafficking components, in delivering HIV Gag to sites of viral assembly have yet to be clearly defined. Monitoring the movement of HIV-1/2 Gag throughout the cell at short time

intervals may provide a clearer indication of the trafficking mechanisms employed by HIV-1 and HIV-2.

7.5 Discussion

In drawing together the results from this thesis it is now apparent that there are numerous ways in which the life cycles of HIV-1 and HIV-2 differ. Rather than a defining, critical step limiting the rate of HIV-2 replication, we have shown that the relative inefficient replicative capacity of HIV-2 compared to HIV-1 is likely to be due to differences at several stages of the life cycle. This work provides a comprehensive, but by no means exhaustive, insight into the rate limiting aspects of HIV-2 Gag expression as a basis to highlight the proficiency of the equivalent stages in the replication of HIV-1. It was hoped that in understanding what makes HIV-1 so formidable and devastating a virus, and equally establishing the areas where HIV-2 fails to be so effective, we may uncover novel targets or mechanisms by which to limit the replicative capacity of HIV-1.

We have shown that HIV-2 is less efficient than HIV-1 during stages of transcription, nuclear export and translation. Both HIV-1 and HIV-2 rely on cap-dependent translation initiation and differences in elongation are unlikely due to the similar codon composition of Gag. However, the lengthier and more structured HIV-2 5' UTR is likely to hinder ribosomal scanning and therefore restrict cap-dependent translation initiation for HIV-2. Novel and uncharacterised HIV RNA-protein interactions have also been identified between the HIV-1/2 5' UTRs which may contribute to transcriptional and translational variations between these two viruses. Taken together, it is therefore not surprising that fewer HIV-2 particles are produced during a HIV-2 infection due to the restrictions which appear to limit many stages of the HIV-2 replication cycle. Although it is well established that HIV-2 infections progress less severely than HIV-1, this work provides a more detailed insight into the causes for this. In better understanding the differences between these two viruses, we are now able to appreciate the ways in which these viruses can be limited at a molecular level; information which is vital for the

development of novel therapies or a protective vaccine to discourage infection by these viruses.

In conclusion, the main aim of this work: to identify and characterise differences in HIV-1/2 replication at the level of gag gene expression, has been achieved. Several differences in HIV-1 and HIV-2 gene expression have been identified and work has progressed to characterise these differences fully or in part. The particular focus of my work: to highlight potential differences between HIV-1/2 translation, has also been accomplished by establishing translation as a less efficient step for HIV-2 and determining that this is not due to initiation strategy or elongation but likely due to inefficient translation initiation. My work has helped to gain a greater understanding of the relationship between viral strategy and HIV-1/2 pathogenesis. Therefore it will hopefully provide a springboard for further work to better characterise these viruses in the hope that, by knowing HIV better, we may finally vanquish its threat to humanity.

REFERENCES

Abbink, T. E. M. and Berkhout, B. (2003). A novel long distance base-pairing interaction in human immunodeficiency virus type 1 RNA occludes the Gag start codon. *The Journal of Biological Chemistry*, **278**, 11601-11611.

Adachi, M., Ohhara, T., Kurihara, K., Tamada, T., Honjo, E., Okazaki, N., Arai, S., Shoyama, Y., Kimura, K., Matsumura, H., Sugiyama, S., Adachi, H., Takano, K., Mori, Y., Hidaka, K., Kimura, T., Hayashi, Y., Kiso, Y. and Kuroki, R. (2009). Structure of HIV-1 Protease in complex with potent inhibitor KNI-272 determined by high-resolution X-ray and neutron crystallography. *Proceedings of the National Academy of Sciences*, **106**, 4641–4646.

Agy, M. B., Sherbert, C. H. and Katze, M. G. (1996). Development of an *in vitro* mRNA degradation assay utilizing extracts from HIV-1- and SIV-infected cells. *Virology*, **217**, 158-166.

Ambrosi, A., Cattoglio, C. and Di Serio, C. (2008). Retroviral integration process in the human genome: is it really non-random? A new statistical approach. *PLoS Computational Biology*, **4**, e1000144.

Anderson, E. C. and Lever, A. M. L. (2006). Human immunodeficiency virus type 1 Gag polyprotein modulates its own translation. *The Journal of Virology*, **80**, 10478-10486.

Arhel, N. (2010). Revisiting HIV-1 uncoating. *Retrovirology*, **7**, 96.

Asai, K., Platt, C. and Cochrane, A. (2003). Control of HIV-1 env RNA splicing and transport: investigating the role of hnRNP A1 in exon splicing silencer (ESS3a) function. *Virology*, **314**, 229-242.

Auewarakul, P., Wacharapornin, P., Srichatrapimuk, S., Chutipongtanate, S. and Puthavathana, P. (2005). Uncoating of HIV-1 requires cellular activation. *Virology*, **337**, 93-101.

Ayukawa, K., Taniguchi, S. i., Masumoto, J., Hashimoto, S., Sarvotham, H., Hara, A., Aoyama, T. and Sagara, J. (2000). La autoantigen is cleaved in the COOH terminus and loses the nuclear localization signal during apoptosis. *The Journal of Biological Chemistry*, **275**, 34465-34470.

Barber, R. D., Harmer, D. W., Coleman, R. A. and Clark, B. J. (2005). GAPDH as a housekeeping gene: analysis of GAPDH mRNA expression in a panel of 72 human tissues. *Physiological Genomics*, **21**, 389-395.

Barre-Sinoussi, F., Chermann, J. C., Rey, F., Nugeyre, M. T., Chamaret, S., Gruest, J., Dauguet, C., Axler-Blin, C., Vezinet-Brun, F., Rouzioux, C., Rozenbaum, W. and Montagnier, L. (1983). Isolation of a T-lymphotropic retrovirus from a patient at risk for acquired immune deficiency syndrome (AIDS). *Science*, **220**, 868-871.

Basu, V. P., Song, M., Gao, L., Rigby, S. T., Hanson, M. N. and Bambara, R. A. (2008). Strand transfer events during HIV-1 reverse transcription. *Virus Research*, **134**, 19-38.

Batonick, M., Favre, M., Boge, M., Spearman, P., Höning, S. and Thali, M. (2005). Interaction of HIV-1 Gag with the clathrin-associated adaptor AP-2. *Virology*, **342**, 190-200.

Baudin, F., Marquet, R., Isel, C., Darlix, J. L., Ehresmann, B. and Ehresmann, C. (1993). Functional sites in the 5' region of human immunodeficiency virus type 1 RNA form defined structural domains. *The Journal of Molecular Biology*, **229**, 382-397.

Berkhout, B., Arts, K. and Abbink, T. E. M. (2011). Ribosomal scanning on the 5′-untranslated region of the human immunodeficiency virus RNA genome. *Nucleic Acids Research*, **39**, 5232-5244.

Berkhout, B. and van Wamel, J. L. (2000). The leader of the HIV-1 RNA genome forms a compactly folded tertiary structure. *RNA*, **6**, 282-295.

Bieniasz, P. D. (2009). The cell biology of HIV-1 virion genesis. *Cell Host and Microbe*, **5**, 550-558.

Blaak, H., van der Ende, M. E., Boers, P. H., Schuitemaker, H. and Osterhaus, A. D. (2006). In vitro replication capacity of HIV-2 variants from long-term aviremic individuals. *Virology*, **353**, 144-154.

Blazkova, J., Trejbalova, K., Gondois-Rey, F., Halfon, P., Philibert, P., Guiguen, A., Verdin, E., Olive, D., Van Lint, C., Hejnar, J. and Hirsch, I. (2009). CpG methylation controls reactivation of HIV from latency. *PLoS Pathogens*, **5**, e1000554.

Blissenbach, M., Grewe, B., Hoffmann, B., Brandt, S. and Uberla, K. (2010). Nuclear RNA export and packaging functions of HIV-1 Rev revisited. *The Journal of Virology*, **84**, 6598-6604.

Bohne, J., Wodrich, H. and Kräusslich, H. G. (2005). Splicing of human immunodeficiency virus RNA is position-dependent suggesting sequential removal of introns from the 5′ end. *Nucleic Acids Research*, **33**, 825-837.

Bousquet, L., Pruvost, A., Didier, N., Farinotti, R. and Mabondzo, A. (2008). Emtricitabine: inhibitor and substrate of multidrug resistance associated protein. *European Journal of Pharmaceutical Sciences*, **35**, 247-256.

Braddock, M., Powell, R., Blanchard, A. D., Kingsman, A. J. and Kingsman, S. M. (1993). HIV-1 TAR RNA-binding proteins control TAT activation of translation in Xenopus oocytes. *The FASEB Journal*, **7**, 214-222.

Brady, J. and Kashanchi, F. (2005). Tat gets the "green" light on transcription initiation. *Retrovirology*, **2**, 69.

Brasey, A., Lopez-Lastra, M., Ohlmann, T., Beerens, N., Berkhout, B., Darlix, J. L. and Sonenberg, N. (2003). The leader of human immunodeficiency virus type 1 genomic RNA harbors an internal ribosome entry segment that is active during the G2/M phase of the cell cycle. *The Journal of Virology*, **77**, 3939-3949.

Brenchley, J. M., Price, D. A. and Douek, D. C. (2006). HIV disease: fallout from a mucosal catastrophe? *Nature Immunology*, **7**, 235-239.

Briggs, J. A. G., Grünewald, K., Glass, B., Förster, F., Kräusslich, H. G. and Fuller, S. D. (2006). The mechanism of HIV-1 core assembly: insights from three-dimensional reconstructions of authentic virions. *Structure*, **14**, 15-20.

Broder, S. (2010). The development of antiretroviral therapy and its impact on the HIV-1/AIDS pandemic. *Antiviral Research*, **85**, 1-18.

Buck, C. B., Shen, X., Egan, M. A., Pierson, T. C., Walker, C. M. and Siliciano, R. F. (2001). The human immunodeficiency virus type 1 *gag* gene encodes an internal ribosome entry site. *The Journal of Virology*, **75**, 181-191.

Buonaguro, L., Tornesello, M. L. and Buonaguro, F. M. (2007). Human immunodeficiency virus type 1 subtype distribution in the worldwide epidemic: pathogenetic and therapeutic implications. *The Journal of Virology*, **81**, 10209-10219.

Cameron, C. E., Ghosh, M., Le Grice, S. F. J. and Benkovic, S. J. (1997). Mutations in HIV Reverse transcriptase which alter RNase H activity and decrease strand transfer efficiency are suppressed by HIV Nucleocapsid protein. *Proceedings of the National Academy of Sciences*, **94**, 6700-6705.

Camus, G., Segura-Morales, C., Molle, D., Lopez-Verges, S., Begon-Pescia, C., Cazevieille, C., Schu, P., Bertrand, E., Berlioz-Torrent, C. and Basyuk, E. (2007). The clathrin adaptor complex AP-1 binds HIV-1 and MLV Gag and facilitates their budding. *Molecular Biology of the Cell*, **18**, 3193-3203.

Cannon, P. M., Matthews, S., Clark, N., Byles, E. D., Iourin, O., Hockley, D. J., Kingsman, S. M. and Kingsman, A. J. (1997). Structure-function studies of the human immunodeficiency virus type 1 Matrix protein, p17. *The Journal of Virology*, **71**, 3474-3483.

Chan, D. C. and Kim, P. S. (1998). Review: HIV entry and its inhibition. *Cell*, **93**, 681-684.

Chang, Y. N., Kenan, D. J., Keene, J. D., Gatignol, A. and Jeang, K. T. (1994). Direct interactions between autoantigen La and human immunodeficiency virus leader RNA. *The Journal of Virology*, **68**, 7008-7020.

Chen, J., Pathak, V. K., Peng, W. and Hu, W. S. (2008). Capsid proteins from human immunodeficiency virus type 1 and simian immunodeficiency virus SIVmac can coassemble into mature cores of infectious viruses. *The Journal of Virology*, **82**, 8253-8261.

Chen, Z., Luckay, A., Sodora, D. L., Telfer, P., Reed, P., Gettie, A., Kanu, J. M., Sadek, R. F., Yee, J., Ho, D. D., Zhang, L. and Marx, P. A. (1997). Human immunodeficiency virus type 2 (HIV-2) seroprevalence and characterization of a distinct HIV-2 genetic subtype from the natural range of simian immunodeficiency virus-infected sooty mangabeys. *The Journal of Virology*, **71**, 3953-3960.

Cheung, P., Zhang, M., Yuan, J., Chau, D., Yanagawa, B., McManus, B. and Yang, D. (2002). Specific interactions of HeLa cell proteins with

Coxsackievirus B3 RNA: La autoantigen binds differentially to multiple sites within the 5' untranslated region. *Virus Research*, **90**, 23-36.

Chevret, S., Costagliola, D., Lefrere, J. J. and Valleron, A. J. (1992). A new approach to estimating AIDS incubation times: results in homosexual infected men. *The Journal of Epidemiology and Community Health*, **46**, 582-586.

Clavel, F., Guétard, D., Brun-Vézinet, F., Chamaret, S., Rey, M. A., Santos-Ferreira, M. O., Laurent, A. G., Dauguet, C., Katlama, C., Rouzioux, C., Klatzmann, D., Champalimaud, J. L. and Montagnier, L. (1986). Isolation of a new human retrovirus from West African patients with AIDS. *Science*, **233**, 343-346.

Clavel, F. and Mammano, F. (2010). Review: role of Gag in HIV resistance to Protease inhibitors. *Viruses*, **7**, 1411-1426.

Coffin, J., Haase, A., Levy, J. A., Montagnier, L., Oroszlan, S., Teich, N., Temin, H., Toyoshima, K., Varmus, H. and Vogt, P. (1986). What to call the AIDS virus? *Nature*, **321**, 1-7.

Coffin, J. M. (1995). HIV population dynamics in vivo: implications for genetic variation, pathogenesis, and therapy. *Science*, **267**, 483-489.

Coffin, J. M., Hughes, S. H. and Varmus, H. E. (1997). Retroviruses.: (Cold Spring Harbor Laboratory Press).

Cole, J. L. (2007). Activation of PKR: an open and shut case? *Trends in Biochemical Sciences*, **32**, 57-62.

Coleman, J. R., Papamichail, D., Skiena, S., Futcher, B., Wimmer, E. and Mueller, S. (2008). Virus attenuation by genome-scale changes in codon pair bias. *Science*, **320**, 1784-1787.

Craigie, R. (2001). HIV Integrase, a brief overview from chemistry to therapeutics. *The Journal of Biological Chemistry*, **276**, 23213-23216.

Cullen, B. R. (2000). Nuclear RNA export pathways. *Molecular and Cellular Biology*, **20**, 4181-4187.

Das, A. T., Klaver, B., Klasens, B. I., van Wamel, J. L. and Berkhout, B. (1997). A conserved hairpin motif in the R-U5 region of the human

immunodeficiency virus type 1 RNA genome is essential for replication. *The Journal of Virology*, **71**, 2346-2356.

Das, S. and Maitra, U. (2001). Functional significance and mechanism of eIF5-promoted GTP hydrolysis in eukaryotic translation initiation. *Progress in Nucleic Acid Research and Molecular Biology*, **70**, 207-231.

Daugas, E., Rougier, J. P. and Hill, G. (2005). HAART-related nephropathies in HIV-infected patients. *Kidney International*, **67**, 393-403.

Dayton, A. (2004). Within you, without you: HIV-1 Rev and RNA export. *Retrovirology*, **1**, 35.

de Béthune, M. P. (2010). Non-nucleoside Reverse transcriptase inhibitors (NNRTIs), their discovery, development, and use in the treatment of HIV-1 infection: A review of the last 20 years (1989-2009). *Antiviral Research*, **85**, 75-90.

de Silva, T. I., Cotten, M. and Rowland-Jones, S. L. (2008). HIV-2: the forgotten AIDS virus. *Trends in Microbiology*, **16**, 588-595.

Dillon, P. J., Nelbock, P., Perkins, A. and Rosen, C. A. (1990). Function of the human immunodeficiency virus types 1 and 2 Rev proteins is dependent on their ability to interact with a structured region present in *env* gene mRNA. *The Journal of Virology*, **64**, 4428-4437.

Dimmock, N. J., Easton, A. J. and Leppard, K. N. (2001). Introduction to modern virology: (Blackwell Publishing).

Dirac, A. M. G., Huthoff, H., Kjems, J. and Berkhout, B. (2001). The dimer initiation site hairpin mediates dimerization of the human immunodeficiency virus, type 2 RNA genome. *The Journal of Biological Chemistry*, **276**, 32345-32352.

Dobrikova, E. Y., Grisham, R. N., Kaiser, C., Lin, J. and Gromeier, M. (2006). Competitive translation efficiency at the picornavirus type 1 internal ribosome entry site facilitated by viral *cis* and *trans* factors. *The Journal of Virology*, **80**, 3310-3321.

Dong, X., Li, H., Derdowski, A., Ding, L., Burnett, A., Chen, X., Peters, T. R., Dermody, T. S., Woodruff, E., Wang, J. J. and Spearman, P. (2005). AP-3 directs the intracellular trafficking of HIV-1 Gag and plays a key role in particle assembly. *Cell*, **120**, 663-674.

Dorman, N. and Lever, A. (2000). Comparison of viral genomic RNA sorting mechanisms in human immunodeficiency virus type 1 (HIV-1), HIV-2, and moloney murine leukemia virus. *The Journal of Virology*, **74**, 11413-11417.

Dugré-Brisson, S., Elvira, G., Boulay, K., Chatel-Chaix, L., Mouland, A. J. and DesGroseillers, L. (2005). Interaction of Staufen1 with the 5′ end of mRNA facilitates translation of these RNAs. *Nucleic Acids Research*, **33**, 4797-4812.

Dulude, D., Théberge-Julien, G., Brakier-Gingras, L. and Heveker, N. (2008). Selection of peptides interfering with a ribosomal frameshift in the human immunodeficiency virus type 1. *RNA*, **14**, 981-991.

Duvall, M. G., Jaye, A., Dong, T., Brenchley, J. M., Alabi, A. S., Jeffries, D. J., van der Sande, M., Togun, T. O., McConkey, S. J., Douek, D. C., McMichael, A. J., Whittle, H. C., Koup, R. A. and Rowland-Jones, S. L. (2006). Maintenance of HIV-specific CD4+ T cell help distinguishes HIV-2 from HIV-1 infection. *The Journal of Immunology*, **176**, 6973-6981.

Elliott, D. and Ladomery, M. (2010). Molecular biology of RNA: (Oxford Unviersity Press).

Forsman, A. and Weiss, R. A. (2008). Why is HIV a pathogen? *Trends in Microbiology*, **16**, 555-560.

Foster, J. L. and Garcia, J. V. (2008). HIV-1 Nef: at the crossroads. *Retrovirology*, **5**, 84.

Fouchier, R. A. M., Meyer, B. E., Simon, J. H. M., Fischer, U., Albright, A. V., Gonzalez-Scarano, F. and Malim, M. H. (1998). Interaction of the human immunodeficiency virus type 1 Vpr protein with the nuclear pore complex. *The Journal of Virology*, **72**, 6004-6013.

Freed, E. O. (2001). HIV-1 replication. *Somatic Cell and Molecular Genetics*, **26**, 13-33.

Fujinaga, K., Taube, R., Wimmer, J., Cujec, T. P. and Peterlin, B. M. (1999). Interactions between human cyclin T, Tat, and the transactivation response element (TAR) are disrupted by a cysteine to tyrosine substitution found in mouse cyclin T. *Proceedings of the National Academy of Sciences*, **96**, 1285-1290.

Gale, M. J., Tan, S. L. and Katze, M. G. (2000). Translational control of viral gene expression in eukaryotes. *Microbiology and Molecular Biology Reviews*, **64**, 239-280.

Gallo, R. C., Salahuddin, S. Z., Popovic, M., Shearer, G. M., Kaplan, M., Haynes, B. F., Palker, T. J., Redfield, R., Oleske, J. and Safai, B. (1984). Frequent detection and isolation of cytopathic retroviruses (HTLV-III) from patients with AIDS and at risk for AIDS. *Science*, **224**, 500-503.

Ganser-Pornillos, B. K., Yeager, M. and Sundquist, W. I. (2008). The structural biology of HIV assembly. *Current Opinion in Structural Biology*, **18**, 203-217.

García-Martínez, L. F., Mavankal, G., Peters, P., Wu-Baer, F. and Gaynor, R. B. (1995). Tat functions to stimulate the elongation properties of transcription complexes paused by the duplicated TAR RNA element of human immunodeficiency virus 2. *The Journal of Molecular Biology*, **254**, 350-363.

Gartner, S., Markovits, P., Markovitz, D. M., Kaplan, M. H., Gallo, R. C. and Popovic, M. (1986). The role of mononuclear phagocytes in HTLV-III/LAV infection. *Science*, **233**, 215-219.

Gatignol, A., Laine, S. and Clerzius, G. (2005). Dual role of TRBP in HIV replication and RNA interference: viral diversion of a cellular pathway or evasion from antiviral immunity? *Retrovirology*, **2**, 65.

Gaudin, C., Mazauric, M. H., Traïkia, M., Guittet, E., Yoshizawa, S. and Fourmy, D. (2005). Structure of the RNA signal essential for translational frameshifting in HIV-1. *The Journal of Molecular Biology*, **349**, 1024-1035.

Glaser, W., Triendl, A. and Skern, T. (2003). The processing of eIF4GI by human rhinovirus type 2 2Apro: relationship to self-cleavage and role of zinc. *The Journal of Virology*, **77**, 5021-5025.

Gottlieb, M. S., Schroff, R., Schanker, H. M., Weisman, J. D., Fan, P. T., Wolf, R. A. and Saxon, A. (1981). Pneumocystis carinii pneumonia and mucosal candidiasis in previously healthy homosexual men. *New England Journal of Medicine*, **305**, 1425-1431.

Gousset, K., Ablan, S. D., Coren, L. V., Ono, A., Soheilian, F., Nagashima, K., Ott, D. E. and Freed, E. O. (2008). Real-time visualization of HIV-1 Gag trafficking in infected macrophages. *PLoS Pathogens*, **4**, e1000015.

Harpen, M., Barik, T., Musiyenko, A. and Barik, S. (2009). Mutational analysis reveals a noncontractile but interactive role of actin and profilin in viral RNA-dependent RNA synthesis. *The Journal of Virology*, **83**, 10869-10876.

Harris, R. S. and Liddament, M. T. (2004). Retroviral restriction by APOBEC proteins. *Nature Reviews Immunology*, **4**, 868-877.

Haubrich, R., Gubernick, S., Yasothan, U. and Kirkpatrick, P. (2008). Etravirine. *Nature Reviews Drug Discovery*, **7**, 287-288.

Hauser, H., Lopez, L., Yang, S., Oldenburg, J., Exline, C., Guatelli, J. and Cannon, P. (2010). HIV-1 Vpu and HIV-2 Env counteract BST-2/tetherin by sequestration in a perinuclear compartment. *Retrovirology*, **7**, 51.

Herbreteau, C. H., Weill, L., Decimo, D., Prevot, D., Darlix, J. L., Sargueil, B. and Ohlmann, T. (2005). HIV-2 genomic RNA contains a novel type of IRES located downstream of its initiation codon. *Nature Structural and Molecular Biology*, **12**, 1001-1007.

Ho, D. D., Neumann, A. U., Perelson, A. S., Chen, W., Leonard, J. M. and Markowitz, M. (1995). Rapid turnover of plasma virions and CD4 lymphocytes in HIV-1 infection. *Nature*, **373**, 123-126.

Hocine, S., Singer, R. H. and Grünwald, D. (2010). RNA processing and export. *Cold Spring Harbor Perspectives in Biology*, **2**.

Imamichi, T., Conrads, T. P., Zhou, M., Liu, Y., Adelsberger, J. W., Veenstra, T. D. and Lane, H. C. (2005). A transcription inhibitor, actinomycin D, enhances HIV-1 replication through an interleukin-6-dependent pathway. *The Journal of Acquired Immune Deficiency Syndromes*, **40**.

Isel, C., Ehresmann, C. and Marquet, R. (2010). Review: initiation of HIV reverse transcription. *Viruses*, ***2***, 213-243.

Jacob, D. T. and DeStefano, J. J. (2008). A new role for HIV Nucleocapsid protein in modulating the specificity of plus strand priming. *Virology*, **378**, 385-396.

Jang, S. K., Krausslich, H. G., Nicklin, M. J., Duke, G. M., Palmenberg, A. C. and Wimmer, E. (1988). A segment of the 5' nontranslated region of

encephalomyocarditis virus RNA directs internal entry of ribosomes during in vitro translation. *The Journal of Virology*, **62**, 2636-2643.

Jolly, C. and Sattentau, Q. J. (2007). Human immunodeficiency virus type 1 assembly, budding, and cell-cell spread in T-cells take place in tetraspanin-enriched plasma membrane domains. *The Journal of Virology*, **81**, 7873-7884.

Jolly, C. and Sattentau, Q. J. (2004). Retroviral spread by induction of virological synapses. *Traffic*, **5**, 643-650.

Joshi, A., Garg, H., Nagashima, K., Bonifacino, J. S. and Freed, E. O. (2008). GGA and Arf proteins modulate retrovirus assembly and release. *Molecular Cell*, **30**, 227-238.

Jossinet, F., Lodmell, J. S., Ehresmann, C., Ehresmann, B. and Marquet, R. (2001). Identification of the *in vitro* HIV-2/SIV RNA dimerization site reveals striking differences with HIV-1. *The Journal of Biological Chemistry*, **276**, 5598-5604.

Kammler, S., Otte, M., Hauber, I., Kjems, J., Hauber, J. and Schaal, H. (2006). The strength of the HIV-1 3' splice sites affects Rev function. *Retrovirology*, **3**, 89.

Kang, H. J. and Park, H. J. (2009). Novel molecular mechanism for actinomycin D activity as an oncogenic promoter G-quadruplex binder. *Biochemistry*, **48**, 7392-7398.

Karn, J. (1999). Tackling tat. *The Journal of Molecular Biology*, **293**, 235-254.

Kasprzak, W., Bindewald, E. and Shapiro, B. A. (2005). Structural polymorphism of the HIV-1 leader region explored by computational methods. *Nucleic Acids Research*, **33**, 7151-7163.

Katzmann, D. J., Babst, M. and Emr, S. D. (2001). Ubiquitin-dependent sorting into the multivesicular body pathway requires the function of a conserved endosomal protein sorting complex, ESCRT-I. *Cell*, **106**, 145-155.

Kaye, J. F. and Lever, A. M. L. (1999). Human immunodeficiency virus types 1 and 2 differ in the predominant mechanism used for selection of genomic RNA for encapsidation. *The Journal of Virology*, **73**, 3023-3031.

Komar, A. A. and Hatzoglou, M. (2011). Cellular IRES-mediated translation: The war of ITAFs in pathophysiological states. *Cell Cycle*, **10**, 229-240.

Komar, A. A. and Hatzoglou, M. (2005). Internal ribosome entry sites in cellular mRNAs: mystery of their existence. *The Journal of Biological Chemistry*, **280**, 23425-23428.

Kwong, P. D., Wyatt, R., Robinson, J., Sweet, R. W., Sodroski, J. and Hendrickson, W. A. (1998). Structure of an HIV gp120 envelope glycoprotein in complex with the CD4 receptor and a neutralizing human antibody. *Nature*, **393**, 648-659.

Lamphear, B. J., Yan, R., Yang, F., Waters, D., Liebig, H. D., Klump, H., Kuechler, E., Skern, T. and Rhoads, R. E. (1993). Mapping the cleavage site in protein synthesis initiation factor eIF-4 gamma of the 2A proteases from human Coxsackievirus and rhinovirus. *The Journal of Biological Chemistry*, **268**, 19200-19203.

Lapointe, J. and Brakier-Gingras, L. (2003). Translation mechanisms: (Kluwer Academic/Plenum Publishers).

Lawrence, D. C., Stover, C. C., Noznitsky, J., Wu, Z. and Summers, M. F. (2003). Structure of the intact stem and bulge of HIV-1 [Psi]-RNA stem-loop SL1. *The Journal of Molecular Biology*, **326**, 529-542.

Le Guenno, B., Jouan, A., Arborio, M., N'Diaye, B., Guiraud, M., Griffet, P., Seignot, P. and Digoutte, J. P. (1987). HIV2 is responsible for AIDS cases in Senegal. *Annales de l'Institut Pasteur. Virologie*, **138**, 397-399.

Le Rouzic, E. and Benichou, S. (2005). The Vpr protein from HIV-1: distinct roles along the viral life cycle. *Retrovirology*, **2**, 11.

Ledford, H. (2008). HIV vaccine developers battle on, despite high-profile failures. *Nature Biotechnology*, **26**, 591-592.

Lee, J. H., Pestova, T. V., Shin, B. S., Cao, C., Choi, S. K. and Dever, T. E. (2002). Initiation factor eIF5B catalyzes second GTP-dependent step in eukaryotic translation initiation. *Proceedings of the National Academy of Sciences of the United States of America*, **99**, 16689-16694.

Leib-Mösch, C., Brack-Werner, R., Werner, T., Bachmann, M., Faff, O., Erfle, V. and Hehlmann, R. (1990). Endogenous retroviral elements in human DNA. *Cancer Research*, **50**, 5636-5642.

Leligdowicz, A., Yindom, L. M., Onyango, C., Sarge-Njie, R., Alabi, A., Cotten, M., Vincent, T., da Costa, C., Aaby, P., Jaye, A., Dong, T., McMichael, A., Whittle, H. and Rowland-Jones, S. (2007). Research article: robust Gag-specific T-cell responses characterize viremia control in HIV-2 infection. *The Journal of Clinical Investigation*, **117**, 3067-3074.

Lever, A. M. L. (2005). HIV: the virus. *Medicine*, **33**, 1-3.

Levesque, K., Zhao, Y. S. and Cohen, É. A. (2003). Vpu exerts a positive effect on HIV-1 infectivity by down-modulating CD4 receptor molecules at the surface of HIV-1-producing cells. *The Journal of Biological Chemistry*, **278**, 28346-28353.

Levy, J. (2007). HIV and the pathogenesis of AIDS., 3rd Edition: (Wiley-Blackwell).

Levy, J. A., Hollander, H., Shimabukuro, J., Mills, J. and Kaminsky, L. (1985). Isolation of AIDS-associated retroviruses from cerebrospinal fluid and brain of patients with neurological symptoms. *The Lancet*, **326**, 585-588.

Li, Y., Bor, Y., Misawa, Y., Xue, Y., Rekosh, D. and Hammarskjold, M. L. (2006). An intron with a constitutive transport element is retained in a Tap messenger RNA. *Nature*, **443**, 234-237.

Locker, N., Chamond, N. and Sargueil, B. (2011). A conserved structure within the HIV gag open reading frame that controls translation initiation directly recruits the 40S subunit and eIF3. *Nucleic Acids Research*, **39**, 2367-2377.

Luo, M. J., Zhou, Z., Magni, K., Christoforides, C., Rappsilber, J., Mann, M. and Reed, R. (2001). Pre-mRNA splicing and mRNA export linked by direct interactions between UAP56 and Aly. *Nature*, **413**, 644-647.

López de Quinto, S., Sáiz, M., de la Morena, D., Sobrino, F. and Martínez-Salas, E. (2002). IRES-driven translation is stimulated separately by the FMDV 3′-NCR and poly(A) sequences. *Nucleic Acids Research*, **30**, 4398-4405.

López-Lastra, M., Rivas, A. and Barría, M. I. (2005). Protein synthesis in eukaryotes: the growing biological relevance of cap-independent translation initiation. *Biological Research*, **38**, 121-246.

MacNeil, A., Sarr, A. D., Sankale, J. L., Meloni, S. T., Mboup, S. and Kanki, P. (2007). Direct evidence of lower viral replication rates *in vivo* in human immunodeficiency virus type 2 (HIV-2) infection than in HIV-1 infection. *The Journal of Virology*, **81**, 5325-5330.

Madani, N. and Kabat, D. (1998). An endogenous inhibitor of human immunodeficiency virus in human lymphocytes is overcome by the viral Vif protein. *The Journal of Virology*, **72**, 10251-10255.

Madsen, J. and Stoltzfus, C. M. (2006). A suboptimal 5' splice site downstream of HIV-1 splice site A1 is required for unspliced viral mRNA accumulation and efficient virus replication. *Retrovirology*, **3**, 10.

Malim, M. H. and Cullen, B. R. (1993). Rev and the fate of pre-mRNA in the nucleus: implications for the regulation of RNA processing in eukaryotes. *Molecular and Cellular Biology*, **13**, 6180-6189.

Malim, M. H. and Emerman, M. (2008). HIV-1 accessory proteins-ensuring viral survival in a hostile environment. *Cell Host and Microbe*, **3**, 388-398.

Mansky, L. M. and Temin, H. M. (1995). Lower in vivo mutation rate of human immunodeficiency virus type 1 than that predicted from the fidelity of purified Reverse transcriptase. *The Journal of Virology*, **69**, 5087-94.

Marcello, A. (2006). Latency: the hidden HIV-1 challenge. *Retrovirology*, **3**, 7.

Marcello, A., Lusic, M., Pegoraro, G., Pellegrini, V., Beltram, F. and Giacca, M. (2004). Nuclear organization and the control of HIV-1 transcription. *Gene*, **326**, 1-11.

Mathews, M. B., Sonenberg, N. and Hershey, J. W. B. (2007). Translational control in biology and medicine. (Cold Spring Harbor, New York.: (Cold Spring Harbor Laboratory Press).

Mazauric, M. H., Seol, Y., Yoshizawa, S., Visscher, K. and Fourmy, D. (2009). Interaction of the HIV-1 frameshift signal with the ribosome. *Nucleic Acids Research*, **37**, 7654-7664.

Meerovitch, K., Svitkin, Y. V., Lee, H. S., Lejbkowicz, F., Kenan, D. J., Chan, E. K., Agol, V. I., Keene, J. D. and Sonenberg, N. (1993). La autoantigen enhances and corrects aberrant translation of poliovirus RNA in reticulocyte lysate. *The Journal of Virology*, **67**, 3798-3807.

Meyer, C., Zizioli, D., Lausmann, S., Eskelinen, E. L., Hamann, J., Saftig, P., von Figura, K. and Schu, P. (2000). [mu]1A-adaptin-deficient mice: lethality, loss of AP-1 binding and rerouting of mannose 6-phosphate receptors. *The EMBO Journal*, **19**, 2193-2203.

Miele, G., Mouland, A., Harrison, G. P., Cohen, E. and Lever, A. M. (1996). The human immunodeficiency virus type 1 5' packaging signal structure affects translation but does not function as an internal ribosome entry site structure. *The Journal of Virology*, **70**, 944-951.

Milev, M., Brown, C. and Mouland, A. (2010). Live cell visualization of the interactions between HIV-1 Gag and the cellular RNA-binding protein Staufen1. *Retrovirology*, **7**, 41.

Miller, M. D., Farnet, C. M. and Bushman, F. D. (1997). Human immunodeficiency virus type 1 preintegration complexes: studies of organization and composition. *The Journal of Virology*, **71**, 5382-5390.

Mitchell, R. S., Beitzel, B. F., Schroder, A. R. W., Shinn, P., Chen, H., Berry, C. C., Ecker, J. R. and Bushman, F. D. (2004). Retroviral DNA integration: ASLV, HIV, and MLV show distinct target site preferences. *PLoS Biology*, **2**, e234.

Mok, H. P. and Lever, A. (2007). Chromatin, gene silencing and HIV latency. *Genome Biology*, **8**, 228.

Montagnier, L., Dauguet, C., Axler, C., Chamaret, S., Gruest, J., Nugeyre, M. T., Rey, F., Barré-Sinoussi, F. and Chermann, J. C. (1984). A new type of retrovirus isolated from patients presenting with lymphadenopathy and acquired immune deficiency syndrome: Structural and antigenic relatedness with equine infectious anaemia virus. *Annales de l'Institut Pasteur. Virologie*, **135**, 119-134.

Montaner, J. S. G., Lima, V. D., Barrios, R., Yip, B., Wood, E., Kerr, T., Shannon, K., Harrigan, P. R., Hogg, R. S., Daly, P. and Kendall, P. (2010). Association of highly active antiretroviral therapy coverage, population viral load, and yearly new HIV diagnoses in British Columbia, Canada: a population-based study. *The Lancet*, **376**, 532-539.

Moreira, D., Kervestin, S., Jean-Jean, O. and Philippe, H. (2002). Evolution of eukaryotic translation elongation and termination factors: variations of evolutionary rate and genetic code deviations. *Molecular Biology and Evolution*, **19**, 189-200.

Morikawa, Y., Goto, T., Yasuoka, D., Momose, F. and Matano, T. (2007). Defect of human immunodeficiency virus type 2 Gag assembly in *Saccharomyces cerevisiae*. *The Journal of Virology*, **81**, 9911-9921.

Narayan, O. and Clements, J. E. (1989). Biology and pathogenesis of lentiviruses. *The Journal of General Virology*, **70**, 1617-1639.

Nevin, W. D. and Dacks, J. B. (2009). Repeated secondary loss of adaptin complex genes in the Apicomplexa. *Parasitology International*, **58**, 86-94.

Odorizzi, G., Cowles, C. R. and Emr, S. D. (1998). The AP-3 complex: a coat of many colours. *Trends in Cell Biology*, **8**, 282-288.

Ohlmann, T., Lopez-Lastra, M. and Darlix, J. L. (2000). An internal ribosome entry segment promotes translation of the simian immunodeficiency virus genomic RNA. *The Journal of Biological Chemistry*, **275**, 11899-11906.

Ono, A. and Freed, E. O. (2004). Cell-type-dependent targeting of human immunodeficiency virus type 1 assembly to the plasma membrane and the multivesicular body. *The Journal of Virology*, **78**, 1552-1563.

Orzech, E., Livshits, L., Leyt, J., Okhrimenko, H., Reich, V., Cohen, S., Weiss, A., Melamed-Book, N., Lebendiker, M., Altschuler, Y. and Aroeti, B. (2001). Interactions between adaptor protein-1 of the clathrin coat and microtubules via type 1a microtubule-associated proteins. *The Journal of Biological Chemistry*, **276**, 31340-31348.

O'Donovan, D., Ariyoshi, K., Milligan, P., Ota, M., Yamuah, L., Sarge-Njie, R. and Whittle, H. (2000). Maternal plasma viral RNA levels determine marked differences in mother-to-child transmission rates of HIV-1 and HIV-2 in The Gambia. *AIDS*, **14**, 441-448.

Paillart, J. C., Skripkin, E., Ehresmann, B., Ehresmann, C. and Marquet, R. (2002). *In vitro* evidence for a long range pseudoknot in the 5′-untranslated and Matrix coding regions of HIV-1 genomic RNA. *The Journal of Biological Chemistry*, **277**, 5995-6004.

Pal, R., Mumbauer, S., Hoke, G. M., Takatsuki, A. and Sarngadharan, M. G. (1991). Brefeldin A inhibits the processing and secretion of envelope glycoproteins of human immunodeficiency virus type 1. *AIDS Research and Human Retroviruses*, **7**, 707-712.

Parkin, N. T., Cohen, E. A., Darveau, A., Rosen, C., Haseltine, W. and Sonenberg, N. (1988). Mutational analysis of the 5' non-coding region of human immunodeficiency virus type 1: effects of secondary structure on translation. *The EMBO Journal*, **7**, 2831-2837.

Patterson, S., Rae, A., Hockey, N., Gilmour, J. and Gotch, F. (2001). Plasmacytoid dendritic cells are highly susceptible to human immunodeficiency virus type 1 infection and release infectious virus. *The Journal of Virology*, **75**, 6710-6713.

Pelletier, J. and Sonenberg, N. (1988). Internal initiation of translation of eukaryotic mRNA directed by a sequence derived from poliovirus RNA. *Nature*, **334**, 320-325.

Perelson, A. S., Neumann, A. U., Markowitz, M., Leonard, J. M. and Ho, D. D. (1996). HIV-1 dynamics *in vivo*: virion clearance rate, infected cell life-span, and viral generation time. *Science*, **271**, 1582-1586.

Pestova, T. V., Shatsky, I. N., Fletcher, S. P., Jackson, R. J. and Hellen, C. U. T. (1998). A prokaryotic-like mode of cytoplasmic eukaryotic ribosome binding to the initiation codon during internal translation initation of hepatitis C and classical swine fever virus RNAs. *Genes and Development*, **12**, 67-83.

Peterlin, B. M. and Trono, D. (2003). Hide, shield and strike back: how HIV-infected cells avoid immune eradication. *Nature Reviews Immunology*, **3**, 97-107.

Poeschla, E. (2008). Integrase, LEDGF/p75 and HIV replication. *Cellular and Molecular Life Sciences*, **65**, 1403-1424.

Pollard, V. W. and Malim, M. H. (1998). The HIV-1 Rev protein. *Annual Review of Microbiology*, **52**, 491-532.

Ponti, D., Troiano, M., Bellenchi, G., Battaglia, P. and Gigliani, F. (2008). The HIV Tat protein affects processing of ribosomal RNA precursor. *BMC Cell Biology*, **9**, 32.

Popov, S., Rexach, M., Zybarth, G., Reiling, N., Lee, M. A., Ratner, L., Lane, C. M., Moore, M. S., Blobel, G. and Bukrinsky, M. (1998). Viral protein R regulates nuclear import of the HIV-1 pre-integration complex. *The EMBO Journal*, **17**, 909-917.

Popper, S. J., Sarr, A. D., Gueye-Ndiaye, A., Mboup, S., Essex, M. E. and Kanki, P. J. (2000). Low plasma human immunodeficiency virus type 2 viral load is independent of proviral load: low virus production *in vivo*. *The Journal of Virology*, **74**, 1554-1557.

Poulsen, A. G., Aaby, P., Larsen, O., Jensen, H., Nauclér, A., Lisse, I. M., Christiansen, C. B., Dias, F. and Melbye, M. (1997). 9-year HIV-2-associated mortality in an urban community in Bissau, west Africa. *The Lancet*, **349**, 911-914.

Proud, C. G. (1994). Peptide-chain elongation in eukaryotes. *Molecular Biology Reports*, **19**, 161-170.

Purcell, D. F. and Martin, M. A. (1993). Alternative splicing of human immunodeficiency virus type 1 mRNA modulates viral protein expression, replication, and infectivity. *The Journal of Virology*, **67**, 6365-6378.

Purzycka, K. J. and Adamiak, R. W. (2008). The HIV-2 TAR RNA domain as a potential source of viral-encoded miRNA. A reconnaissance study. *Nucleic Acids Symposium Series*, **52**, 511-512.

Raijmakers, R., Schilders, G. and Pruijn, G. J. M. (2004). The exosome, a molecular machine for controlled RNA degradation in both nucleus and cytoplasm. *The European Journal of Cell Biology*, **83**, 175-183.

Ramirez, B. C., Simon-Loriere, E., Galetto, R. and Negroni, M. (2008). Implications of recombination for HIV diversity. *Virus Research*, **134**, 64-73.

Ratner, L., Gallo, R. C. and Wong-Staal, F. (1985). HTLV-III, LAV, ARV are variants of same AIDS virus. *Nature*, **313**, 636-637.

Reeves, J. D. and Doms, R. W. (2002). Human immunodeficiency virus type 2. *The Journal of General Virology*, **83**, 1253-1265.

Rerks-Ngarm, S., Pitisuttithum, P., Nitayaphan, S., Kaewkungwal, J., Chiu, J., Paris, R., Premsri, N., Namwat, C., de Souza, M., Adams, E., Benenson, M., Gurunathan, S., Tartaglia, J., McNeil, J. G., Francis, D. P.,

Stablein, D., Birx, D. L., Chunsuttiwat, S., Khamboonruang, C., Thongcharoen, P., Robb, M. L., Michael, N. L., Kunasol, P. and Kim, J. H. (2009). Vaccination with ALVAC and AIDSVAX to prevent HIV-1 infection in Thailand. *The New England Journal of Medicine*, **361**, 2209-2220.

Ricci, E. P., Rifo, R. S., Herbreteau, C. H., Decimo, D. and Ohlmann, T. (2008). Lentiviral RNAs can use different mechanisms for translation initiation. *Biochemical Society Transactions*, **036**, 690-693.

Robinson, M. S., Sahlender, D. A. and Foster, S. D. (2010). Rapid inactivation of proteins by Rapamycin-induced rerouting to mitochondria. *Developmental Cell*, **18**, 324-331.

Rogowska-Szadkowska, D. and Chlabicz, S. (2008). Primary HIV infection. *HIV and AIDS Review*, **7**, 10-14.

Rospert, S., Rakwalska, M. and Dubaquié, Y. (2005). Polypeptide chain termination and stop codon readthrough on eukaryotic ribosomes. In *Reviews of Physiology Biochemistry and Pharmacology*, pp. 1-30. Edited by S. G. Amara, E. Bamberg, S. Grinstein, S. C. Hebert, R. Jahn, W. J. Lederer, R. Lill, A. Miyajima, H. Murer, S. Offermanns, G. Schultz and M. Schweiger: Springer Berlin Heidelberg.

Russell, R., Liang, C. and Wainberg, M. (2004). Is HIV-1 RNA dimerization a prerequisite for packaging? Yes, no, probably? *Retrovirology*, **1**, 23.

Saad, J. S., Ablan, S. D., Ghanam, R. H., Kim, A., Andrews, K., Nagashima, K., Soheilian, F., Freed, E. O. and Summers, M. F. (2008). Structure of the myristylated human immunodeficiency virus type 2 Matrix protein and the role of phosphatidylinositol-(4,5)-bisphosphate in membrane targeting. *The Journal of Molecular Biology*, **382**, 434-447.

Santiago, M. L., Range, F., Keele, B. F., Li, Y., Bailes, E., Bibollet-Ruche, F., Fruteau, C., Noe, R., Peeters, M., Brookfield, J. F. Y., Shaw, G. M., Sharp, P. M. and Hahn, B. H. (2005). Simian immunodeficiency virus infection in free-ranging sooty mangabeys (*Cercocebus atys atys*) from the Tai forest, Cote d'Ivoire: implications for the origin of epidemic human immunodeficiency virus type 2. *The Journal of Virology*, **79**, 12515-12527.

Sarafianos, S. G., Das, K., Tantillo, C., Clark, A. D., Ding, J., Whitcomb, J. M., Boyer, P. L., Hughes, S. H. and Arnold, E. (2001). Crystal structure of HIV-1 Reverse transcriptase in complex with a polypurine tract RNA:DNA. *The EMBO Journal*, **20**, 1449-1461.

Savarino, A. (2007). In-Silico docking of HIV-1 Integrase inhibitors reveals a novel drug type acting on an enzyme/DNA reaction intermediate. *Retrovirology*, **4**, 21.

Schröder, A. R. W., Shinn, P., Chen, H., Berry, C., Ecker, J. R. and Bushman, F. (2002). HIV-1 integration in the human genome favors active genes and local hotspots. *Cell*, **110**, 521-529.

Seewald, M. J., Korner, C., Wittinghofer, A. and Vetter, I. R. (2002). RanGAP mediates GTP hydrolysis without an arginine finger. *Nature*, **415**, 662-666.

Sharp, P. M., Bailes, E., Chaudhuri, R. R., Rodenburg, C. M., Santiago, M. O. and Hahn, B. H. (2001). The origins of acquired immune deficiency syndrome viruses: where and when? *Philosophical Transactions of the Royal Society of London. Series B: Biological Sciences*, **356**, 867-876.

Shun, M. C., Raghavendra, N. K., Vandegraaff, N., Daigle, J. E., Hughes, S., Kellam, P., Cherepanov, P. and Engelman, A. (2007). LEDGF/p75 functions downstream from preintegration complex formation to effect gene-specific HIV-1 integration. *Genes and Development*, **21**, 1767-1778.

Sleasman, J. W. and Goodenow, M. M. (2003). 13. HIV-1 infection. *The Journal of Allergy and Clinical Immunology*, **111**, 582-592.

Slomovic, S., Fremder, E., Staals, R. H. G., Pruijn, G. J. M. and Schuster, G. (2010). Addition of poly(A) and poly(A)-rich tails during RNA degradation in the cytoplasm of human cells. *Proceedings of the National Academy of Sciences*, **107**, 7407-7412.

Stopak, K., de Noronha, C., Yonemoto, W. and Greene, W. C. (2003). HIV-1 Vif blocks the antiviral activity of APOBEC3G by impairing both its translation and intracellular stability. *Molecular Cell*, **12**, 591-601.

Strong, C. L., Lanchy, J. M., Dieng-Sarr, A., Kanki, P. J. and Lodmell, J. (2009). A 5' UTR-spliced mRNA isoform is specialized for enhanced HIV-2 Gag translation. *The Journal of Molecular Biology*, **391**, 426-437.

Sund, J., Ander, M. and Aqvist, J. (2010). Principles of stop-codon reading on the ribosome. *Nature*, **465**, 947-950.

Suzuki, Y. and Craigie, R. (2007). The road to chromatin -nuclear entry of retroviruses. *Nature Reviews Microbiology*, **5**, 187-196.

Svitkin, Y. V., Imataka, H., Khaleghpour, K., Kahvejian, A., Liebig, H. D. and Sonenberg, N. (2001). Poly(A)-binding protein interaction with eIF4G stimulates picornavirus IRES-dependent translation. *RNA*, **7**, 1743-1752.

Svitkin, Y. V., Pause, A. and Sonenberg, N. (1994). La autoantigen alleviates translational repression by the 5' leader sequence of the human immunodeficiency virus type 1 mRNA. *The Journal of Virology*, **68**, 7001-7007.

Svitkin, Y. V. and Sonenberg, N. (2004). An efficient system for cap- and poly(A)-dependent translation *in vitro*. In *mRNA Processing and Metabolism*, pp. 155-170. Edited by.

The Antiretroviral Therapy Cohort Collaboration, A. (2008). Life expectancy of individuals on combination antiretroviral therapy in high-income countries: a collaborative analysis of 14 cohort studies. *The Lancet*, **372**, 293-299.

Tong-Starksen, S. E., Welsh, T. M. and Peterlin, B. M. (1990). Differences in transcriptional enhancers of HIV-1 and HIV-2. Response to T cell activation signals. *The Journal of Immunology*, **145**, 4348-4354.

UNAIDS (2010). *UNAIDS report on the global AIDS epidemic 2010*. **In**: http://www.unaids.org/globalreport/documents/20101123_GlobalReport_full_en.pdf.

Vallejos, M., Deforges, J., Plank, T. D. M., Letelier, A., Ramdohr, P., Abraham, C. G., Valiente-Echeverría, F., Kieft, J. S., Sargueil, B. and López-Lastra, M. (2011). Activity of the human immunodeficiency virus type 1 cell cycle-dependent internal ribosomal entry site is modulated by IRES trans-acting factors. *Nucleic Acids Research*, **39**, 6186-6200.

Venkat, A., Piontkowsky, D. M., Cooney, R. R., Srivastava, A. K., Suares, G. A. and Heidelberger, C. P. (2008). Care of the HIV-positive patient in the emergency department in the era of highly active antiretroviral therapy. *Annals of Emergency Medicine*, **52**, 274-285.

Ventoso, I., Blanco, R., Perales, C. and Carrasco, L. (2001). HIV-1 Protease cleaves eukaryotic initiation factor 4G and inhibits cap-dependent translation. *Proceedings of the National Academy of Sciences*, **98**, 12966-12971.

Waheed, A. A. and Freed, E. O. (2009). Lipids and membrane microdomains in HIV-1 replication. *Virus Research*, **143**, 162-176.

Wan, M., Takagi, M., Loh, B. N., Xu, X. Z. and Imanaka, T. (1996). Autoprocessing: an essential step for the activation of HIV-1 Protease. *The Biochemical Journal*, **316**, 569-573.

Watts, J. M., Dang, K. K., Gorelick, R. J., Leonard, C. W., Bess Jr, J. W., Swanstrom, R., Burch, C. L. and Weeks, K. M. (2009). Architecture and secondary structure of an entire HIV-1 RNA genome. *Nature*, **460**, 711-716.

Wei, X., Ghosh, S. K., Taylor, M. E., Johnson, V. A., Emini, E. A., Deutsch, P., Lifson, J. D., Bonhoeffer, S., Nowak, M. A., Hahn, B. H., Saag, M. S. and Shaw, G. M. (1995). Viral dynamics in human immunodeficiency virus type 1 infection. *Nature*, **373**, 117-122.

Weill, L., James, L., Ulryck, N., Chamond, N., Herbreteau, C. H., Ohlmann, T. and Sargueil, B. (2010). A new type of IRES within *gag* coding region recruits three initiation complexes on HIV-2 genomic RNA. *Nucleic Acids Research*, **38**, 1367-1381.

WHO, U., Unicef: Geneva. (2009). *Towards universal access; scaling up priority HIV/AIDS interventions in the health sector: progress report 2009.* **In**: http://www.who.int/hiv/pub/tuapr_2009_en.pdf.

Wilson, J. E., Pestova, T. V., Hellen, C. U. T. and Sarnow, P. (2000). Initiation of protein synthesis from the A site of the ribosome. *Cell*, **102**, 511-520.

Wu, F., Garcia, J., Sigman, D. and Gaynor, R. (1991). Tat regulates binding of the human immunodeficiency virus trans-activating region RNA loop-binding protein TRP-185. *Genes and Development*, **5**, 2128-2140.

Wu, Y. and Marsh, J. W. (2003). Gene transcription in HIV infection. *Microbes and Infection*, **5**, 1023-1027.

Yakovchuk, P., Protozanova, E. and Frank-Kamenetskii, M. D. (2006). Base-stacking and base-pairing contributions into thermal stability of the DNA double helix. *Nucleic Acids Research*, **34**, 564-574.

Yang, H. C., Shen, L., Siliciano, R. F. and Pomerantz, J. L. (2009). Isolation of a cellular factor that can reactivate latent HIV-1 without T cell

activation. *Proceedings of the National Academy of Sciences*, **106**, 6321-6326.

Yedavalli, V. S. R. K., Neuveut, C., Chi, Y., Kleiman, L. and Jeang, K. T. (2004). Requirement of DDX3 DEAD box RNA helicase for HIV-1 Rev-RRE export function. *Cell*, **119**, 381-392.

Yusim, K., Peeters, M., Pybus, O. G., Bhattacharya, T., Delaporte, E., Mulanga, C., Muldoon, M., Theiler, J. and Korber, B. (2001). Using human immunodeficiency virus type 1 sequences to infer historical features of the acquired immune deficiency syndrome epidemic and human immunodeficiency virus evolution. *Philosophical transactions of the Royal Society of London. Series B: Biological sciences*, **356**, 855-66.

Zaher, H. S. and Green, R. (2009). Quality control by the ribosome following peptide bond formation. *Nature*, **457**, 161-166.

Zhang, G., Hubalewska, M. and Ignatova, Z. (2009). Transient ribosomal attenuation coordinates protein synthesis and co-translational folding. *Nature Structural and Molecular Biology*, **16**, 274-280.

Zouridis, H. and Hatzimanikatis, V. (2007). A model for protein translation: polysome self-organization leads to maximum protein synthesis rates. *Biophysical journal*, **92**, 717-730.

APPENDIX

1: HIV Gag-Luc reporter plasmid maps

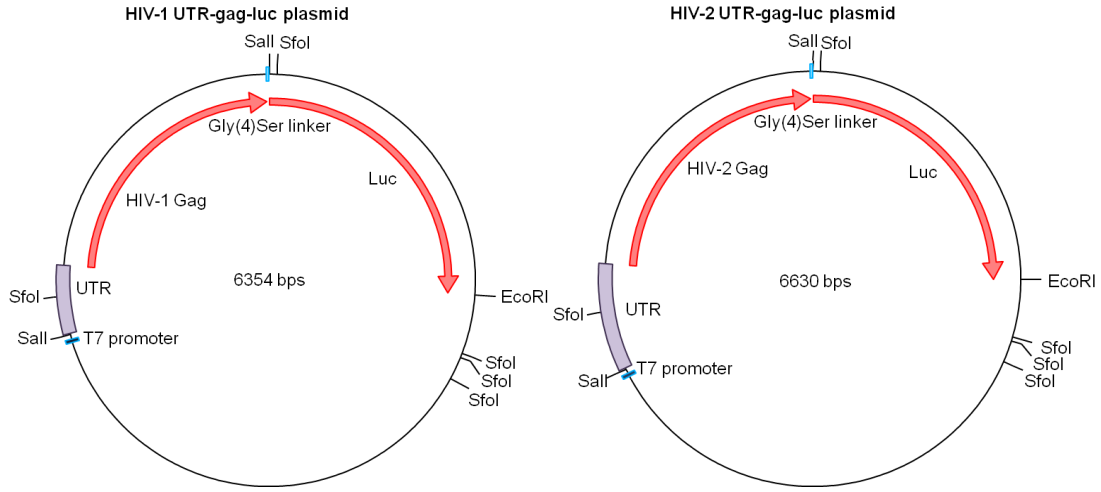

2: HIV ΔTAR Gag-Luc reporter plasmid maps

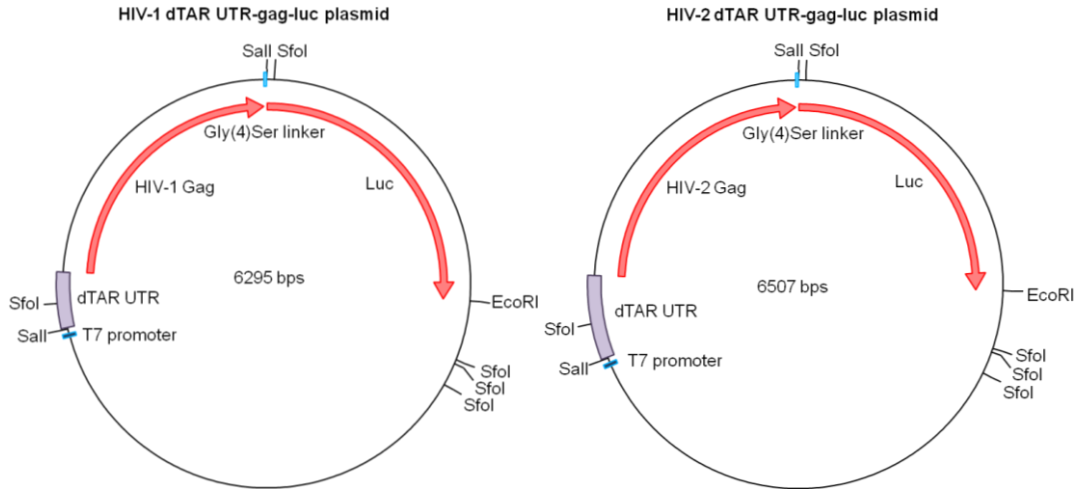

3: pcDNA3-2A plasmid map

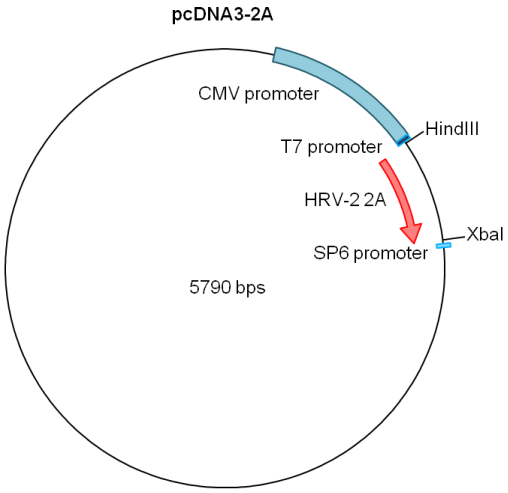

4: pcDNA3-2A-IRES plasmid map